## ABSTRACT

HELAL, AMR AWAD MOHAMED TAHA ALMANSY. Analysis of Earth Embankment Structures using Performance-based Probabilistic Approach including the Development of Artificial Neural Network Tool. (Under the direction of Dr. Mohammed A. Gabr and Dr. Roy H. Borden).

Earth embankment structures such as dams and levees are essential in our nation's infrastructure; being used for flood protection, water storage and hydropower generation. Frequent storms showed the deteriorating condition of dams and levees and urgent the need for a better condition assessment and stability evaluation. Past dams and levees failures have proved that the use of factor of safety approach is not an effective indicator of these structures' performance given the uncertainties in design input parameters (soil properties, loading history, etc.). An evaluation of the existing FEMA risk prioritization tool was performed along with sensitivity analysis. Numerical analysis of the Howard A. Hanson dam using PLAXIS 2D is preformed and its results within the context of limit states and FEMA risk tool is presented and discussed. A contour approach is proposed for risk estimation using various combinations of probabilities of exceeding limit states for seepage, earthquake and LSIII. A new risk tool is developed with MATLAB graphical user interface (GUI) to implement the finite element program PLAXIS 2D results. A total of 363 cases of numerical analysis using the finite element program PLAXIS 2D are performed varying key parameters including: i) geometry and properties of embankment ii) cycles of rising and falling water levels simulating the consecutive storms. MATLAB was used to develop a neural network which showed a training and prediction regression ($R^2$) of 98%. A parametric study on the effect of geometry, soil parameters and cycles of loading is performed using a base embankment model. As side slopes becomes steeper, shear strain increased from 0.1 to 0.5 to 3.8% going from 4:1 to 3:1 to 2:1 slope at time of 30 days. As embankment friction angle increased from 25$^o$ to 36$^o$, there was a

decrease in shear strain at toe from 2.4 to 0.5%. Cohesion of embankment, foundation and alluvial had a limited effect on the shear strain at toe. The embankment and alluvial permeability had a slight effect on the shear strain values. Increasing the foundation permeability from $6.8*10^{-5}$ to $1*10^{-3}$ cm/s caused an increase in toe shear strain to exceed LSIII. Increasing cycles of loading from 1 to 6 cycles, increased the shear strain by a factor of 10. Relative importance of the input parameters, indicated that side slopes and foundation permeability have the most effect on the shear strain at toe. The results of an integrated remote-sensing program and finite element modeling for a Sherman Island levee section is presented. Sherman island levee is constructed over peat deposit which experience large land subsidence and decomposition over time. Remote sensing data were used for the calibration of a numerical model using the finite element program PLAXIS 2D with mesh updating. Amorphous peat showed stiffer response and lower compressibility than fibrous peat. The assumption of amorphous peat led to computed displacements that ranged from 10 to 30% less than those with the fibrous peat properties, depending on the location within the domain. The analyses indicated a relatively small mechanistic deformation induced by an “extreme” water level under transient conditions. A study on the effect of peat different states of decomposition varies from H1 to H10 on the Von Post scale is performed. Deformed shape and probability of exceedance for both shear strain and gradient is shown. H1-H3 case reached probability of exceeding LSI of 1 after 270 days while H4-H7 peat took approximately 10,000 days to reach PE of 1. H8-H10 peat reached a PE of 1 at around 300,000 days.

# Analysis of Earth Embankment Structures using Performance-based Probabilistic Approach including the Development of Artificial Neural Network Tool

by
Amr Awad Mohamed Taha Almansy Helal

A dissertation submitted to the Graduate Faculty of
North Carolina State University
in partial fulfillment of the
requirements for the degree of
Doctor of Philosophy

Civil Engineering

Raleigh, North Carolina

2017

APPROVED BY:

| | |
|---|---|
| _____ | _____ |
| Dr. Mohammed A. Gabr<br>Committee Co-Chair | Dr. Roy H. Borden<br>Committee Co-Chair |
| _____ | _____ |
| Dr. Shamim Rahman | Dr. Abhinav Gupta |

## DEDICATION

*To my father, awesome mother and two beautiful siblings.*

*To my wife and my son "Yousef"*

*To my dear friends and colleagues*

*To whom I dedicate this work hoping it would be of benefit!*

## BIOGRAPHY

Amr Awad Mohamed Taha Almansy Helal was born on March 5th, 1986 in Damietta, Egypt. He got his Bachelor's degree from the Civil Engineering program in Mansoura University, Egypt in 2008. Being the top student in his class, his family encouraged him to complete his graduate studies in the US. He got admitted into the Master's program into the University of Alabama in Huntsville in 2011, where he was awarded his Master's degree in Civil Engineering in December 2012. Then, he got accepted into the Ph.D. program in North Carolina State University, one of the top-ranked universities in engineering, in spring 2013. He will continue to seek further opportunities in teaching and research in the geotechnical field transferring the knowledge he gained throughout his academic journey.

## ACKNOWLEDGMENTS

My thanks and sincere appreciation to my doctoral committee co-chairs, Dr. Mohammed Gabr and Dr. Roy Borden. Their guidance and support has always been a motivation to complete this thesis work. I would also like to thank Dr. Shamim Rahman and Dr. Abhinav Gupta for accepting to be in my doctoral committee. I also want to thank Dr. M. Masud Hasan for his significant help in developing the risk tool coding used in this research work. My family and wife also has been a great motivational aspect and gave me support and encouragement to travel abroad and study in the US. Lastly, I would like to thank all my friends in Raleigh who has eased the time I spent here with their companionship and encouragement. Thanks, Nafadi, Moataz, Abdelrahman, Islam, Ahmed, Omar, Yousef, Mahmoud, Hani, Midani, Sayed, Mostafa, Karim, Hassan, Elbadry and many others more. Thanks Ching-ting, Jungmok, Hamed, Kayser, Yuilian, Tim, Atefeh, Ahsan, Shahin, Casey, Mona, Jadid, Afshin, Zahra, Jinung, Ashkan, Arash, and Amin for keeping company in our geotechnical graduate office in Mann Hall 402.

# TABLE OF CONTENTS

## LIST OF TABLES

## LIST OF FIGURES

# CHAPTER 1. INTRODUCTION

## 1.1 Research motivation

Earth embankment structures such as levees and dams play an important role during extreme flooding events as well as during normal operating conditions. In addition to providing flood protection, these structures serve as a key-part of our critical civil infrastructure as they are also used for water storage and hydropower generation. According to the Association of State Dam Safety Officials, approximately one third of the "high hazard" earth dams are considered deficient in some aspects of their integrity and many are older than 50 years. ASCE reported that the 5 year funds needed for rehabilitation and upgrade of these structures is on the order of $12.5 billion but what is allocated nationwide is only $5.05 billion. Therefore, there is a clear need for accurate evaluation of stability and functionality level of these types of structures for condition assessment as well as cost effective specification and implementation of the remedial actions. Given the short fall of $7.45 billion in rehabilitation funds, the development of better condition assessment and efficient specification of rehabilitation approaches will have a positive impact on the welfare and safety of the communities served by these types of structures, and contribute to our nation's security and economic wellbeing.

The experience of past levee failures during storms like hurricane Katrina (Daniel, 2014) has proved that the use of the state of practice "factor of safety" approach is not an effective indicator of the safety level or expected performance of earth structures given uncertainties in loading history and stress path, soil properties, and changes in geometry with time. Therefore,

an approach based on the definition of limit states (Khalilzad and Gabr, 2011) has been implemented to assess the condition of protective earth structures and specify the probabilities of exceeding a predefined limit state and its associated risk value. The emerging need for evaluation of stability and functionality levels of earth structures rises from the frequent failures and the limited fund available for rehabilitation.

The integrity and reliability of levees are essential components of homeland safety. The failure of such systems due to a natural or manmade hazard can have monumental repercussions, sometimes with dramatic consequences on human life, property and the country's economy. There is lack of models in the literature that simulates effect of peat aging/decomposition over time from a probabilistic limit states prospective. The concept of performance limit states of these critical structures provides a means to quantitatively assess the functionality of an earth structure under severe storm loading events. The probability of exceeding a prescribed limit state is defined based on the strain or hydraulic gradient levels in potential emerging failure zones.

Innovative approaches that uses probabilistic and reliability analysis should become familiar inside the practical geotechnical community to allow decision-makers in allocating expenditure for such structure's rehabilitation. Also, tools for estimating risk that can facilitate engineering decisions should be developed. The research here on aims at applying coupled numerical probabilistic approaches to estimate probabilities of failure for earth embankment structures and develop simple tools to aid in the decision-making process. Also, study on the effect of peat decomposition on the performance of embankment levee in terms of strain or hydraulic gradient and probabilities of exceeding predefined limit states is performed.

## 1.2 Research objectives

The objectives of work in this study is to use coupled numerical probabilistic approaches to estimate functionality for embankment structures using probabilities of exceeding limit states and loss of life risk

- Investigation of the validity of using available risk tools (FEMA risk tool) to estimate associated risk for embankment structures and study of Howard A. Hanson dam as a case study using numerical analysis and probability approach.
- Implementation of the limit states concept developed by Khalilzad (2011) to estimate probabilities of exceeding a predefined limit state and its associated risk for embankment structures.
- Perform a parametric study on earth embankment structures using finite element program (PLAXIS 2D) and the effect of changing side slopes, soil friction angle, cohesion, permeability and cycles of loading on probabilities of exceeding a predefined limit state.
- Development of risk tool for dams and levees "*REES*: *R*isk *E*stimator for *E*mbankment *S*tructures", using Artificial Neural Network (ANN) approach and MATLAB coding for the prediction of risk for various combinations of loads, dam geometry and cyclic loading.
- Application of the implemented approach using field measurements by analyzing Sherman Island levees system in California in support of the DHS effort to estimate the risk of these levees failures from subsequent storms and salt-water intrusion issue

in the Sacramento San Joaquim Delta. The effect of peat decomposition/aging is investigated within the probabilities of limit state approach.

### 1.3 Thesis organization

This thesis was organized in a paper format having introduction and literature review chapters along with chapters discussing the research work and summary and conclusions.

*Chapter 1: Introduction*

This chapter represents research motivation, research objectives and thesis organization.

*Chapter 2: Literature review*

Literature review about limit states, probabilistic approach, Three-Sigma rule, Artificial Neural Networks (ANN), Numerical constitutive soil models and unsaturated soil hydraulic models.

*Chapter 3: Evaluation of FEMA risk tool and estimation of probabilities of exceeding limits states for embankment dams using numerical analysis*

This chapter discusses and evaluates the FEMA risk tool with an implementation for Howard A. Hanson dam using numerical analysis and probabilistic approach.

*Chapter 4: Development of risk estimator tool for embankment structures (REES) using coupled numerical-probabilistic approaches and artificial neural network.*

This chapter introduces the Artificial Neural Networks approach (ANN) and its incorporation into a GUI interface in developing the risk tool that eliminates the need for extensive finite element analysis to predict the probability of exceeding limit states. It also presents a parametric study on the effect of embankment side slopes, soil parameters and loading cycles.

*Chapter 5: Effect of peat decomposition on the performance of embankment levee using limit state probabilistic approaches and numerical analysis*

This chapter represents a study on the effect of peat decomposition on the deformation response of the Sacramento delta levee system. A numerical model is calibrated using PLAXIS 2D and in-situ field measurements.

*Chapter 6: Summary and conclusions*

This chapter summarize research work performed and its conclusion, contribution to the state of art.

*Appendix A: Properties of PLAXIS 2D cases for current study*

This appendix contains properties for PLAXIS 2D cases that was used to develop the ANN tool.

*Appendix B. MATLAB parameters randomization effect and probability sheet calculation*

This appendix contains ANOVA analysis details conducted in MATLAB along with probability sheet calculation procedure.

*Appendix C. MATLAB code and REES tool*

This appendix contains the MATLAB code for REES tool and ANN along with an explanation of the various components of the tool.

# CHAPTER 2. LITTERATURE REVIEW

## 2.1 Limit state design

Limit state design problems in geotechnical engineering design have been historically divided into two main groups of problems, stability and elasticity problems, in other words, ultimate and serviceability limit states (Meyerhof, 1995; Terzaghi, 1943). Meyerhof (1995), mentioned that stability or ultimate state problems deals with conditions just before failure happens by plastic flow without any consideration of strain effects. Serviceability limit state problems only consider deformations of soil due to soil-structure interaction and doesn't account for the stress conditions for failure. Generally, limit states are conditions where a structure no longer performs its designed function. Whenever a structure doesn't satisfy any of its performance standards, it can be said it reached a limit state (Becker, 1996).

Several studies used factor of safety approach (FS) by applying it to ultimate resistance to account for the ultimate state for earthwork's design (i.e. earth retaining structures, foundation, embankment structures and other construction problems). Factor of safety approach in stability estimates was first introduced in the $18^{th}$ century (Belidor, 1792; Coulomb, 1773). Factor of safety represents a ratio between the ultimate resistance of the earth structure or foundation to the applied load. Terzaghi and Peck (1948) gave ranges for total factors of safety for geotechnical structures with upper and lower ranges from 1.2 up to 3 based on the structure type and the failure mode. Various researchers suggested factors of safety for settlement analysis (Terzaghi, 1943; Terzaghi and Peck, 1948; Meyerhof, 1953; Skempton and MacDonald, 1953; Bjerrum, 1963). Another approach was implemented by Brinch Hansen

(1953) to estimate partial factors of safety on different types of loads, soil shear strength parameters and pile capacities. In European codes, limit state design is based on partial factors approach for both load and strength parameters of soils, while in North America codes, it favors load and resistance factors which is referred to as load-resistance factor design approach (LRFD) (Meyerhof, 1995). LRFD approach has the advantage of incorporating the variabilities in soil properties, site investigation methods, as-built dimensions, failure mode uncertainties and analysis method. These types of analysis also stand for serviceability limit states to estimate deformations of geotechnical structures. Uncertainties in the soil strength parameters (i.e. cohesion and friction angle) and the soil profile geometry give a great unreliability in the stability of structures and suggests that traditional factor of safety design doesn't provide a good indication of the performance and stability of structures.

The main concern raised when first LSD was first presented during the 1970's, was that it would be too complicated for practitioners. Although Allen (1994) stated that LSD can be as simple or as complicated as required "to do the job". Although many researches has published paper in the limit state topic such as Meyerhof (1970, 1982, 1984, 1993, and 1995), Ovesen (1981, 1993), Oveson and Orr (1991) and an international symposium on limit state design was held in Copenhagen, Denmark in 1993, which included more than 68 papers and discussion on limit state design.

Although the application of the limit state design (LSD) has increased over the last two decades. It has not been widely used in the dam safety evaluation (Farinha et. al, 2015). More committees are aware of the shortcomings of the overall factory of safety approach and moving forward toward probability approaches such as International Commission of Large Dams

(ICOLD, 1988, 1993) as traditional factor of safety design doesn't provide a good indication of the performance and stability of earth structures (Duncan, 1991; USACE, 2006).

Nian et.al (2008) used limit state and limit analysis to analyze the stability of reinforced slopes with piles in anisotropic and nonhomogeneous soils. Konstantakos (2010) discussed ultimate limit state method (ULS) advantages and limitations for braced excavations design. He stated that in Europe codes, in contrast with US, geotechnical engineers uses ULS design to estimate a factor of safety to be greater than one for all structures. A reduction factors is applied for soil strength parameters. On the other hand, US engineers uses a serviceability approach where soil parameters is estimated and then analysis is preformed to obtain service displacement, moments and forces. Design forces is then estimated by applying a factor of safety on the service results and factor of safety between 1.2 and 1.5 is applied to estimate wall embedment. Farinha et al. (2015) applied the limit state design (LSD) approach to the foundation of a concrete gravity dam with the joint application of the concepts of ultimate limit states and numerical methods. The authors adopted a criteria to determine the characteristic values of the soil properties. In their paper, they concluded that the LSD method can be used for dam foundation design with the partial factor values described in Eurocode 7. Limit state design has also been used to design cast-in-place piles, drilled shafts and sheet piles (Zaretskii et al., 1985; Misra and Roberts, 2009; Krabbenhoft et al., 2005).

Given the shortage ability of the traditional factor of safety approach to present the stability and the functionality of earth structures and the continuous research towards using probabilistic approaches along with limit states, This study will implement an approach proposed by Khalilzad and Gabr (2013, 2011b). This approach proposed a new platform for deformation

based limit state analysis for embankment dams. The approach was implemented into simple probabilistic analysis using approach by Duncan (2000). The authors defined limit state values by the horizontal deformation values at the toe location that can indicate the stability of the embankment. Then the shear strain values is correlated to the horizontal deformation on the failure surface. They used a qualitative definition for the limit states (LS) and divided as follows:

1) LS(I): minor deformations, no discernible shear zones, low gradients (i.e. $i < 1$) throughout the embankment dam and foundation,
2) LS(II): medium (repairable) deformations, limited piping problems (i.e. $i > 0.67$ within a shallow depth at the location of toe), dispersed plastic zones with moderate strain values, tolerable gradients less than critical,
3) LS(III): major deformations, breaches and critical gradients at key locations (i.e. boiling and fine material washing at the location of toe), high strain plastic zones and emerging shear bands

Although it seems from literature that the limit state design approach has been well-established, there is research gaps on how to quantify the limit state upper and lower bounds due to lack of sufficient data to estimate failure, also due to the uncertainties presented in the strength parameters and load conditions for structures. Limit states approaches have to be incorporated with probabilistic and statistical methods to be able to estimate probabilities of failure and exceeding or reaching a limit state bound.

## 2.2 Probabilistic approaches (Reliability-based design)

Recently, the interest has increased to the use of probability theory and reliability concepts to model uncertainties in earth embankments design. Geotechnical engineering is a field that contains lots of uncertain parameters in the soil strength parameters. In reliability-based design, parameters are treated as random variables with a probability density function or frequency distribution. This gives the perspective of including the variability of these functions and concluding a more representative safety measure as a probability of failure value (Harr, 1987; Christian et al., 1994; Khalilzad et al., 2015). Probability of failure in LRFD design can be defined as the shaded overlap area between resistance and load curves as in Figure 2.1.

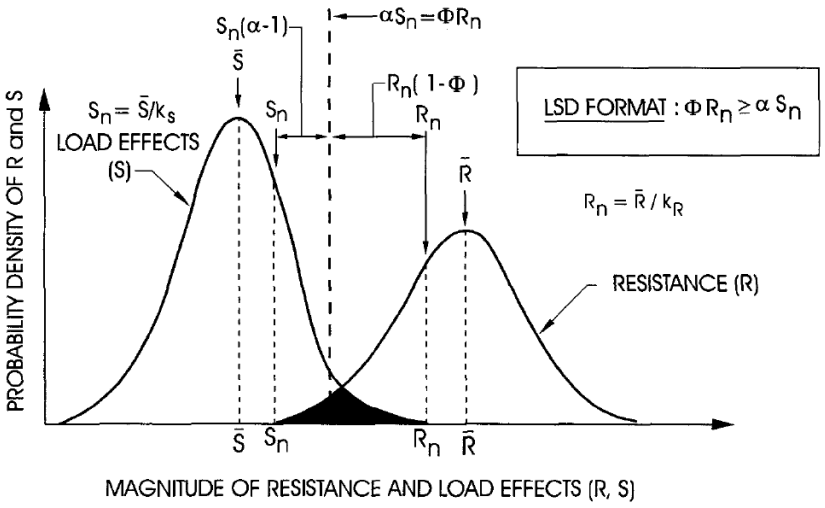


**Figure 2.1. Load and resistance factor design (LRFD) with probability of failure (Becker, 1996)**

Reliability-based design unlike the factor of safety design approach (which sometimes is based on engineering experience and judgment), takes into account the uncertainties associated with the design variables. Although the absolute values of probabilities of failure is difficult to estimate, because of the lack of understanding and lack of data for actual structures behavior

(Becker, 1996). The reliability methods use reliability index (β) as an indicator of the probability of failure or measure of safety. In many design codes, the reliability index values β ranges between 2.5 and 4 which corresponds to a probability of failure from about $1x10^{-2}$ to $1x10^{-5}$ (MacGregor, 1976; Allen, 1975). AAHSTO and OHBDC bridge codes use a target reliability index value of $\beta = 3.5$ and it is also used for code calibration for the foundations in the NBCC.

The main disadvantages in using reliability-based design are the requirement of sufficient and proper information about the probability distribution of the parameters which is seldom available. Probabilistic design approaches can be divided into three main categories: i) A fully probabilistic method in which the actual distribution is known or measured and this could be time-consuming and expensive to determine, so it is only recommended to be done in large special projects, ii) Approximate probability method that doesn't require knowing the actual probability distribution and it can be assumed. Typically, normal and log-normal distributions are assumed for soil properties (Becker, 1996). Lumb (1966) concluded that the variations in properties of four natural soils follow normal distribution and it can be safe to use normal distribution for properties that follows log-normal and bi-normal distributions. This can be defined by the second moment probabilistic method which uses two moments of mean and coefficient of variation, iii) The third level is the semi-probabilistic method which used separate load and resistance factors and this one by far the most simple and convenient method to apply. The LRFD is an example of this third category level. The main challenge in applying the reliability method is how to select an appropriate probability distribution for the parameters to meet the design level of safety specified by β value.

The probability distribution depends greatly on the mean, standard deviation or the coefficient of variation values. Many researchers have summarized the coefficients of variation for several geotechnical properties and in-situ test (Harr, 1984; Kulhawy, 1992; Lacasse and Nadim, 1997; Meyerhof, 1993, 1995 and Duncan, 2000). Table 2.1 summarizes the values for the coefficient of variation found in the literature. It must be noted while these values in the Table represent a large amount of test data, it covers extremely wide ranges of values for the same parameter and the conditions of sampling and testing are not specified. These values in Table 2.1 only provide guidance but engineering sense must be used when choosing the coefficient of variation value. Once the coefficient is assumed properly, the standard deviation can be estimated and the probability distribution is available in order to use in the probability of failure calculations. Duncan (2000) in his paper "Factors of safety and reliability in geotechnical engineering" uses Taylor series method to determine the probability of failure using the estimation of standard deviations values which he proposed to get using either available sufficient data or published values for coefficient of variations, or using the Three – Sigma rule which is used within this research.

In recent years, many studies have been done to explore possibility of risk in dam safety. Von Thun (1987) studied risk methodology with U.S. Bureau of Reclamation in order to estimate dam risk and risk expense. Two conferences were held (McCann, 1985; Haimes and Stakhiv, 1986; Moser and Stakhiv, 1987) where dam safety is discussed. When the safety of a dam is evaluated, the risk analysis is applied to estimate failure probability related to rare events. Foufoula- Georgiou (1989) showed how the exceedance probability of extreme

precipitation could be derived and applied to two watersheds in Iowa. Langseth and Perkins (1983) proposed a procedure for dam safety analysis.

Moreover, numerous studies have attempted to evaluate the safety of dams (Bowles, 1987; McCann et al., 1985; Von Thun, 1987; Resendiz-Carrill and Lave, 1987; Karlsson and Haimes, 1988a, 1988b; Haimes et al., 1988; Karlsson and Haimes, 1989; Petrakian et al., 1989). Wood (1977) in his paper "An Analysis of Flood Levee Reliability" evaluated the overtopping risk for levee by applying the integral transformation approach**.** Karlsson and Haimes (1988) in their paper "Risk-Based Analysis of Extreme Events" discussed how mathematical expectation has traditionally been used in solving risk-based problems and that it is no appropriate for decision making that affecting public policy because it conceals extremes by combining events of different magnitudes and probabilities of occurrence. Goodarzi et al. (2012) presented risk and uncertainty analysis to dam overtopping based on univariate and bivariate flood frequency by applying Gumbel logistic distribution. This shows the growing use of probabilistic approaches and risk towards estimating earth structures adequate functionality and risk under various failure modes such as piping, seepage, earthquake, overtopping and global stability failure.

**Table 2.1. Summary of coefficient of variation (V) for some geotechnical properties**

| Geotechnical Characteristics | Coefficient of Variation, V (%) | References |
|---|---|---|
| **Index properties** | | |
| Unit weight ($\gamma$) | 3 – 7 % | Harr (1984), Kulhawy (1992) |
| Liquid and plastic limit (LL, PL) | 11 % | Kulhawy (1992) |
| SPT blow count resistance (N) | 15 – 50 % | Harr (1984), Kulhawy (1992), Meyerhof (1993, 1995) |
| **Strength parameters** | | |
| Effective friction angle ($\varphi$') | 2 – 13 % | Harr (1984), Kulhawy (1992), Meyerhof (1993) |
| Undrained shear strength ($S_u$) | 13 – 40 % | Harr (1984), Kulhawy (1992), Lacasse and Nadim (1997), Duncan (2000), Meyerhof (1993) |
| Undrained strength ratio ($S_u$ /$\sigma_v$') | 5 – 15 % | Lacasse and Nadim (1997), Duncan (2000) |
| **Deformation parameters** | | |
| Elastic modulus (E) | 2 – 5 % | Meyerhof (1993, 1995) |
| Coefficient of consolidation ($C_v$) | 33 – 68 % | Duncan (2000) |
| Compression index ($C_c$) | 10 – 55 % | Harr (1984), Kulhawy (1992), Duncan (2000), Meyerhof (1993, 1995) |
| Coefficient of permeability for saturated clay (k) | 68 – 90 % | Harr (1984), Duncan (2000) |

## 2.3 Three-sigma rule

Estimation of standard deviation of soil parameters is a challenging task and requires enough data. Although, there are methods that can be used to estimate standard deviations if no enough data is present. Duncan (2000) proposed three methods that can be used to estimate standard deviation: i) If sufficient data is available, one can use the formal definition equation of standard deviation. ii) Published values for coefficient of variation which is available in number of published work at shown in Table 2.1. iii) The three-sigma rule. Dai and Wang (1992) described that we can use the fact that 99.73% of all values of a normally distributed parameter always fall within three standard deviations of the average. Three-sigma rule is shown in Figure 2.2.

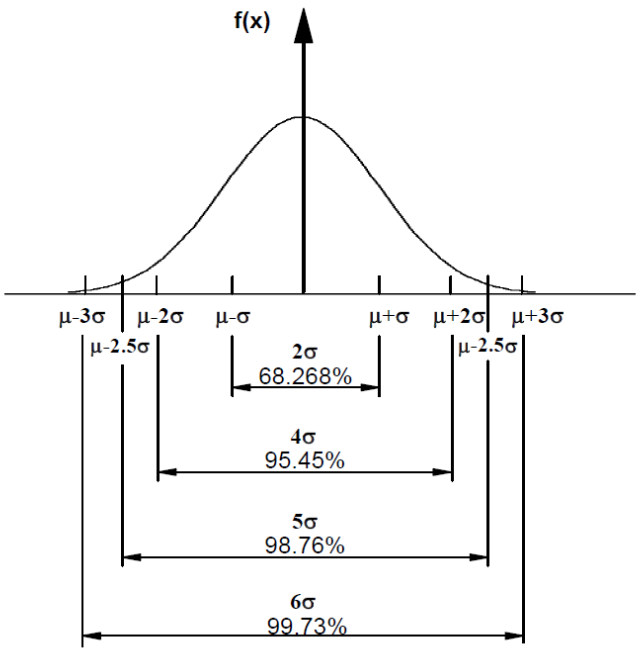


**Figure 2.2. Three-sigma rule representation for a normal distribution (US Army Corps of Engineers ETL 1110-2-561, 2006)**

Therefore, if HCV = highest conceivable value of the parameter, and LCV = lowest conceivable value of the parameter, these are approximately three standard deviations above and below the average value. The Three-Sigma rule can be used to estimate a value of standard deviation by first estimating the highest and the lowest conceivable values of the parameter and then dividing the difference between them by six:

$$\sigma = \frac{HCV - LCV}{6}$$

When limited data are obtainable or not data are available, then the three-sigma rule can be applied. Some research papers call it “Six sigma rule”.

### 2.4 Numerical constitutive soil models

Due to the high expenses of soil testing, stress-strain curves input data is very limited (Schanz et al., 1999). Use of numerically developed soil models to simulate soil behavior is of a tremendous help in understanding complex problems in geotechnical engineering where no or limited data is available. Various constitutive models can be used to simulate soil behavior; some assumes linear stress-strain relationships (i.e. linear Elastic, linear elastic perfectly-plastic) such as Mohr-Coulomb model. Other models incorporate nonlinear behavior as the isotropic hardening model or hardening soil model. These models use basic soil strength parameters and results from lab test to simulate the non-linear soil behavior. Although all the existing efforts to develop numerical models to simulate soil behavior, extensive care should be taken when choosing the appropriate soil model for a specific problem to get near-to-reality outcomes.

The linear elastic perfectly-plastic model (Mohr-Coulomb) has some limitation and only to use for first analysis of the problems. Although it takes in account stiffness increase with depth, it doesn't include either stress-dependency or stress-path dependency of stiffness or anisotropic stiffness. Various models have been developed to describe the non-linear behavior of soil such as Cam-Clay model (Hashiguchi, 1985, 1993), the pseudo-elastic (hypo-elastic) model, the hyperbolic model (Duncan and Chang, 1970) and the hardening soil model (Schanz et al., 1999). The hardening soil model is selected in this research to run the analysis for the embankment as the problem is of a large strain problem and the stiffness parameters change with pressure and with cycles of water level rising and drawdown. The hardening soil model supersedes the other nonlinear models by using the theory of plasticity instead of theory of elasticity, including soil dilatancy and introducing a yield cap. Hardening soil model (HS) is a more accurate model that takes into account more soil parameters such as triaxial loading stiffness $E_{50}$, the triaxial unloading stiffness, $E_{ur}$ and the Oedometer loading stiffness, $E_{oed}$. PLAXIS assumes default values as an average value for various soil types, $E_{ur} \sim 3E_{50}$ and $E_{oed} \sim E_{50}$. Also, the HS model accounts for the stress-dependency of stiffness moduli (i.e. all stiffnesses increases with pressure). The HS model simulates both soft and stiff soils. In comparison to the Mohr-Coulomb model, the yield surface of the HS model is not fixed in the principal stress space and can expand due to plastic strain. The stiffness of the soil decreases under deviatoric stress, resulting in irrecoverable plastic strain. In a drained triaxial test, hardening soil model can be approximated with a hyperbola similar to the hyperbolic model by Kondner (1963) and Duncan and Chang (1970), but different in that it utilizes the theory of plasticity instead of the theory of elasticity, includes soil dilation effects, and provides for a

yield cap. More details the formulation and equations of the hardening soil model are presented in PLAXIS material models manual. Hardening soil model is used in this thesis to simulate the nonlinear soil behavior and the input parameters are presented in Table 2.2.

**Table 2.2. Hardening soil model input parameters (PLAXIS 2016)**

| Parameter | Definition | Units |
|---|---|---|
| $E_{50}^{ref}$ | Secant stiffness in standard drained triaxial test | kN/m$^2$ |
| $E_{oed}^{ref}$ | Tangent stiffness in for primary oedemter loading | kN/m$^2$ |
| $E_{ur}^{ref}$ | Unloading/ reloading stiffness (default $E_{ur}^{ref} = E_{50}^{ref}$) | kN/m$^2$ |
| **m** | power for stress-level dependency of stiffness | ---- |
| **C'** | Effective cohesion | kN/m$^2$ |
| **φ' (phi)** | Effective angle of internal friction | ($^o$) |
| **Ψ (psi)** | Angle of dilatancy | ($^o$) |
| $\nu_{ur}$ | Poisson's ration for unloading-reloading (default=0.2) | ---- |
| $p^{ref}$ | Reference stress for stiffnesses (default $p^{ref}$ = 100 kN/m$^2$) | kN/m$^2$ |

Zain et al. (2011) in their paper modeled the lateral movement in soft clay due to excavation using finite element PLAXIS program with two soil models, Mohr-Coloumb and Hardening soil model. For simulation in PLAXIS, they created a geometry model which consists of sand and clay layer and a vertical sheet pile as driven downwards until bottom of the soil layer. The authors mentioned that the failure was resulted due to excavations done in stages on one side of the soil to the sheet pile. The results they obtained concluded that Mohr-Coulomb model are nearly equal to Hardening-Soil model if comparing horizontal displacements. However, for the soil stresses, the researcher found that the percentage differences between the both models are higher which is caused by characteristic of Hardening-Soil model that accounted for stress dependency of stiffness moduli, where all stiffness increase with pressure. They mentioned that Hardening soil model are more accurate because it uses three different inputs of stiffness

parameters which are $E_{50}$, $E_{ur}$ and $E_{oed}$ while Mohr-Coloumb model only consider for E value which is limited number of features that soil behavior show. For MC-model, Hooke's single stiffness model with linear elasticity in combination with an ideal plasticity, whereas the HS-model use double stiffness model for elasticity in combination with isotropic strain.

**2.5 Artificial Neural Networks (ANN)**

Artificial neural networks as its name indicates are soft computational approaches that try to simulate the decision process of the human brain nerve system. It learns from the knowledge of the neurons networks and uses that to predict outcomes. It is sometimes referred to as ANNs. A question may come in mind, why we should use ANNs and view it as more than a simulation approach although, computationally, any conventional computer can do what any ANNs can offer. The answer lies in two aspects; ANN allows simple computations to solve complex problems and can stand for wide range of problems given its self-organizing feature (Graupe, 2013). Simplicity is the key of ANNs solving algorithm, think of a fly avoiding an obstacle or a mouse running from a cat. They don't solve differential equations or complex computational algorithms, they simply use their neural cells to identify these obstacles and learn from experience to gain knowledge. Same as when kid observe his parents and learn from them, then simulate their movements. In short, ANNs is a computational approach inspired by the human brain neural system that has the ability to learn, recall, generalize and predict from a training set of data. If enough training data is available, we can use it to train the network and get a reasonable approximation for outcomes. MATLAB has an artificial neural network framework that will be used in this research to train an ANN network and then build a GUI (graphical user interface) for a risk estimation tool as will be explained later.

### 2.5.1 Artificial Neural Network approach (ANN)

Artificial Neural Network (ANN) approach can offer a simple platform for solving complex problems and can also learn and predict outcomes using training set of data. Neural Networks first caught interest after McCulloch and Pitts introduced simplified neurons in 1943. Usage of Neural networks and fuzzy logic has been missing in the dam safety community research till the 1980s. From the 1980s, analysis on dam observation data has developed greatly and new theories have been presented such as Grey Theory, fuzzy mathematics and neural networks. Liu Guanbiao (Liu, 1989) used fuzzy clustering method to analyze the displacement of a concrete dam. Other researchers used fuzzy logic and neural networks to predict earth dam's deformations (Chen, 2000; Deng, 2007). Artificial neural network has a set of simple units called neurons which send signals between each other and depends on a number of weighted connections. Any neural network consists of input units, activation functions, connection between units, external input (or bias) and learning rule (Rumelhart and McCleland, 1986). We can distinguish three types of neural network elements: input units which receive data form outside the neural network, output units which send data out of the neural network, and hidden units whose input and output signals remain within the neural network. Figure 2.3 shows a typical arrangement of an artificial neuron. For more details about activation functions and learning rules, refer to MATLAB neural network tool manual (MATLAB, 2014).

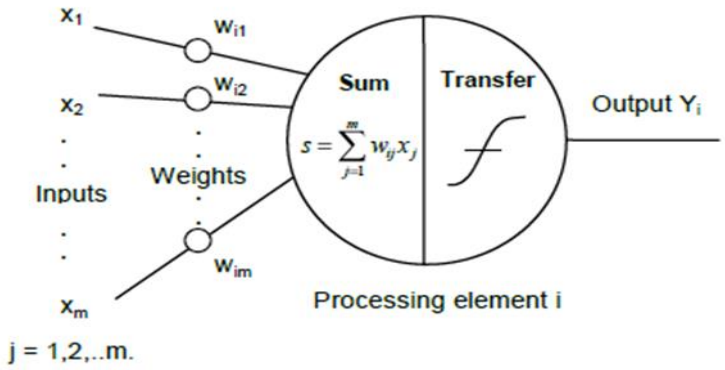


**Figure 2.3. Typical arrangement of an artificial neuron (JongKoo Jeon, 2007)**

### 2.5.2 Back-propagation algorithm (Feedforward ANN)

Literature has showed that a two-layer feed forward network can fit most complicated problems (Minsky and Papert, 1969). The main idea begins that the errors for the units of the hidden layers is determined by back-propagating the errors for the output layers, that's why it is called back-propagation algorithm. This has been used widely as a learning algorithm in feedforward neural networks. The algorithm works in two steps: first, propagate inputs forward to get an actual output. Then, the error (difference between target and output layers) is propagated backward to previous hidden layers to update their weights. Figure 2.4 shows a multilayer feedforward neural network.

### 2.5.3 Number of hidden layers

To design a good neural network model, number of hidden layers is needed as one of the first concerns. It is currently known that there is no need to have more than two hidden layers, as there is no improvement in the results with more hidden layers (Kecman, 2001, Masters, 1993, and Chester, 1990).

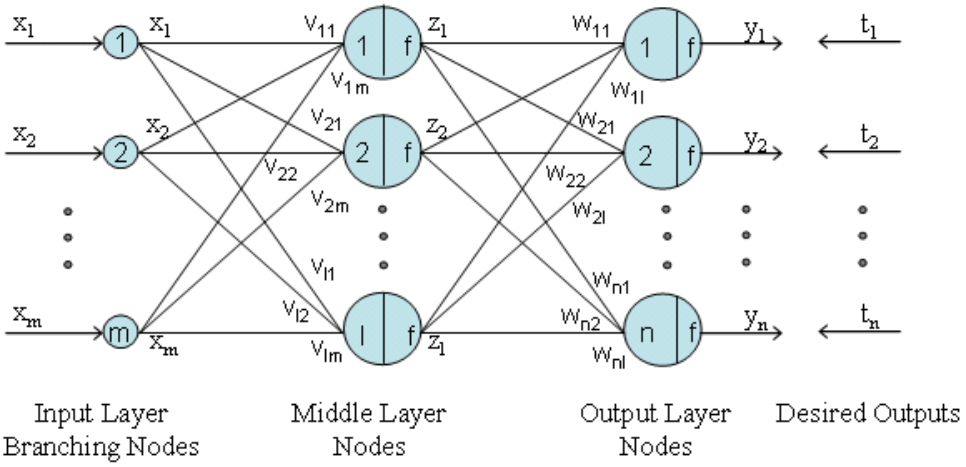


**Figure 2.4. Typical multilayer feedforward neural networks (JongKoo Jeon, 2007)**

## 2.6 Unsaturated soil hydraulic models

Embankment soil usually have parts that can be considered as unsaturated soil in-which the matric suction and the capillary action plays a significant role in altering soil stresses. Soil–water characteristic curve (SWCC) contains the fundamental information required for describing mechanical behaviors of unsaturated soil. SWCC relates the soil water content or degree of saturation to matric suction. Various equations were developed to describe SWCC. Pedroso et al. (2009) and Pedroso and Williams (2010) proposed a model to describe SWCC and SWCC with hysteresis. Pedroso and Williams (2011) also proposed a genetic algorithm method to determine the best fitting parameters of the different SWCC models. Some SWCC variables such as air-entry value, residual water content and residual suction are commonly used to describe the SWCC characteristics and are associated properties such as shear strength and permeability. Fredlund and Xing's (1994) equation with correction factor C(w) gives fitting result for a wide range of soil over the entire range of matric suction. Similar equations

can also be derived for Van Genuchten's equation (1980). Figure 2.5 shows a general shape of the SWCC along with its variables.

Unsaturated hydraulic properties are used for the embankment layer as all or some parts of the layer are above the phreatic surface at the different stages of modeling simulating rising reservoir level. The other two layers are saturated during the simulation time. There are several models that describe the hydraulic behavior of unsaturated soils. PLAXIS incorporates two hydraulic models for unsaturated soils, Van Genuchten and the approximate Van Genuchten model. Van Genuchten is a three-parameter function that relates saturation to the suction pore pressure head $\emptyset_p$ as follows:

$$S(\emptyset_p) = S_{residu} + (S_{sat} - S_{residu}) \left[1 + (\frac{g_a}{\emptyset_p})^{g_n}\right]^{g_c}$$

Where $S_{residu}$ is the residual saturation which describes the part of water that remains in soil even at high suction heads. $S_{sat}$ is the saturation when pores are filled with water. $g_a$, $g_n$ and $g_c$ are empirical parameters. PLAXIS converts a two-parameter equation as Mualem (1976) as

$$g_c = \frac{1 - g_n}{g_n}$$

The parameter $g_a$ is related to the air entry value (AEV) of the soil. The parameter $g_n$ is a function of the rate of water extraction once the AEV has been exceeded while the parameter $g_c$ is a function of the residual water content (due to the curvature in high suction range). More details about these models can be in the PLAXIS manual. No hysteresis effect has been considered for the SWCC in this study.

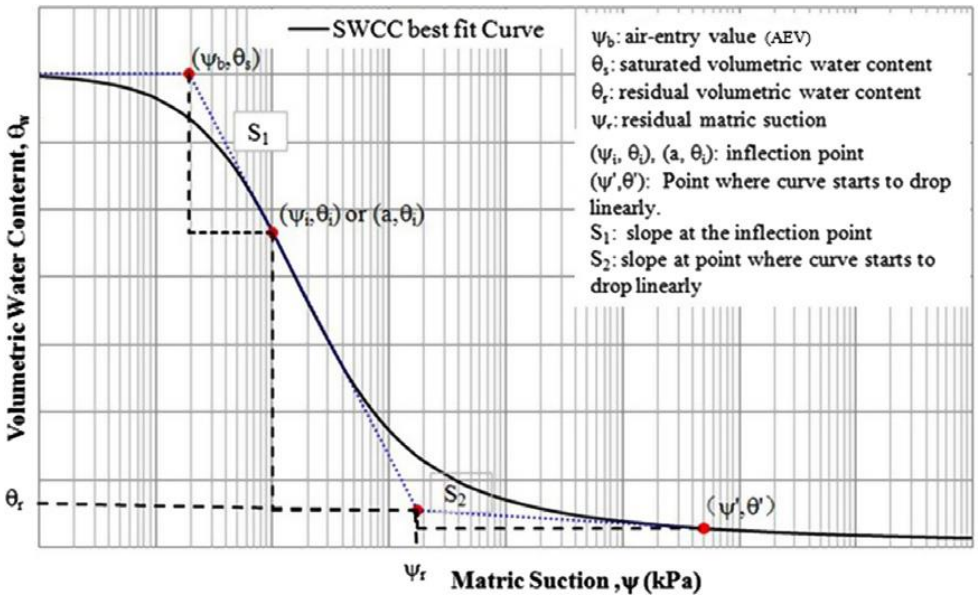


**Figure 2.5. General soil water characteristic curve (SWCC) (Zhai, 2012)**

## References


1- Allen, R. G. D. (1975). Index numbers in theory and practice. *Chicago, Aldine.*

2- Allen, D. E. (1994). The history of future of limit states design. *Journal of Thermal Insulation and Building Envelopes, 18*, 3-20.

3- Becker, D. E. (1996). Eighteenth Canadian geotechnical colloquium: limit states design for foundations. Part I. An overview of the foundation design process. *Canadian Geotechnical Journal, 33(6)*, 956-983.

4- Becker, D. E. (1996). Eighteenth Canadian geotechnical colloquium: limit states design for foundations. Part II. Development for the national building code of Canada. *Canadian Geotechnical Journal, 33*, 984-1007.

5- Bjerrum, L. and Eggestad A. (1963). Interpretation of loading tests on sand. *Norwegian Geotechnical Institute Publication, 58,* 23-27.

6- Bowles, D. S. (1987). A comparison of methods for risk assessment of dams. *NATO Advanced Study Institute, Tucson, AZ.*

7- Brinch J. Hansen. (1953). Earth pressure calculation. *Copenhagen*.

8- Chester, D. L. (1990). Why two hidden layers are better than one. *IJCNN 90, Washington, DC, Lawrence Erlbaum, 1,* 265-268.

9- Christian, J. T., Ladd, C. C. and Baecher, G. B. (1994). Reliability and Probability in Stability Analysis. *Journal of Geotechnical Engineering, ASCE. 120,* 1071-1111.

10- Dai, S. H. and Wang, M. O. (1992). Reliability analysis in engineering applications. *New York, Van Nostrand Reinhold.*

11- Deng, X. and Wang X., (2007). Application of dynamic fuzzy neural network to dam deformation prediction. *Hydropower Automation and Dam Monitoring, 4,* 64-67

12- Duncan, J. M. and Chang, C. Y. (1970). Nonlinear analysis of stress and strain in soils. *Journal of the Soil Mechanics and Foundations Division, ASCE, 96(SM5),* 1629-1653.

13- Duncan, J. M. and Tan, C. K. (1991). Settlement of Footings on Sands: Accuracy and Reliability. *Geotechnical Engineering Congress, ASCE, 1,* 446-455.

14- Duncan, J. M. (2000). Factors of Safety and Reliability in Geotechnical Engineering. *Journal of Geotechnical and Geoenvironmental Engineering, 126(4).*

15- Farinha, M. L., Caldeira, L. and Maranha das Neves, E. (2015). Limit state design approach for the safety evaluation of the foundations of concrete gravity dams. *Structure and Infrastructure Engineering, 11,* 1306-1322.

16- Foufoula-Georgiou, E. (1989). A probabilistic storm transposition approach for estimating exceedance probabilities of extreme precipitation depths. *Water Resources Research, 25(5),* 799-815.

17- Fredlund, D. G. and Xing, A. (1994). Equations for the soil-water characteristic curve. *Canadian Geotechnical Journal, 32,* 521-532.

18- Goodarzi, E., Shui, L. T. and Ziaei, M. (2012). Dam overtopping risk using probabilistic concepts-Case study: The Meijaran Dam, Iran. *Ain Shams Engineering Journal.*

19- Graupe, D. (2013). Principles of Artificial Neural Networks. *World Scientific.*

20- Haimes, Y. Y., and E. Z. Stakhiv (1986). Risk-Based decision making in water resources. *Proceeding of an Engineering Foundation Conference, Santa Barbara, CA, American Society of Civil Engineers, New York, NY.*

21- Haimes, Y. Y., R. Petrakian, P. O. Karlsson, and J. Mitsiopoulos. (1988). Risk analysis of dam failure and extreme floods: application of the partitioned multi-objective risk method. *Environmental Systems Management, Inc., Charlottesville, VA.*

22- Harr, M. E. (1987). Reliability-based design in civil engineering. *New York: McGraw-Hill.*

23- Harr, M. E. (1984). Reliability-based design in civil engineering. *Henry M. Shaw Lecture, Dept. of Civil Engineering, North Carolina State University, Raleigh, N.C.*

24- Hashiguchi. K. (1985). Macrometric approaches-static-instrincsically time-independent. *Proceedings XI ICSMFE, San Francisco, Constitutive laws for soils, 25-65*.

25- Hashiguchi, K. (1993). Fundamental requirements and formulations of elastoplastic constitutive equations with tangential plasticity. *International Journal of Plasticity, 9,* 525-549.

26- ICOLD. (1984). World register of dams: updating. *International Commission of Large Dams, Paris.*

27- ICOLD. (1993). Embankment dams-Upstream slope protection, Review and recommendations. *International Commission of Large Dams, Paris, 91*.

28- JongKoo, J. (2007). Fuzzy and Neural Network Models for Analyses of Piles. *Ph.D Thesis, Civil Engineering Department, North Carolina State University.*

29- Karlsson, P. O., and Y. Y. Haimes. (1988a). Risk-Based Analysis of Extreme Events. *Water Resources Research, 24(1),* 9-20.

30- Karlsson, P. O., and Y. Y. Haimes. (1988b). Probability Distributions and Their Partitioning. *Water Resources Research, 24(1),* 21-29.

31- Karlsson, P. O., and Y. Y. Haimes. (1989). Risk assessment of extreme events: application. *Journal of Water Resources Planning and Management, 115(3),* 299-320.

32- Kecman, V. (2001). Learning and Soft Computing: Support Vector Machines, Neural Networks, and Fuzzy Logic Models. *MIT Press.*

33- Khalilzad, M. and Gabr, M. A. (2011). Deformation-Based Limit States for Earth Embankments. *ASCE Conference Proceeding, 36,* 39-48.

34- Kondner. R. B. (1963). Hyperbolic stress-strain response: Cohesive soils. *Journal of SMF Div. Proceedings, ASCE, 89(SM1),* 115-143.

35- Konstantakos, D. C. (2010). Advantages and Limitations of Ultimate Limit State Design Methods for Braced Excavations. *Earth Retention Conference 3, GSP 208.*

36- Krabbenhoft, K., Damkilde, L. and Krabbenhoft, S. (2005). Ultimate limit state design of sheet pile walls by finite elements and nonlinear programming. *Computers and Structures, 83,* 383-393.

37- Kulhawy, F. H. (1992). On the evaluation of soil properties. *Geotechnical Special Publicaiton, 31,* 95-115.

38- Lacasse, S. and Nadim, F. (1997). Uncertainties in characterizing soil properties. *Norwegian Geotechnical Institute, Oslo, Norway, 201, 49-75*.

*39-* Langseth, A. M., and Perkins, M. (1983). The influence of dam failure probabilities on spillway analysis. *Proceedings of Conference on Frontiers in Hydraulic Engineering. ASCE, New York.*

*40-* Liu, L. (1989). Optical Pattern Fuzzy Logic. *Japanese Journal of Applied Physics, 29(2).*

41- Lumb, P. (1966). The variability of natural soils. *Canadian Geotechnical Journal, 2.*

42- MacGregor, J. G. (1976). Safety and limit state design for reinforced concrete. *Canadian Journal of Civil Engineering, 3(4),* 484-513.

43- Masters, T. (1993). Practical Neural Network Recipes in C++. *Morgan Kaufmann*.

44- McCann, M. W., Franzini, J. B. Kavazanjian, E. and Shah, H.C. (1985). Preliminary safety evaluation of existing dams. *John A. Blume. Earthquake Engineering Center, Stanford University, 69.*

45- Meyerhof, G. G. and Murdock, L. J. (1953). An investigation of the bearing capacity of some bored and driven piles in London clay. *Geotechnique, 3*, 267-282.

46- Meyerhof, G. G. (1970). Safety factors in soil mechanics. *Canadian Geotechnical Journal, 7,* 349-355.

47- Meyerhof, G. G. (1982). Limit states design in geotechnical engineering. *Structural Safety, 1*, 67-71.

48- Meyerhof, G. G. (1984). Safety factors and limit states analysis in geotechnical engineering. *Canadian Geotechnical Journal, 21*, 1-7.

49- Meyerhof, G. G. (1993). Development of geotechnical limit state design. *Proceedings of the International Symposium on Limit State Design in Geotechnical Engineering, Copenhagen, Danish Geotechnical Society, Copenhagen, 1(3),* 1-12.

50- Meyerhof G. G. (1995). Development of geotechnical limit state design. *Canadian Geotechnical Journal, 32(1),* 128-136.

*51*- Minsky M. L. and Papert S. (1969). Perceptrons. *MIT Press, Cambridge MA.*

52- Misra, A. and Roberts, L. A. (2009). Service limit state resistance factors for drilled shafts. *Geotechnique 59(1),* 53–61.

*53*- Moser, D. A., and E. Z. Stakhiv. (1987). Risk analysis considerations for dam safety, in engineering reliability and risk in water resources. *NATO Advanced Study Institute, Tucson, AZ*

54- Ovesen, N. K. (1981). Towards a European code for foundation engineering. *Ground Engineering, 14(7),* 25-28.

55- Ovesen, N. K. and Orr, T. (1991). Limit States Design: the European perspective. *Proceedings of Geotechnical Engineering Congress, American Society of Civil Engineers, Special Publication, 27(2),* 1341-1352.

56- Ovesen, N. K. (1993). Eurocdoe 7: a European code of practice for geotechnical design. *Proceedings of the International Symposium on Limit State Design in Geotechnical Engineering, 3,* 691-710.

57- Pedroso, D. M., Chao, D. S. and Dong, J.Z. (2009). The concept of reference curves for constitutive modeling in soil mechanics. *Computers and Geotechnics, 36,* 149–165.

58- Pedroso, D. M., Williams, D. J. (2010). A novel approach for modelling soil water characteristic curves with hysteresis. *Computers and Geotechnics 37 (3),* 374–380.

59- Petrakian, R., Y.Y. Haimes, E. Stakhiv, and D. Moser. (1989). Risk analysis of dam failure and extreme floods. *American Society of Civil Engineers, New York, NY.*

60- Resendiz-Carrillo, D., and L.B. Lave. (1987). Optimizing Spillway Capacity with an Estimated Distribution of Floods. *Water Resources Research, 23(11),* 2043-49.

61- Rumelhart, D. E. and McClelland (1986). Parallel Distributed Processing: Explorations in the Microstructure of Cognition. *MIT Press, Cambridge, MA.*

62- Schanz, T., Vermeer, P. A. and Bonnier, P. G. (1999). Formulation and verification of the Hardening-Soil Model. *Beyond 2000 in Computational geotechnics, Amsterdam.*

63- Skempton A. W., MacDonald D. H. (1956). The allowable settlements of buildings. *Proceedings I.C.E., 5,* 727-768.

64- Terzaghi, K. (1943). Theoretical soil mechanics. *John Wiley & Sons, New York*

65- Terzaghi, K. and Peck, R. B. (1948). Soil mechanics in engineering practice. *John Wiley & Sons, New York.*

66- US Army Corps of Engineers (USACE). (2006). Reliability analysis and risk assessment for seepage and slope stability failure modes for embankment dams. *ETL 1110-2-561.*

67- Van Genuchten, M. Th. (1980). A closed-form equation for predicting the hydraulic conductivity of unsaturated soils. *Soil Science Society of America Journal, 44,* 892–898.

68- Von Thun L. (1987). *Use of risk-based analysis in making decision on dam safety. Engineering Reliability and Risk in Water Resources*, 205-221.

69- Zain, N. H., Ahmad, J., Ashaari, Y., Shaffie, E. and Mustaffa, N. K. (2011). Modelling of lateral movement in soft soil using hardening soil model. *Proceedings, UKSim 13th International Conference on Modelling and Simulation, 195-200.*

70- Zaretskii, Yu, K. and Karabaev, M. I. (1985). Limit-state design of cast-in-place piles. *Soil Mechanics and Foundation Engineering, 22,* 169-175.

71- Zhai, Q. and Rahardjo, H. (2012). Determination of soil-water characteristic curve variables. *Computers and Geotechnics, 42,* 37-43.

# CHAPTER 3. EVALUATION OF FEMA RISK TOOL AND ESTIAMTION OF PROBABILITIES OF EXCEEDING LIMIT STATES FOR EMBANKMENT DAMS USING NUMERICAL ANALYSIS

## 3.1 Abstract

Climate change is causing a rise in sea level, which increases the likelihood of recurring damaging floods from storm surges for embankment structures (i.e., dams and levees). To help mitigate these damages, precise techniques must be developed for risk assessment and probability of exceeding limit states estimation for these structures; being the first defense line against flood all over the country. Existing risk estimation tool estimates probabilities of exceeding limit states in a qualitative manner that doesn't necessarily represent actual structure behavior or damage level. It also has no way of taking storm cycles history or soil profile into consideration. This along with limited allocated nation's budget for remediation, urges the need for development of approaches that estimates probabilities in a quantitative way. Therefore, work inhere evaluates existing risk tool that was developed for the Federal Emergency Management Agency (FEMA) for risk estimation for dams along with sensitivity analysis using contour plots. An approach for quantitative probability estimation using PLAXIS 2D numerical analysis and a probability estimation sheet is proposed. The Howard A. Hanson (HHD), located on the Green river near Seattle, Washington, is used as a case study. Numerical analysis results showed a probability of exceeding limit state III of $1.2*10^{-6}$ for normal stability and $2*10^{-5}$ for seepage after 6 storm cycles and a loss of life risk ranging from 0.001 to 0.25 for an overtopping probability of failure from $1*10^{-1}$ to $1*10^{-8}$ (Point x on the contour plot). Also, increasing storm cycles increased the probability of exceeding LSI from $2*10^{-6}$ to $3.9*10^{-3}$, LSII from $1.2*10^{-10}$ to $4.5*10^{-5}$, LSIII from $5.3*10^{-14}$ to $1.2*10^{-6}$ going from 3 to 6 cycles respectively.

## 3.2 Introduction

Climate change and global warming are leading to rise in the sea level. In the coming centuries, Sea level rise will be a threat to coastal land, infrastructures and ecosystems (Overpeck et al. 2006; Titus et al. 1991; Wu et al. 2009). More than 160 million people lives in a coastal region that are less than 1 m below sea level (Allison et al. 2009; Peters et al. 2013). Several researchers predicted sea level rise projections in the 21$^{st}$ century to be in the range of 50 to 150 cm (Chang et al. 2015). A recent study in Nature magazine showed that Antarctica alone will contribute with more than 1 m of sea-level rise by 2100 and more than 15 meters by 2500 (DeConto et al. 2016**)**. The climate central report (2012) showed that global warming more than doubles the odds of severe floods to happen over the coming 18 years.

Rising sea level will increase the likelihood of recurring damaging floods from storm surges and will necessitate the precise assessment of risk related to severe surge storms. Across the country, nearly 5 million people live in 2.6 million houses on land less than 4 feet above high tide (Ben Strauss et al. 2012). This population is at risk in case of flooding without efficient protection and emergency response plan. On the other hand, earth embankment structures (dams and levees) are a main defense line that are used to mitigate flooding damage all over the country. The emerging climate change and sea level rise implies the need for accurate estimation of the probability of exceeding limit states defining distinct levels of structural stability, and its consequences due to storms, surges or flooding. Existing FEMA risk estimation tool (URS, 2007) estimates probabilities of exceeding limit states in a qualitative manner that doesn't necessarily represent structure actual behavior or damage level. Also, it also has no way of taking storm cycles history or soil profile into consideration. This

along with limited allocated nation's budget for remediation, urges the need for development of tools that estimates probabilities in a quantitative way.

Work in this paper evaluates and modifies existing risk tool that was developed for the Federal Emergency Management Agency (FEMA) to be able use it for quantitative, rather than qualitative risk assessment analyses. The Howard A. Hanson (HHD), located on the Green river near Seattle, Washington, is used as a case study to demonstrate such quantitative assessment. The tool considers four failure modes due to the occurrence of flood overtopping, earthquakes, excessive seepage, and normal stability based on observation. The loss of life potential (LLP) is calculated and then combined with the probability of failure (POF) to estimate loss of life risk. An evaluation of existing FEMA tool for risk estimation is performed and a sensitivity analysis is presented and discussed. Also, numerical analysis for the Howard A. Hanson dam (HHD) near Seattle, Washington under cycles of rising and lowering water levels is performed. The numerical analysis results are used along with probabilistic approaches to estimate probability of exceeding predefined limit states of deformation.

### 3.3 Limit states and probability approaches

Traditional factor of safety design doesn't provide a good indication of the performance and stability of earth structures (Duncan, 1991; USACE, 2006). Though, the application of the limit state design (LSD) has increased over the last two decades but it has not been widely used in the dam safety evaluation (Farinha et. al, 2015). For example, Nian et.al (2008) used limit state and limit analysis to analyze the stability of reinforced slopes with piles in anisotropic and nonhomogeneous soils. Konstantakos (2010) discussed ultimate limit state method (ULS)

advantages and limitations for braced excavations design. Farinha et al. (2015) applied the limit state design (LSD) approach to the foundation of a concrete gravity dam with the joint application of the concepts of ultimate limit states and numerical methods. Limit state design has also been used to design cast-in-place piles, drilled shafts and sheet piles (Krabbenhoft et al., 2005). The International Commission of Large Dams (ICOLD, 1988, 1993) are aware of the shortcomings of the overall factory of safety approach and moving forward toward probability approaches.

On the hydrological side of the analyses, the risk analysis is applied to estimate failure probability related to rare events. Foufoula- Georgiou (1989) showed how the exceedance probability of extreme precipitation could be derived and applied to two watersheds in Iowa. Wood (1977) evaluated the overtopping risk for levee by applying the integral transformation approach. Karlsson and Haimes (1988) discussed how mathematical expectation has traditionally been used in solving risk-based problems and that it is no appropriate for decision making that affecting public policy because it conceals extremes by combining events of different magnitudes and probabilities of occurrence. Goodarzi et al. (2012) presented risk and uncertainty analysis to dam overtopping based on univariate and bivariate flood frequency by applying Gumbel logistic distribution. These studies show the growing use of probabilistic approaches and risk towards estimating earth structures adequate functionality and risk under overtopping. There is a lack however in parallel analyses and method development for other failure modes such as piping, seepage, earthquake, overtopping and global stability failure. Calamak et al. (2014) used probabilistic slope stability analyses of earth-fill dams considering hydraulic conductivity, unit weight, cohesion and internal friction angle as random variables

using Monte Carlo simulation method (MCSM). They showed that ignoring the random field of hydraulic conductivity may result in underestimation of reliability indices and probability of failure, though, spatial variation of hydraulic conductivity should also be considered in probabilistic stability analyses. Various approaches in the literature are used for probabilistic slope stability analysis such as First order second moment method (FOSM) (Wu & Kraft, 1970; Cornel, 1971; Alonso, 1976; Tang et al, 1976; Vanmarcke, 1977; Li & Lumb, 1987; Barbosa et al, 1989; Christian et al, 1994; Hassan & Wolff, 1999). With increasing computer capabilities, Monto Carlo simulations are adopted by some researchers (Tobutt, 1982; Husein Malkawi et al., 2000; Griffiths and Fenton, 2004; Cho 2007; Hammah and Yacoub, 2009; Srivastava et al., 2010). Also, numerous studies on probabilistic seepage analysis through earth-fill dams are mentioned in the literature (Fenton & Griffiths, 1996; Ahmed, 2009; Calamak et al, 2012; Cho, 2012; Le et al, 2012; Calamak et al, 2013)

Khalilzad and Gabr (2013, 2011b) proposed a new platform for deformation based limit state analysis for embankment dams. The approach was implemented into simple probabilistic analysis using approach by Duncan (2000). The authors defined performance limit states based on horizontal deformation values at the toe location than can indicate the stability of the embankment. Then the deviatoric shear strain values are correlated to the horizontal deformation on the failure surface. They used a definition for the limit states (LS) and categorized it as follows:

- LS(I): minor deformations, no discernible shear zones, low gradients (i.e. $i < 1$) throughout the embankment dam and foundation, deviatoric shear strain values of 1% or less;

- LS(II): medium (repairable) deformations, limited piping problems (i.e. i > 0.67 within a shallow depth at the location of toe), dispersed plastic zones with moderate strain values, tolerable gradients less than critical; deviatoric shear strain values of 3%;
- LS(III): major deformations, breaches and critical gradients at key locations (i.e. boiling and fine material washing at the location of toe), high strain plastic zones and emerging shear bands, deviatoric shear strain values of 5%.

### 3.4 Earth embankment structures risk estimation

Estimation of risk value for earth embankment structures such as dams and levees, is challenging due to the difficulty in quantifying the probabilities of failure for these structures. Due to the lack of data on current state, soil profiles, and a reliable system to track earth structures performance and maintain inspection through its design life, many of these structures need urgent rehabilitation plan. According to the Association of State Dam Safety Officials (ASDSO), approximately one third of the "high hazard" earth dams are considered deficient in some aspects of their integrity and many are older than 50 years.

Many states have approached this issue using different techniques. Washington State for example has established a semi-quantitate system for dam risk ranking (FEMA tool user manual, 2008). United Research Services Corporation (URS) developed a risk prioritization tool for the Federal Emergency Management Agency (FEMA) to help decision making process for dam rehabilitation. This tool is investigated in this study and used to estimate the risk values for the Howard A. Hanson dam in Seattle, Washington. Advantages and drawbacks for this tool is presented in detail.

### 3.5 FEMA risk prioritization tool

The FEMA risk prioritization tool for dams is a standards-based decision-making tool for risk-based dam safety prioritization meant to be used by state dam safety regulators to identify dams that most urgently need attention. Once a dam has been prioritized, then the risk acceptance is based on state policy. The tool was not meant to judge the dam safety. The tool is quick and easy to implement although it lacks a way to identify probability of failure in a quantitative manner. The risk output depends heavily on the assigned failure modes probability values which is based on observations and engineering judgment. The tool considers four failure modes: flood overtopping, earthquakes, piping, and normal stability. In each column of the tool worksheet, there are bins of descriptors to aid in selecting magnitude of failure probability (F) ranging from 1 to 1 x $10^{-6}$ as shown in Figure 3.1. In addition, there is a column of specific observations which provide clues about which bin might be appropriate. General guidelines in making subjective judgements of failure probability are provided based on Barneich et Al. (1996). The tools calculate the failure consequences as loss of life potential (LLP), the tool prioritizes the dam by plotting LLP versus probability of failure on a risk plot and divide dams into three zones: priority A (urgent action recommended), B (Risk should be reduced in accordance to priorities) and C (diminished need to reduce risk) (Figure 3.2). Work here-in aims at modifying the tool and incorporating a quantitative approach to assign probabilities of exceeding limit states to the existing FEMA risk tool.

FEMA risk tool assigns probabilities of failures based on visual observations, design, construction or maintenance information. Each failure mode is characterized by column of physical observations, geometric details, analysis results and other pertinent information. The

columns are made up of bins with ranges of failure probability corresponding to the noted information about the dam in each bin. It is mentioned in the FEMA tool manual that "If possible, average dam conditions and failure probabilities are described to provide a means to benchmark the user's frame of reference. This allows the evaluation to judge whether this dam is better or worse than the defined average. Since each bin covers 1 to 2 orders of magnitude, relying only on visual observation could lead to a difference of one order of magnitude of probability values. Also, in the bin description, the probability of failure assignment is based on factor of safety criteria along with observations of the condition of the embankment structure. This is also shown in figure 3.1 as the probability of failure. This factor of safety-based probability estimation urges the need for a modified approach to estimate it based on a probabilistic approach taking uncertainty in the soil parameters and storms cycles for the embankment structure.

The piping (Seepage) probability of failure is probably the most difficult mode to assign. The tool uses historical performance method developed by Dr. Mark Foster. According to Foster et al (1998), an average homogeneous earthfill dam with no filters has an annualized probability of piping failure of $2*10^{-4}$. However, if there are known defects, the presence of dispersive clay, observed piping, etc. then the risk levels should be higher. Although, this method has some limitations: it is based on large dams (>15 m height) so it may underestimate the probabilities of failure for smaller dams. Also, as it is based on accidents and failures, so care should be taken in applying probabilities of failure specially at lower ranges.

The flood (overtopping) probability of failure still a challenge to estimate as it depends on the recurrence period of the flood when all that is available is the percentage of the PMF passed

through the spillway. Earthquake probability of failure also requires some analysis on whether liquefaction might be a problem and recurrence interval of the threshold earthquake. Slope stability probability of failure could be estimated if factor of safety analysis is available. The FEMA risk tool manual suggests that if no data is available, user should use conservative approach to assign failure probabilities.

### 3.6 FEMA risk tool drawbacks:

- The use of the risk tool provides an estimate of the probability of failure in a qualitative way that doesn't reflect the soil profile and site conditions of the dam. Also the tool uses factor of safety-based visual observation to estimate probability. The output risk value heavily depends on the assigned values for the failure probabilities. There should be a way to link probability of failure values with the surface deformation of the dam under loading conditions, with the logic being deformation is measurable through in situ or remote sensing surveying.
- The use of the tool doesn't account for the impact of cycles of storms and spatial variability of soil properties on the probability of failure. The guidelines provided in FEMA risk tool estimate the probability of failure based on observations and engineering judgment. A robust approach should consider soil profile properties, geometry variation, and water level cycles and can use statistical and probabilistic approaches to estimate risk value based on probability of exceeding a desired performance limit state.

| OBSERVATIONS | FAILURE MODES | | | |
|---|---|---|---|---|
| | Earthquake [2] ▲ | Flood[1] ○ | Piping ■ | Normal Stability ◇ |
| Significant deformation and transverse cracking<br>Concentrated seepage with turbidity<br>Large slumps<br>Large Trees | Not designed for EQ loading in high hazard area<br>Soils liquefy<br>FS<1.0* in EQ AEP $10^{-1}$ | TFF < $10^{-1}$ | Observed piping of embankment or foundation<br>Erodable / poorly compacted / dry and brittle soils* and Incompatible or Internally unstable soils<br>No filter<br>Unprotected seepage exit with high gradient | FS < 1.0*<br>Slopes steeper than 1.5H:1V<br>High Pore Pressures Very weak foundation |
| Observed deformation and cracking, steep or stepped abutments<br>Significant seepage or wet areas<br>Trees on slope or toe | Loose soils present in fdn or embankment<br>Soils liquefy or FS<1.0* under Operating Basis Earthquake (OBE) | TFF < $10^{-2}$ | | FS < 1.1*<br>Slopes steeper than 2H:1V<br>High phreatic surface<br>Poor foundation |
| Infrequent Inspection<br>(none in last 10 years)<br>Limited Cracking<br>Small Trees<br>Minor Animal Burrows<br>Clear, Consistent Seepage | Marginal soils<br>FS>1.0* under OBE<br>FS<1.0* for Maximum Design Earthquake (MDE) | TFF < 10-3 | Compacted clay core<br>No observed piping<br>Uncertain Filter Compatibility<br>Uncertain Foundation<br>Nonerodible soils<br>Toe Drain<br>Partial Fdn. Cutoff<br>**(Average 2 E-4)** | FS < 1.2*<br>Slopes steeper than 2H:1V<br>Uncertain foundation |
| | | TFF < $10^{-4}$ | | FS < 1.3<br>Slopes steeper than 3H:1V |
| Embankment condition satisfactory confirmed by regular inspection<br>**(Note: with embankment concrete corewall or cutoff wall reduce by one order of magnitude)** | Dense foundation or compacted embankment soils<br>FS>1.1 under MDE | TFF < $10^{-5}$ | No known cracks<br>Modern, fully penetrating filter<br>Full Foundation Cutoff<br>Modern Foundation Treatment | FS > 1.3<br>Regular monitoring Slopes flatter than 3H:1V<br>Good foundation |
| | FS>1.3 under MDE | TFF > PMPDF or Probable Maximum Flood | Wide filter and blanket drain<br>Extensive monitoring | FS > 1.5<br>Regular monitoring |
| Failure Mode F | 1.00E-04 | 1.00E-05 | 1.00E-06 | 1.00E-05 |
| Life Loss Potential | 1 | 2 | 1 | 2 |
| Failure Mode F with Storage | 1.00E-04 | 1.00E-05 | 1.00E-06 | 1.00E-05 |

Notes: (* or unknown)

1. TFF - threshold failure flood flood which overtops sufficent to cause breach
2. Skip earthquake failure mode if in low seismicity area where Maximum Design Earthquake (MDE) pga < 0.1g

Input Required
Ignore if not applicable

**Figure 3.1. FEMA risk tool failure modes estimation table (FEMA risk tool)**

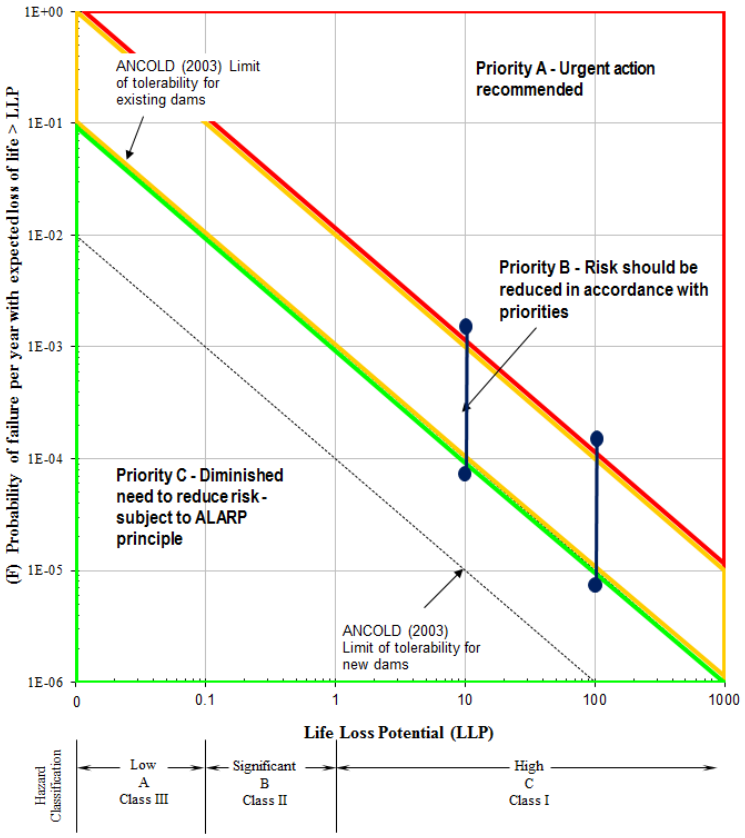


**Figure 3.2. FEMA risk tool risk plot using Loss of life and annual probability of failure (FEMA risk tool)**

### 3.7 FEMA risk tool consequences of failure

The FEMA risk tool considers loss of life potential (LLP) as its consequences of failure. LLP is a critical term in risk assessment for dams, however, methods used for its estimation are highly variable. Flood depth, dam floodplain, time of the day and year, population at risk, warning time, dam spillway capacity and evacuation time are some of the factors that should be considered in estimating LLP. The flood comparison method is implemented in the FEMA tool and it provides an estimate of the loss of life based on the ratio between peak dam

discharges to the 10 year flood discharge ($Q_b/Q_{10}$). It assumes higher fatality rates near the dam than further downstream which gives reasonable values away from the flooding area compared to areas close to the dam. For this work, ($Q_b/Q_{10}$) was estimated to be 10 which gives fatality rate of 0.02 from zero to 3 miles. Having different population at risk (PAR) leads to different loss of life potential values (LLP). The increase of PAR from 500 to 5000 people will change LLP from 10 to 100. These values were used to investigate the effect of changing the probability of failure (POF) for and the resulting risk calculated by the FEMA risk tool on the Howard A. Hanson as explained later.

### 3.8 Case study: Howard A. Hanson Dam (HHD)

The Howard A. Hanson Dam (HHD) is located on the Green river, 21 miles east of Auburn, near Seattle, Washington. The dam is an earthen embankment structure and serves as a flood control along with water supply for the city of Tacoma, Washington. In January 2009, 38 cm (15 inches) of rainfall raised the Howard A. Hanson reservoir level to a record high of 362.4 m (1189 ft.) in comparison with the maximum storage level is 384 m (1260 ft.) This caused some depressions on the right abutment of the dam. The Army Corps of Engineers, Seattle district started controlling the reservoir level and performing remedial measures to the dam to mitigate risk. While the probability of overtopping is reduced, the probability of a critical condition due to through and under seepage, earthquakes or embankment stability is still a possibility. The impact of the probability of occurrence of these potential failure modes on the potential loss of life risk is analyzed herein.

### 3.9 FEMA risk tool sensitivity analysis

A sensitivity analysis is performed to investigate the effect of changing the probability of failure (POF) on the different dam categories and the total risk calculated by the FEMA risk tool. In a study by Eddleston et al. (2006), they performed a comparison between methods used to determine the probability of failure due to internal erosion in embankment dams for 6 dams. They used the Stanford University, University of New South Wales and DEFRA methods which used data from reported dam incidents around the world to access the likelihood of failure for different failure modes. The results showed a wide spread of values for the probability of failure calculation. The difference ranged from between 1.5 and 34 with a mean variation of 9 i.e. nearly an order of magnitude for probability of failure. Figure 3.2 shows a plot of flood probability leading to overtopping, with this probability varied between 1 in 10000 up to 1 in 10, and the associated loss of life potential (LLP) is taken as 10 and 100, corresponding to base and maximum flood, respectively. Increasing the probability of failure from $8*10^{-5}$ to $2*10^{-3}$ for the same LLP of 10 moved the dam from priority (C) zone to priority (A) respectively. Based on the study by Eddleston (2006), different methods could assign probabilities values that vary by one order of magnitude and that can change the risk region where the embankment structures will fall in. Therefore, there is a need for a quantitative way to calculate probability of failure instead of assigning it in a qualitative way based on observations.

A contour plot approach is proposed for the representation of the total risk as a function of the individual probabilities of exceeding a prescribed performance limit state with failure being the ultimate limit state. Total risk is calculated as the sum of the individual probabilities of

failure in terms of loss of life risk. Figures 3.3 through 3.5 shows plots of total risk value contours based on 512 different combinations of seepage and limit state III probability of exceedance, while changing overtopping probability from $1*10^{-1}$ up to $1*10^{-8}$. Earthquake probability of failure is kept constant at $1x10^{-6}$ and LLP is assumed as 2 and 1 for flood and sunny day situations respectively. The X axis (seepage probability of failure), Y axis (probability of exceeding limit state III) in the contour plot have values from $1*10^{-1}$ up to $1*10^{-8}$. Risk values are represented using contours and values are written on the contour lines. In Figure 3.3, there is a large gap between the 0.2 and 0.25 risk contour lines, as the combinations of the two probabilities of failure remains small till it reaches around $4*10^{-2}$ value then it starts to have a major contribution in the contour values. It is noticeable that the risk values are constant for all overtopping probabilities less than $1*10^{-3}$ as shown in Figure 3.5 due to the small contribution of the overtopping probability of failure to the total risk. Although these contour graphs represent a way to estimate risk based on combinations of probability of failure, it still requires a quantitative way to assign probabilities based on deformation of the embankment structures due to storm cycles and soil profile. Point x on the contour plots represents risk based on probabilities of failure for Howard A. Hanson dam calculated using PLAXIS 2D 2016 and probability sheet as will be explained later.

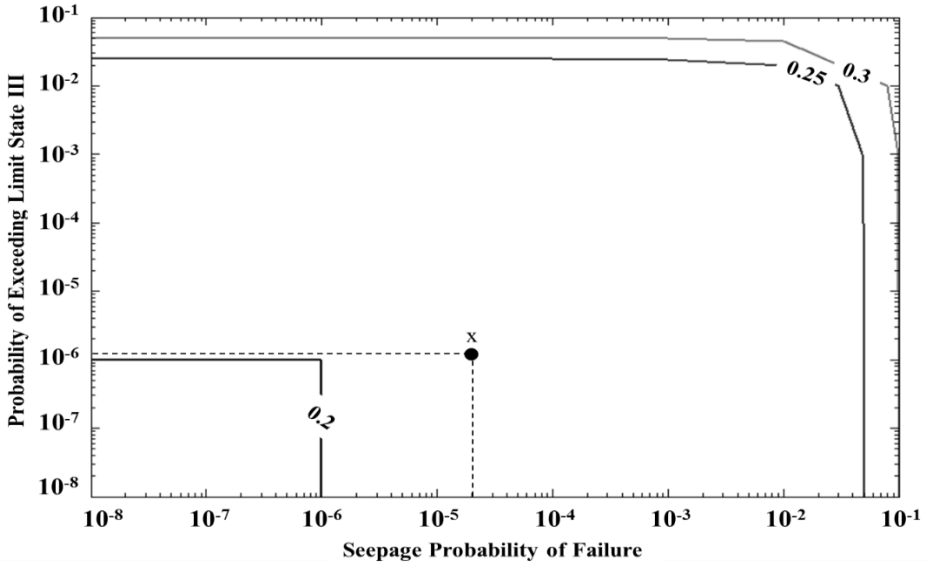


**Figure 3.3. Loss of life risk for combinations of seepage and LSIII probabilities (Overtopping probability of failure = $1*10^{-1}$, Earthquake probability of failure = $1*10^{-6}$)**

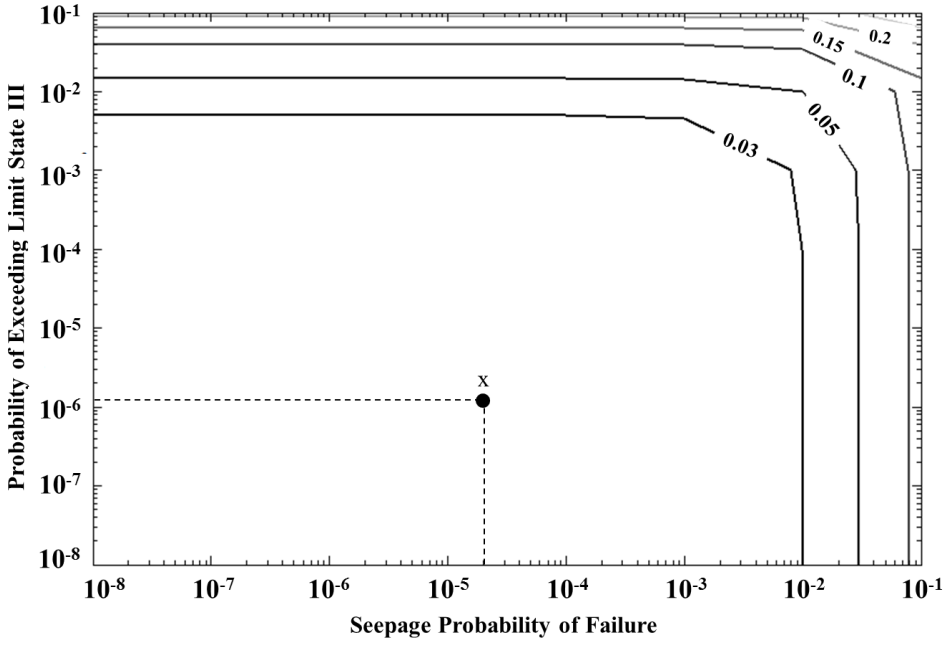


**Figure 3.4. Loss of life risk values for combinations of seepage and LSIII probabilities (Overtopping probability of failure = $1*10^{-2}$, Earthquake probability of failure = $1*10^{-6}$)**

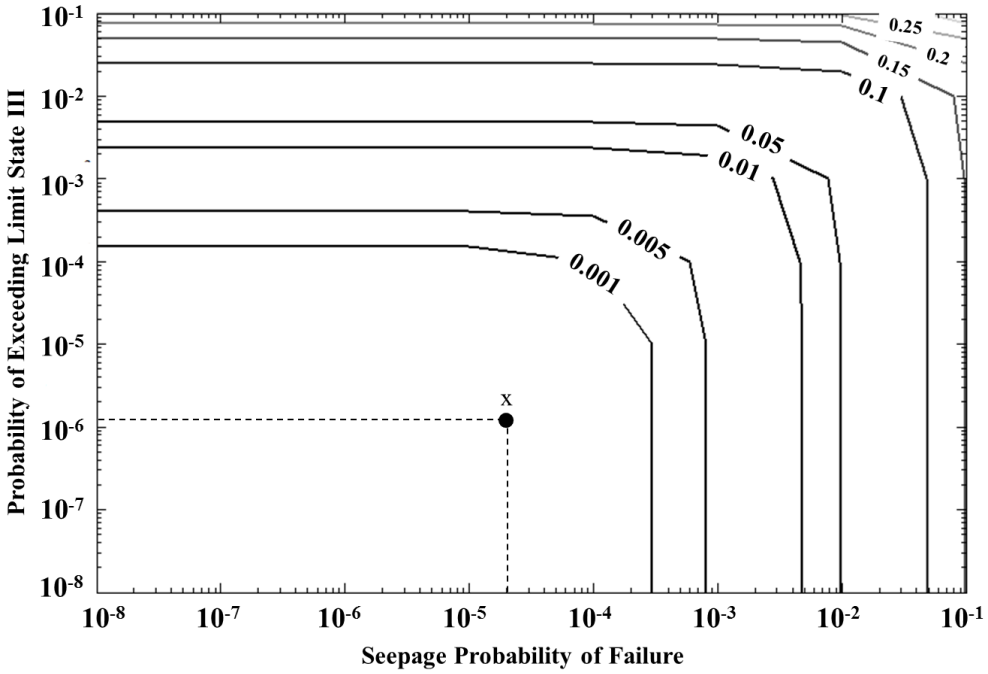


**Figure 3.5. Loss of life risk values for combinations of seepage and LSIII probabilities (Overtopping probability of failure $\leq 1*10^{-3}$, Earthquake probability of failure = $1*10^{-6}$)**

### 3.10 PLAXIS 2D numerical analysis

Analysis of the dam using the finite element program PLAXIS 2D is performed to estimate its probability of exceeding limit states. The variable parameters are assumed to friction angle in the embankment, slope and lower alluvial layer. The dam geometry and soil properties are based on the log and the hydraulic reports by the USACE Seattle district as shown in Table 3.1. The model configuration and meshing are shown in Figure 3.6. Three finite element mesh resolutions were investigated from coarse to fine to very fine mesh. Changing the mesh from coarse to fine, caused a 2% change in displacement at point A, for example. No significant change was observed when using a very fine mesh in comparison to fine mesh, thus a fine 15-

node elements mesh was used with the domain having 1187 soil elements and 9723 nodes as in Figure 3.6.

Boundary conditions for the embankment model includes horizontal and vertical deformations restricted at the bottom boundary of the bedrock layer, hence the bottom of the model. Horizontal deformations only are restricted on the right and left side of the model.

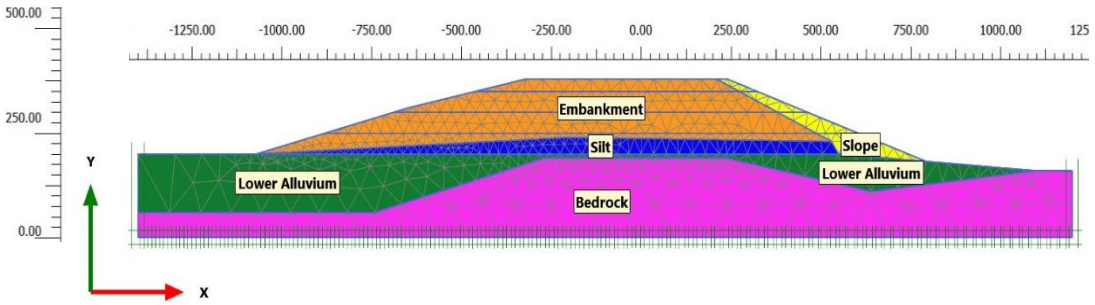


**Figure 3.6. Howard A. Hanson dam model and mesh in PLAXIS 2D**

Flow boundary conditions has a no-flow boundary at the lower boundary of the model and a free-flow boundary at the downstream slope of the embankment. Upstream face of the embankment has either a steady state seepage during "sunny day" where constant head condition is applied, followed by a time-dependent head condition for the rise of water elevation representing the flood cycles conditions.

**Table 3.1. Howard A. Hanson dam soil input parameters***

| Parameter | Embankment | Slope | Silt | Lower Alluvium | Units |
|---|---|---|---|---|---|
| Material model | Hardening soil | Hardening soil | Hardening soil | Hardening soil | - |
| Type of material behavior | Drained | Drained | Drained | Drained | - |
| Soil unit weight below phreatic level, $\gamma_{sat}$ | 21.2 (135) | 21.7 (138) | 120 | 18.8(125) | kN/m$^3$(pcf) |
| Cohesion, $c'_{ref}$ | 0 | 0 | 0 | 0.0 | kN/m$^3$(pcf) |
| Friction angle, $\varphi'$ | 38 | 38 | 30 | 35 | (º) |

* US Army Corps of Engineers report on Howard A. Hanson dam

### 3.11 Modeling phases

The embankment dam is modeled using stage construction phases to simulate embankment construction, sunny day and flood day conditions. 7 Flood cycles are then introduced and deformations and shear strains is measured. The stages used to model the embankment are described as follows:

*1*- **Initial phase:** Geostatic stress state using the $K_o$ procedure (Direct generation of initial effective stresses, pore pressures and state parameters) is generated in the embankment foundations before construction of the embankment.

*2*- **Embankment Construction:** Starting from initial phase, construction of embankment and slope layers by placing it in four layers with the water level assumed at low elevation as the initial phase. In these phases, the undrained behavior was ignored and in each phase, the displacements are reset to zero and small strains is reset to zero.

*3*- **Steady state normal water level:** The water level is raised from its original elevation to the sunny day normal elevation of 355.7 m (1167 ft.) and allow for steady state condition. This calculation was done using plastic calculation type and uses steady state groundwater flow for pore pressure calculations. Steady state groundwater flow calculates flow to determine steady-state pore pressures and phreatic level based on hydraulic conditions.

*4*- **Water level rise to max level:** After reaching a steady state condition and water level is at sunny day elevation, storm situation is simulated by raising the water level to reach maximum elevation of 373.1 m (1224 ft.) (Probable maximum flood, PMF) (1.2 m below crest elevation). This calculation type was selected as a fully coupled flow-

deformation (performs time-dependent analysis of deformation and total pore water pressures). The water level rise was assumed to be with a rate of 0.07 m/hr. (0.23 ft./hr.) with linear head function rise (Average rate observed during hurricane Katrina and Isaac). The time taken to reach the maximum elevation of was 10 days and 8 hours. After reaching this maximum elevation, the water level was maintained at its current level for 12 hours (Observed during hurricane Katrina 2005) and a transit analysis with fully coupled flow-deformation analysis was performed.

5- **Flood cycle effect:** To simulate the flood cycle effect on the embankment, Water level was raised to the max elevation with a linear rate of 0.07 m/hr. (0.23 ft./hr.) and kept there for 12 hours, then lowered to sunny day elevation with a linear rate of 0.04 m/hr. (0.13 ft./hr.). Several cycles are repeated and deformation and shear strain values are monitored. Different water levels for the phases explained are shown in Figure 3.7.

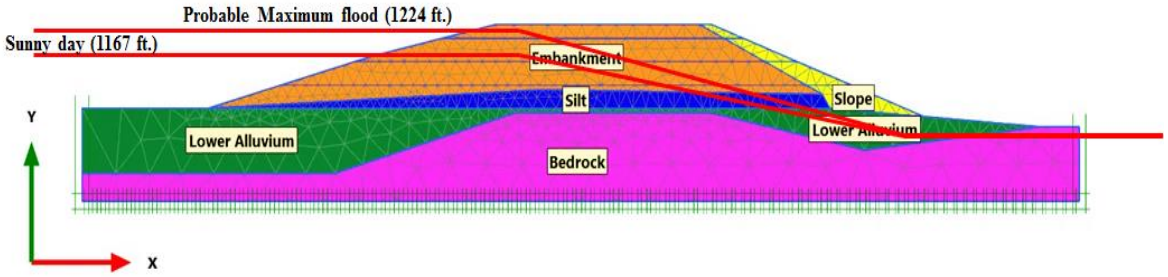


**Figure 3.7. Howard A. Hanson dam water level at different model phases**

## 3.12 Probability of exceeding limit states

To estimate the probability of exceedance for each limit state, an approach similar to Duncan (2000) is employed. Duncan in his paper "*Factors of safety and reliability in geotechnical engineering"* implemented a methodology to estimate standard deviation for a parameter when limited data are available to do so. The variable parameter is the soil friction

angle, φ for Embankment, slope and lower Alluvium layer. Mean value and standard deviation was assigned as shown in Table 3.2 (USACE slope stability report). The finite element model was then processed for the friction angle, one with one standard deviation above the mean and one below the mean. Once shear strains values are obtained for key locations (toe area) in the embankment dam, it is normalized with respect to the predefined limit states. Predefined limit state is taken as three limit states: LSI, LSII and LSIII at 1, 3 and 5% deviatoric strain values respectively as proposed by Khalilzad (2011). Next, the Taylor series Technique (Wolff, 1994; USACE, 1997; 1998) is used to find the standard deviation and coefficient of variation of these normalized values. Then, a reliability index based on lognormal distribution of the normalized deformation is calculated (Duncan, 2000). Hence, the reliability is calculated based on a normal distribution of the reliability index and the probability of exceeding the limit states is estimated. Table 3.2 explains the steps to estimate the probability of exceedance after 6 cycles of loading for the embankment dam. Also, the probability of exceeding limit states with respect to gradient values is estimated using the same technique given values of 0.4, 0.6 and 1 for LS I, II and III gradients. Progression of probability of exceeding limit state I, II and III values is shown in Figure 3.8a with storm cycles. The figure shows that the probability values increases with number of cycles as the shear strain accumulates at the toe location with the storm loading history. Also, it is noticeable going from 5 to 7 cycles, the probability of failure has a lower slope and then almost goes with a constant rate. That is mainly due to the material softening and the strain rate slow decrease due to that softening as shown in Figure 3.8b as shear strain rate tends to decrease as cycles increase from 5 to 7 cycles. Figure 3.8b shows the shear strain value at toe due to friction angle variation in embankment layer.

**Table 3.2. Probability of exceeding limit states calculation after 6 storm cycles**

| **Limit state pertinent to shear strain at Toe ($\gamma_S$)** | | | | | **LSI ($\gamma_{S1}$ = 1%)** | | **LSII ($\gamma_{S2}$ = 3%)** | | **LSIII ($\gamma_{S3}$ = 5%)** | |
|---|---|---|---|---|---|---|---|---|---|---|
| | **E(φ)** | **σ(φ)[1]** | **E(φ)+/- σ(φ)** | **$\gamma_S$ (%)[2]** | **$N_1$= $\gamma_{S1}$/ $\gamma_S$** | **$\Delta N_1$[3]** | **$N_2$= $\gamma_{S2}$/ $\gamma_S$** | **$\Delta N_2$[3]** | **$N_3$= $\gamma_{S3}$/ $\gamma_S$** | **$\Delta N_3$[3]** |
| **Embankment** | 38 | 3.8 | 41.8 | 0.026 | 38.462 | -31.215 | 115.385 | -93.645 | 230.769 | -187.291 |
| | | | 34.2 | 0.138 | 7.246 | | 21.739 | | 43.478 | |
| **Slope** | 38 | 4.2 | 42.2 | 0.102 | 9.804 | -1.257 | 29.412 | -3.771 | 58.824 | -7.541 |
| | | | 33.8 | 0.117 | 8.547 | | 25.641 | | 51.282 | |
| **Lower Alluvium** | 35 | 3.5 | 38.5 | 0.065 | 15.480 | -5.771 | 46.440 | -17.313 | 92.879 | -34.627 |
| | | | 31.5 | 0.103 | 9.709 | | 29.126 | | 58.252 | |
| **Limit state of with the predefined limit states** | | | | | **LSI** | | **LSII** | | **LSIII** | |
| Notations: | | | **Standard deviation[4]** | | 15.885 | | 47.654 | | 95.307 | |
| E=Expected value of parameter | | | **Mean($\mu_{\Delta N}$) [5]** | | 14.875 | | 44.624 | | 89.247 | |
| σ=Standard deviation of parameter | | | **C.O.V.($V_{\Delta N}$) [6]** | | 1.068 | | 1.068 | | 1.068 | |
| LSI=Limit State (1) | | | **Beta (β)[7]** | | 2.659 | | 3.918 | | 4.712 | |
| R=Reliability | | | **R=Φ(β)[8]** | | 0.996076 | | 0.999955 | | 0.99999878 | |
| P(E)=Probability of exceeding limit state | | | **P(E)=1-R[9]** | | **$3.92*10^{-3}$** | | **$4.5*10^{-5}$** | | **$1.2*10^{-6}$** | |

[1] σ: Standard deviation of parameter

[2] $\gamma_S$: Shear strain values measured from PLAXIS finite element analysis for the parameter proposed value.

[3] ΔN: Difference in the normalized values of shear strain with respect to the predefined limit states

[4] $\sigma_{\Delta N}$: Standard deviation of ΔN's using the Taylor series $\sigma_{\Delta N} = \sqrt{\left(\frac{\Delta N_1}{2}\right)^2_{Embankment} + \left(\frac{\Delta N_1}{2}\right)^2_{Slope} + \left(\frac{\Delta N_1}{2}\right)^2_{Lower\ Alluvium}}$ (Wolff, 1994; USACE1997)

[5] $\mu_{\Delta N}$: Mean value for normalized shear strain values.

[6] $V_{\Delta N}$: Coefficient of variation for mean and standard deviation of normalized values. $V_{\Delta N1} = \frac{\sigma_{\Delta N}}{\mu_{\Delta N}}$

[7] $\beta_{ln}$: lognormal distributed reliability index. $\beta_{ln} = \frac{ln\left\{(\mu_{\Delta N})\left(\sqrt{1+(V_{\Delta N}{}^2)}\right)\right\}}{\sqrt{1+(V_{\Delta N}{}^2)}}$ (Duncan, 2000)

[8] R: Reliability value based on normal distribution of the reliability index (Duncan, 2000) $R = \text{NORMSDIST}(\beta_{ln})$

[9] P(E): Probability of exceeding limit state. $P(E) = 1 - R$

The probability of exceeding limits states is calculated based on the values of shear strain at the toe from the three soil layers' friction angles. Point x on the contour plot (Figures 3.3 through 3.5) shows the risk value for the HHD with probability of exceeding limit state III of $1.2*10^{-6}$ and $2*10^{-5}$ for stability and seepage respectively. The seepage probability of exceeding limit state was estimated using gradient values. Point x shows a loss of life risk value ranging from less than 0.001 to around 0.25 for an overtopping probability of failure form $1*10^{-1}$ to $1*10^{-8}$. It should be noted that the risk value is based on loss of life potential of 2 and 1 for flood and sunny day and earthquake probability of failure of $1*10^{-6}$. For zero to 2 cycles, the values for probabilities of exceeding limit states is very small and close to zero which makes it hard to plot it on Figure 3.8a. Any values lower than $1*10^{-14}$ were not plotted on the graph.

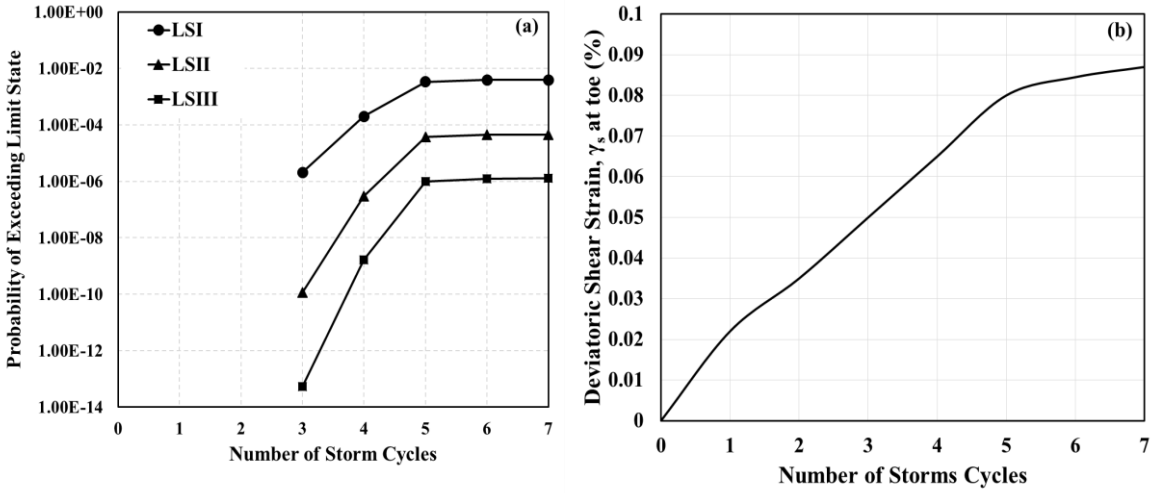


**Figure 3.8 a) Effect of storm cycles on probability of exceeding limit states for Howard A. Hanson dam b) deviatoric shear strain at toe with storm cycles**

### 3.13 Summary and conclusions

An approach is presented herein to show an expedient procedure of quantifying the probabilities of exceeding limit states using numerical analyses coupled with simple probabilistic model. The FEMA risk tool doesn't have a quantitative way of assigning probabilities of exceeding limit states. That quantitative methodology allows for representation of the structure geometry, soil conditions and storm cycle history. Contour plots is proposed to estimate risk based on assumption for earthquake probability of failure and loss of life potential. The HHD has been analyzed to show the effect of POF on the total risk value using the FEMA risk tool. Based on the results presented in this study, it can be concluded that:

1. Numerical analysis of the Howard A. Hanson dam (HHD) showed a probability of exceeding LSI of $3.9*10^{-3}$, LSII of $4.5*10^{-5}$ and LSIII of $1.2*10^{-6}$ for normal stability, and $2*10^{-5}$ for seepage after 6 cycles. Also, increasing storm cycles increased the probability of exceeding LSI from $2*10^{-6}$ to $3.9*10^{-3}$, LSII from $1.2*10^{-10}$ to $4.5*10^{-5}$, LSIII from $5.3*10^{-14}$ to $1.2*10^{-6}$ going from 3 to 6 cycles respectively. Also, due to material softening, the rate of increase from 5 to 7 cycles has a lower slope than going from 3 to 5 cycles as shear strain rate becomes lower and reaches almost a constant rate.
2. Using the contour plot approach and implementing the probabilities of exceeding limit state III for Howard A. Hanson dam, a loss of life risk values ranging from less than 0.001 to around 0.25 for an overtopping probability of failure form $1*10^{-1}$ to $1*10^{-8}$ (Point x on the contour plot) were estimated. It should be noted that the risk value is based on loss of life potential of 2 and 1 for flood and sunny day respectively,

population at risk of 100 people and earthquake probability of failure of $1*10^{-6}$. These contour plots can be used along with quantitative calculation of probabilities of failure using PLAXIS 2D numerical analysis to estimate risk value.

3. Using the FEMA tool for analysis of the HHD and increasing the probability of failure from $8*10^{-5}$ to $2*10^{-3}$ for the same LLP of 10 moved the dam from priority (C) zone to priority (A) respectively. Different methods assign probabilities values that vary by one order of magnitude (Eddleston, 2006). This change the structure hazard classification and urges the need for a quantitative way to calculate probability of failure instead of assigning it in a qualitative way based on observations and engineering judgment.

**References**


*1.* Ahmed, A. A. (2009). Stochastic analysis of free surface flow through earth dams. *Computers and Geotechnics, 36(7),* 1186-1190.

*2.* Allison, I., et al. (2009). The Copenhagen diagnosis: Updating the world on the latest climate science. *Climate Change Research Centre (CCRC), Univ. of New South Wales, Sydney, Australia*.

3. Alonso, E. E. (1976). Risk analysis of slopes and its application to slopes in Canadian sensitive clays. *Geotechnique, 26,* 453-472.

4. Barbosa, M. R., Morris, D. V. and Sarma, S. K. (1989). Factor of safety and probability of failure of rockfill embankments. *Géotechnique, 39(3),* 471-483.

5. Barneich et al. (1996). The reliability analysis of a major dam project. uncertainty in geologic environment from theory to practice. *Geotechnical Special Publication, 2,* 58.
6. Ben Strauss, Claudia Tebaldi and Remik Ziemlinski. (2012). Sea level rise, storms and global warming's threat to the US coast: A Climate Central Report. *Surging Seas.*
7. Calamak, M., Kentel, E. and Yanmaz, A. M. (2012). Seepage analysis through earth-fill dams having random fields. *10th International Congress on Advances in Civil Engineering, Ankara, Turkey,* 97.
8. Calamak, M., Kentel, E. and Yanmaz, A. M. (2013). Spatial variability in seepage flow through earth-fill dams. *Canadian Dam Association 2013 Annual Conference, Montreal, Quebec, Canada, 37.*
9. Calamak, M. and Yanmaz, A. M. (2014). Probabilistic assessment of slope stability for earth-fill dams having random soil parameters. *5th International Symposium on Hydraulic Structures Brisbane, Australia.*
10. Cho, S.E. (2007). Effects of spatial variability of soil properties on slope stability. *Engineering Geology, 92(3–4),* 97-109.
11. Cho, S.E. (2012). Probabilistic analysis of seepage that considers the spatial variability of permeability for an embankment on soil foundation. *Engineering Geology, 133–134(0),* 30-39.
12. Christian, J., Ladd, C. and Baecher, G. (1994). Reliability applied to slope stability analysis. *Journal of Geotechnical Engineering, 120(12),* 2180-2207.

13. Cornell, C. A. (1971). First-order uncertainty analysis of soils deformation and stability. *Proceedings of the 1st International Conference on Application of Statistics and Probability to Soil and Structural Engineering, Hong Kong,* 130-143.
14. DeConto, R. and Pollard, D. (2016). Contribution of Antarctica to past and future sea-level rise. *Nature.*
15. Department of Homeland Security (2011). Methods for estimating loss of life resulting from dam failure. *Dams Sector report.*
16. Duncan, J. M. and Tan, C. K. (1991). Settlement of Footings on Sands: Accuracy and Reliability. *Geotechnical Engineering Congress, ASCE, 1,* 446-455.
17. Duncan, J. M. (2000). Factors of safety and reliability in geotechnical engineering. *Journal of Geotechnical and Geoenvironmental Engineering, 126,* 307-316.
18. Eddleston, M. W. H. and Carter, I. C. (2006). Comparison of methods used to determine the probability of failure due to internal erosion in embankment dams. *Improvements in reservoir construction, operation and maintenance, Thomas Telford, London.*
19. Farinha, M. L., Caldeira, L. and Maranha das Neves, E. (2015). Limit state design approach for the safety evaluation of the foundations of concrete gravity dams. *Structure and Infrastructure Engineering, 11,* 1306-1322.
20. Fenton, G. A. and Griffiths, D. V. (1996). Statistics of free surface flow through stochastic earth dam. *Journal of Geotechnical Engineering, 122(6),* 427-436.

21. Foster, M., Fell, R and Spannagle M. (1998). Risk assessment, estimating the probability of failure of embankment dams by piping. *ANCOLD 98 Conference on dams.*

22. Foufoula G. E. (1989). A probabilistic storm transposition approach for estimating exceedance probabilities of extreme precipitation depths. *Water Resource Research, 25,* 799-815.

23. Goodarzi, E., Mirzaei, M. and Ziaei, M. (2012). Evaluation of dam overtopping risk based on univariate and bivariate flood frequency analyses. *Canadian Journal of Civil Engineering, 39 (4).*

24. Griffiths, D. and Fenton, G. (2004). Probabilistic slope stability analysis by finite elements. *Journal of Geotechnical and Geoenvironmental Engineering, 130(5),* 507-518.

*25.* Hammah, R. E. and Yacoub, T. E. (2009). Probabilistic slope analysis with the finite element method. *43rd US Rock Mechanics Symposium and 4th U.S. Canada Rock Mechanics Symposium, Asheville, NC, United States.*

26. Hassan, A. and Wolff, T. (1999). Search algorithm for minimum reliability index of earth slopes. *Journal of Geotechnical and Geoenvironmental Engineering, 125(4),* 301-308.

27. Husein Malkawi, A. I., Hassan, W. F. and Abdulla, F. A. (2000). Uncertainty and reliability analysis applied to slope stability. *Structural Safety, 22(2),* 161-187.

28. International Commission on Large Dams. (1988). Dam design criteria. The philosophy of their selection. *Bulletin 61*.

29. International Commission on Large Dams. (1993). Rock foundations for dams. *Bulletin 88*.

30. Karlsson, P. O. and Haimes Y. Y. (1988a). Risk-based analysis of extreme events. *Water Resource Research, 24(1),* 9-20.

31. Khalilzad, M. and Gabr, M. A. (2011). Deformation-Based Limit States for Earth Embankments. *ASCE Conference Proceeding*. 3639-48.

32. Khalilzad, M., Gabr, M. A.; Hynes, M.E. (2015). Deformation-Based Limit State Analysis of Embankment Dams Including Geometry and Water Level Effects. *International Journal of Geomechanics, 15 (5),* 0401-4086.

33. Konstantakos, D. C. (2010). Advantages and limitations of ultimate limit state design methods for braced excavations. *Geotechnical Special Publication, 384 (208),* 818-825.

34. Li, K. S. and Lumb, P. (1987). Probabilistic design of slopes. *Canadian Geotechnical Journal, 24,* 520-31.

35. Nian, T. K., Chen, G. Q., Luan, M. T., Yang, Q., Zheng, D. F. (2008). Limit analysis of the stability of slopes reinforced with piles against landslide in nonhomogeneous and anisotropic soils. *Canadian Geotechnical Journal. 45(8),* 1092-1103.

36. Overpeck, J. T., Otto-Bliesner, B. L., Miller, G. H., Muhs, D. R., Alley, R. B. and Kiehl, J. T. (2006). Paleoclimatic evidence for future ice-sheet instability and rapid sea-level rise. *Science, 311,* 1747-1750.

37. Peters, G. P., et al. (2013). The challenge to keep global warming below 2°C. *National Climate Change, 3,* 4-6.

*38.* Risk Prioritization Tool for Dams User's manual (2008); *prepared for the Federal Emergency Management Agency (FEMA).*

39. Srivastava, A., Babu, G. L. S. and Haldar, S. (2010). Influence of spatial variability of permeability property on steady state seepage flow and slope stability analysis. *Engineering Geology, 110(3-4),* 93- 101.

40. Tang, W. H., Yucemen, M. S. and Ang, A. S. (1976). Probability-based short term design of soil slopes. *Canadian Geotechnical Journal, 13,* 201-215.

41. Titus, J. G., Park, R. A., Leatherman, S. P., Weggel, J. R., Greene, M. S., Mausel, P. W., Brown, S., Gaunt, C., Trehan, M. and Yohe, G. (1991). Greenhouse effect and sea level rise: the cost of holding back the sea. *Coastal Management, 19(2),* 171-204.

42. Tobutt, D. C. (1982). Monte Carlo simulation methods for slope stability. *Computers & Geosciences, 8(2),* 199-208.

*43.* U.S. Army Corps of Engineers. (1997). Engineering and design introduction to probability and reliability methods for use in geotechnical engineering. *Engr. Tech. Letter No. 1110-2-547, Department of the Army, Washington, D.C.*

*44.* U.S. Army Corps of Engineers. (1998). Risk-based analysis in geotechnical engineering for support of planning studies. *Engrg. Circular No. 1110-2-554, Department of the Army, Washington, D.C.*

45. US Army Corps of Engineers (USACE). (2006). Reliability analysis and risk assessment for seepage and slope stability failure modes for embankment dams. *ETL 1110-2-561.*

46. United States Department of the Interior, Bureau of Reclamation (2003). Guidelines for achieving public protection in dam safety decision making.

47. Vanmarcke, E. H. (1977). Probabilistic modeling of soil profiles. *Journal of Geotechnical Engineering, 103,* 1227-1246.

48. Wolff, T. F. (1994). Evaluating the reliability of existing levees. *Report Research Project: Reliability of existing levees, prepared for U.S. Army Engineer Waterways Experiment Station Geotechnical Laboratory, Vicksburg, Miss.*

49. Wood, E. F. (1977). An analysis of flood levee reliability. *Water Resources Research, 13,* 665-671.

50. Wu, T. H. and Kraft, L. M. (1970). Safety analysis of slopes. *Journal of Soil Mechanics and Foundation Division, 96, 609-630.*

51. Wu, S. Y., Najjar, R. and Siewert, J. (2009). Potential impacts of sea-level rise on the mid- and upper Atlantic region of the United States. *Climate Change, 95,* 121–38.

# CHAPTER 4. DEVELOPMENT OF RISK ESTIMATOR TOOL FOR EMBANKMENT STRUCTURES (REES) USING COUPLED NUMERICAL-PROBABILISTIC APPROACH AND ARTIFICIAL NEURAL NETWROK

## 4.1 Abstract

Earth embankment structures (i.e. levees and dams) plays a critical role during extreme flooding and storm events. Given the nation's deteriorated state of these structures and the shortage in rehabilitation fund, there is a clear need for accurate evaluation of stability and functionality level of these types of structures for better condition assessment. Although probabilistic and reliability analysis techniques are widely used within the geotechnical community, risk estimation tools that implements coupled numerical probabilistic approaches are lacking in the literature. Therefore, work here-in presents a new risk estimation tool for embankment structures that uses coupled numerical probabilistic approach and artificial neural networks. REES (Risk Estimator for Embankment Structures) is developed with MATLAB graphical user interface (GUI) to implement the finite element program PLAXIS 2D results. 363 case runs with PLAXIS 2D are used to train and test the tool. The trained neural network showed a regression values of $R^2$ of 0.98, 0.97 and 0.98 for the training, validation and testing data respectively. Performance of the REES tool to testing cases showed a close trend between predicted and calculated numerical shear strains. A parametric study on the effect of geometry, embankment, foundation and alluvial soil parameters and cycles of loading is performed and its results is discussed. Embankment side slopes and foundation permeability has the most effect on the shear strain values at toe. The developed REES tool allows for a robust and easy estimation of probabilities of exceeding limit states to help with the decision-making process and presents a promising advancement in the risk tools within the geotechnical community. It also eliminates the need for performing sophisticated finite element analysis to estimate the risk probabilities. As more data becomes available, fine-tuning of the REES tool could be

performed to enhance the tool prediction accuracy. Explanation of the tool components and MATLAB code is provided for REES in Appendix C.

## 4.2 Introduction

Earth embankment structures such as levees and dams play a key role during extreme flooding events as well as during normal operating conditions. In addition to providing flood protection, these structures serve as a key-part of our critical civil infrastructure as they are also used for water storage and hydropower generation. According to the Association of State Dam Safety Officials, approximately one third of the "high hazard" earth dams are considered deficient in some aspects of their integrity and many are older than 50 years. ASCE reported that the 5-year funds needed for rehabilitation and upgrade of these structures are on the order of $12.5 billion but what are allocated nationwide is only $5.05 billion. Therefore, there is a clear need for accurate evaluation of stability and functionality level of these types of structures for condition assessment as well as cost effective specification and implementation of the remedial actions. Given the short fall of $7.45 billion in rehabilitation funds, the development of better condition assessment and efficient specification of rehabilitation approaches will have a positive impact on the welfare and safety of the communities served by these types of structures, and contribute to our nation's security and economic wellbeing.

The emerging need for evaluation of stability and functionality levels of earth structures rises from the frequent failures and the limited fund available for rehabilitation. New approaches that uses probabilistic and reliability analysis should become familiar inside the practical geotechnical community to allow decision-makers in allocating expenditure for such

structure's rehabilitation. Also, simple tools for estimating risk that facilitate engineering decision-making process is not common in the literature. More efforts should be taken to develop such tool. The research here applies coupled numerical probabilistic approaches to estimate probabilities of failure for earth embankment structures and develop a simple tool using MATLAB and Artificial Neural Network (ANN) approach to aid in the decision-making process.

### 4.3 Artificial Neural Networks

Artificial neural networks are soft computational approaches that try to simulate the decision process of the human brain nerve system. ANN can offer a simple platform for solving complex problems and can also learn and predict outcomes using training set of data. Artificial neural network has a set of simple units called neurons which send signals between each other and depends on a number of weighted connections. Any neural network consists of input units, activation functions, connection between units, external input (or bias) and learning rule (Rumelhart and McCleland, 1986). Figure 4.1 shows a typical arrangement of an artificial neuron. If enough training data is available, we can use it to train the network and get a reasonable approximation for outcomes. MATLAB has an artificial neural network toolbox that is used in this work to train an ANN network and then build a GUI (graphical user interface) for a risk estimation tool structure. More details is explained later.

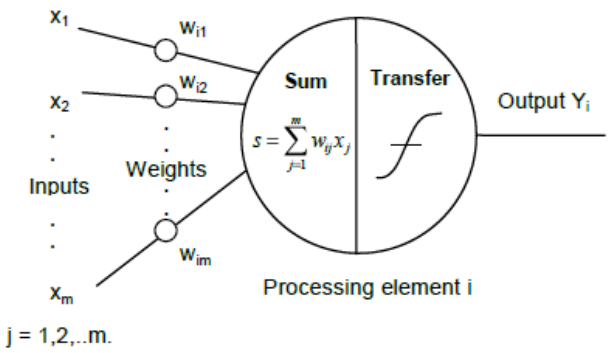


**Figure 4.1. Typical arrangement of an artificial neuron (JongKoo Jeon, 2007)**

### 4.4 PLAXIS 2D model description

To train a risk tool using Artificial Neural Network (ANN) approach. A base model with the geometry shown in Figure 4.2 is used. Cases with varying embankment height, side slope, crest width and soil properties were performed in PLAXIS 2D 2016. All these parameters were kept constant during each case while treating Elastic modulus, $E_{50}$, of the embankment layer as random variable with mean and standard deviation calculated using the three-sigma rule. 121 cases were analyzed, having three runs for each case to vary the random variable by one standard deviation below the mean and one plus the mean for the Embankment layer (total of 363 embankment finite element models). The output results were used to train the ANN and construct the risk tool.

### 4.5 Analyses of parameters

Soil parameters (i.e. Effective friction angle, φ', effective cohesion, c', saturated unit weight, $\gamma_{sat}$, elastic modulus, $E_{50}$, and coefficient of permeability, κ) are varied randomly to cover a wide range of geometry and layers possibilities. Reasonable upper and lower values ranges have been assumed based on literature as in Table 4.2a. Then, a probability distribution is assumed for each parameter as suggested by literature as summarized in Table 4.1. As

summarized by Lacasse and Nadim (1996), most of the soil parameters can be assumed to have a normal distribution function except for clay undrained shear strength and permeability which tend to follow log-normal distribution. The three-sigma rule (which states that 99.73% of the data will fall within a three-standard deviation around the mean value) was used to estimate standard deviation values for each parameter. Other embankment structures geometry parameters (i.e. Embankment height, upstream and downstream slopes, crest width) are assumed based on a normal distribution function with ranges shown in Table 4.2b.

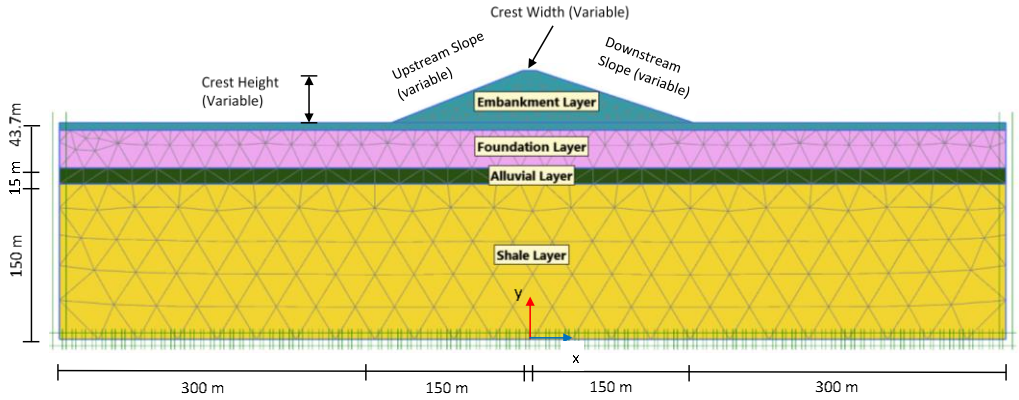


**Figure 4.2. PLAXIS 2D base model with variable parameters**

**Table 4.1. Soil parameters suggested probability distribution from literature**

| Property | Symbol (Units) | Soil type | probability distribution | Reference |
|---|---|---|---|---|
| Moisture content | $W_n$ (%) | All soils | Normal | 1, 3, 4 |
| Unit Weight | $\gamma$, $\gamma_d$, $\gamma_b$ (kN/m3) | | Normal | 1, 2, 3, 4 |
| Relative density | $D_r$ (%) | | Normal | 1 |
| Specific gravity | $G_s$ | | Normal | 3 |
| Degree of saturation | S (%) | | Normal | 3 |
| Liquid limit | LL (%) | Clay | Normal | 1, 2, 4 |
| Plastic limit | PL (%) | | Normal | 1, 2, 4 |
| Plasticity index | PI (%) | | Normal | 1 |
| Friction angle | $\varphi$ ($^o$) | Sand | Normal | 1, 2, 3, 4 |
| Undrained shear strength | $S_u$ (kPa) | Clay | Log-normal | 2 |
| Hydraulic conductivity | k (cm/s) | All soils | Log-normal | 5, 6, 7 |
| (1) Phoon and Kulhawy (1999), (2) Lacasse and Nadim (1996), (3) Harr (1987)<br>(4) Kulhawy (1992), (5) Benson (1993), (6) Bogardi et al (1989), (7) Freeze (1975) | | | | |

**Table 4.2a. Embankment soil parameters ranges and statistical parameters**

| Parameter | Sand | | | Clay | | | Silt | | |
|---|---|---|---|---|---|---|---|---|---|
| | Range | μ | σ | Range | μ | σ | Range | μ | σ |
| φ' (º)[1] | 27-38 | 32.5 | 1.83 | 18-30 | 24 | 2 | 26-30 | 28 | 0.67 |
| | 38-42 | 40 | 0.67 | 30-38 | 34 | 1.33 | 30-36 | 33 | 1 |
| | 42-45 | 43.5 | 0.50 | | | | | | |
| c' (kPa)[2] | 0 | 0 | 0 | 0-13 | 6.5 | 2.17 | 0-5 | 2.5 | 0.83 |
| | 0 | 0 | 0 | 13-26 | 19.5 | 2.17 | 5-10 | 7.5 | 0.83 |
| | 0 | 0 | 0 | | | | | | |
| $\rho_{sat}$ (kN/m$^3$)[1] | 19.3-21.2 | 20.3 | 0.03 | 13.9-17.7 | 15.8 | 0.06 | 13.8-17.6 | 15.7 | 0.06 |
| | 21.2-22.5 | 21.9 | 0.02 | 17.7-21.6 | 19.7 | 0.07 | 17.6-21.3 | 19.4 | 0.06 |
| | 22.5-24.3 | 23.4 | 0.03 | | | | | | |
| k (cm/s)[3] | $1*10^{-3}$- $2*10^{-1}$ | $1*10^{-1}$ | $3*10^{-2}$ | $2*10^{-9}$-$1*10^{-5}$ | $5*10^{-6}$ | $1.67*10^{-6}$ | $1*10^{-8}$-$1*10^{-6}$ | $5*10^{-7}$ | $1.65*10^{-7}$ |
| | $1*10^{-3}$- $2*10^{-1}$ | $1*10^{-1}$ | $3*10^{-2}$ | $2*10^{-10}$-$4*10^{-6}$ | $2*10^{-6}$ | $6.67*10^{-7}$ | $1*10^{-8}$-$1*10^{-4}$ | $5*10^{-5}$ | $1.67*10^{-5}$ |
| | $1*10^{-3}$- $2*10^{-1}$ | $1*10^{-1}$ | $3*10^{-2}$ | | | | | | |
| $E_{50}$ (kPa)[4] | $1*10^4$-$2.5*10^4$ | $1.75*10^4$ | 2500 | $5*10^3$-$2.5*10^4$ | $1.5*10^4$ | $3.33*10^3$ | $2*10^3$-$1*10^4$ | $6*10^3$ | $1.3*10^3$ |
| | $2.5*10^4$-$5*10^4$ | $3.75*10^4$ | $4.17*10^3$ | $1.5*10^4$-$5*10^4$ | $3.25*10^4$ | $5.8*10^3$ | $1*10^4$-$2*10^4$ | $1.5*10^4$ | $1.6*10^3$ |
| | $5*10^4$-$8.1*10^4$ | $6.55*10^4$ | $5.17*10^3$ | | | | | | |

[1]Holtz and Kovacs. (2011). "An Introduction to Geotechnical Engineering" 2nd Edition. Pearson Publishing- Figure 12.15

[2]Mesri et al. (1993). "Cohesion Intercept in Effective Stress-Stability Analysis" Journal of Geotechnical Engineering, 119(8): 1229-1249

[3]Lamb and Whitman (1969). "Soil Mechanics" Figure 19.5

[4]Bowles (1997). "Foundation Analysis and Design" 5th Edition. The McGraw-Hill Companies Publishing. Table 2-8

**Table 4.2b. Embankment geometry parameters ranges and statistical parameters**

| Parameter | Dam | | | Levee | | |
|---|---|---|---|---|---|---|
| | Range | μ | σ | Range | μ | σ |
| Crest Width (m) | 2-20 | 11 | 3 | 1.6-2.4 | 2 | 0.13 |
| Crest Height (m) | 20-100 | 60 | 13.33 | 2-5.2 | 3.6 | 0.53 |
| Upstream& Downstream slope (V:H) | 2:1- 4:1 | 3:1 | - | 2:1- 4:1 | 3:1 | - |

### 4.6 Parameters randomization

To cover a wide range of parameters to train the ANN tool, geometry and embankment parameters were randomized using MATLAB randomization function based on each parameter's assumed distribution. Then, probability distribution plots are generated to confirm that the selected values follow the assumed distribution. This randomization procedure insures that generalization within the assumed range could be achieved. To check the randomization effect of selecting different random sets for the friction angle of all assumed soil types and the difference between the output means, a one-way ANOVA analysis was conducted using MATLAB (Appendix B). The resulting p value was equal to 0.9496 > 0.05, which shows that there is no statistical significant difference between the means at 5% significance level.

### 4.7 Storm hydrograph and duration

Storms varies in intensity and duration throughout the nation. To determine a representative storm cycle for the research study analysis, hydrographs of two major hurricanes in the US history are investigated and presented. The hydrographs for Hurricane Katrina (2005) and Hurricane Isaac (2012) are shown in Figures 4.3a and b. The average rates of 0.07 and 0.04 m/hr for rate of rise and drawdown respectively was estimated using the hydrograph data. A storm duration of 12 hr is used in the analysis as shown in Table 4.3.

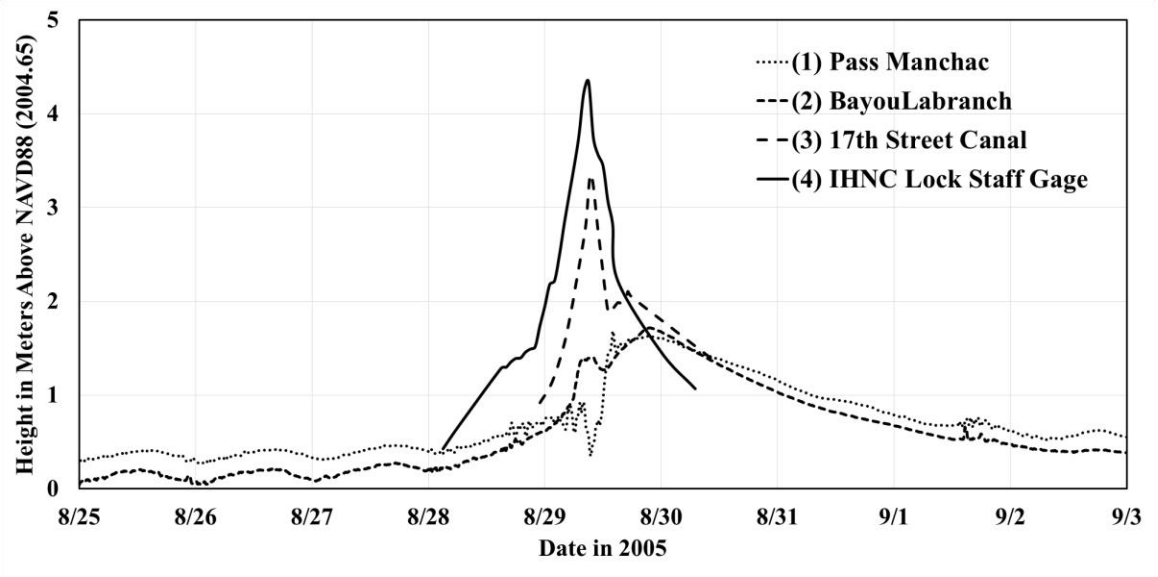


**Figure 4.3a. Hurricane Katrina (2005) hydrograph at various locations in New Orleans (Bunya et al. 2010)**

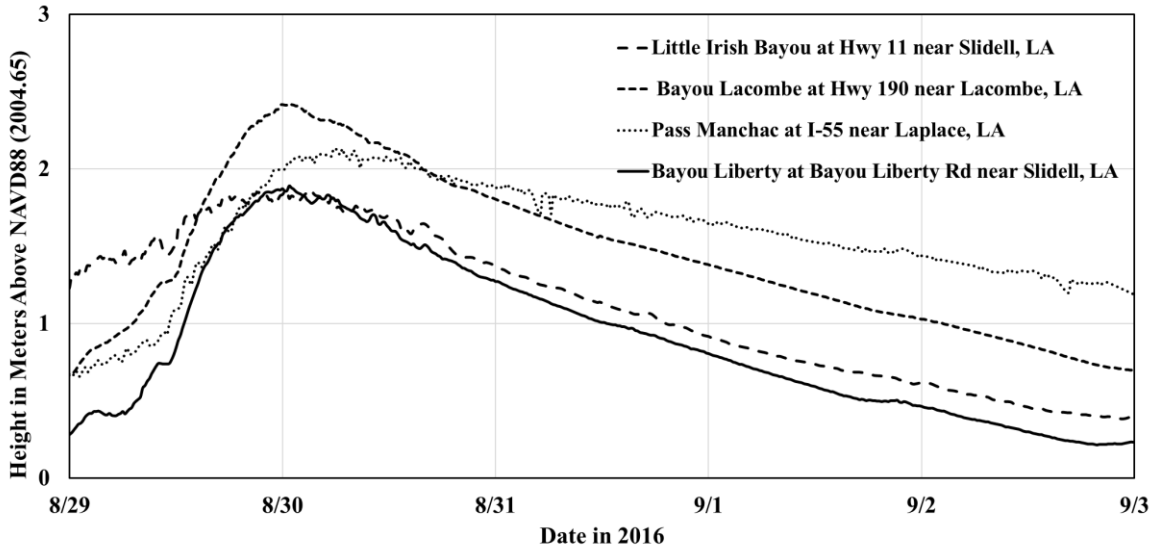


**Figure 4.3b. Hurricane Isaac (2012) hydrograph at various locations in State of Louisiana (Dietrich et al. 2012)**

**Table 4.3. Rate of rise, drawdown and storm duration for Hurricane Katrina and Isaac**

| Hurricane Katrina (2005) | | | |
|---|---|---|---|
| **Location** | **rate of rise (m/hr)** | **rate of drawdown (m/hr)** | **Storm duration (hr)** |
| Pass Manchac | 0.01 | 0.01 | 12 |
| Bayou LaBranche | 0.01 | 0.01 | 2 |
| 17th Street Canal | 0.20 | 0.08 | 1 |
| IHNC LockStaff Gage | 0.13 | 0.14 | 1 |
| **Hurricane Isaac (2012)** | | | |
| Little Irish Bayou at Hwy 11 near Slidell, LA | 0.04 | 0.02 | 1 |
| Bayou Lacombe at Hwy 190 near Lacombe, LA | 0.05 | 0.02 | 1 |
| Pass Manchac at I-55 near Laplace, LA | 0.04 | 0.01 | 11 |
| Bayou Liberty at Bayou Liberty Rd near Slidell, LA | 0.05 | 0.02 | 2 |
| | **0.07 m/hr** | **0.04 m/hr** | |

## 4.8 Number of cases (samples)

The required number of samples to cover a certain population is a key question in this study. Two methods are used to estimate the number of required samples. Robert Krejcie (1970) uses equation 4.1 based on Chi-Square distribution table to estimate number of samples which gives number of samples of 96 samples.

$$n = \frac{\chi^2 * N * p * (1-p)}{(e^2 * (N-1)) + (\chi^2 * p * (1-p)}$$ Equation (4.1)

Where:

$\chi^2$: Chi-Square table value for 1 degree of freedom at the confidence level of 95% (3.841)

$N$: Population size (assumed to be 84,000 based on ASCE report, 2013)

P: proportion (assumed value of 0.5 since this would provide the maximum sample size)

e: margin of error of 10%

Another method from Research Advisors (2006) estimated the required number of samples for desired confidence levels and variable margin of error and population size. Assuming margin of error of 10% at confidence level of 95% and a population level of

84,000 yields number of samples of 96 as well. 108 cases of combinations have been selected as shown in Figure 4.4 with assumed soil types for embankment, foundation and alluvial layers. Embankment layer was assumed to be only silt or clay while having the foundation and alluvial layer to be sand, silt or clay. Number of cases were assumed to be 6 for each possibility to give it equal chances of happening and to exceed the total number of cases required.

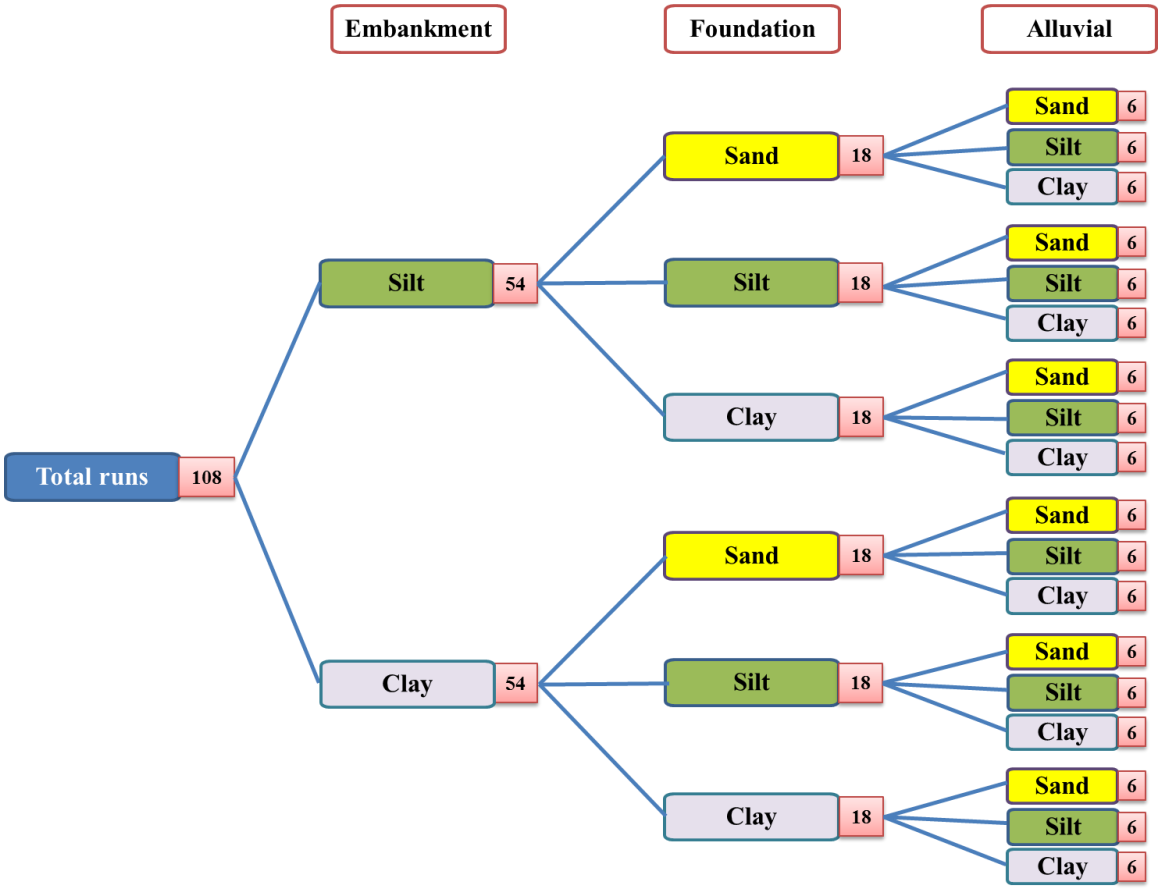


**Figure 4.4. PLAXIS 2D study cases combinations**

Appendix A shows the combinations used for the parametric study with the randomly assumed values for soil properties. Cases are numbered A, B and C having 3 runs for each case. Case B corresponds to the one with the mean value and A with one standard deviation above mean and C with one below. Various parameters for each case is shown along with output horizontal deformation and shear strain at toe location.

### 4.9 Probabilities of exceeding limit states calculation

To find the probability of exceedance for each limit state, an approach like Duncan (2000) is employed. Duncan in his paper "*Factors of safety and reliability in geotechnical engineering"* implemented a methodology to estimate standard deviation for a parameter when limited data are available to do so. Given the limited data available to define standard deviation for earth embankment structures, the three-sigma rule is used in this study to estimate the standard deviation for parameters of the embankment soil layers assuming the highest and lowest value based on literature while mean values was introduced to the model. The finite element model was then processed for each parameter, one with one standard deviation above the mean and one below the mean. Once shear strain values are obtained for key locations (toe area) in the embankment dam, it is normalized with respect to the predefined limit states. Predefined limit state is taken as three limit states: LSI, LSII and LSIII at 1, 3 and 5% deviatoric strain values respectively as proposed by Khalilzad (2011). The corresponding deformation value to the limit states deviatoric strain is exported from the finite element program PLAXIS and the output deformation values is normalized with respect to it. Next, the Taylor series the Taylor Series Technique (Wolff, 1994; USACE, 1997; 1999) is used to find the standard

deviation and coefficient of variation of these normalized values. Then, a reliability index based on lognormal distribution of the normalized deformation is calculated (Duncan, 2000). Hence, the reliability is calculated based on a normal distribution of the reliability index and the probability of exceeding the limit states is estimated. Table A-2 (Appendix) explains the steps to estimate the probability of exceedance with an illustrative example run from the finite element program PLAXIS along with all the equations used for estimation of these parameters.

## 4.10 Parametric study

An embankment base model is selected to perform a parametric study to study the effect of geometry, soil parameters and loading cycle effect on the shear strain. The embankment geometry has properties from case number 30 in Appendix A. Effect of upstream and downstream side slopes, embankment, foundation and alluvial soil properties and cycles of loading on the deviatoric shear strain is investigated and results are discussed and presented as follows. The loading and rates of rise and drawdown follows the same steps as explained earlier in sections 4.4 through 4.7 for the average of hurricane Katrina and Isaac. Water elevations, geometry dimensions and meshing is shown in Figure 4.5

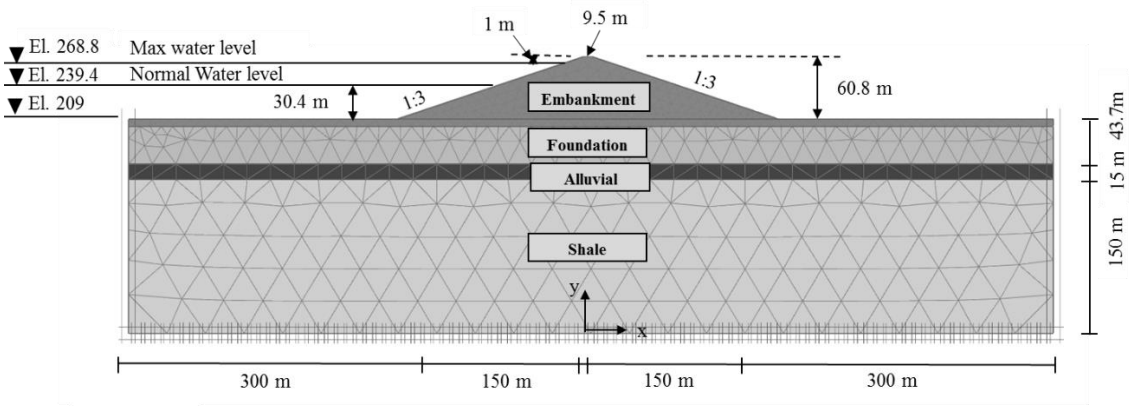


**Figure 4.5. Embankment base model for parametric study**

### 4.10.1 Effect of upstream and downstream side slopes

The effect of the embankment upstream and downstream slopes magnitudes on the strain levels is investigated using the geometry of the base case. Three side slopes (Horizontal: Vertical):, 2:1, 3:1 and 4:1 are modeled and its effects on the deviatoric strain parameter are presented. All other geometry and soil parameters are kept at its original values only changing the upstream and downstream side slopes. Figure 4.6a through f shows side slopes effect for one loading cycle.

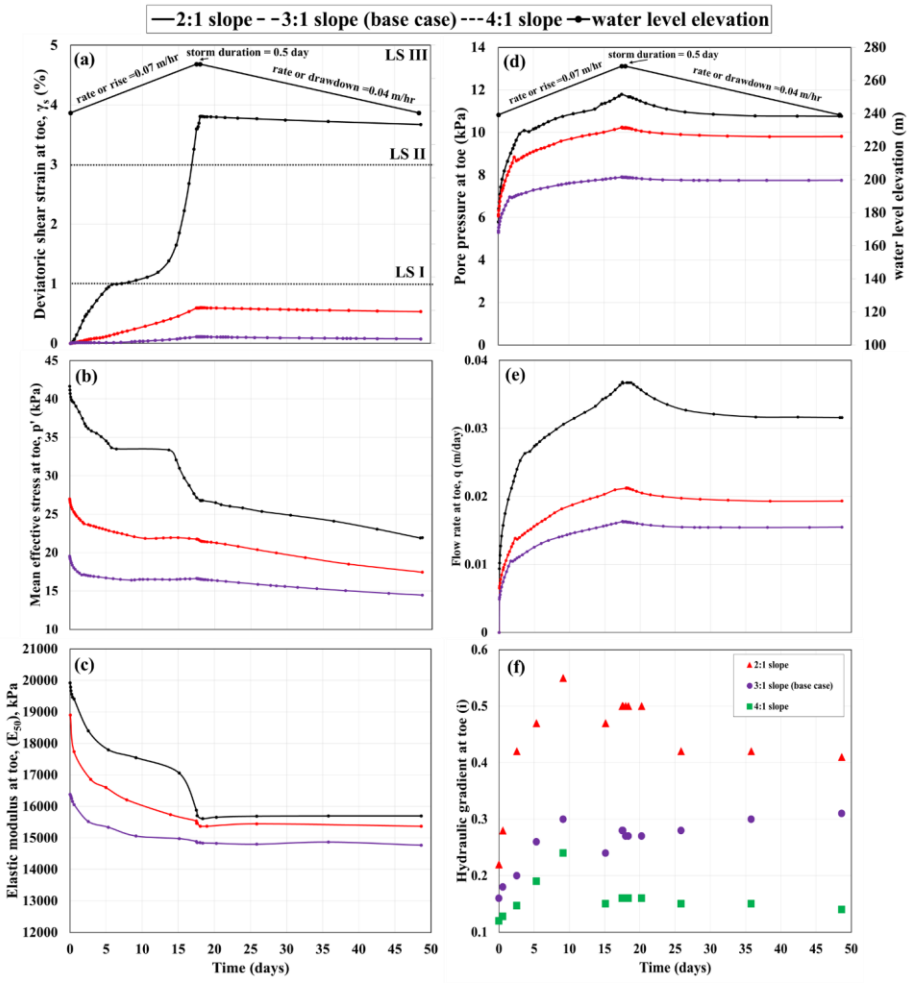


**Figure 4.6. Effect of side slopes on a) deviatoric shear strain b) mean effective stress c) Elastic modulus d) pore pressure e) flow and f) hydraulic gradient at toe location**

Figure 4.6a shows the state of deviatoric strain at toe with time and LSI, LSII and LSIII. The water level elevation in the embankment with time is also shown. From zero to 5 days, there is sharp increase in the shear strain for the 2:1 slope compared to the 3:1 and 4:1 slopes (Figure 4.6a). This can be explained by the higher mean effective stress at toe (Figure 4.6b) due to the higher overburden pressure for steeper slope, also the large decrease in the elastic modulus at toe from 20000 to 18000 kPa during that period (Figure 4.6c). Pore pressure increase is shown in Figure 4.6d where the 2:1 case shows higher values than the other two cases. Also, the flow at toe plays a significant role as has a significant amount of around 0.027 m/day in the first 5 days (Figure 4.6e). The hydraulic gradient values are higher as well for the 2:1 case to reach 0.5 compared with 0.27 and 0.2 for the 3:1 and 4:1 cases (Figure 4.6f). These results show the high contribution from flow and pore pressure to the strain at toe for the steeper slope embankment.

As water rise keeps going with time, going from 5 to 15 days, the shear strain for the 2:1 case stays constant for a while then starts increasing with a higher rate. This could be attributed to the constant value for the mean effective stress shown and the different rate of decrease for elastic modulus. Also, the hydraulic gradient values tend to increase and then decrease during that time to show that shear strain rate of increase will be slower. Towards the end of the water rise phase (i.e. 17.5 days), the shear strain at toe keeps increasing to its max value exceeding LSII for the 2:1 case while keeping it under LSI for both 3:1 and 4:1 cases. The sharp increase in the shear strain for 2:1 cases is due to the sharp decrease in the mean effective stress and the elastic modulus as well. The flow kept increasing for that period to reach a max value of 0.035 m/day. The hydraulic gradient value is increasing as well to reach 0.5 during that time. As the

storm duration is 0.5 day of sustaining water level at the higher elevation, there is a slight change in shear strain, mean effective stress, elastic modulus at toe. This brief period didn't allow the excess pore pressure to dissipate quickly, that's why there is a slight decrease in pore pressure, flow and hydraulic gradient at toe. After that, from 18 days up to the end of the time as water level drawdown, there is a slight decrease in the shear strain at toe for the three cases. Excess pore pressure will begin to dissipate with time, decreasing the flow rate and the hydraulic gradient values to lower values. Also, the elastic modulus will start to gain a little bit of its value or stay constant during that phase. At time of 30 days, going from 4:1 to 3:1 to 2:1 increase the shear strain value from 0.1 to 0.5 to 3.8% exceeding LSI and LSII. The hydraulic gradient value also increased to be 0.42 versus 0.26 and 0.15 for the 3:1 and 4:1 case. These results show that as slope gets steeper, the effect of the flow and pore pressure is higher and causes higher hydraulic gradient at toe. Figure 4.7 shows the phreatic water level inside the embankment for the three slope cases at 15 days. It shows that with steeper stope, the water level rises quickly inside the embankment causing the pore pressure and flow effect to be greater at the toe area.

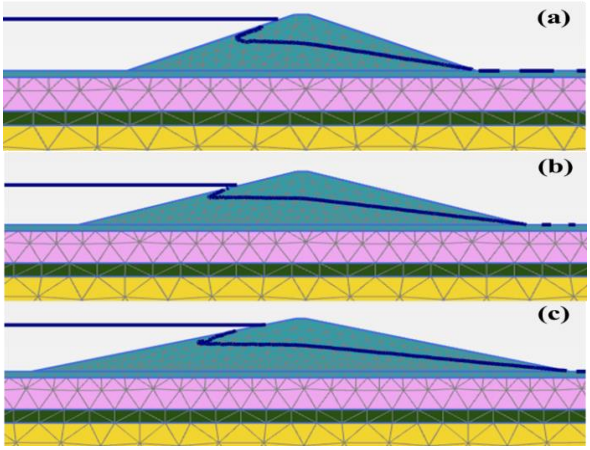


**Figure 4.7. Phreatic level for a) 2:1 b) 3:1 and c) 4:1 slope at 15 days**

### 4.10.2 Effect of friction angle

The effect of the embankment, foundation and alluvial layer friction angle (φ) on the strain levels is investigated using the geometry of the base case. Values of friction angle were assumed to have values of 25$^o$, 33$^o$ (base case) and 36$^o$. Figure 4.8a through f shows the effect for embankment friction angle for one cycle of loading. Results shows that the deviatoric shear strain for the case of 25$^o$ has the highest value that exceeds LS I at around 10 days. This was due to the low elastic modulus that the embankment soil started with that corresponds to that low friction angle. The initial elastic modulus was 10000 kPa compared to 15000 kPa and 20000 kPa for the friction angles of 33 and 36$^o$ (Figure 4.8c). Also, the decrease in the mean effective stress was noticeable in the case of friction angle of 25$^o$ which explains the sharp increase in the deviatoric shear strain in the time from zero to 17.5 days (Figure 4.8b). Flow and pore pressure at toe was similar as the phreatic surface follows the same path inside the embankment as the friction angle won't have an effect on flow and pore pressure(Figures 4.8d, e). Another analysis for the foundation and alluvial friction angles showed that they have a slight effect on the deviatoric shear strain values at toe.

Decreasing the friction angle of embankment from 36$^o$ to 25$^o$ caused an increase from 0.5 to 2.4 % for deviatoric shear strain, which is an increase by a factor of 4.8. The hydraulic gradient is almost the same for times during the whole period for the three-friction angle case (Figure 4.8f). This shows that the friction angle has a smaller effect than side slopes and mainly are due the different value of the initial elastic modulus that was assigned to the model corresponding to each friction angle value.

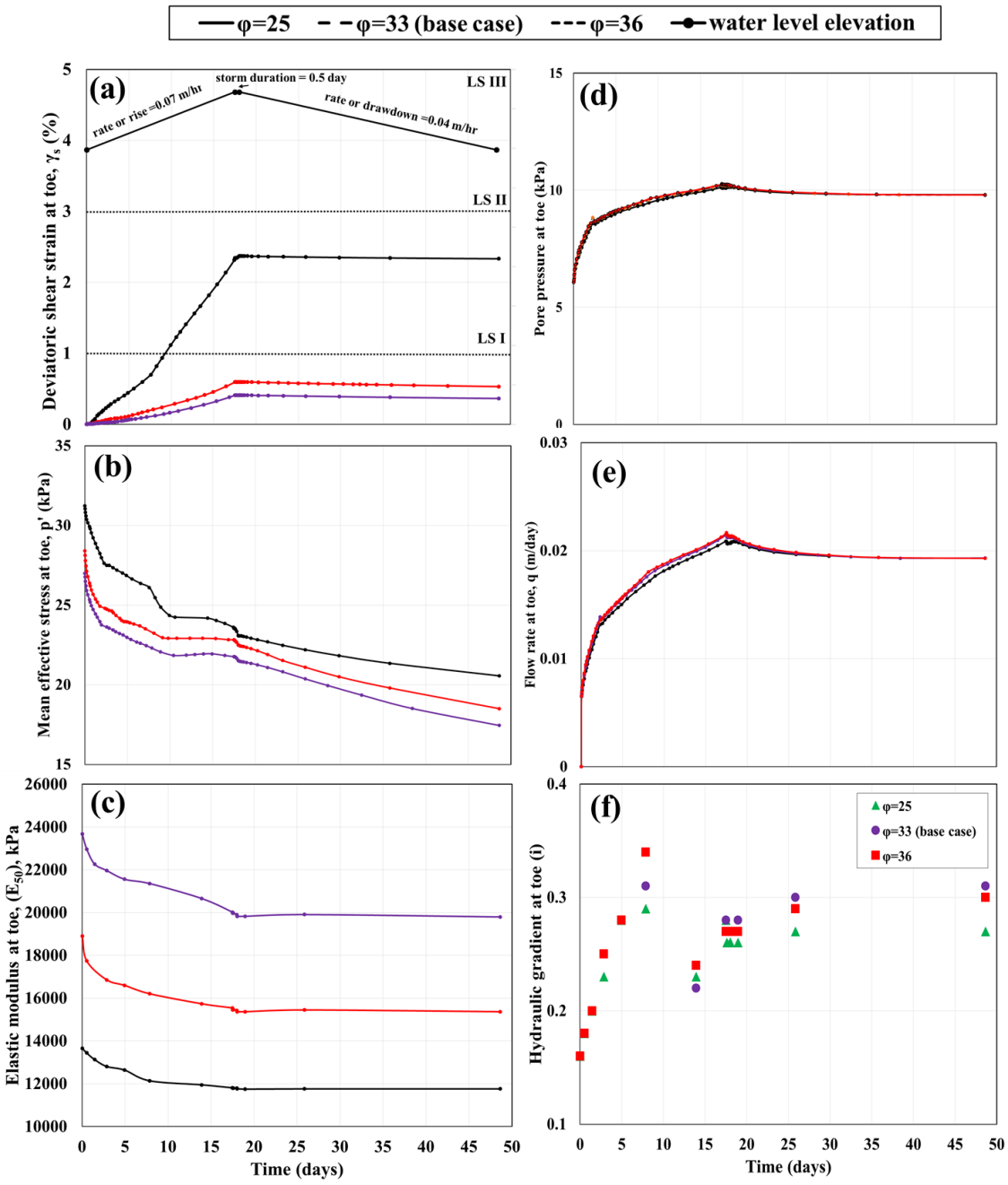


**Figure 4.8. Effect of embankment friction angle on a) deviatoric shear strain b) mean effective stress c) Elastic modulus d) pore pressure e) flow and f) hydraulic gradient at toe location**

### 4.10.3 Effect of permeability

The effect of the embankment, foundation and alluvial layer permeability (k) on the strain levels is investigated using the geometry of the base case. Values of permeability were assumed to be $1*10^{-3}$, $4.8*10^{-5}$ (base case) and $1*10^{-4}$ for embankment layer. For foundation layer, $1*10^{-3}$, $6.8*10^{-5}$ (base case) and $1*10^{-4}$. For alluvial layer, $1*10^{-3}$, $4.5*10^{-5}$ (base case) and $1*10^{-4}$. Figure 4.9 shows the effect of changing permeability for embankment and alluvial layer on the deviatoric shear strain at toe for one storm cycle for the embankment. They had a slight effect on the shear strain value at toe. Investigation of the effect of foundation permeability on the shear strain response at tor location resulted that it has higher effect on the shear strain than embankment and alluvial permeability. Figure 4.10a through f shows that effect on various parameters at the toe.

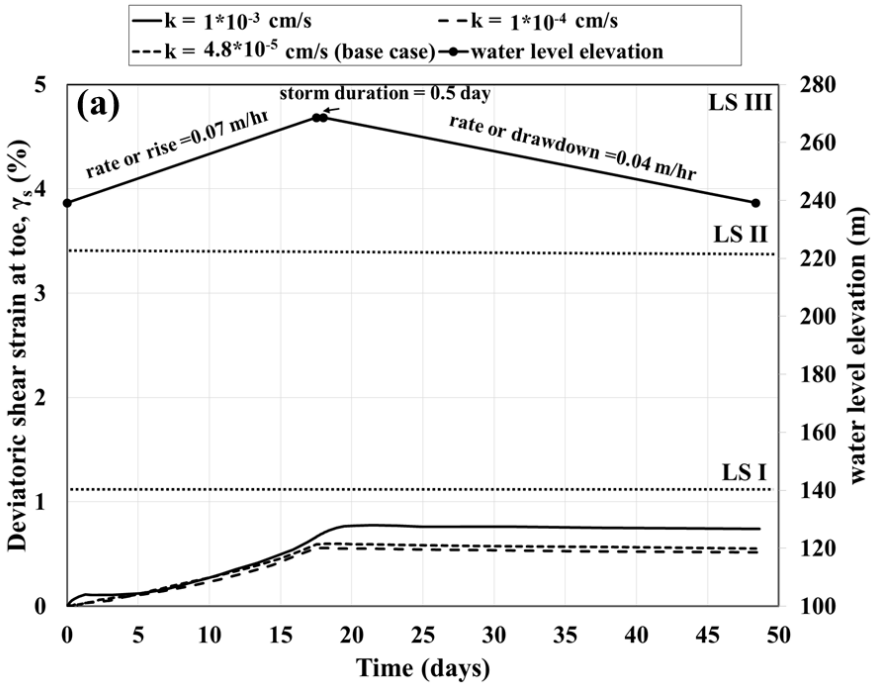


**Figure 4.9a. Effect of embankment permeability on the deviatoric shear strain at toe location**

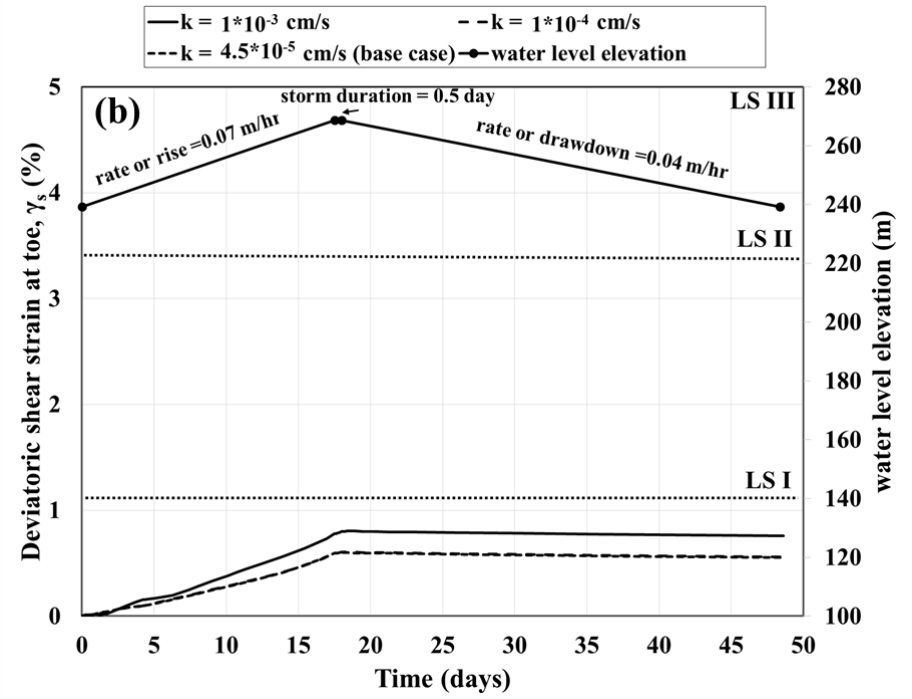


**Figure 4.9b. Effect of alluvial permeability on the deviatoric shear strain at toe location**

Changing the foundation permeability from $6.8*10^{-5}$ to $1*10^{-3}$ caused significant increase in the shear strain at toe to exceed LSI and LSII and it keeps increasing not reaching a steady state even after water drawdown (Figure 4.10a). Also, the elastic modulus at toe and the mean effective stress has a sharp decrease during water level rise and storm duration but the decrease is minimal once drawdown begins (Figure 4.10b and c). The foundation layer with higher permeability acts as a drainage layer for the embankment, causing more deformation to happen at toe during water rise. Pore pressure also will increase at toe location as the foundation permeability allows the water to rise faster inside the embankment. From the results, pore pressure are higher during water level rise up, also flow and hydraulic gradient at toe (Figure 4.10d, e and f). Once drawdown stage begins, the dissipation in pore pressure and flow are sharp as the drainage effect of the foundation begins. During that phase, the shear strain keeps

increasing even with the pore pressure dissipation as the hydraulic gradient at the end of the storm cycles has a high value around 0.48. This value of gradient and shear strain will accumulate for the next cycle to have shear strain to exceed LSIII.

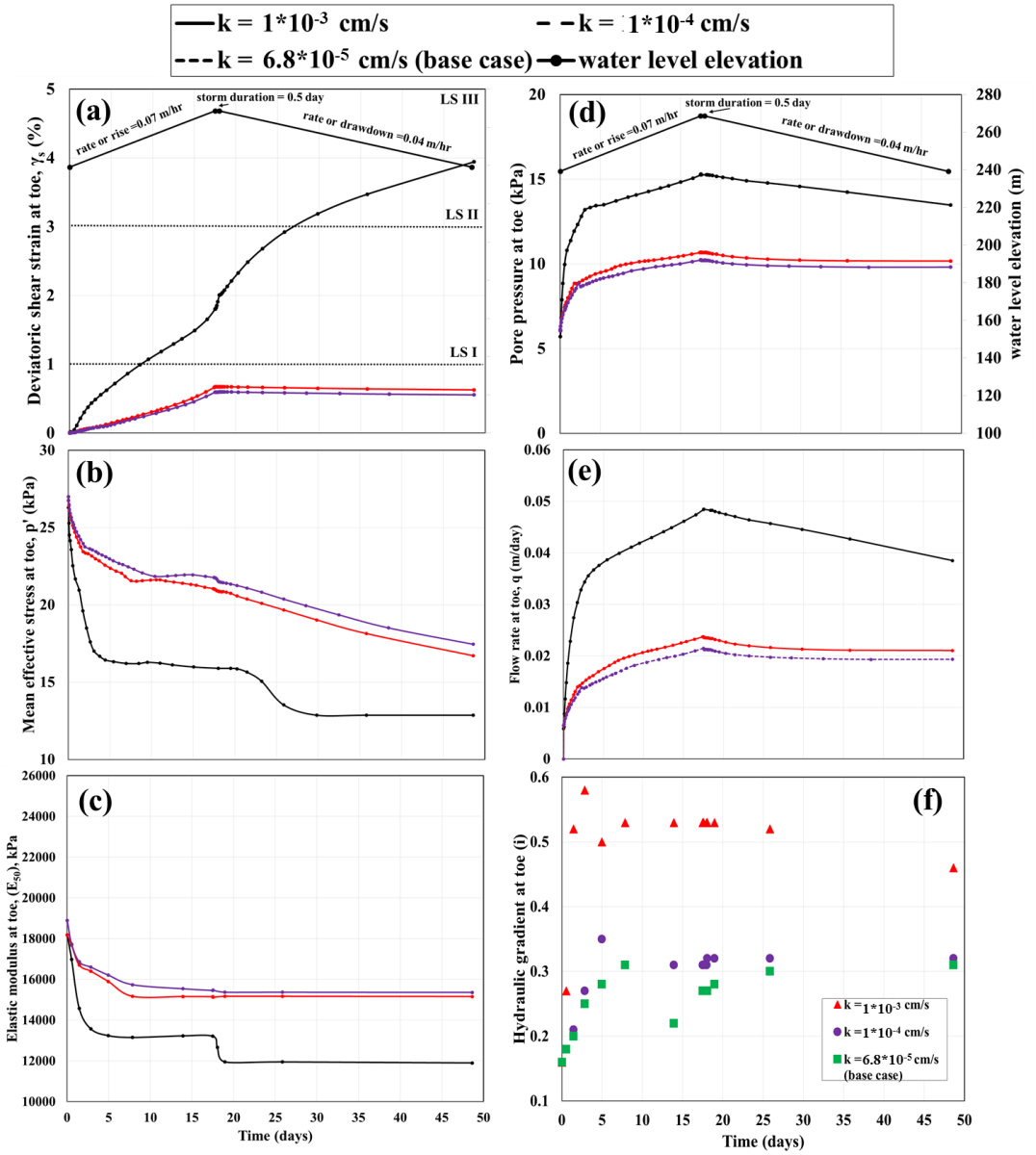


**Figure 4.10. Effect of foundation permeability on a) deviatoric shear strain b) mean effective stress c) Elastic modulus d) pore pressure e) flow and f) hydraulic gradient at toe location**

### 4.10.4 Effect of cycles of water level rise and drawdown

The effect of the cycles of loading or storm cycles is investigated using the geometry of the base case. The storm cycle includes water level rise from the mid-height level with a rate of 0.07 m/hr., to an elevation of 1 m below crest. Then, keeping water at that elevation for 12 hrs to represent the storm duration. Then, water level drawdown with a rate of 0.04 m/hr to the mid-height water level, and a plastic phase for 90 days. These rates and duration are incorporated from two hurricanes Katrina and Isaac as explained before. Cycles of loading are increased up to 6 cycles. Figure 4.11 shows the deviatoric shear strain at toe with time and cycles of loading along with the storm cycles water level elevation.

As more cycles is introduced, deformation and deviatoric strain values increases at toe as shear strain accumulates and shear band grows in each cycle. Shear strain increased from 0.58 to 5.8 % going from 1 to 6 cycles, this is a factor of increase of 10. This also increases the probability of exceeding limit states and move its value from LS I up to LS III. It is noticeable from figure 4.11 that having a plastic phase (no loading phase allowing water level to reach steady state) between cycles doesn't change the shear strain value. Having longer periods between storms will not affect the shear strain value at toe and it will keep accumulating as new storms is introduced later. This analysis confirms that it is crucial to take the embankment storm loading history into account with time as it affects the probability of the structure to exceed limit states and has an increasing deformation that may lead to failure. Stark and Duncan (1991) made a similar observation in relation to the forensic analyses of the failure occurred at the St. Luis dam in California. Also, having longer or shorter duration between storms will not affect the shear strain value and it will keep accumulating as new storms is

present. Figure 4.12 shows the shear bands in the embankment as it grows during cycles of loading

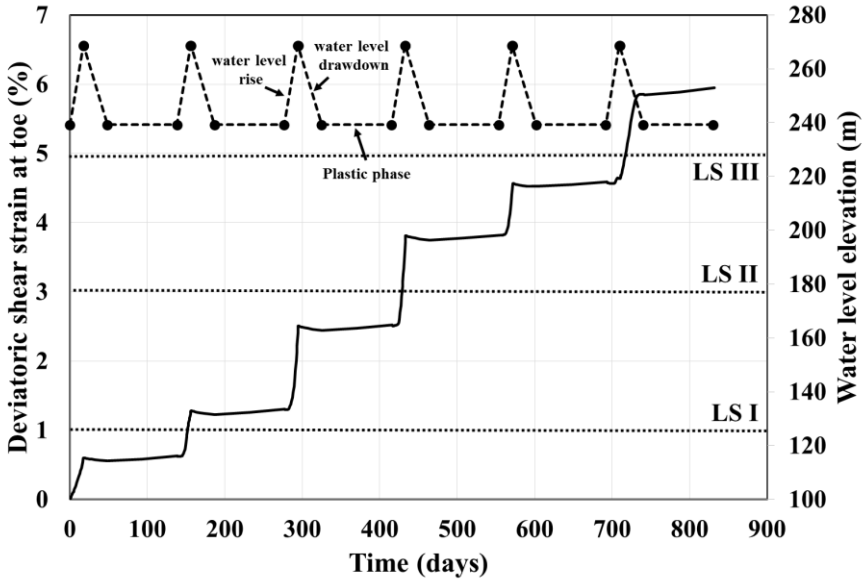


**Figure 4.11. Effect of cycles of loading on deviatoric shear strain at toe location**

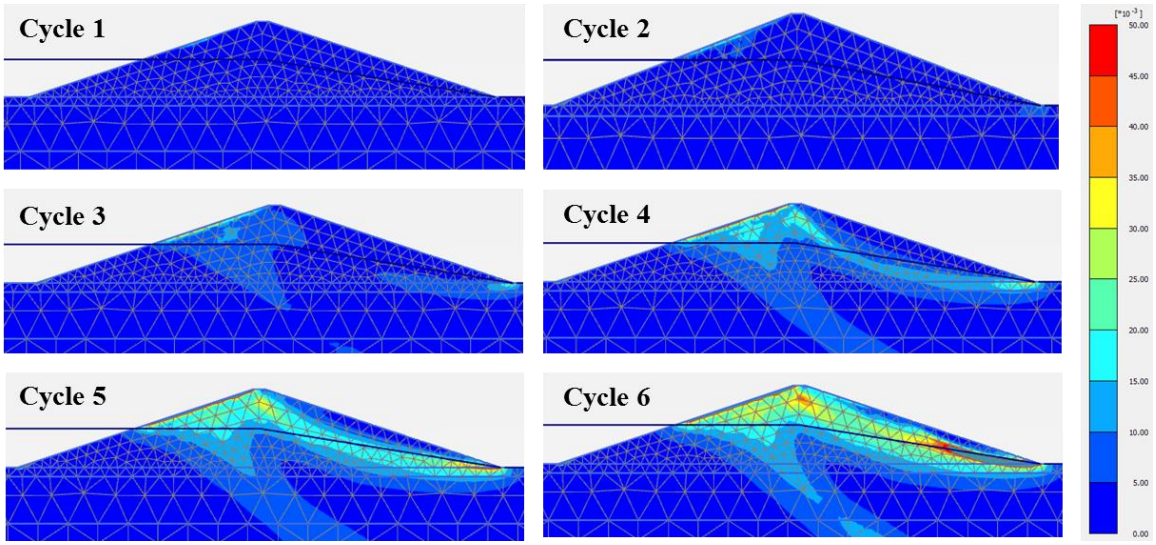


**Figure 4.12. Shear strain bands in embankment with cycles of loading**

## 4.11 ANN model development

### 4.11.1 Training function

MATLAB coding was used to allow for training and testing the REES tool, using known input and its corresponding output data set to predict unknown output data with error precision. As several training functions are implemented in MATLAB to train neural networks, a study on the performance of each training function is performed. The performance is measured via the mean squared error (mse) on the testing dataset and the regression analysis on the divided dataset within the network. The data was divided into 90% (109 cases) to train, validate and test the network, and 10% (12 cases) to test the network independently and estimate the mean square error as a measure of best performance. MATLAB code was developed to train 1000 neural networks for each training function and results and performance is shown in Table 4.4. Each network is trained starting from different initial weights and biases, and with a different division of the first dataset into training, validation, and test sets. Note that the test sets are a good measure of generalization for each respective network, but not for all the networks, because data that is a test set for one network will likely be used for training or validation by other neural networks. This is why the original dataset was divided into two parts, to ensure that a completely independent test set is preserved. The neural network with the lowest mean squared error is the one that generalized best to the second part of the dataset. Scaled conjugate gradient backpropagation showed the least mean square error on the testing data and it was selected to train the network and further investigate the effect of number of neurons on its performance.

**Table 4.4. Effect of neural network training function on performance**

| Neural network training functions | | Mean Square Error (mse) |
|---|---|---|
| **trainlm** | Levenberg-Marquardt backpropagation | 2.79 |
| **trainbr** | Bayesian regularization | 6.33 |
| **trainscg** | Scaled conjugate gradient backpropagation | **0.88** |
| **trainb** | Batch training with weight & bias learning rules | 4.89 |
| **trainbfg** | BFGS quasi-Newton backpropagation | 2.52 |
| **traincgb** | Powell -Beale conjugate gradient backpropagation | 2.45 |
| **traincgf** | Fletcher-Powell conjugate gradient backpropagation | 2.69 |
| **traincgp** | Polak-Ribiere conjugate gradient backpropagation | 1.98 |
| **traingd** | Gradient descent backpropagation | 43.87 |
| **traingdm** | Gradient descent with momentum backpropagation | 1.16 |
| **traingda** | Gradient descent with adaptive lr backpropagation | 4.22 |
| **traingdx** | Gradient descent w/momentum & adaptive lr backpropagation | 2.14 |
| **trainoss** | One step secant backpropagation | 2.53 |
| **trainrp** | Resilient backpropagation (Rprop) | 4.62 |

### 4.11.2 Number of neurons in hidden layer effect

Once the optimum training function is selected, the effect of number of neurons in the hidden layers is investigated. There is some guidelines on how to select the number of hidden neurons in the literature (Lin & Lee, 1996, and Masters, 1993). They suggested using the minimum and maximum number of neurons using the following equations:

$$\text{N (neurons)}_{\text{minimum}} = \sqrt{m * n}$$

$$\text{N (neurons)}_{\text{maximum}} = \text{m}$$

Where

m = Number of input variables = 17 in this study

n = number of output variables = 3 in this study

Based on that, number of neurons were selected to be 7, 12 and 17 and their effect on the performance of mean squared error and regression is investigated as shown in Table 4.5. Having a number of neurons of 7 gave the least mean squared error of 0.27, 0.22 and 0.11 for training, validation and testing data and thus was selected to be the optimum number of hidden neurons.

**Table 4.5. Effect of number of hidden neurons on network performance**

| Training functions | Number of neurons | MSE (Training) | MSE (Validation) | MSE (Testing) |
|---|---|---|---|---|
| Scaled conjugate gradient backpropagation (trainscg) | **7** | 0.27 | 0.22 | 0.11 |
| | 12 | 0.53 | 0.33 | 0.23 |
| | 17 | 0.55 | 0.22 | 0.55 |

### 4.11.3 Neural network structure

The network selected consists of three layers; an input layer of 17 neurons which corresponds to the 17 input parameters; a hidden layer of 7 neurons and a target output layer of 3 neurons. Weights (w) and bias were introduced into the network to allow for backpropagation technique to back-calculate the error. To train the network, such that the proper weights and biases are calculated, the input layer was fed with the 17 input parameters for embankment geometry and soil parameters, and the target layer was fed with shear strain values for mean and two upper and lower shear strain. The network structure is shown in Figure 4.13.

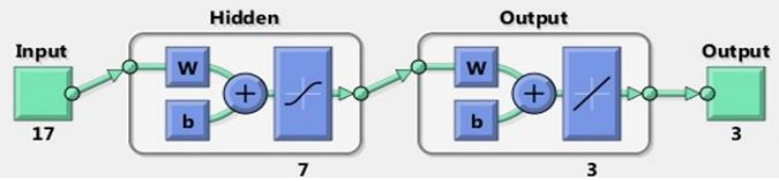


**Figure 4.13. Neural network structure**

A total of 363 Finite element runs (121 models with 3 runs each) were simulated using PLAXIS 2D and were used to train and test the neural network toolbox. The data were divided into 60% (73 cases) for training, 20% (24 cases) for validation and 20% (24 cases) for testing set. As the testing data had no effect on the training process, it was used to provide an independent measure of the performance of the neural network. To avoid overfitting and to increase the network generalization ability, training was halted when the validation set error stopped decreasing. The network was trained for 10000 times using MATLAB to reach error convergence (Code in Appendix C). The model gave a prediction accuracy of $R^2$ of 0.98 for the testing data, 0.98 for the training and 0.97 for the validation data which is within a reasonable accuracy. Figure 4.14 shows the regression plots for the shear strains along with $R^2$ values. These neural networks will be implemented in a tool developed by GUI to allow for the estimation of probabilities of exceeding limit states as will be explained later. A statistical analysis to show the accuracy of ANN prediction was performed. For the calculated shear strain values from PLAXIS 2D and ANN, its mean values were 2.33 and 2.35 respectively, and a standard deviation of 3.73 and 3.69, respectively. This shows the close performance for each of the numerical analysis and artificial neural network prediction.

## 4.12 Relative importance of input parameters

To estimate the relative importance of each of the input parameters to the predicted shear strain output value, Weights of the ANN should be used to estimate the individual contribution of each parameter. As the weights are not unique and changes as different initial weights is used for each training trail. Using ANN to estimate relative importance could be

misleading and won't give an idea of how each parameter is contributing to the output shear strain values. Although, results from PLAXIS parametric study could be used to estimate relative importance for each input parameter. Side slopes and foundation permeability seems like the most factors influencing the shear strain values at toe location. Changing the side slopes from the base case from 1:4 to 1:2 caused an increase in the shear strain at toe with a factor of 38. Also, the permeability for foundation layer caused an increase by a factor of 7 by increasing its value by one order of magnitude. Embankment friction angle and cohesion comes after in the importance and contribution to shear strain values at toe based on the parametric study results.

### 4.13 Risk Estimator for Embankment Structures "REES" tool development

After the development of the ANN model and checking its performance, MATLAB was used to develop a graphical user interface (GUI) tool that implements the ANN model and allows for a friendly user input estimate the output probabilities of exceeding limit states. The tool was named "***REES***" which stands for "Risk Estimator for Embankment Structures". ***REES*** also estimates failure consequence as function of fatality rates with distance away from the embankment structure using peak breach discharge (cfs) and 10-year discharge (cfs) values from the FEMA loss of life risk sheet (FEMA risk tool, 2008). Using fatality rates and probability of exceeding limit state III (to be the probability of failure), ***REES*** then calculates risk value for embankment structures based on population at risk (PAR) of 1000 people. ***REES*** uses Artificial Neural Network (ANN) model to predict output for cases that were not included in the training set.

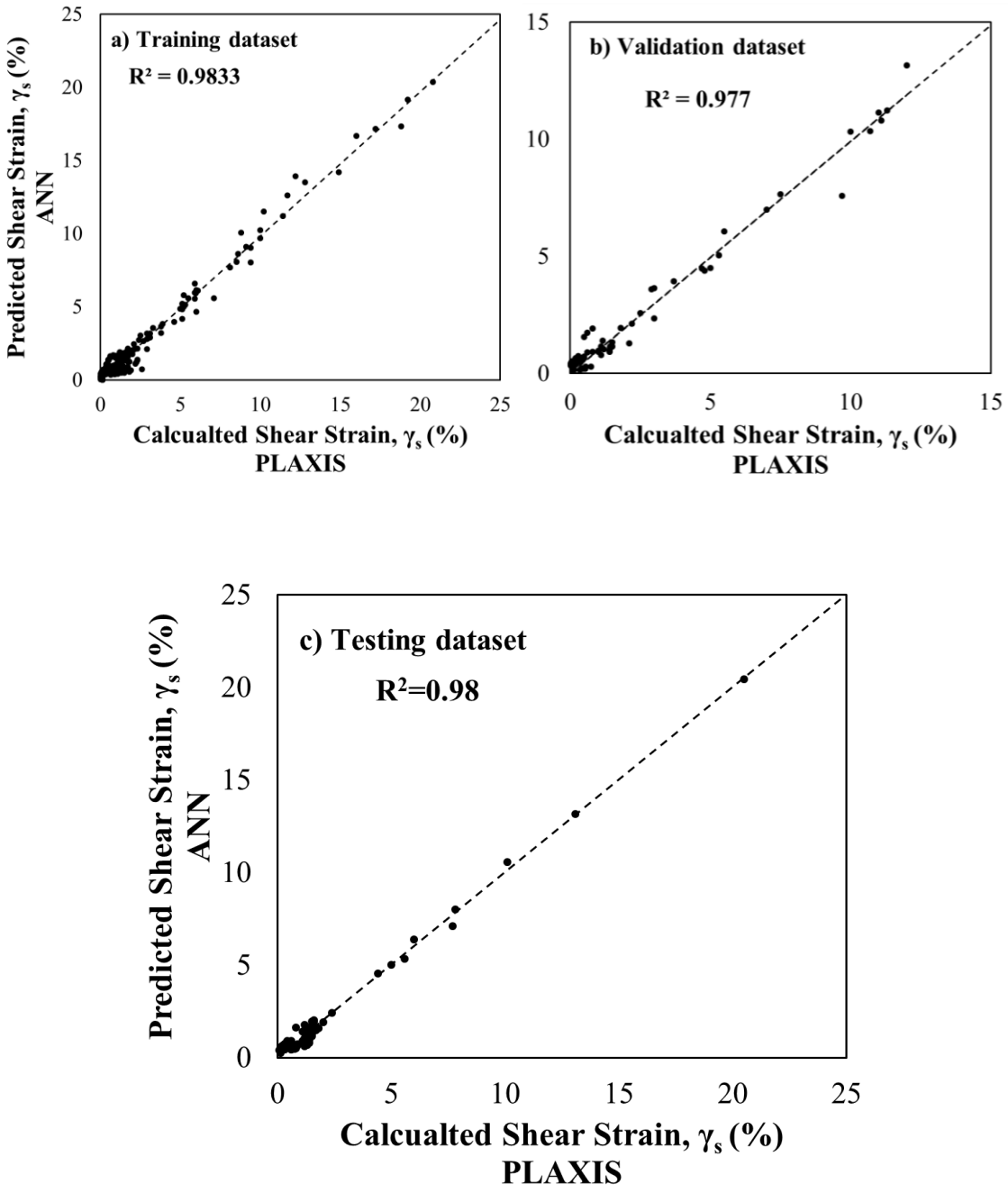


**Figure 4.14. ANN regression plots for (a) training (b) validation and (c) testing data set**

The accuracy of prediction depends on the amount of data used for training and as more data becomes available, fine-tuning of the tool is possible. A user manual also has been developed to guide the user through operating the tool with examples.

### 4.13.1 REES performance and validation

The testing data set used in the artificial neural network procedure allows for the validation of the prediction accuracy of the REES tool. As the testing data had no effect on the training process, it was used to provide an independent measure of the performance of the neural network. 10 cases from Appendix A are selected to estimate probabilities of exceeding LSI, II and III using the results from PLAXIS 2D versus what REES tool predicts. Both shear strain values is extracted from PLAXIS 2D and REES and the probability excel sheet is used to estimate probabilities of exceeding the three limit states. Table 4.6 shows the shear strain from PLAXIS 2D and REES along with probabilities of exceeding limit states from each methodology. Shear strain values for the mean case and the case with one standard deviation above and one below are presented. Although the shear strain values are not close at times, the results showed that the probabilities of exceeding limit states are very close. The highest difference between PE (LSI) was around three order of magnitude from $1*10^{-9}$ to $1*10^{-6}$ which still puts the structure into the same risk region as discussed in chapter (3). This small variation in values show the promising application of the REES tool to estimate shear strain and probabilities of exceeding limit states. As more data becomes available, more fine-tuning of the tool will improve its prediction accuracy. Figure 4.15 and 4.16 shows the values from Table 4.6 along with 1:1 line and regression parameter. For the shear strain values had an $R^2$ of

0.9965 and had a matching 1:1 and regression line. For the probability of exceedance, $R^2$ was 0.9989 with matching 1:1 and regression line as well.

**Table 4.6. Deviatoric shear strain and probabilities of exceedance from PLAXIS & REES**

| Deviatoric Shear Strain (%) | | | | | | Probabilities of exceeding limit state | | | | | |
|---|---|---|---|---|---|---|---|---|---|---|---|
| PLAXIS 2D | | | REES | | | PLAXIS | | | REES | | |
| $\gamma_s$ (μ-σ) | $\gamma_s$ (μ) | $\gamma_s$ (μ+σ) | $\gamma_s$ (μ-σ) | $\gamma_s$ (μ) | $\gamma_s$ (μ+σ) | PE (LSI) | PE (LSII) | PE (LSIII) | PE (LSI) | PE (LSII) | PE (LSIII) |
| 0.3 | 0.4 | 0.6 | 0.73 | 0.80 | 0.89 | $4*10^{-3}$ | 0 | 0 | $1*10^{-2}$ | 0 | 0 |
| 0.18 | 0.23 | 0.3 | 0.59 | 0.64 | 0.71 | $1*10^{-9}$ | 0 | 0 | $1*10^{-6}$ | 0 | 0 |
| 7.7 | 7.8 | 10.1 | 7.10 | 8.01 | 10.56 | 1 | 1 | 1 | 1 | 1 | 1 |
| 1.4 | 1.5 | 1.6 | 1.56 | 1.73 | 1.95 | 1 | 0 | 0 | 1 | $5*10^{-7}$ | 0 |
| 5 | 5.6 | 6 | 5.01 | 5.35 | 6.37 | 1 | 1 | 0.84 | 1 | 1 | 0.85 |
| 1.5 | 1.55 | 1.6 | 1.17 | 1.78 | 2.01 | 1 | 0 | 0 | 0.95 | 0 | $3*10^{-6}$ |
| 4.4 | 13.1 | 20.5 | 4.55 | 13.16 | 20.43 | 1 | 0.96 | 0.82 | 1 | 0.97 | 0.83 |
| 1.8 | 2 | 2.4 | 1.59 | 1.90 | 2.43 | 1 | 0 | $3*10^{-10}$ | 1 | 0.02 | $3*10^{-6}$ |
| 1.1 | 1.2 | 1.3 | 1.41 | 1.38 | 1.38 | 0.98 | 0 | 0 | 1 | 0 | 0 |
| 1.1 | 1.2 | 1.3 | 0.89 | 1.03 | 1.21 | 1 | 0 | 0 | 1 | 0.07 | 0 |

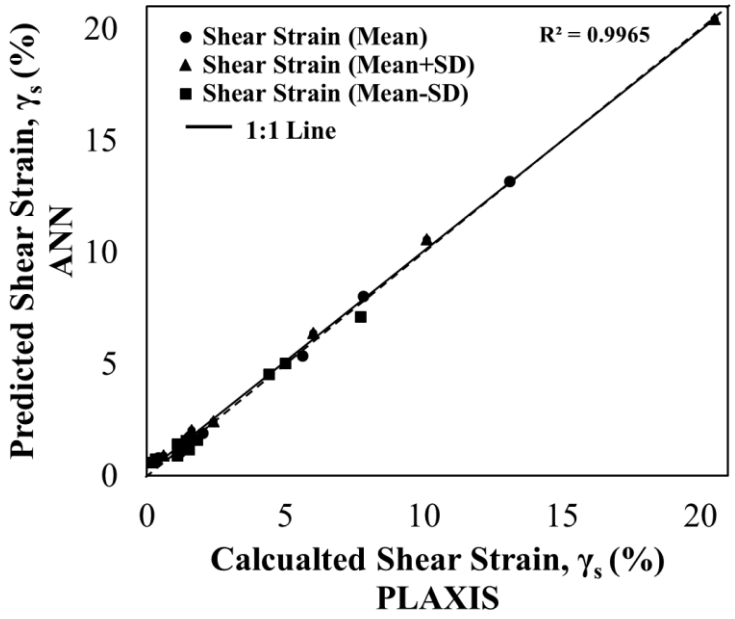


**Figure 4.15. Testing and validation data for REES tool versus PLAXIS 2D**

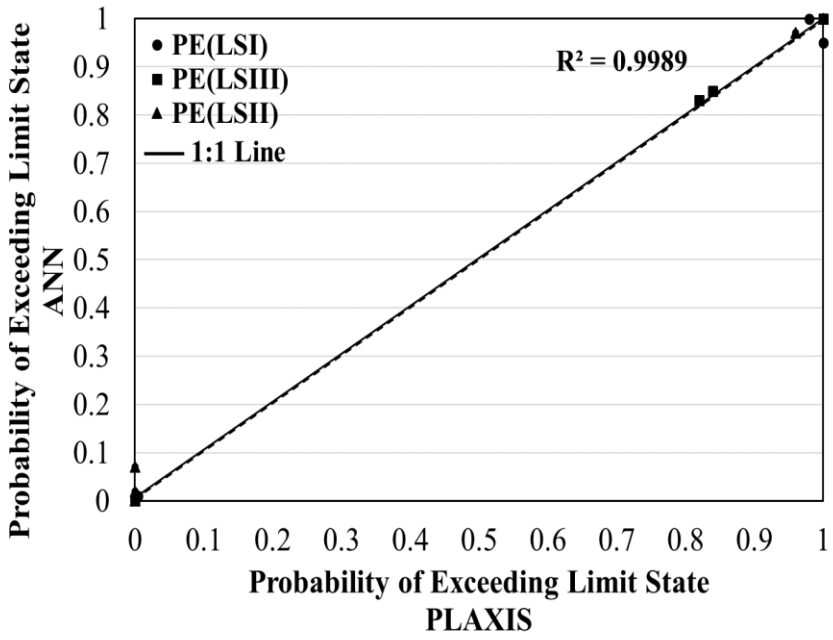


**Figure 4.16. Probability of exceeding limit states for REES tool versus PLAXIS 2D**

The proposed artificial neural network approach could be used in practice to estimate probability of exceeding limit states for an existing levee during coming storms. If the hydrograph data is available for the levee site, the geotechnical engineer can estimate how many storms the levee has experienced over its lifetime and use the tool to predict the shear strain at that specific number of storm events. Care should be taken to the magnitude of the storms that the levee has experienced with comparison to the average storm analyzed here-in from Katrina and Isaac hurricane. Finite element analysis showed a linear relationship between the storm height and shear strain values at toe location. This could be used to scale the shear strain value with correspondence to storm intensity in terms of storm height.

Accurate analysis of the hydrograph for the levee should be carried out in order to insure representative results from the neural network tool and REES.

### 4.14 Summary and conclusions

A new risk estimation tool for embankment structures that uses coupled numerical probabilistic approach and artificial neural networks is presented in this study. REES (Risk Estimator for Embankment Structures) is developed with MATLAB graphical user interface (GUI) to implement the finite element program PLAXIS 2D results.

1- ***REES*** presents a robust and user-friendly way for geotechnical engineers to estimate probabilities of exceeding limit states for embankment structures along with its loss of life risk. These values along with engineering judgment could be used for rehabilitation prioritization and decision-making process. The ***REES*** tool developed using Graphical User Interface (GUI) in MATLAB is presented along with description attached in Appendix C.

2- Appropriate soil and geometry parameters ranges have been assigned from the literature to cover a wide range of soil types. Storm effect was introduced using rate of rise of 0.07 m/hr and rate of drawdown of 0.04 m/hr using average values from hydrographs of Hurricane Katrina and Isaac. A base embankment model was analyzed in PLAXIS 2D and 363 run cases with the different properties combinations were performed. The output shear strain values were used to train and test the artificial neural network. Artificial neural network toolbox within MATLAB was used to produce a neural network which showed a training $R^2$ of 98% and prediction $R^2$ of 98% which is an acceptable accuracy. Statistical Analysis

of the date showed a mean of the calculated and the predicted shear strains 2.33 and 2.35 respectively, and a standard deviation of 3.73 and 3.69.

3- A parametric study on the effect of geometry, soil parameters and cycles of loading is performed using a base embankment model. As side slopes becomes steeper, shear strain increased from 0.1 to 0.5 to 3.8% going from 4:1 to 3:1 to 2:1 slope at time of 30 days. As embankment friction angle increases from 25 to 36$^{o}$, there was a decrease in shear strain at toe from 2.4 to 0.5%. For foundation and alluvial friction angle, they had a slight effect on the shear strain at toe. Cohesion of embankment, foundation and alluvial has also a limited effect on the shear strain at toe. The embankment and alluvial permeability had a slight effect on the shear strain values. The permeability effect of the foundation layer was more significant than embankment and alluvial layer. Increasing the foundation permeability from $6.8*10^{-5}$ to $1*10^{-3}$ cm/s caused an increase in toe shear strain to exceed LSIII. Increasing cycles of loading from 1 to 6 cycles, increased the shear strain by a factor of 10. This illustrates the importance of including loading history in embankment analysis.

4- Relative importance of the input parameters based on parametric study, indicated that side slopes and foundation permeability has the most effect on the shear strain at toe. Side slopes change from the 4:1 to 2:1 caused an increase in the shear strain at toe with a factor of 38. Also, increasing the foundation permeability by one order of magnitude caused an increase in the shear strain at toe by a factor of 7.

5- A study on the ***REES*** performance is performed. 10 testing cases were used to compare the predicted shear strain and probabilities of exceeding LS I, LS II and LS III using ***REES*** versus PLAXIS 2D. A slight difference is observed between the calculated and the predicted values. This shows the promising use of the REES tool for prediction of probabilities of exceeding limit state for embankment structures.

**References**


1. Benson, C. H. (1993). Probability distributions for hydraulic conductivity of compacted soil liner. *Journal of Geotechnical and Geoenvironmental Engineering, ASCE, 119(3),* 471-486.
2. Bogardi, I., Kelly, W. E., and Bardossy, A. (1989). Reliability model for soil liners; Initial design. *Journal of Geotechnical and Geoenvironmental Engineering, ASCE, 115(5),* 658-669.
3. Bowles, J. E. (1997). Foundation analysis and design. *McGraw-Hill.*
4. Duncan, J. M. (2000). Factors of safety and reliability in geotechnical engineering. *Journal of Geotechnical and Geoenvironmental Engineering, 126(4).*
5. Freeze, R. A. (1975). A stochastic conceptual analysis of one dimensional ground water flow in nonuniform homogeneous media. *Water Resources Research, 11,* 725-741
6. Harr, M. E. (1987). Reliability-based design in civil engineering. *New York: McGraw-Hill.*
7. Holtz, R. D., Kovacs, W. D. and Sheahan, T. C. (2011). Introduction to geotechnical engineering, 2nd Edition. *Pearson.*

8. Khalilzad, M. and Gabr, M. A. (2011). Deformation-based limit states for earth embankments. *ASCE Conference Proceeding*. 3639-48.
9. Krejcie, R. V. and Morgan, D. W. (1970). Determining sample size for research activities. *Educational and Psychological Measurement, 30,* 607-610.
10. Kulhawy, F. H. (1992). On the evaluation of soil properties. *Geotechnical Special Publicaiton, 31,* 95-115.
11. Lacasse, S. and Nadim, F. (1997). Uncertainties in characterizing soil properties. *Norwegian Geotechnical Institute, Oslo, Norway, 201, 49-75*.
12. Lamb, T. W., and Whitman, R. V. (1969). Soil mechanics. *John Wiley & Sons.*
13. Lin. C. T., Lee, C.S. (1996). Neural fuzzy systems: a neuro-fuzzy synergism to intelligent systems, *Prentice-Hall, Inc., Upper Saddle River, NJ*
14. Masters, T. (1993). Practical neural network recipes in C++. *Morgan Kaufmann.*
15. Mesri et al. (1993). Cohesion intercept in effective stress-stability analysis. *Journal of Geotechnical Engineering, 119(8),* 1229-1249.
16. Phoon, K. K. and Kulhawy, F. H. (1999). Characterization of geotechnical variability. *Canadian Geotechnical Journal, 36(4),* 612-624
17. Rumelhart, D. E. and McClelland (1986). Parallel distributed processing: explorations in the microstructure of cognition. *MIT Press, Cambridge, MA.*
18. Stark, T. D., and Duncan, J. M (1991). Mechanisms of strength loss in stiff clays. *Journal of Geotechnical Engineering, ASCE, 117(1), 139-154.*

19. U.S. Army Corps of Engineers. (1997). Engineering and design introduction to probability and reliability methods for use in geotechnical engineering. *Engr. Tech. Letter No. 1110-2-547, Department of the Army, Washington, D.C.*
20. U.S. Army Corps of Engineers. (1998). Risk-based analysis in geotechnical engineering for support of planning studies. *Engrg. Circular No. 1110-2-554, Department of the Army, Washington, D.C.*
21. Wolff, T. F. (1994). Evaluating the reliability of existing levees. *Report Research Project: Reliability of existing levees, prepared for U.S. Army Engineer Waterways Experiment Station Geotechnical Laboratory, Vicksburg, Miss.*

# CHAPTER 5. EFFECT OF PEAT DECOMPOSTION ON THE PERFORMANCE OF EMBANKMENT LEVEE USING LIMIT STATE PROBABILISTIC APPROACHES AND NUMERICAL ANALYSIS

## 5.1 Abstract

The integrity and reliability of levees are essential components of homeland safety. The failure of such systems due to a natural or manmade hazard can have monumental repercussions, sometimes with dramatic consequences on human life, property and the country's economy. There is lack of models in the literature that simulates effect of peat aging/decomposition over time from a probabilistic limit states prospective. This paper presents some results of integrated remote-sensing monitoring and modeling to assess the performance-based response of a levee section. The modeled levee is part of the Whale's Mouth section on Sherman Island where satellite images and in-ground GPS sensors are used for displacement measurements. The Whale's Mouth levee is modeled using the large deformation option of the finite element program PLAXIS 2D. The model is used to establish a deterministic performance response under maximum water level loading and to investigate the effect of peat decomposition on the deformation response of the levee section. The remote sensing data are used to calibrate the numerical model. The results are compared to the pre-defined limit state and illustrate how the peat layer decomposition affects the modeled levee section performance. The concept of performance limit states of these critical structures provides a means to quantitatively assess the functionality of an earth structure under severe storm loading events. The probability of exceeding a prescribed limit state is defined based on the strain or hydraulic gradient levels in potential emerging failure zones. The variation in strength properties and hydraulic conductivity of the levee embankment, as well as the rate of rising water level and duration of flooding, may lead to the progression of the structure state from a low probability of exceeding adequate functionality to a high probability of exceeding

the limit state, i.e., imminent failure. The remote sensing data collected during these loading and unloading events is used to establish the levee condition assessment based on the performance limit states.

## 5.2 Introduction

The levee network in the Sacramento-San Joaquin Delta supports an exceptionally rich agricultural area (over a $500 million annual crop value). Currently, the risk of levee failure in this area from extreme storms and earthquakes not only threatens the lives of individuals living behind the levees, but also the water quality in this water-transfer system. The California Department of Water Resources (DWR) provided possible scenarios for levee breaches, most of which predicted flooding of most of the islands and major repair costs (Lund et al., 2007). In the Sacramento Delta, for example, 300 billion gallons of salt water would be expected to flow into the Delta in the first few days after levee failure (DWR, 2008), compromising the water quality for Southern California. Concern about the Delta levees also exists from ongoing land subsidence due to the peat layer decomposition. Amorphous peat has particles that are mainly colloidal and the majority of porewater is adsorbed around the grain structure while fibrous peat has an open structure with interstices filled with a secondary structural arrangement of non-woody, fine fibrous material. In this case, most of the water occurs as free water (MacFarlane and Radforth, 1965).

Amorphous peat is the product of biochemical decomposition and breakdown of fibrous components and other plant remains. It includes a significant amount of inorganic matter. Mesri and Ajlouni (2007) mentioned that there is not a significant difference between the biochemical composition of amorphous and fibrous peat particles, although the organic grains

for amorphous peat are smaller and equi-dimensional (Ng and Eischens, 1983). The difference in settlement response for the two states in the Sherman Island levee profile is investigated in this work as the two extremes of the peat cases.

Given the hundreds of miles of levees with potential subsidence issues, the use of a remote sensing-based health assessment can quantitatively identify weak sections and impending failures. Continuous remote sensing technology, such as satellite and airborne monitoring, can serve as an accurate early warning system, as well as a valuable resource for assessing gradual and abrupt ground subsidence. The use of such monitored data within the context of performance limit states, as for example those presented by Khalilzad and Gabr (2014, 2011), allows for assessment of functionality levels as well as the fragility (in terms of probability of exceedance versus flood level). For each of the three limit states, probabilities of exceedance will be established for the instrumented levee section.

Khalilzad and Gabr (2011) defined earth embankment limit states by correlating shear strain values to the horizontal deformation at the toe location. They presented definitions for the limit states (LS) as follows - LS(I): minor deformations, no discernible shear zones (max deviatoric strain less than 1%), low gradients (i.e., $i < 1$) throughout the embankment dam and foundation; LS(II): medium (repairable) deformations, limited piping problems (i.e., $i > 0.67$ within a shallow depth at the location of toe), dispersed plastic zones with moderate strain values (maximum deviatoric strain less than 3%), tolerable gradients less than critical; LS(III): major deformations, breaches and critical gradients at key locations (i.e., $i>1$, boiling and fine material washing at the location of toe), high strain plastic zones (maximum deviatoric strain > 5%).

This work presents some results of integrated remote-sensing monitoring and modeling to assess the performance-based response of a levee section. The modeled levee is part of the Whale's Mouth section on Sherman Island where satellite images and in-ground GPS sensors are used for displacement measurements. The Whale's Mouth levee is modeled using the large deformation option of the finite element program PLAXIS 2D. The model is used to establish a deterministic performance response under maximum water level loading and to investigate the effect of peat decomposition on the deformation response of the levee section. The remote sensing data are used to calibrate the numerical model. The results are compared to the pre-defined limit state and illustrate how the peat layer decomposition affects the modeled levee section performance.

### 5.3 Sacramento-San Joaquin Delta and Sherman island

Sacramento-San Joaquin delta in Sacramento, California is a web of channels that is protected with more than 1100 miles of levees. The levees network in the Sacramento-San Joaquin Delta supports exceptionally rich agricultural area (over a $500 million annual crop value). Currently, the risk of levee failure in this area from potential flooding, earthquakes and normal day operation not only threatens the lives of individuals living behind the levees, but also, the water quality in this water-transfer system due to salt-water intrusion into the fresh water. Preliminary risk assessment demonstrated a 40% chance that at least 30 islands within the Delta area would be flooded by simultaneous levee failures in a major earthquake in the next 25 years. Sherman Island is one of many islands located on the Sacramento-San Joaquin Delta which has around 18 miles of levee protection. Sherman Lake is considered a natural

preserve and the district has an emergency response plan in case of any event that can comprise the levee system safety. Sherman Island has a population of around 233 people (Census, 2000).

Several flood events affected Sherman's island levees through history. Firstly, was during the 1861/62 season and caused lots of damage that the farmers almost lost most of their livestock. Significant levee failure happened later during the winters of 1871/72, 1874/75, 1876, and 1878. The subsequent levee reconstruction featured a 12-foot high levee with 120 feet base width. The flood of 1878 devastated the entire island. Another flood event happened on 1969 and caused a major pumping effort to dewater the island. After the 1969 break, Seepage and settlement in the area of the break have been ongoing issues requiring constant levee improvements.

**5.4 Sherman Island levee site and field instrumentation**

The monitoring and modeling utilized herein is a step towards establishing a platform for a long-term assessment of the levee system health based on local measurement of deformation (Bennett et al., 2011) due to natural cycles of water elevation loading and unloading associated with rain storms, flood cycles, tides, tremors, and traffic loads, as well as aging, consolidation and creep. Thus, federal and local governments will be able to prioritize and implement repairs and rehabilitation, as well as assess the effectiveness of these repairs before major events. This approach attempts to reduce the risk of having a catastrophic failure of a flood-control system similar to that of Hurricane Katrina and Superstorm Sandy. The levee test site is located on Sherman Island in Sacramento County, California. Sherman Island is at the confluence of the Sacramento and San Joaquin Rivers, approximately two-kilometer northeast of Antioch, CA.

The instrumented levee section is known as the setback levee and is owned by California Department of Water Resources.

In situ instrumentation was installed along the setback levee on Sherman Island in April 2015. Three stand-alone, continuously monitoring GPS stations were anchored to the ground surface as shown in Figure 5.1a. Locations of GPS stations compared to modeled cross-section are shown in Figure 5.1b. Each station contains a Novatel ProPak 6 receiver and a dual-frequency GPS plus GLONASS pinwheel antenna. The ProPak 6 is a high performance Global Navigation Satellite System (GNSS) receiver capable of receiving and tracking different combinations of GNSS signal and integrated L-Band on 240 channels. The receivers have a built in cellular modem and are connected to the AT&T network for remote data transmission.

**5.5 Fibrous and Amorphous peat**

Peat soils are organic deposits that are classified to have an organic content of more than 75% (ASTM D4427, 2013). Peat soil has high content of fibrous organic matter. Huat et al. (2004) reported that peat content will differ depending on location and various factors such as origin, fiber content, temperature, climate and humidity. Peat goes through a process of decomposition with time. Decomposition or humification is a process that leads to decreasing the organic matter and changing the chemical composition and its structure. The organic content usually has a rate of decay slower than its rate of accumulation. There are several approaches to classify peat based on its degree of decomposition, including the classification system by Von Post (1922). This scale system is based on factors that include botanical composition, degree of humification and color of the peat water after squeezing. It has ten degrees of decomposition from $H_1$ (very fibrous) to $H_{10}$ (totally decomposed or amorphous) as

in Table 5.1. Amorphous peat is likely to exist at lower void ratios, has relatively low permeability anisotropy, lower compressibility, lower friction angle and higher coefficient of earth pressure at rest (Mesri et al., 2007; Edil and Wang, 2000).

Fibrous peat has a high compressibility that causes the permeability to decrease dramatically as it is compressed under embankment load (Miyakawa, 1960; Lea and Brawner, 1963). Fibrous peat has the highest values of the compression index ($C_c$) and the highest values of $C_\alpha/C_c$. The primary consolidation completes within a few weeks or months (Mesri et al., 2007). Table 5.2 summarizes strength parameters (friction angle, φ; cohesion, c and coefficient of earth pressure at rest, $K_o$) and compression parameters (Compression index, $C_c$; Swelling index, $C_s$; Secondary compression to compression index ratio $C_\alpha/C_c$ and change in permeability coefficient, $C_k$) from the literature for fibrous versus amorphous peat.

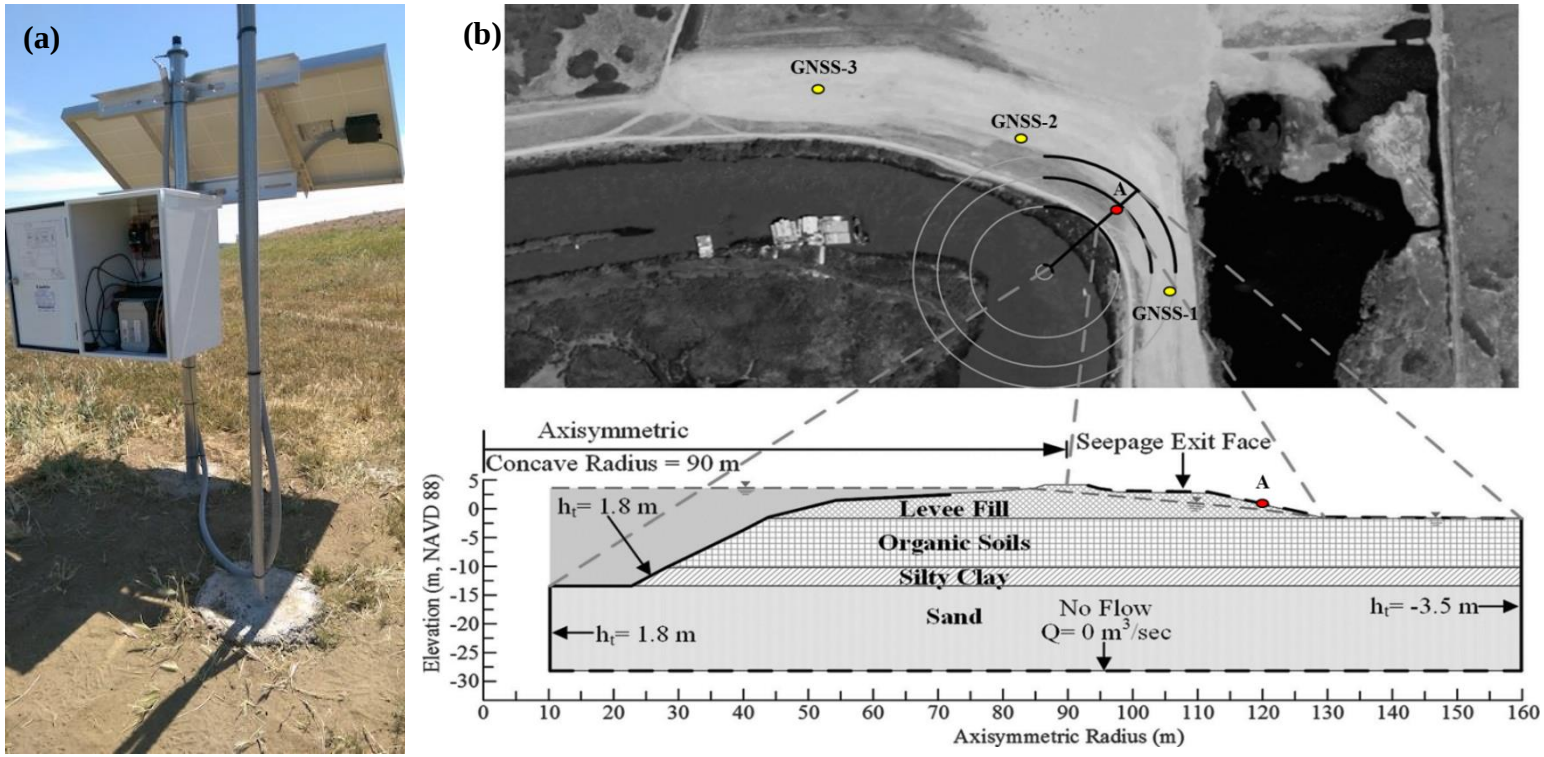


**Figure 5.1.a. One of three stand-alone GPS stations installed in Sherman Island setback levee.**
**b. Model of Sherman Island proposed by Jafari et al. (2016).**

**Table 5.1 Von Post classification system for peat**

| Degree of humification | Decomposition | Plant structure | Content of amorphous material | Material extruded on squeezing (passing between fingers | Nature of residue |
|---|---|---|---|---|---|
| $H_1$ | None | Easily identified | None | Clear, Colorless water | -------- |
| $H_2$ | Insignificant | Easily identified | None | Yellowish water | -------- |
| $H_3$ | Very slight | Still identifiable | Slight | Brown, muddy water; no peat | Not pasty |
| $H_4$ | Slight | Not easily identified | Some | Dark brown, muddy water; no peat | Somewhat pasty |
| $H_5$ | Moderate | Recognizable, but vague | Considerable | Muddy water and some peat | Strongly pasty |
| $H_6$ | Moderately strong | Indistinct (More distinct after squeezing) | Considerable | About one third of peat squeezed out; water dark brown | |
| $H_7$ | Strong | Faintly recognizable | High | About one half of peat squeezed out; any water very dark brown | Fibres and roots more resistant to decomposition |
| $H_8$ | Very strong | Very indistinct | High | About two third of peat squeezed out; also some pasty water | |
| $H_9$ | Nearly complete | Almost unrecognizable | -------- | Nearly all of peat squeezed out as a fairly uniform past | -------- |
| $H_{10}$ | Complete | Not discernible | -------- | All of the peat passes between the fingers; no free water visible | -------- |

The values in table 5.2 show the variability for these two types of peat. Although the ranges can be close at times, the peat behavior changes with location, water content, fiber content and other factors.

**Table 5.2. Compression and strength parameters for fibrous and amorphous peats**

| Peat type | Compression parameters | | | | Strength parameters | | | Ref. | Notes |
|---|---|---|---|---|---|---|---|---|---|
| | $C_c$ | $C_s$ | $C_\alpha/C_c$ | $C_k$ | $K_o$ | φ' | c' (kpa) | | |
| **Fibrous** | 2 - 9.5 | ---- | 0.0003-0.11 | ---- | ---- | ---- | ---- | Fox et al. (1992) | ---- |
| **Fibrous** | ---- | ---- | ---- | ---- | 0.33 | 53 | ---- | Edil et al. (2000) | Minnesota |
| **Fibrous** | 0.2-10 | (0.1-0.3) $C_c$ | 0.06+-0.01 | 0.25 $e_o$ | 0.3-0.35 | 40-60 | ---- | Mesri et al. (2007) | ---- |

| | | | | | | | | | |
|---|---|---|---|---|---|---|---|---|---|
| **Fibrous** | 4.7 | $C_c/10$ | ---- | ---- | ---- | ---- | ---- | Dhowian et al. (1981) | ---- |
| **Fibrous** | ---- | ---- | ---- | ---- | ---- | 3-20 | 9-17 | Bujang et al. (2014) | Malaysia |
| **Fibrous** | 3.9 | 0.4 | 0.05 | 2.4 | ---- | ---- | ---- | Shafie et al. (2013) | Sherman Island |
| **Fibrous** | 0.34-0.68 | ---- | ---- | ---- | ---- | 28 | 18 | Marachi et al. (1983) | |
| **Amorphous** | ---- | ---- | ---- | ---- | 0.49 | 53 | ---- | Edil et al. (2000) | Minnesota |
| **Amorphous** | ---- | ---- | ---- | ---- | ---- | 6-20 | 7-12 | Bujang et al. (2014) | Malaysia |

### 5.6 Finite element and domain model

The finite element program PLAXIS 2-D 2016 is used to model a levee section on Sherman Island, within the California Delta area. The section geometry was selected on the basis of the information presented by Jafari et al. (2016), as shown in Figure 5.1b. Global Navigation Satellite System (GNSS) remote sensing displacement recording locations (GNSS-1, 2 and 3) are shown in Figure 5.1b. Displacements at point A on the levee landslide side slope from numerical modeling will be compared to those measured in the field. The modeled soil profile consists of 4 layers, which include a levee fill underlain by approximately 8 m of organic soil (peat). This organic layer is underlain by a silty clay over a thick layer of sand. Soil properties are extracted from data by Jafari et al. (2016) with some of the parameters assumed based on information from borehole logs performed on the Sherman island setback levee project. The borehole logs suggested that the peat soil is highly fibrous, so the initial model utilized the fibrous peat data in Table 5.2.

Soil properties for domain profile are summarized in Table 5.3. Different finite element mesh resolutions were investigated from coarse to fine to very fine mesh. Changing the mesh from coarse to fine, caused a 5% increase in displacement at point A, for example. No notable change was observed when using a very fine mesh in comparison to fine mesh, thus a fine 15-

node elements mesh was used with the domain having 1961 elements and 15,975 nodes. Horizontal and vertical deformations were restricted at the bottom boundary of the shale layer. Only the horizontal deformations are restricted at the lateral boundaries of the model. Flow boundary conditions included a no-flow boundary at the lower boundary of the model (boundary of shale layer) and a free-flow boundary at the downstream slope of the embankment. The upstream face of the levee was defined as steady state seepage. The modeled embankment and boundary conditions are shown in Figure 5.2.

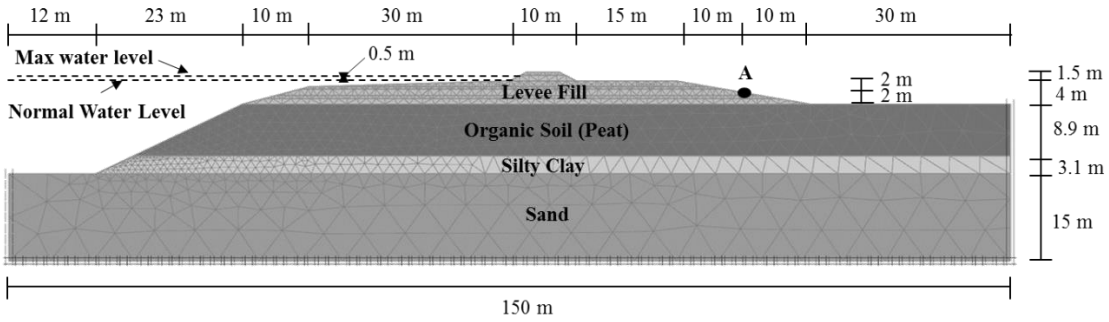


**Figure 5.2. Finite element PLAXIS 2D levee mesh and boundary conditions**

### 5.7 Peat model: Soft Soil Creep (SSC)

The Soft Soil Creep Model (SSC) in PLAXIS was used to model to the peat layer to account for the viscous effects including creep and stress relaxation. This model takes into account secondary (time-dependent) compression (creep) and utilizes stress-dependent stiffness with the failure behavior conforming to the Mohr-Coulomb criterion. The soft soil creep model requires the same input parameters as the soft soil model in addition to a creep parameter in the form of the Modified Creep Index (μ*). The specific parameters used in this study are shown in Table 5.4. As a limited amount of data were available for the compression parameters for amorphous peat, values were assumed based on water content correlation with compression

index. A compression index, $C_c$ = 8 corresponds to a water content of 700%. Taking $C_\alpha/C_c$ ratio to have an average value of 0.06, yields a $C_\alpha$ = 0.48 and $C_s$ = 0.8. Also, the friction angle and the cohesion were selected to be 6$^o$ and 12 kPa, respectively, after Bujang et al. (2014). The remainder of the soil layers in the finite element domain were modeled using the Mohr-Coulomb criterion.

### 5.8 Modeling phases and calibration

The levee was modeled using staged construction in 7 layers. Direct generation of initial effective stresses, and pore pressures and state parameters in the foundation layers were performed before construction of the embankment. The groundwater level was assumed at the boundary between the fill layer and the peat layer. The time interval for placing each layer was set to 2 days and the consolidation phase time was estimated using trial runs. In these phases, the displacements and strains are reset to zero before placement of the next layer. To simulate the extreme loading condition, the water level was raised to the max elevation (1 m below crest elevation) and allowed to reach a steady state condition. In the final phase, a consolidation analysis was performed to capture secondary compression settlement (creep effect) for 20,000 days (over 50 years). Point A along the landslide side slope were chosen to investigate the displacement response given the change in the peat properties and to place such a response within the context of the defined limit states. Results for vertical displacement (negative sign means settlement) versus time for fibrous peat are shown in Figure 5.3 for point A (designated on Figure 5.1).

This point was chosen to allow for the model calibration with the GNSS-1 and GNSS-2 remote sensing records available near to these locations in the Sherman Island levee. These

GNSS data are for a one-year period from 4/1/2015 up to 4/1/2016. In this case, the rate of deformation with time shows a relatively close trend to the model results of point A. As the GNSS data start time is not known after the construction of the levee, the rate of decrease with time is the value of concern and not the actual deformation values. The GNSS data showed an average of 0.13 m of deformation per year compared to the 0.12 m per year computed for point A. The starting time in Figure 5.3 is 50,000 days which is the lifetime that the Sherman Island has been in place. This corresponds to 1.7 m of deformation at levee toe location. It is assumed that the GNSS data starts from the same value of deformation to be able to compare the rate of vertical displacement with time. Reinert (2014) in his Ph.D thesis mentioned that land subsidence in the delta area has an average rate of 3.2 to 4.8 cm/year (Mount and Twiss, 2005). Also some other sources mentioned rates as low as 1.5 in/year up to 6 in/year. These values are comparable to 0.13 m/year that was observed by the GNSS measured data.

**Table 5.3. Soil profile parameters for Sherman Island model**

| Model | | Mohr-Coulomb | Soft soil creep | Soft soil creep | Mohr-Coulomb | Mohr-Coulomb | Model | |
|---|---|---|---|---|---|---|---|---|
| **Layer** | | **Fill** | **Peat (Fibrous)** | **Peat (Amorphous)** | **Silty Clay** | **Sand** | **Units** | **Ref.** |
| material behavior | | Drained | Undrained (A) | Undrained (A) | Undrained (A) | Drained | - | - |
| unit weight above phreatic level | $\gamma_{unsat}$ | 16 | 9 | 9 | 15 | 18 | kN/m$^3$ | Jafari (2016) |
| saturated unit weight | $\gamma_{sat}$ | 17.7 | 11.6 | 11.6 | 16.7 | 19.5 | kN/m$^3$ | Jafari (2016) |
| Initial void ratio | $e_{int}$ | 0.5 | 17.5 | 10 | 0.5 | 0.5 | - | Borehole logs (2008) |
| ***Parameters*** | | | | | | | | |
| Poisson's ratio | $\nu'$ | 0.33 | 0.15 | 0.15 | 0.3 | 0.2 | - | Default |
| Modified compression index | $\lambda^*$ | - | $C_c$=10<br>$\lambda^*$= 0.2350 | $C_c$=8<br>$\lambda^*$= 0.3162 | - | - | - | Mesri et al. (2007) |
| Modified swelling index | $\kappa^*$ | - | $C_s$=3<br>$\kappa^*$= 0.1410 | $C_s$=0.8<br>$\kappa^*$= 0.0632 | - | - | - | Mesri et al. (2007) |
| Modified creep index | $\mu^*$ | - | Cα=0.6<br>$\mu^*$= 0.0141 | Cα=0.48<br>$\mu^*$= 0.0190 | - | - | | Mesri et al. (2007) |
| Cohesion | $c'_{ref}$ | 0.0 | 7 | 12 | 5 | 0 | kN/m$^2$ | Borehole logs (2008) |
| Friction angle | $\varphi'$ | 33 | 11.3 | 6 | 33 | 30 | (º) | |
| Dilatancy angle | $\psi$ | 0.0 | 0.0 | 0.0 | 0 | 0 | (º) | Default |
| Advanced: Set to default | – | Yes | Yes | Yes | Yes | Yes | - | - |
| Horizontal permeability | $k_x$ | 1*10$^{-3}$ | 5.5*10$^{-5}$ | 5.5*10$^{-7}$ | 1*10$^{-6}$ | 1*10$^{-2}$ | cm/s | Jafari (2016) |
| Vertical permeability | $k_v$ | 0.25*10$^{-3}$ | 5.5*10$^{-5}$ | 5.5*10$^{-7}$ | 1*10$^{-5}$ | 1*10$^{-1}$ | cm/s | Jafari (2016) |
| Change in permeability | $c_k$ | 1*10$^{15}$ | 1 | 1 | 1*10$^{15}$ | 1*10$^{15}$ | - | Mesri et al. (2007) |
| Interface strength | - | Rigid | Rigid | Rigid | Rigid | Rigid | - | Default |
| Strength reduction factor | $R_{inter}$ | 1.0 | 1.0 | 1.0 | 1.0 | 1.0 | - | Default |
| ***Initial*** | | | | | | | | |
| $K_o$ determination | - | Auto | Auto | Auto | Auto | Auto | - | Default |
| $K_{o,x} = K_{o,z} = (1-\sin \varphi)$ | - | 0.455 | - | - | 0.455 | 0.5 | - | Default |

**Table 5.4. Fibrous and amorphous peat parameters used for finite element modeling**

| Peat type | Compression parameters | | | | Strength parameters | | | Reference |
|---|---|---|---|---|---|---|---|---|
| | $C_c$ | $C_s$ | $C_\alpha$ | $C_k$ | $e_o$ | φ' | c'(kpa) | |
| **Fibrous** | 10 | 3 | 0.6 | 1.0 | 17.5 | 11.3 | 7 | Mesri et al. (2007) |
| **Amorphous** | 8 | 0.8 | 0.48 | ---- | 10 | 6 | 12 | Bujang et al. (2014). |

## 5.9 Model scenarios for long term assessment

Similar to the approach for model calibration, the levee was modeled using staged construction in 7 layers. Direct generation of initial effective stresses, and pore pressures and state parameters in the foundation layers was performed before construction of the embankment. The groundwater level was assumed at the boundary between the fill layer and the peat layer. The time interval for placing each layer was set to 1 day. In these phases, the displacement and strains were reset to zero before placement of the next layer and undrained behavior was ignored. The large deformation option was used (updated mesh technique) in all phases.

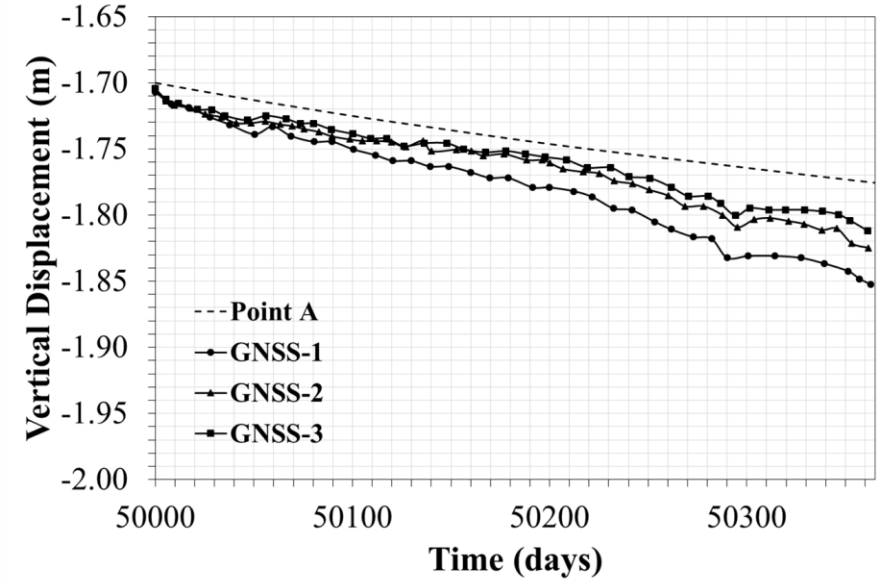


**Figure 5.3. Displacement with time for fibrous peat versus measured data**

The water level was raised in two stages; first to reach its normal elevation (sunny day) of 1.5 m below crest. Second, a transit analysis was performed where water level was raised at a rate of 0.08 m/hr to reach its max elevation (1 m below crest), then leaving it there for a week (7 days) while performing a consolidation analysis. The water level was then lowered at the same rate of 0.08 m/hr to the sunny day level of 1.5 m below crest. At this point in time, a consolidation analysis of 1,000 days was performed to capture the deformation response with time. After the end of the consolidation stage, another cycle of raising and lowering the water level was performed with the exact same rate and stages as before. Finally, a consolidation phase of another 1,000 days was carried out.

The results of such analyses are shown in Figure 5.4. The displacement as a function of time at point A showed that the effect of the transient highwater level loading on the displacement magnitude is insignificant compared to the secondary compression due to the presence of the peat layer. The assumption of having an amorphous peat layer results in less settlement of the levee section with time compared to fibrous peat. The rate of deformation increases with time in the case of the amorphous peat, as shown in Figure 5.4, due to the smaller change in void ratio as compared to the amorphous peat, and therefore a greater secondary compressibility rate with time. As peat properties transition with time from the fibrous to amorphous case, the vertical deformation will be bounded by the trend lines shown in Figure 5.4. Figure 5.5 shows the change in the deviatoric strain with time and the associated limit states based on using the mean value of $C_\alpha/C_c=0.06$ for the assessment of deformation. Equation 1 shows the expression for estimating the deviatoric strain, which is a function of Cartesian strains $\varepsilon_{xx}$ and $\varepsilon_{yy}$ and volumetric strain, $\varepsilon_{v.}$

$$\gamma_s = \sqrt{\frac{2}{3}\left[\left(\varepsilon_{xx} - \frac{\varepsilon_v}{3}\right)^2 + \left(\varepsilon_{yy} - \frac{\varepsilon_v}{3}\right)^2 + \left(\varepsilon_{zz} - \frac{\varepsilon_v}{3}\right)^2 + \frac{1}{2}(\gamma_{xy}{}^2 + \gamma_{yz}{}^2 + \gamma_{zx}{}^2)\right]} \quad (1)$$

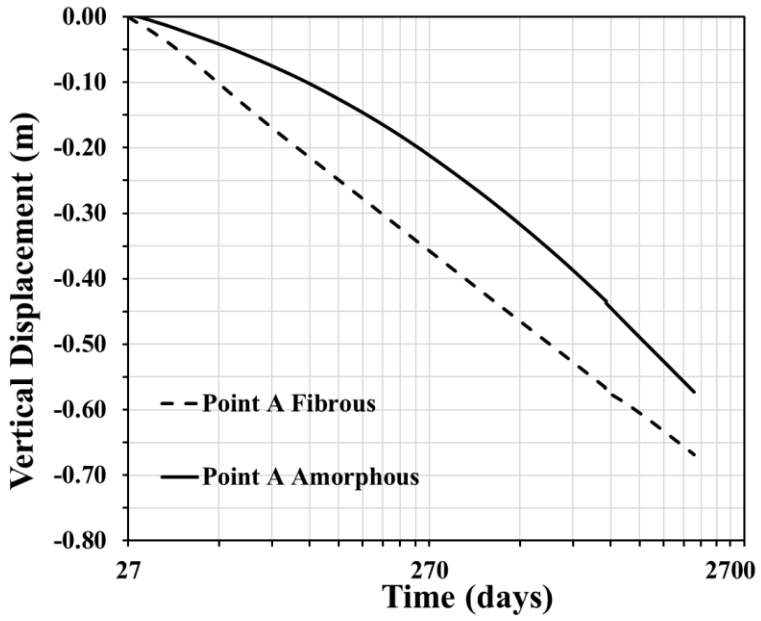


**Figure 5.4. Vertical displacement with time for fibrous and amorphous peat.**

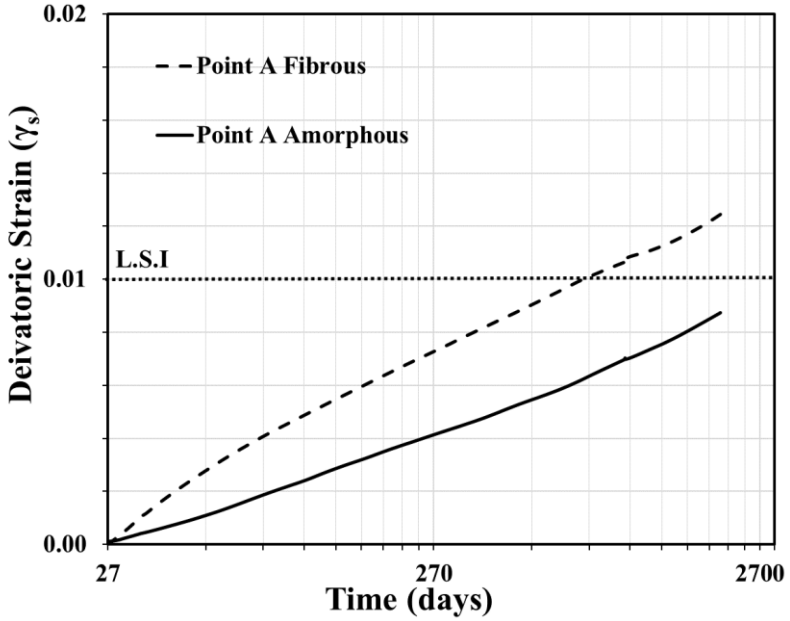


**Figure 5.5. Deviatoric strain ($\gamma_s$) with time and limit state criteria for mean value of $C_\alpha/C_c$=0.06.**

The results show that the deviatoric strain is higher for the fibrous peat assumption than when the amorphous case is assumed. These strain magnitudes will exceed limit state I (Khalilzad and Gabr, 2011) after approximately 750 days at point A. As presented by Edil and Wang (2000) shear resistance in peat continues to develop with increasing strain levels without evidence of clear failure surface. The concern here, however, is the occurrence of translational embankment sliding with the continuing deformation in the fashion described by Duncan and Houston (1983).

## 5.10 Peat decomposition effect on probability of exceeding limit states

Peat decomposition/aging with time effect on the limit state response of the Sacramento delta levee is investigated in this study. Peats with three degree of decomposition from fibrous (H1-H3) to hemic (H4-H7) to amorphous (H8-H10) are selected to investigate its deformation behavior using numerical analysis and limit states. Table 5.5 shows the consolidation and permeability properties for these cases. $C_c$ values for (H1-H3) and (H8-H10) are assigned from Mesri et al. (2007). For the hemic or moderately humified peat (H4-H7), its $C_c$ value was taken as the average value between fibrous and amorphous case. Other properties are assumed from the literature as noted in Table 5.5. $C_\alpha/C_c$ ratio were assigned using the same literature to calculate $C_\alpha$. The secondary compression coefficient values are of immense importance in this study due to the considerable effect of creep in peat. Void ratio values are assumed reasonably according to data from literature to simulate a high void ratio for fibrous peat and the lowest value being for amorphous peat. Then, hemic peat to be taken as an average value between both cases. The values of hydraulic permeability are assigned based on Ryden et al. (1990) in

Magnussen (1994). The change in permeability coefficient $C_k$ which represents the change in void ratio with permeability change ($\Delta e/\log\Delta k$) and is calculated from the Ajlouni et al. (2000) which proposes that it value changes with peat degree of decomposition.

**Table 5.5. Peat parameters with different state of decomposition used for PLAXIS 2D**

| Peat Degree of decomposition | $C_c$[1] | $C_\alpha/C_c$[1] | $C_\alpha$** | $C_k$[2] | $e_0$* | $k_v$ (cm/s)[4] |
|---|---|---|---|---|---|---|
| **H1-H3** | 10 | 0.1 | 1 | $e_o/4.5=4.4$ | 20* | $10^{-5}$ |
| **H4-H7** | 7.5* | 0.06 | 0.45 | $e_o/4 =2.8$ | 11.5* | $10^{-8}$ |
| **H8-H10** | 5 | 0.035 | 0.175 | $e_o/3 =1$ | 3* | $10^{-10}$ |

[1]Mesri et al. (2007); [2]AJLOUNI et al. (2000); [4]Ryden (1990) in Magnussen (1994); *Assumed; **Calculated.

As peat ages with time and transition from H1 to H10 category, its physical, consolidation and hydraulic properties changes. The study here aims at modeling peat at different time stages going from H1 to H10 and assigning representative parameters for each stage to account for peat decomposition. Numerical modeling is performed and its deformation responses is presented and discussed. PLAXIS 2D assumes constant coefficient of compression ($C_c$) and coefficient of secondary compression ($C_\alpha$) for the soft soil creep used to model peat soils. That contradicts the assumption proposed by Mesri et al. (2007) that $C_\alpha/C_c$ ratio changes with peat type and its degree of decomposition. To model that in PLAXIS 2D, H1-H3 (Fibrous) peat is assumed to be an initial state having properties as in Table 5.5. Then after 8 years, peat properties is manually changed to simulate peat transition to H4-H7 (Moderately humified). After another 8 years, modeling simulated the last stage of peat decomposition of H8-H10 (Amorphous). These peat properties were assigned to the embankment levee in the Sherman Island in the Sacramento San Joaquin delta as shown in Figure 5.2.

The embankment construction and consolidation phase were modeled with the same time steps explained in section 5.8, with changing peat decomposition for each time. Also, three cases that represents peat with only one degree of decomposition is modeled for comparison. Deformation and shear strain values were extracted and presented. Figure 5.6 shows the vertical displacement at point A (Figure 5.2) versus time for the three (H1-H3), (H4-H7) and (H8-H10) peats. Also, the case where peat decomposition was modeled with time steps changing the peat properties as it ages according to Table 5.5 is presented. For the model case where peat aging is modeled, vertical displacement yielded an intermediate curve between moderately decomposed and low decomposed (Fibrous) peat case. Also, deformation rate changed going from moderately case into more decomposed peat to follow the amorphous peat deformation curve. Shear strain values followed fibrous trend then transitioned more into amorphous peat as it ages. Although, the case where peat ages with time presented less vertical displacement than fibrous case, it is still important to know which stage of decomposition the peat is currently in to adequately design for the right amount of deformation. Figure 5.7 shows deviatoric strain at toe for peat with three decomposition cases for up to 50,000 days. For the case where peat decomposition is modeled with time steps every 8 year, after 10,000 days the peat was assumed to have the same properties of amorphous peat as the shear strain rate observed to have a constant rate. H1-H3 peat experiences the highest values of shear strain at toe to exceed LSI limit of 1% shear strain at 235 days and reach LSII limit of 3% shear strain at approximately 20,000 days. On the other hand, H4-H7 and H8-H10 peat took 2700 days to exceed LSI and didn't reach LSII at the end time of 50,000 days. Many factors still unclear

about how much time is needed in the field for peat to decompose as many factors is involved in the decomposition process (i.e. temperature, aerobic and anaerobic activity, pH, etc.).

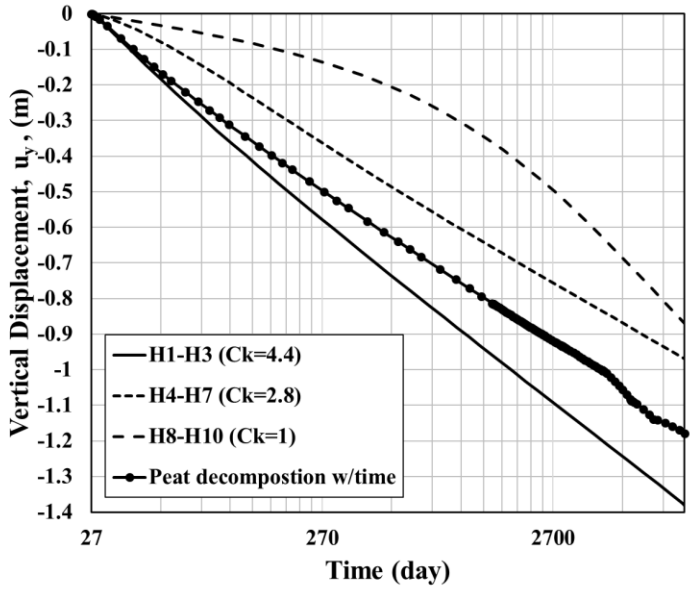


**Figure 5.6. Vertical displacement for peat with different degree of decomposition**

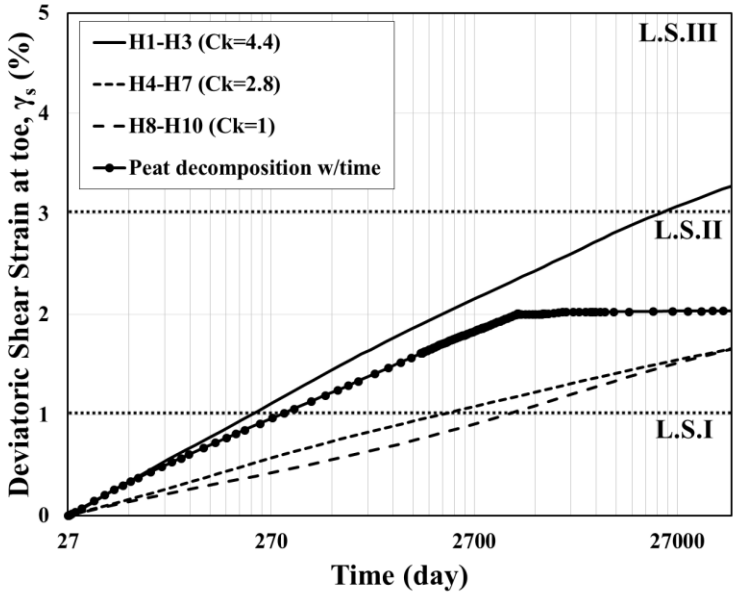


**Figure 5.7. Deviatoric shear strain at toe for peat with different degree of decomposition (H1-H3, H4-H7 and H8-H10)**

Figure 5.8 shows the deformation values within the levee at consolidation time of 10,000 days for the three-peat decomposition cases. Figure 5.8a shows higher deformation especially at toe location for fibrous (H1-H3) peat compared to H4-H7 and H8-H10 peats. As peat decomposition increases, the deformation values decrease as it experiences less compression with time.

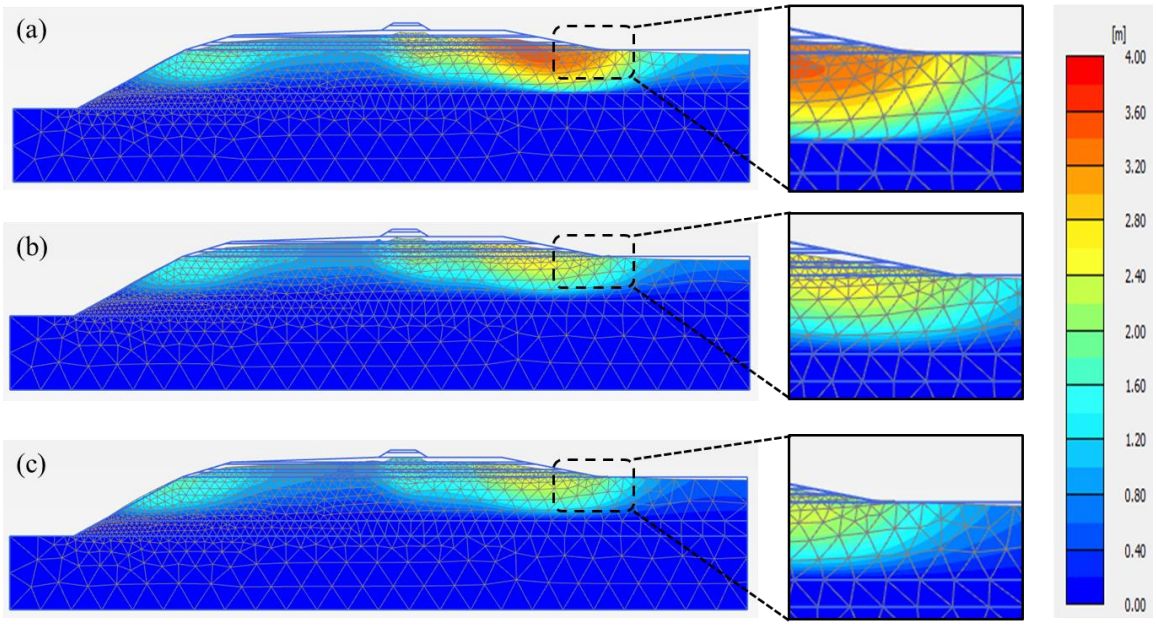


**Figure 5.8. Deformation of levee for a) H1-H3 peat b) H4-H7 peat c) H8-H10 peat at 10,000 days.**

## 5.11 Probabilities of exceeding limit states

To estimate the probability of exceedance for each limit state, an approach similar to Duncan (2000) is employed. Duncan in his paper "*Factors of safety and reliability in geotechnical engineering"* implemented a methodology to estimate standard deviation for a parameter when limited data are available to do so. The variable parameter is the $C_\alpha/C_c$ for peat layer. Mean value and standard deviation was assigned as in Table 5.5. The finite element model was then processed for the variable parameter, one with one standard deviation above

the mean and one below the mean. Once shear strains values are obtained for toe area in the embankment dam, it is normalized with respect to the predefined limit states. Predefined limit state is taken as three limit states: LSI, LSII and LSIII at 1, 3 and 5% deviatoric strain values respectively as proposed by Khalilzad (2011). Next, the Taylor series the Taylor Series Technique (Wolff, 1994; USACE, 1997; 1999) is used to find the standard deviation and coefficient of variation of these normalized values. Then, a reliability index based on lognormal distribution of the normalized deformation is calculated (Duncan, 2000). Hence, the reliability is calculated based on a normal distribution of the reliability index and the probability of exceeding the limit states is estimated. Progression of probability of exceeding LSI and LSII is shown in Figure 5.9 with time.

For Fibrous (H1-H3) peat, as shear strain increases and exceeds a shear strain value of 1% at approximately 270 days, the probability of exceeding LSI reaches 1 slightly after 270 days and keeps constant till the end of consolidation phase. Probability of exceeding LSII begins to increase starting at around 9100 days when shear strain reaches 2.6% (Figure 5.7) and keeps increasing to reach probability of exceeding LSII of 0.95 at 50,000 days. For (H4-H7), it takes 10,000 days to reach probability of exceeding LSI 1 as its shear strain trend doesn't exceed 1% value till 1800 days. Amorphous peat (H8-H10) takes more time around 300,000 days to reach probability of 1. As peats ages and have more decomposition, it needs more time to develop shear strain and ultimately reaches probability of exceeding LSI of 1. This also is affected by the shear strain values that results from the models with one standard deviation above and below the mean. Although the mean case exceeds the 1% limits value for shear strain, the one above and one below mean cases could lead to the probabilities of exceeding LS I not to reach

1. Probability of exceeding LSII for both H4-H7 and H8-H10 peat was very small as the shear strain values didn't reach LSII by 50,000 days.

Sherman island levees have been constructed since around 1870's. This implies around 147 years of consolidation for these levees (~50,000 days). This included primary and secondary consolidation within the peat layer under embankment. The soil testing from the Sherman island site characterized the peat as highly fibrous peat. Within the context of modeling, H1-H3 peat (Fibrous) yielded a shear strain value around 3.2% at 50,000 days which corresponds to the lifetime of Sherman island levee (Figure 5.7). This value of shear strain gives a probability of exceeding LSI of 1 and a probability of exceeding LSII of 0.95 (Figure 5.9) . As peat ages with time, more shear strain will be developed causing the probability of exceeding LSII to reach 1 and may reach LSIII which represents failure based on the approach implemented herein.

Same probability technique could be applied to hydraulic gradient probabilities of exceedance. The probability of exceeding limit states with respect to gradient values is estimated using the values of hydraulic gradient (i) of 0.3, 0.6 and 1 for LS I, II and III gradients respectively. These values for gradient were proposed by Khalilzad and Gabr (2011). Hydraulic gradient values are extracted from PLAXIS 2D at toe location using flow net generated.

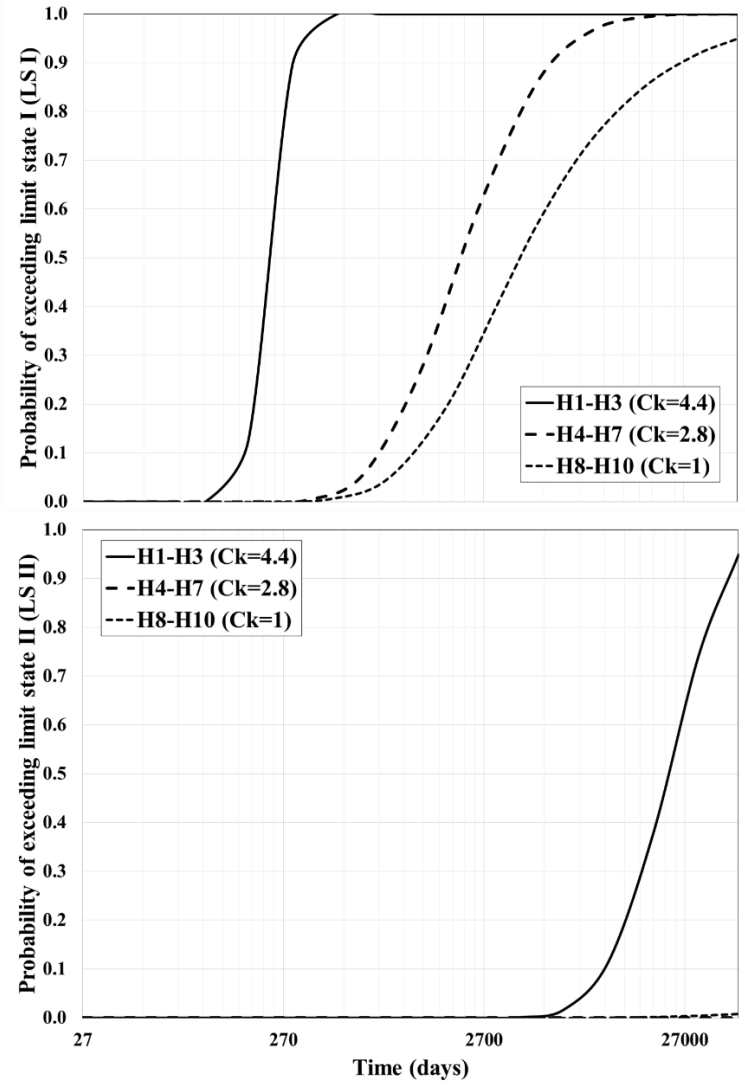


**Figure 5.9. Probability of exceeding LS I and LSII for shear strain for peat with different degree of decomposition**

Figure 5.10 shows the hydraulic gradient values at toe for different peat decomposition state. Hydraulic gradient values were in the range from zero to 0.2 and that gives a probability of exceedance of LS I for gradient to be zero as its limit is 0.3. These ranges of gradient values for around 0.2 agrees with the ranges determined by Jafari at the Sherman island levee location (Jafari et al., 2016). The gradient values had a trend of slight decrease once consolidation

happens for all peat cases. The fibrous peat had the least hydraulic gradient at toe due to the low permeability compared to the other two peat case. H4-H7 and H8-H10 had higher permeability which leads to higher shear strain, higher pore pressure and higher gradient at toe decreasing with time as consolidation happens and the high permeability effect allows for faster dissipation of excess pore water pressure. This shows the importance of including the hydraulic gradient effect with peat decomposition as permeability and void ratio changes with peat aging and time.

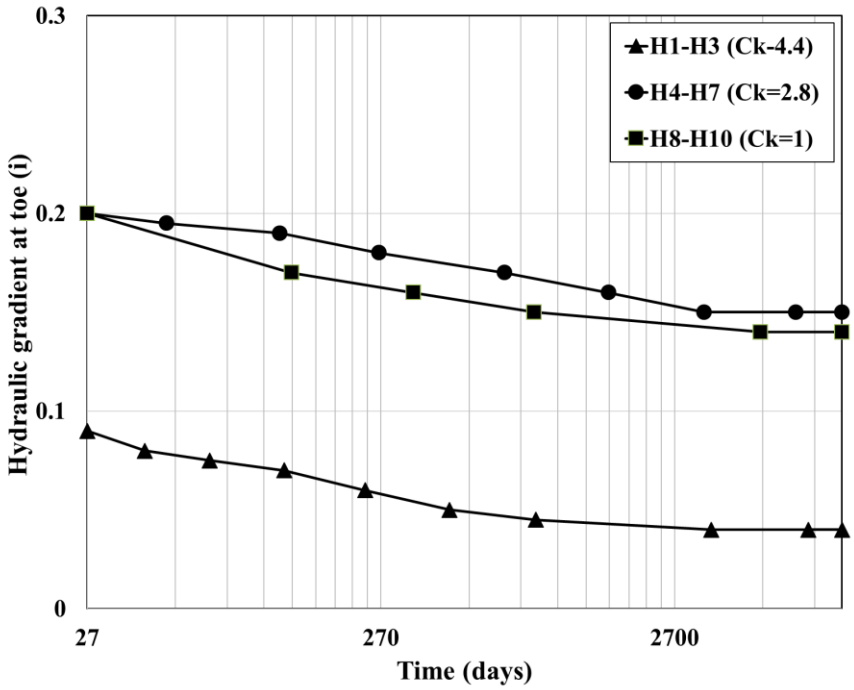


**Figure 5.10. Hydraulic gradient at toe location for peat with different degree of decomposition**

## 5.12 Summary and conclusions

This paper presents the results of an integrated remote-sensing program and finite element modeling for a Sherman Island levee section. At this location, satellite images and in-ground GPS sensors are collecting displacement measurements. These measurements were used for the calibration of a numerical model using the finite element program PLAXIS 2D with mesh updating. The model was used to establish a deterministic performance response under rising water level loading and to investigate the effect of peat decomposition on the deformation response of the levee section. Based on the results presented in this paper, the following conclusions are advanced:

1- Amorphous peat shows stiffer response and lower compressibility than fibrous peat, which agrees with findings reported in the literature (Mesri et al., 2007). The assumption of amorphous peat led to computed displacements that ranged from 10 to 30% less than those with the fibrous peat properties, depending on the location within the domain.

2- The analyses indicated a relatively small mechanistic deformation induced by an "extreme" water level under transient conditions. This is in comparison to the continuous and large deformation induced by the compression of the peat layer. The high-water level will however affect the exit hydraulic gradients and may lead to critical conditions as was discussed by Jafari et al (2016).

3- The variability in the reported values for compression coefficients ($C_c$ and $C_\alpha$) for fibrous and amorphous peat suggests these values need to be better defined as a function of fiber content, state of decomposition and water content. A parameter in

terms of cellulose and lignin content can provide insight as to the chemical composition of the materials and the related shear strength with aging for more accurate performance assessment of the levee.

4- A study on the effect of peat different states of decomposition varies from H1 to H10 on the Von Post scale is performed. Appropriate consolidation and hydraulic properties are assigned. Results are compared with a model where the peat decomposition state is varied manually at time intervals. The deformation and shear strain results showed that it is important to model the real behavior for aging as it does change the deformation response with time. Deformed shape and probability of exceedance for both shear strain and gradient is shown. H1-H3 case reached probability of exceeding LSI of 1 after 270 days. H4-H7 peat took approximately 10,000 days to reach PE of 1. H8-H10 peat had a PE of 1 at around 300,000.

5- Hydraulic gradient at toe values was in the range of 0.1 to 0.2 at the end of the consolidation phase which agree with the results discoed by Jafari et al. (2016) at the Sherman island levee location.

6- The analyses presented indicated the exceedance of LS (I) in terms of deviatoric strain, with the main driving factor being the compressibility of the peat layer. The deformation of the embankment levee is non-uniform due to stress variability with location. Continuous large deformation can lead to compromising the levee hydraulic performance function and translational sliding of the embankment, as presented by Duncan and Houston (1983).

**References**


1. Ajlouni, M. A. (2000). Geotechnical properties of peat and related engineering problems. *PhD Dissertation, University of Illinois at Urbana-Champaign. 15-189.*
2. ASTM International. (2013) ASTM D4427-13. Standard Classification of Peat Samples by Laboratory Testing. West Conshohocken.
3. Edil, T. B., and Wang, X. (2000). Shear strength and $K_o$ of peats and organic soils. *Geotechnics of high water content materials, ASTM STP 1374, West Conshohocken, Pa.,* 209–225.
4. Bennett, V., Abdoun, T., Zeghal, M., Koelewijn, A., Barendse, M., and Dobry, R. (2011). Real-Time Monitoring System and Advanced Characterization Technique for Civil Infrastructure Health Monitoring. *Advances in Instrumentation and Monitoring in Geotech. Eng. Special Issue – Advances in Civil Eng. J., Hindawi Publishing.*
5. Bujang, B. K. Huat, Sina Kazemian, Arun Prasad and Maassoumeh Barghchi (2011). State of an art review of peat: General perspective. *International Journal of the Physical Sciences, 6(8),* 1988-1996.
6. Dhowian, A. W., Edil, T. B. (1980). Consolidation behavior of peats. *Geotech. Testing J., 3(3),* 105-114.
7. Duncan, J. M. (2000). Factors of safety and reliability in geotechnical engineering. *Journal of Geotechnical and Geoenvironmental Engineering, 126,* 307-316.
8. Duncan, James M., and William N. Houston (1983). Estimating failure probabilities for California levees. *Journal of Geotechnical Engineering, 109 (2),* 260-268.

9. DWR, California Department of Water Resources. (2008). Managing an Uncertain Future – Climate change adaptation strategies for California's Water. *White Paper, October, www.climatechange.water.ca.gov*
10. Edil, T. B. (2001). Site characterization in peat and organic soils. *Proc. Int. Conf. In-situ Meas. Soil Properties and Case Histories, Bali, Indonesia,* 49-59.
11. Fox, P. J. (1992). An analysis of one-dimensional creep of peat. *Ph.D. Thesis, University of Wisconsin-Madison, Department of Civil and Environmental Engineering, Madison, Wisconsin.*
12. Huat, B. B. K. (2004). Organic and Peat Soils Engineering. *University Putra, Malaysia Press Serdang, Malaysia.*
13. Khalilzad, M., Gabr, M., and Hynes, M. (2014). Effects of Woody Vegetation on Seepage-Induced Deformation and Related Limit State Analysis of Levees. *Int. J. Geomech., ASCE,* 302-312.
14. Khalilzad, M., Gabr, M. A. (2011), Deformation-Based Limit States for Earth Embankments. *Proceedings of the GeoFrontiers 2011 Conference, Texas, Dallas.*
15. Lea, N., and Brawner, C. O. (1963). Highway design and construction over peat deposits in the lower British Colombia. *Highway Research Rec., 7,* 1–32.
16. Lund, J., Hanak, E., Fleenor, W., Howitt, R., Mount, J., and Moyle, P. (2007). Envisioning Futures for the Sacramento-San Joaquin Delta. *Public Policy Institute of California.*

17. MacFarlane, I. C. and Radforth, N. W. (1965). A study of the physical behavior of peat derivatives under compression. *Proc. 10th Muskeg Res. Conf., National Research Council of Canada.*

18. Magnussen, T. (1994). Studies of the soil atmosphere and related physical characteristics in peat forest soils. *Forest Ecol. Mgmt., 67,* 203–224.

19. Mesri, G. and Ajlouni, M. (2007). Engineering Properties of Fibrous Peats. *Journal of Geotechnical and Geoenvironmental Engineering, ASCE, 7(850),* 850-866.

20. Miyakawa, I. (1960). Some aspects of road construction on peaty or marshy areas in Hokkaido, with particular reference to filling methods. *Civil Engineering Research Institute, Hokkaido Development Bureau, Sapporo, Japan, 54.*

*21.* Mount, J., and Twiss, R. (2005). Subsidence, sea level rise, seismicity in the Sacramento-San Joaquin Delta. *San Francisco Estuary and Watershed Science. Vol. 3, Issue 1*

22. Article 5. http://repositories.cdlib.org/jmie/sfews/vol3/iss1/art5

23. Navid, H., Jafari, Stark, T., Leopold, A., Merry, S. (2016). Three-dimensional levee and floodwall underseepage. *Canadian Geotechnical Journal, 53,* 72-84.

24. Ng, S. Y., and Eischens, G. R. (1983). Repeated short-term consolidation of peats. *Proc. Symp. Testing of Peats and Organic Soils, STP 820, ASTM, W. Conshohocken, Pa.,* 192–206.

*25.* Reinert, Edward Thomas. (2014). Dynamic shake testing of a model levee on peaty organic soil in the Sacramento-San Joaquin Delta. *Ph.D Thesis, UCLA Electronic Theses and Dissertations.*

26. U.S. Army Corps of Engineers. (1997). Engineering and design introduction to probability and reliability methods for use in geotechnical engineering. *Engr. Tech. Letter No. 1110-2-547, Department of the Army, Washington, D.C.*
27. U.S. Army Corps of Engineers. (1998). Risk-based analysis in geotechnical engineering for support of planning studies. *Engrg. Circular No. 1110-2-554, Department of the Army, Washington, D.C.*
28. Von Post, L. (1922). Sveriges geologiska undersoknings torvinventering och nagre av dess hittills vunna resultat. *Sr. Mosskulturfor, 1:* 1–27.
29. Wolff, T. F. (1994). Evaluating the reliability of existing levees. *Rep., Res. Proj.: Reliability of existing levees, prepared for U.S. Army Engineer Waterways Experiment Station Geotechnical Laboratory, Vicksburg, Miss*

# CHAPTER 6. SUMMARY AND CONCLUSIONS

## 6.1 Regarding evaluation of FEMA risk tool and estimation of probabilities of exceeding limit states for embankment dams using numerical analysis

An approach is presented herein to show an expedient procedure of quantifying the probabilities of exceeding limit states using numerical analyses coupled with simple probabilistic model. The FEMA risk tool doesn't have a quantitative way of assigning probabilities of exceeding limit states. That quantitative methodology allows for representation of the structure geometry, soil conditions and storm cycle history. Contour plots is proposed to estimate risk based on assumption for earthquake probability of failure and loss of life potential. The HHD has been analyzed to show the effect of POF on the total risk value using the FEMA risk tool. Based on the results presented in this study, it can be concluded that:

1. Numerical analysis of the Howard A. Hanson dam (HHD) showed a probability of exceeding LSI of $3.9*10^{-3}$, LSII of $4.5*10^{-5}$ and LSIII of $1.2*10^{-6}$ for normal stability, and $2*10^{-5}$ for seepage after 6 cycles. Also, increasing storm cycles increased the probability of exceeding LSI from $2*10^{-6}$ to $3.9*10^{-3}$, LSII from $1.2*10^{-10}$ to $4.5*10^{-5}$ LSIII from $5.3*10^{-14}$ to $1.2*10^{-6}$ going from 3 to 6 cycles respectively. Also, due to material softening, the rate of increase from 5 to 7 cycles has a lower slope than going from 3 to 5 cycles as shear strain rate becomes lower and reaches almost a constant rate.
2. Using the contour plot approach and implementing the probabilities of exceeding limit state III for Howard A. Hanson dam, a loss of life risk values ranging from less than

0.001 to around 0.25 for an overtopping probability of failure form $1*10^{-1}$ to $1*10^{-8}$ (Point x on the contour plot) were estimated. It should be noted that the risk value is based on loss of life potential of 2 and 1 for flood and sunny day respectively, population at risk of 100 people and earthquake probability of failure of $1*10^{-6}$. These contour plots can be used along with quantitative calculation of probabilities of failure using PLAXIS 2D numerical analysis to estimate risk value.

3. Using the FEMA tool for analysis of the HHD and increasing the probability of failure from $8*10^{-5}$ to $2*10^{-3}$ for the same LLP of 10 moved the dam from priority (C) zone to priority (A) respectively. Different methods assign probabilities values that vary by one order of magnitude (Eddleston, 2006). This change the structure hazard classification and urges the need for a quantitative way to calculate probability of failure instead of assigning it in a qualitative way based on observations and engineering judgment.

### 6.2. Regarding development of risk estimator tool for embankment structures (REES) using coupled numerical-probabilistic approach and artificial neural network

A new risk estimation tool for embankment structures that uses coupled numerical probabilistic approach and artificial neural networks is presented in this study. REES (Risk Estimator for Embankment Structures) is developed with MATLAB graphical user interface (GUI) to implement the finite element program PLAXIS 2D results.

1- ***REES*** presents a robust and user-friendly way for geotechnical engineers to estimate probabilities of exceeding limit states for embankment structures along with its loss of life risk. These values along with engineering judgment could be

used for rehabilitation prioritization and decision-making process. The ***REES*** tool developed using Graphical User Interface (GUI) in MATLAB is presented along with description attached in Appendix C.

2- Appropriate soil and geometry parameters ranges have been assigned from the literature to cover a wide range of soil types. Storm effect was introduced using rate of rise of 0.07 m/hr and rate of drawdown of 0.04 m/hr using average values from hydrographs of Hurricane Katrina and Isaac. A base embankment model was analyzed in PLAXIS 2D and 363 run cases with the different properties combinations were performed. The output shear strain values were used to train and test the artificial neural network. Artificial neural network toolbox within MATLAB was used to produce a neural network which showed a training $R^2$ of 98% and prediction $R^2$ of 98% which is an acceptable accuracy. Statistical Analysis of the date showed a mean of the calculated and the predicted shear strains 2.33 and 2.35 respectively, and a standard deviation of 3.73 and 3.69.

3- A parametric study on the effect of geometry, soil parameters and cycles of loading is performed using a base embankment model. As side slopes becomes steeper, shear strain increased from 0.1 to 0.5 to 3.8% going from 4:1 to 3:1 to 2:1 slope at time of 30 days. As embankment friction angle increases from 25 to 36º, there was a decrease in shear strain at toe from 2.4 to 0.5%. For foundation and alluvial friction angle, they had a slight effect on the shear strain at toe. Cohesion of embankment, foundation and alluvial has also a limited effect on the shear strain at toe. The embankment and alluvial permeability had a slight effect on the shear

strain values. The permeability effect of the foundation layer was more significant than embankment and alluvial layer. Increasing the foundation permeability from $6.8*10^{-5}$ to $1*10^{-3}$ cm/s caused an increase in toe shear strain to exceed LSIII. Increasing cycles of loading from 1 to 6 cycles, increased the shear strain by a factor of 10. This illustrates the importance of including loading history in embankment analysis.

4- Relative importance of the input parameters based on parametric study, indicated that side slopes and foundation permeability has the most effect on the shear strain at toe. Side slopes change from the 4:1 to 2:1 caused an increase in the shear strain at toe with a factor of 38. Also, decreasing the foundation permeability by one order of magnitude caused an increase in the shear strain at toe by a factor of 7.

5- A study on the ***REES*** performance is performed. 10 testing cases were used to compare the predicted shear strain and probabilities of exceeding LS I, LS II and LS III using ***REES*** versus PLAXIS 2D. A slight difference is observed between the calculated and the predicted values. This shows the promising use of the REES tool for prediction of probabilities of exceeding limit state for embankment structures.

### 6.3. Regarding effect of peat decomposition on the performance of embankment levee using limit state probabilistic approaches and numerical analysis

This paper presents the results of an integrated remote-sensing program and finite element modeling for a Sherman Island levee section. At this location, satellite images and in-ground GPS sensors are collecting displacement measurements. These measurements were used for

the calibration of a numerical model using the finite element program PLAXIS 2D with mesh updating. The model was used to establish a deterministic performance response under rising water level loading and to investigate the effect of peat decomposition on the deformation response of the levee section. Based on the results presented in this paper, the following conclusions are advanced:

1- Amorphous peat shows stiffer response and lower compressibility than fibrous peat, which agrees with findings reported in the literature (Mesri et al., 2007). The assumption of amorphous peat led to computed displacements that ranged from 10 to 30% less than those with the fibrous peat properties, depending on the location within the domain.

2- The analyses indicated a relatively small mechanistic deformation induced by an "extreme" water level under transient conditions. This is in comparison to the continuous and large deformation induced by the compression of the peat layer. The high-water level will however affect the exit hydraulic gradients and may lead to critical conditions as was discussed by Jafari et al (2016).

3- The variability in the reported values for compression coefficients ($C_c$ and $C_\alpha$) for fibrous and amorphous peat suggests these values need to be better defined as a function of fiber content, state of decomposition and water content. A parameter in terms of cellulose and lignin content can provide insight as to the chemical composition of the materials and the related shear strength with aging for more accurate performance assessment of the levee.

4- A study on the effect of peat different states of decomposition varies from H1 to H10 on the Von Post scale is performed. Appropriate consolidation and hydraulic properties are assigned. Results are compared with a model where the peat decomposition state is varied manually at time intervals. The deformation and shear strain results showed that it is important to model the real behavior for aging as it does change the deformation response with time. Deformed shape and probability of exceedance for both shear strain and gradient is shown. H1-H3 case reached probability of exceeding LSI of 1 after 270 days. H4-H7 peat took approximately 10,000 days to reach PE of 1. H8-H10 peat had a PE of 1 at around 300,000.

5- Hydraulic gradient at toe values was in the range of 0.1 to 0.2 at the end of the consolidation phase which agree with the results discoed by Jafari et al. (2016) at the Sherman island levee location.

6- The analyses presented indicated the exceedance of LS (I) in terms of deviatoric strain, with the main driving factor being the compressibility of the peat layer. The deformation of the embankment levee is non-uniform due to stress variability with location. Continuous large deformation can lead to compromising the levee hydraulic performance function and translational sliding of the embankment, as presented by Duncan and Houston (1983).

## 6.4. Contributions to the state of the art

1. Development of a user-friendly risk tool “REES: Risk estimator for Embankment Structures” to estimate deviatoric shear strain, probability of

exceeding limit states and loss of life risk for earth embankment structures. The tool could be fine-tuned when more data becomes available.

2. Research study of the effect of embankment geometry, soil properties and storm cycles on the deformation and shear strain response at key locations of the embankment. Crest width, crest height and upstream and downstream slopes was varied as geometry parameters according to a probability distribution. Soil properties such as friction angle, unit weight, cohesion and permeability was also assumed based on probability distribution to vary within ranges from the literature. Storm cycle effect was introduced using average rate of rise and drawdown from hurricanes Katrina and Isaac.
3. Research study of the effect of peat decomposition of the Sacramento delta levee using PLAXIS 2D and remote sensing and field monitoring. Calibration of the numerical model using field data was introduced and presented. Peat decomposition states ranging from fibrous to amorphous case was investigates using numerical analysis. More research should be performed to develop a constitutive soil model that takes into account peat decomposition with time based on peat properties and link that to its geotechnical properties.

## 6.5. Future work

1. Development of a model to simulate peat decomposition with time and its effect on geotechnical properties of peat. This model could be incorporated into the finite element program PLAXIS as a user-defined soil model in

FORTRAN coding language. This new model will be a big step forward in modeling peat behavior and its decomposition effects.

2. Expanding the finite element analysis to investigate more soil profile combinations in order to be able to fine-tune REES tool and enhance its predication ability. Also, finite element runs for embankment profiles that includes peat and soft soils could be incorporated into the tool and update the graphical user interface and the neural network accordingly. A study on the effect of varying thicknesses for foundation, alluvial layers could be carried out as a future study. Also, a more non-homogenous embankment profiles could be investigates such as using a core layer, a drainage layer, etc.
3. Adding the economic risk as an additional risk criteria based on economic consequences. The economic consequences were already defined as a part on the REES tool in this research, but linking it to the risk calculation could be carried out as future work.
4. Transferring the knowledge about probabilistic limit-state into decision makers and private sector and encourage its usage along with traditional approaches (i.e. Factor of safety)

# Appendices

# APPENDIX A. Properties of PLAXIS 2D cases for current study

| Case no | Crest Width (m) | Upstream slope | Downstream slope | Crest Height (m) | Embankment | | | | | Foundation | | | | | Alluvial | | | | |
|---|---|---|---|---|---|---|---|---|---|---|---|---|---|---|---|---|---|---|---|
| | | | | | φ' (o) | $E_{50}$ (kPa) | c' (kPa) | $\gamma_{sat}$ (kN/m3) | k (cm/s) | φ' (o) | $E_{50}$ (kPa) | c' (kPa) | $\gamma_{sat}$ (kN/m3) | k (cm/s) | φ' (o) | $E_{50}$ (kPa) | c' (kPa) | $\gamma_{sat}$ (kN/m3) | k (cm/s) |
| 1A | 1.8 | 3.0 | 2.5 | 3.0 | 28 | 7333 | 3 | 16.21 | 5.15E-07 | 33 | 17500 | 0 | 20.49 | 4.88E-02 | 32 | 17500 | 0 | 20.44 | 1.33E-01 |
| 1B | 1.8 | 3.0 | 2.5 | 3.0 | 28 | 6000 | 3 | 16.21 | 5.15E-07 | 33 | 17500 | 0 | 20.49 | 4.88E-02 | 32 | 17500 | 0 | 20.44 | 1.33E-01 |
| 1C | 1.8 | 3.0 | 2.5 | 3.0 | 28 | 4667 | 3 | 16.21 | 5.15E-07 | 33 | 17500 | 0 | 20.49 | 4.88E-02 | 32 | 17500 | 0 | 20.44 | 1.33E-01 |
| 2A | 2.0 | 2.5 | 3.0 | 3.4 | 29 | 7333 | 3 | 14.59 | 5.41E-07 | 35 | 17500 | 0 | 20.54 | 8.87E-02 | 32 | 17500 | 0 | 20.71 | 9.26E-02 |
| 2B | 2.0 | 2.5 | 3.0 | 3.4 | 29 | 6000 | 3 | 14.59 | 5.41E-07 | 35 | 17500 | 0 | 20.54 | 8.87E-02 | 32 | 17500 | 0 | 20.71 | 9.26E-02 |
| 2C | 2.0 | 2.5 | 3.0 | 3.4 | 29 | 4667 | 3 | 14.59 | 5.41E-07 | 35 | 17500 | 0 | 20.54 | 8.87E-02 | 32 | 17500 | 0 | 20.71 | 9.26E-02 |
| 3A | 1.9 | 3.0 | 2.0 | 3.3 | 27 | 7333 | 3 | 15.58 | 2.74E-07 | 32 | 17500 | 0 | 20.03 | 9.37E-02 | 40 | 37500 | 0 | 21.90 | 1.64E-01 |
| 3B | 1.9 | 3.0 | 2.0 | 3.3 | 27 | 6000 | 3 | 15.58 | 2.74E-07 | 32 | 17500 | 0 | 20.03 | 9.37E-02 | 40 | 37500 | 0 | 21.90 | 1.64E-01 |
| 3C | 1.9 | 3.0 | 2.0 | 3.3 | 27 | 4667 | 3 | 15.58 | 2.74E-07 | 32 | 17500 | 0 | 20.03 | 9.37E-02 | 40 | 37500 | 0 | 21.90 | 1.64E-01 |
| 4A | 2.4 | 3.0 | 3.0 | 4.0 | 28 | 7333 | 3 | 15.86 | 5.35E-07 | 35 | 17500 | 0 | 20.35 | 8.32E-02 | 40 | 37500 | 0 | 21.89 | 6.05E-02 |
| 4B | 2.4 | 3.0 | 3.0 | 4.0 | 28 | 6000 | 3 | 15.86 | 5.35E-07 | 35 | 17500 | 0 | 20.35 | 8.32E-02 | 40 | 37500 | 0 | 21.89 | 6.05E-02 |
| 4C | 2.4 | 3.0 | 3.0 | 4.0 | 28 | 4667 | 3 | 15.86 | 5.35E-07 | 35 | 17500 | 0 | 20.35 | 8.32E-02 | 40 | 37500 | 0 | 21.89 | 6.05E-02 |
| 5A | 2.2 | 3.0 | 3.0 | 4.9 | 28 | 7333 | 3 | 15.31 | 6.58E-07 | 33 | 17500 | 0 | 20.78 | 9.23E-02 | 44 | 65500 | 0 | 23.80 | 8.85E-02 |
| 5B | 2.2 | 3.0 | 3.0 | 4.9 | 28 | 6000 | 3 | 15.31 | 6.58E-07 | 33 | 17500 | 0 | 20.78 | 9.23E-02 | 44 | 65500 | 0 | 23.80 | 8.85E-02 |
| 5C | 2.2 | 3.0 | 3.0 | 4.9 | 28 | 4667 | 3 | 15.31 | 6.58E-07 | 33 | 17500 | 0 | 20.78 | 9.23E-02 | 44 | 65500 | 0 | 23.80 | 8.85E-02 |
| 6A | 1.6 | 2.5 | 3.0 | 1.9 | 29 | 7333 | 3 | 15.99 | 4.87E-07 | 35 | 17500 | 0 | 20.33 | 6.46E-02 | 43 | 65500 | 0 | 23.10 | 1.03E-01 |
| 6B | 1.6 | 2.5 | 3.0 | 1.9 | 29 | 6000 | 3 | 15.99 | 4.87E-07 | 35 | 17500 | 0 | 20.33 | 6.46E-02 | 43 | 65500 | 0 | 23.10 | 1.03E-01 |
| 6C | 1.6 | 2.5 | 3.0 | 1.9 | 29 | 4667 | 3 | 15.99 | 4.87E-07 | 35 | 17500 | 0 | 20.33 | 6.46E-02 | 43 | 65500 | 0 | 23.10 | 1.03E-01 |
| 7A | 1.7 | 2.5 | 2.0 | 5.5 | 27 | 7333 | 3 | 15.66 | 7.64E-07 | 40 | 37500 | 0 | 21.88 | 1.19E-01 | 27 | 6000 | 2 | 14.38 | 5.11E-07 |
| 7B | 1.7 | 2.5 | 2.0 | 5.5 | 27 | 6000 | 3 | 15.66 | 7.64E-07 | 40 | 37500 | 0 | 21.88 | 1.19E-01 | 27 | 6000 | 2 | 14.38 | 5.11E-07 |
| 7C | 1.7 | 2.5 | 2.0 | 5.5 | 27 | 4667 | 3 | 15.66 | 7.64E-07 | 40 | 37500 | 0 | 21.88 | 1.19E-01 | 27 | 6000 | 2 | 14.38 | 5.11E-07 |
| 8A | 1.6 | 4.0 | 3.0 | 4.3 | 28 | 7333 | 4 | 15.14 | 5.97E-07 | 39 | 37500 | 0 | 21.76 | 2.88E-02 | 29 | 6000 | 2 | 15.36 | 4.45E-07 |
| 8B | 1.6 | 4.0 | 3.0 | 4.3 | 28 | 6000 | 4 | 15.14 | 5.97E-07 | 39 | 37500 | 0 | 21.76 | 2.88E-02 | 29 | 6000 | 2 | 15.36 | 4.45E-07 |
| 8C | 1.6 | 4.0 | 3.0 | 4.3 | 28 | 4667 | 4 | 15.14 | 5.97E-07 | 39 | 37500 | 0 | 21.76 | 2.88E-02 | 29 | 6000 | 2 | 15.36 | 4.45E-07 |
| 9A | 2.2 | 2.5 | 2.5 | 3.0 | 28 | 7333 | 3 | 15.80 | 4.36E-07 | 40 | 37500 | 0 | 21.97 | 1.06E-01 | 27 | 6000 | 2 | 15.83 | 5.30E-07 |
| 9B | 2.2 | 2.5 | 2.5 | 3.0 | 28 | 6000 | 3 | 15.80 | 4.36E-07 | 40 | 37500 | 0 | 21.97 | 1.06E-01 | 27 | 6000 | 2 | 15.83 | 5.30E-07 |
| 9C | 2.2 | 2.5 | 2.5 | 3.0 | 28 | 4667 | 3 | 15.80 | 4.36E-07 | 40 | 37500 | 0 | 21.97 | 1.06E-01 | 27 | 6000 | 2 | 15.83 | 5.30E-07 |
| 10A | 2.1 | 3.5 | 3.0 | 3.4 | 29 | 7333 | 2 | 15.54 | 4.80E-07 | 39 | 37500 | 0 | 22.37 | 1.23E-01 | 29 | 6000 | 8 | 20.61 | 3.52E-05 |
| 10B | 2.1 | 3.5 | 3.0 | 3.4 | 29 | 6000 | 2 | 15.54 | 4.80E-07 | 39 | 37500 | 0 | 22.37 | 1.23E-01 | 29 | 6000 | 8 | 20.61 | 3.52E-05 |
| 10C | 2.1 | 3.5 | 3.0 | 3.4 | 29 | 4667 | 2 | 15.54 | 4.80E-07 | 39 | 37500 | 0 | 22.37 | 1.23E-01 | 29 | 6000 | 8 | 20.61 | 3.52E-05 |
| 11A | 1.3 | 3.0 | 3.0 | 3.8 | 29 | 7333 | 4 | 15.45 | 4.60E-07 | 41 | 37500 | 0 | 21.80 | 7.28E-02 | 32 | 15000 | 8 | 19.42 | 5.14E-05 |
| 11B | 1.3 | 3.0 | 3.0 | 3.8 | 29 | 6000 | 4 | 15.45 | 4.60E-07 | 41 | 37500 | 0 | 21.80 | 7.28E-02 | 32 | 15000 | 8 | 19.42 | 5.14E-05 |
| 11C | 1.3 | 3.0 | 3.0 | 3.8 | 29 | 4667 | 4 | 15.45 | 4.60E-07 | 41 | 37500 | 0 | 21.80 | 7.28E-02 | 32 | 15000 | 8 | 19.42 | 5.14E-05 |
| 12A | 1.2 | 2.5 | 2.5 | 3.8 | 28 | 7333 | 2 | 15.27 | 5.45E-07 | 40 | 37500 | 0 | 22.03 | 9.91E-02 | 30 | 15000 | 8 | 19.58 | 3.99E-05 |
| 12B | 1.2 | 2.5 | 2.5 | 3.8 | 28 | 6000 | 2 | 15.27 | 5.45E-07 | 40 | 37500 | 0 | 22.03 | 9.91E-02 | 30 | 15000 | 8 | 19.58 | 3.99E-05 |
| 12C | 1.2 | 2.5 | 2.5 | 3.8 | 28 | 4667 | 2 | 15.27 | 5.45E-07 | 40 | 37500 | 0 | 22.03 | 9.91E-02 | 30 | 15000 | 8 | 19.58 | 3.99E-05 |

| | | | | | | | | | | | | | | | | | | |
|---|---|---|---|---|---|---|---|---|---|---|---|---|---|---|---|---|---|---|
| **13A** | **2.0** | **3.5** | **4.0** | **4.7** | **27** | **7333** | **2** | **15.74** | **6.30E-07** | **44** | **65500** | **0** | **22.72** | **1.11E-01** | **26** | **15000** | **14** | **15.66** | **7.96E-06** |
| **13B** | **2.0** | **3.5** | **4.0** | **4.7** | **27** | **6000** | **2** | **15.74** | **6.30E-07** | **44** | **65500** | **0** | **22.72** | **1.11E-01** | **26** | **15000** | **14** | **15.66** | **7.96E-06** |
| **13C** | **2.0** | **3.5** | **4.0** | **4.7** | **27** | **4667** | **2** | **15.74** | **6.30E-07** | **44** | **65500** | **0** | **22.72** | **1.11E-01** | **26** | **15000** | **14** | **15.66** | **7.96E-06** |
| **14A** | **2.3** | **3.0** | **3.0** | **4.6** | **28** | **7333** | **3** | **14.59** | **4.57E-07** | **43** | **65500** | **0** | **22.91** | **8.06E-02** | **21** | **15000** | **17** | **15.91** | **5.37E-06** |
| **14B** | **2.3** | **3.0** | **3.0** | **4.6** | **28** | **6000** | **3** | **14.59** | **4.57E-07** | **43** | **65500** | **0** | **22.91** | **8.06E-02** | **21** | **15000** | **17** | **15.91** | **5.37E-06** |
| **14C** | **2.3** | **3.0** | **3.0** | **4.6** | **28** | **4667** | **3** | **14.59** | **4.57E-07** | **43** | **65500** | **0** | **22.91** | **8.06E-02** | **21** | **15000** | **17** | **15.91** | **5.37E-06** |
| **15A** | **2.1** | **2.0** | **3.0** | **3.2** | **27** | **7333** | **3** | **15.46** | **5.81E-07** | **43** | **65500** | **0** | **23.52** | **1.01E-01** | **24** | **15000** | **11** | **15.95** | **9.56E-06** |
| **15B** | **2.1** | **2.0** | **3.0** | **3.2** | **27** | **6000** | **3** | **15.46** | **5.81E-07** | **43** | **65500** | **0** | **23.52** | **1.01E-01** | **24** | **15000** | **11** | **15.95** | **9.56E-06** |
| **15C** | **2.1** | **2.0** | **3.0** | **3.2** | **27** | **4667** | **3** | **15.46** | **5.81E-07** | **43** | **65500** | **0** | **23.52** | **1.01E-01** | **24** | **15000** | **11** | **15.95** | **9.56E-06** |
| **16A** | **1.4** | **2.5** | **3.0** | **3.4** | **30** | **16667** | **4** | **15.37** | **7.95E-07** | **44** | **65500** | **0** | **23.20** | **1.15E-01** | **33** | **32500** | **11** | **18.76** | **1.52E-06** |
| **16B** | **1.4** | **2.5** | **3.0** | **3.4** | **30** | **15000** | **4** | **15.37** | **7.95E-07** | **44** | **65500** | **0** | **23.20** | **1.15E-01** | **33** | **32500** | **11** | **18.76** | **1.52E-06** |
| **16C** | **1.4** | **2.5** | **3.0** | **3.4** | **30** | **13333** | **4** | **15.37** | **7.95E-07** | **44** | **65500** | **0** | **23.20** | **1.15E-01** | **33** | **32500** | **11** | **18.76** | **1.52E-06** |
| **17A** | **1.4** | **3.0** | **2.5** | **4.3** | **28** | **7333** | **3** | **15.15** | **6.59E-07** | **43** | **65500** | **0** | **23.31** | **6.99E-02** | **36** | **32500** | **22** | **18.67** | **2.03E-06** |
| **17B** | **1.4** | **3.0** | **2.5** | **4.3** | **28** | **6000** | **3** | **15.15** | **6.59E-07** | **43** | **65500** | **0** | **23.31** | **6.99E-02** | **36** | **32500** | **22** | **18.67** | **2.03E-06** |
| **17C** | **1.4** | **3.0** | **2.5** | **4.3** | **28** | **4667** | **3** | **15.15** | **6.59E-07** | **43** | **65500** | **0** | **23.31** | **6.99E-02** | **36** | **32500** | **22** | **18.67** | **2.03E-06** |
| **18A** | **2.4** | **3.0** | **3.5** | **3.7** | **29** | **7333** | **3** | **16.09** | **6.41E-07** | **43** | **65500** | **0** | **22.95** | **1.29E-01** | **35** | **32500** | **17** | **19.67** | **1.56E-06** |
| **18B** | **2.4** | **3.0** | **3.5** | **3.7** | **29** | **6000** | **3** | **16.09** | **6.41E-07** | **43** | **65500** | **0** | **22.95** | **1.29E-01** | **35** | **32500** | **17** | **19.67** | **1.56E-06** |
| **18C** | **2.4** | **3.0** | **3.5** | **3.7** | **29** | **4667** | **3** | **16.09** | **6.41E-07** | **43** | **65500** | **0** | **22.95** | **1.29E-01** | **35** | **32500** | **17** | **19.67** | **1.56E-06** |
| **19A** | **1.9** | **2.0** | **3.0** | **4.7** | **28** | **7333** | **2** | **15.26** | **3.71E-07** | **28** | **6000** | **3** | **16.37** | **1.38E-07** | **30** | **17500** | **0** | **20.44** | **3.61E-02** |
| **19B** | **1.9** | **2.0** | **3.0** | **4.7** | **28** | **6000** | **2** | **15.26** | **3.71E-07** | **28** | **6000** | **3** | **16.37** | **1.38E-07** | **30** | **17500** | **0** | **20.44** | **3.61E-02** |
| **19C** | **1.9** | **2.0** | **3.0** | **4.7** | **28** | **4667** | **2** | **15.26** | **3.71E-07** | **28** | **6000** | **3** | **16.37** | **1.38E-07** | **30** | **17500** | **0** | **20.44** | **3.61E-02** |
| **20A** | **1.8** | **2.0** | **3.0** | **2.9** | **29** | **7333** | **3** | **16.02** | **4.17E-07** | **28** | **6000** | **3** | **15.11** | **5.79E-07** | **32** | **17500** | **0** | **20.79** | **1.20E-01** |
| **20B** | **1.8** | **2.0** | **3.0** | **2.9** | **29** | **6000** | **3** | **16.02** | **4.17E-07** | **28** | **6000** | **3** | **15.11** | **5.79E-07** | **32** | **17500** | **0** | **20.79** | **1.20E-01** |
| **20C** | **1.8** | **2.0** | **3.0** | **2.9** | **29** | **4667** | **3** | **16.02** | **4.17E-07** | **28** | **6000** | **3** | **15.11** | **5.79E-07** | **32** | **17500** | **0** | **20.79** | **1.20E-01** |
| **21A** | **2.5** | **3.0** | **2.5** | **4.0** | **27** | **7333** | **1** | **16.29** | **5.45E-07** | **29** | **6000** | **3** | **14.60** | **5.05E-07** | **39** | **37500** | **0** | **22.49** | **1.04E-01** |
| **21B** | **2.5** | **3.0** | **2.5** | **4.0** | **27** | **6000** | **1** | **16.29** | **5.45E-07** | **29** | **6000** | **3** | **14.60** | **5.05E-07** | **39** | **37500** | **0** | **22.49** | **1.04E-01** |
| **21C** | **2.5** | **3.0** | **2.5** | **4.0** | **27** | **4667** | **1** | **16.29** | **5.45E-07** | **29** | **6000** | **3** | **14.60** | **5.05E-07** | **39** | **37500** | **0** | **22.49** | **1.04E-01** |
| **22A** | **1.7** | **3.0** | **2.0** | **3.8** | **27** | **7333** | **3** | **15.61** | **4.88E-07** | **27** | **6000** | **1** | **16.53** | **3.80E-07** | **40** | **37500** | **0** | **21.77** | **1.04E-01** |
| **22B** | **1.7** | **3.0** | **2.0** | **3.8** | **27** | **6000** | **3** | **15.61** | **4.88E-07** | **27** | **6000** | **1** | **16.53** | **3.80E-07** | **40** | **37500** | **0** | **21.77** | **1.04E-01** |
| **22C** | **1.7** | **3.0** | **2.0** | **3.8** | **27** | **4667** | **3** | **15.61** | **4.88E-07** | **27** | **6000** | **1** | **16.53** | **3.80E-07** | **40** | **37500** | **0** | **21.77** | **1.04E-01** |
| **23A** | **2.1** | **2.5** | **2.5** | **4.9** | **27** | **7333** | **3** | **15.87** | **2.37E-07** | **28** | **6000** | **2** | **15.66** | **5.72E-07** | **44** | **65500** | **0** | **23.95** | **1.27E-01** |
| **23B** | **2.1** | **2.5** | **2.5** | **4.9** | **27** | **6000** | **3** | **15.87** | **2.37E-07** | **28** | **6000** | **2** | **15.66** | **5.72E-07** | **44** | **65500** | **0** | **23.95** | **1.27E-01** |
| **23C** | **2.1** | **2.5** | **2.5** | **4.9** | **27** | **4667** | **3** | **15.87** | **2.37E-07** | **28** | **6000** | **2** | **15.66** | **5.72E-07** | **44** | **65500** | **0** | **23.95** | **1.27E-01** |
| **24A** | **2.2** | **3.0** | **3.0** | **2.2** | **28** | **7333** | **3** | **16.08** | **2.55E-07** | **29** | **6000** | **4** | **15.97** | **3.74E-07** | **44** | **65500** | **0** | **23.29** | **1.36E-01** |
| **24B** | **2.2** | **3.0** | **3.0** | **2.2** | **28** | **6000** | **3** | **16.08** | **2.55E-07** | **29** | **6000** | **4** | **15.97** | **3.74E-07** | **44** | **65500** | **0** | **23.29** | **1.36E-01** |
| **24C** | **2.2** | **3.0** | **3.0** | **2.2** | **28** | **4667** | **3** | **16.08** | **2.55E-07** | **29** | **6000** | **4** | **15.97** | **3.74E-07** | **44** | **65500** | **0** | **23.29** | **1.36E-01** |
| **25A** | **2.3** | **2.0** | **2.5** | **3.5** | **28** | **7333** | **3** | **15.65** | **6.74E-07** | **28** | **6000** | **2** | **15.48** | **6.47E-07** | **28** | **6000** | **1** | **16.27** | **1.84E-07** |
| **25B** | **2.3** | **2.0** | **2.5** | **3.5** | **28** | **6000** | **3** | **15.65** | **6.74E-07** | **28** | **6000** | **2** | **15.48** | **6.47E-07** | **28** | **6000** | **1** | **16.27** | **1.84E-07** |
| **25C** | **2.3** | **2.0** | **2.5** | **3.5** | **28** | **4667** | **3** | **15.65** | **6.74E-07** | **28** | **6000** | **2** | **15.48** | **6.47E-07** | **28** | **6000** | **1** | **16.27** | **1.84E-07** |

| | | | | | | | | | | | | | | | | | | |
|---|---|---|---|---|---|---|---|---|---|---|---|---|---|---|---|---|---|---|
| **26A** | **1.7** | **3.0** | **3.0** | **3.6** | **28** | **7333** | **4** | **16.02** | **3.80E-07** | **28** | **6000** | **3** | **15.09** | **5.16E-07** | **28** | **6000** | **3** | **15.76** | **7.56E-07** |
| **26B** | **1.7** | **3.0** | **3.0** | **3.6** | **28** | **6000** | **4** | **16.02** | **3.80E-07** | **28** | **6000** | **3** | **15.09** | **5.16E-07** | **28** | **6000** | **3** | **15.76** | **7.56E-07** |
| **26C** | **1.7** | **3.0** | **3.0** | **3.6** | **28** | **4667** | **4** | **16.02** | **3.80E-07** | **28** | **6000** | **3** | **15.09** | **5.16E-07** | **28** | **6000** | **3** | **15.76** | **7.56E-07** |
| **27A** | **2.1** | **3.0** | **2.5** | **1.2** | **29** | **7333** | **3** | **14.94** | **8.48E-07** | **27** | **6000** | **2** | **13.86** | **2.35E-07** | **28** | **6000** | **1** | **15.03** | **5.95E-07** |
| **27B** | **2.1** | **3.0** | **2.5** | **1.2** | **29** | **6000** | **3** | **14.94** | **8.48E-07** | **27** | **6000** | **2** | **13.86** | **2.35E-07** | **28** | **6000** | **1** | **15.03** | **5.95E-07** |
| **27C** | **2.1** | **3.0** | **2.5** | **1.2** | **29** | **4667** | **3** | **14.94** | **8.48E-07** | **27** | **6000** | **2** | **13.86** | **2.35E-07** | **28** | **6000** | **1** | **15.03** | **5.95E-07** |
| **28A** | **8.3** | **3.0** | **3.0** | **58.4** | **31** | **16667** | **8** | **20.55** | **4.45E-05** | **29** | **6000** | **8** | **19.72** | **4.16E-05** | **30** | **15000** | **7** | **18.84** | **4.38E-05** |
| **28B** | **8.3** | **3.0** | **3.0** | **58.4** | **31** | **15000** | **8** | **20.55** | **4.45E-05** | **29** | **6000** | **8** | **19.72** | **4.16E-05** | **30** | **15000** | **7** | **18.84** | **4.38E-05** |
| **28C** | **8.3** | **3.0** | **3.0** | **58.4** | **31** | **13333** | **8** | **20.55** | **4.45E-05** | **29** | **6000** | **8** | **19.72** | **4.16E-05** | **30** | **15000** | **7** | **18.84** | **4.38E-05** |
| **29A** | **10.5** | **2.0** | **2.0** | **42.8** | **29** | **7333** | **8** | **19.17** | **5.79E-05** | **35** | **15000** | **7** | **20.31** | **5.68E-05** | **32** | **15000** | **8** | **20.40** | **3.60E-05** |
| **29B** | **10.5** | **2.0** | **2.0** | **42.8** | **29** | **6000** | **8** | **19.17** | **5.79E-05** | **35** | **15000** | **7** | **20.31** | **5.68E-05** | **32** | **15000** | **8** | **20.40** | **3.60E-05** |
| **29C** | **10.5** | **2.0** | **2.0** | **42.8** | **29** | **4667** | **8** | **19.17** | **5.79E-05** | **35** | **15000** | **7** | **20.31** | **5.68E-05** | **32** | **15000** | **8** | **20.40** | **3.60E-05** |
| **30A** | **9.5** | **3.0** | **3.0** | **60.8** | **33** | **16667** | **8** | **19.65** | **4.78E-05** | **34** | **15000** | **7** | **20.48** | **6.79E-05** | **33** | **15000** | **7** | **19.47** | **4.53E-05** |
| **30B** | **9.5** | **3.0** | **3.0** | **60.8** | **33** | **15000** | **8** | **19.65** | **4.78E-05** | **34** | **15000** | **7** | **20.48** | **6.79E-05** | **33** | **15000** | **7** | **19.47** | **4.53E-05** |
| **30C** | **9.5** | **3.0** | **3.0** | **60.8** | **33** | **13333** | **8** | **19.65** | **4.78E-05** | **34** | **15000** | **7** | **20.48** | **6.79E-05** | **33** | **15000** | **7** | **19.47** | **4.53E-05** |
| **31A** | **10.3** | **2.5** | **2.5** | **53.1** | **32** | **16667** | **6** | **18.71** | **4.01E-05** | **32** | **6000** | **8** | **19.33** | **6.62E-05** | **20** | **15000** | **11** | **15.86** | **4.51E-06** |
| **31B** | **10.3** | **2.5** | **2.5** | **53.1** | **32** | **15000** | **6** | **18.71** | **4.01E-05** | **32** | **6000** | **8** | **19.33** | **6.62E-05** | **20** | **15000** | **11** | **15.86** | **4.51E-06** |
| **31C** | **10.3** | **2.5** | **2.5** | **53.1** | **32** | **13333** | **6** | **18.71** | **4.01E-05** | **32** | **6000** | **8** | **19.33** | **6.62E-05** | **20** | **15000** | **11** | **15.86** | **4.51E-06** |
| **32A** | **11.8** | **2.5** | **3.0** | **43.0** | **31** | **16667** | **7** | **19.03** | **4.26E-05** | **29** | **6000** | **8** | **19.21** | **5.45E-05** | **26** | **15000** | **16** | **15.30** | **5.94E-06** |
| **32B** | **11.8** | **2.5** | **3.0** | **43.0** | **31** | **15000** | **7** | **19.03** | **4.26E-05** | **29** | **6000** | **8** | **19.21** | **5.45E-05** | **26** | **15000** | **16** | **15.30** | **5.94E-06** |
| **32C** | **11.8** | **2.5** | **3.0** | **43.0** | **31** | **13333** | **7** | **19.03** | **4.26E-05** | **29** | **6000** | **8** | **19.21** | **5.45E-05** | **26** | **15000** | **16** | **15.30** | **5.94E-06** |
| **33A** | **7.5** | **3.0** | **3.0** | **59.3** | **31** | **16667** | **7** | **18.70** | **2.79E-05** | **30** | **15000** | **7** | **19.89** | **3.94E-05** | **26** | **15000** | **11** | **15.59** | **7.64E-06** |
| **33B** | **7.5** | **3.0** | **3.0** | **59.3** | **31** | **15000** | **7** | **18.70** | **2.79E-05** | **30** | **15000** | **7** | **19.89** | **3.94E-05** | **26** | **15000** | **11** | **15.59** | **7.64E-06** |
| **33C** | **7.5** | **3.0** | **3.0** | **59.3** | **31** | **13333** | **7** | **18.70** | **2.79E-05** | **30** | **15000** | **7** | **19.89** | **3.94E-05** | **26** | **15000** | **11** | **15.59** | **7.64E-06** |
| **34A** | **7.3** | **3.0** | **3.0** | **57.2** | **31** | **16667** | **7** | **19.64** | **3.56E-05** | **31** | **15000** | **6** | **19.69** | **6.05E-05** | **35** | **32500** | **16** | **19.27** | **1.58E-06** |
| **34B** | **7.3** | **3.0** | **3.0** | **57.2** | **31** | **15000** | **7** | **19.64** | **3.56E-05** | **31** | **15000** | **6** | **19.69** | **6.05E-05** | **35** | **32500** | **16** | **19.27** | **1.58E-06** |
| **34C** | **7.3** | **3.0** | **3.0** | **57.2** | **31** | **13333** | **7** | **19.64** | **3.56E-05** | **31** | **15000** | **6** | **19.69** | **6.05E-05** | **35** | **32500** | **16** | **19.27** | **1.58E-06** |
| **35A** | **4.7** | **2.5** | **2.0** | **62.6** | **28** | **7333** | **8** | **20.18** | **2.64E-05** | **32** | **15000** | **7** | **19.86** | **4.87E-05** | **34** | **32500** | **19** | **20.62** | **2.41E-06** |
| **35B** | **4.7** | **2.5** | **2.0** | **62.6** | **28** | **6000** | **8** | **20.18** | **2.64E-05** | **32** | **15000** | **7** | **19.86** | **4.87E-05** | **34** | **32500** | **19** | **20.62** | **2.41E-06** |
| **35C** | **4.7** | **2.5** | **2.0** | **62.6** | **28** | **4667** | **8** | **20.18** | **2.64E-05** | **32** | **15000** | **7** | **19.86** | **4.87E-05** | **34** | **32500** | **19** | **20.62** | **2.41E-06** |
| **36A** | **9.8** | **3.5** | **2.5** | **73.2** | **31** | **16667** | **7** | **19.04** | **4.14E-05** | **29** | **6000** | **6** | **19.87** | **7.30E-05** | **35** | **32500** | **6** | **18.68** | **2.52E-06** |
| **36B** | **9.8** | **3.5** | **2.5** | **73.2** | **31** | **15000** | **7** | **19.04** | **4.14E-05** | **29** | **6000** | **6** | **19.87** | **7.30E-05** | **35** | **32500** | **6** | **18.68** | **2.52E-06** |
| **36C** | **9.8** | **3.5** | **2.5** | **73.2** | **31** | **13333** | **7** | **19.04** | **4.14E-05** | **29** | **6000** | **6** | **19.87** | **7.30E-05** | **35** | **32500** | **6** | **18.68** | **2.52E-06** |
| **37A** | **13.0** | **3.0** | **2.5** | **67.7** | **30** | **7333** | **7** | **19.66** | **3.19E-05** | **25** | **15000** | **12** | **15.11** | **3.38E-06** | **32** | **17500** | **0** | **19.69** | **1.28E-01** |
| **37B** | **13.0** | **3.0** | **2.5** | **67.7** | **30** | **6000** | **7** | **19.66** | **3.19E-05** | **25** | **15000** | **12** | **15.11** | **3.38E-06** | **32** | **17500** | **0** | **19.69** | **1.28E-01** |
| **37C** | **13.0** | **3.0** | **2.5** | **67.7** | **30** | **4667** | **7** | **19.66** | **3.19E-05** | **25** | **15000** | **12** | **15.11** | **3.38E-06** | **32** | **17500** | **0** | **19.69** | **1.28E-01** |
| **38A** | **8.9** | **2.5** | **3.0** | **77.4** | **29** | **7333** | **7** | **19.10** | **3.82E-05** | **26** | **15000** | **12** | **16.20** | **5.34E-06** | **33** | **17500** | **0** | **20.17** | **8.54E-02** |
| **38B** | **8.9** | **2.5** | **3.0** | **77.4** | **29** | **6000** | **7** | **19.10** | **3.82E-05** | **26** | **15000** | **12** | **16.20** | **5.34E-06** | **33** | **17500** | **0** | **20.17** | **8.54E-02** |
| **38C** | **8.9** | **2.5** | **3.0** | **77.4** | **29** | **4667** | **7** | **19.10** | **3.82E-05** | **26** | **15000** | **12** | **16.20** | **5.34E-06** | **33** | **17500** | **0** | **20.17** | **8.54E-02** |

| | | | | | | | | | | | | | | | | | | |
|---|---|---|---|---|---|---|---|---|---|---|---|---|---|---|---|---|---|---|
| **39A** | **12.5** | **2.5** | **3.0** | **50.3** | **29** | **7333** | **7** | **19.46** | **4.50E-05** | **26** | **15000** | **15** | **15.40** | **4.42E-06** | **40** | **37500** | **0** | **21.89** | **9.95E-02** |
| **39B** | **12.5** | **2.5** | **3.0** | **50.3** | **29** | **6000** | **7** | **19.46** | **4.50E-05** | **26** | **15000** | **15** | **15.40** | **4.42E-06** | **40** | **37500** | **0** | **21.89** | **9.95E-02** |
| **39C** | **12.5** | **2.5** | **3.0** | **50.3** | **29** | **4667** | **7** | **19.46** | **4.50E-05** | **26** | **15000** | **15** | **15.40** | **4.42E-06** | **40** | **37500** | **0** | **21.89** | **9.95E-02** |
| **40A** | **12.6** | **2.5** | **2.5** | **48.5** | **30** | **16667** | **8** | **20.12** | **3.00E-05** | **23** | **15000** | **15** | **15.56** | **7.15E-06** | **39** | **37500** | **0** | **22.44** | **1.13E-01** |
| **40B** | **12.6** | **2.5** | **2.5** | **48.5** | **30** | **15000** | **8** | **20.12** | **3.00E-05** | **23** | **15000** | **15** | **15.56** | **7.15E-06** | **39** | **37500** | **0** | **22.44** | **1.13E-01** |
| **40C** | **12.6** | **2.5** | **2.5** | **48.5** | **30** | **13333** | **8** | **20.12** | **3.00E-05** | **23** | **15000** | **15** | **15.56** | **7.15E-06** | **39** | **37500** | **0** | **22.44** | **1.13E-01** |
| **41A** | **14.0** | **2.5** | **3.5** | **58.7** | **28** | **7333** | **7** | **19.47** | **4.97E-05** | **25** | **15000** | **16** | **15.40** | **7.24E-06** | **44** | **65500** | **0** | **22.96** | **5.93E-02** |
| **41B** | **14.0** | **2.5** | **3.5** | **58.7** | **28** | **6000** | **7** | **19.47** | **4.97E-05** | **25** | **15000** | **16** | **15.40** | **7.24E-06** | **44** | **65500** | **0** | **22.96** | **5.93E-02** |
| **41C** | **14.0** | **2.5** | **3.5** | **58.7** | **28** | **4667** | **7** | **19.47** | **4.97E-05** | **25** | **15000** | **16** | **15.40** | **7.24E-06** | **44** | **65500** | **0** | **22.96** | **5.93E-02** |
| **42A** | **14.0** | **3.0** | **3.0** | **78.4** | **33** | **16667** | **8** | **18.78** | **5.57E-05** | **22** | **15000** | **21** | **16.15** | **4.03E-06** | **44** | **65500** | **0** | **23.21** | **6.66E-02** |
| **42B** | **14.0** | **3.0** | **3.0** | **78.4** | **33** | **15000** | **8** | **18.78** | **5.57E-05** | **22** | **15000** | **21** | **16.15** | **4.03E-06** | **44** | **65500** | **0** | **23.21** | **6.66E-02** |
| **42C** | **14.0** | **3.0** | **3.0** | **78.4** | **33** | **13333** | **8** | **18.78** | **5.57E-05** | **22** | **15000** | **21** | **16.15** | **4.03E-06** | **44** | **65500** | **0** | **23.21** | **6.66E-02** |
| **43A** | **8.9** | **3.0** | **3.5** | **77.4** | **32** | **16667** | **8** | **18.89** | **3.39E-05** | **21** | **15000** | **18** | **15.33** | **6.46E-06** | **28** | **6000** | **3** | **15.88** | **8.37E-07** |
| **43B** | **8.9** | **3.0** | **3.5** | **77.4** | **32** | **15000** | **8** | **18.89** | **3.39E-05** | **21** | **15000** | **18** | **15.33** | **6.46E-06** | **28** | **6000** | **3** | **15.88** | **8.37E-07** |
| **43C** | **8.9** | **3.0** | **3.5** | **77.4** | **32** | **13333** | **8** | **18.89** | **3.39E-05** | **21** | **15000** | **18** | **15.33** | **6.46E-06** | **28** | **6000** | **3** | **15.88** | **8.37E-07** |
| **44A** | **8.4** | **3.0** | **3.0** | **58.3** | **31** | **16667** | **9** | **19.30** | **6.86E-05** | **26** | **15000** | **7** | **15.16** | **7.33E-06** | **28** | **6000** | **3** | **15.00** | **7.39E-07** |
| **44B** | **8.4** | **3.0** | **3.0** | **58.3** | **31** | **15000** | **9** | **19.30** | **6.86E-05** | **26** | **15000** | **7** | **15.16** | **7.33E-06** | **28** | **6000** | **3** | **15.00** | **7.39E-07** |
| **44C** | **8.4** | **3.0** | **3.0** | **58.3** | **31** | **13333** | **9** | **19.30** | **6.86E-05** | **26** | **15000** | **7** | **15.16** | **7.33E-06** | **28** | **6000** | **3** | **15.00** | **7.39E-07** |
| **45A** | **11.1** | **3.0** | **3.0** | **52.0** | **31** | **16667** | **7** | **19.28** | **2.35E-05** | **24** | **15000** | **3** | **16.13** | **5.54E-06** | **28** | **6000** | **2** | **15.12** | **5.07E-07** |
| **45B** | **11.1** | **3.0** | **3.0** | **52.0** | **31** | **15000** | **7** | **19.28** | **2.35E-05** | **24** | **15000** | **3** | **16.13** | **5.54E-06** | **28** | **6000** | **2** | **15.12** | **5.07E-07** |
| **45C** | **11.1** | **3.0** | **3.0** | **52.0** | **31** | **13333** | **7** | **19.28** | **2.35E-05** | **24** | **15000** | **3** | **16.13** | **5.54E-06** | **28** | **6000** | **2** | **15.12** | **5.07E-07** |
| **46A** | **9.0** | **2.5** | **2.5** | **39.7** | **30** | **16667** | **7** | **18.88** | **4.35E-05** | **34** | **32500** | **17** | **20.07** | **1.48E-06** | **29** | **6000** | **7** | **19.72** | **1.10E-04** |
| **46B** | **9.0** | **2.5** | **2.5** | **39.7** | **30** | **15000** | **7** | **18.88** | **4.35E-05** | **34** | **32500** | **17** | **20.07** | **1.48E-06** | **29** | **6000** | **7** | **19.72** | **1.10E-04** |
| **46C** | **9.0** | **2.5** | **2.5** | **39.7** | **30** | **13333** | **7** | **18.88** | **4.35E-05** | **34** | **32500** | **17** | **20.07** | **1.48E-06** | **29** | **6000** | **7** | **19.72** | **1.10E-04** |
| **47A** | **15.4** | **3.5** | **3.0** | **69.0** | **33** | **16667** | **7** | **19.51** | **2.52E-05** | **33** | **32500** | **5** | **20.30** | **1.76E-06** | **33** | **15000** | **7** | **18.83** | **1.07E-04** |
| **47B** | **15.4** | **3.5** | **3.0** | **69.0** | **33** | **15000** | **7** | **19.51** | **2.52E-05** | **33** | **32500** | **5** | **20.30** | **1.76E-06** | **33** | **15000** | **7** | **18.83** | **1.07E-04** |
| **47C** | **15.4** | **3.5** | **3.0** | **69.0** | **33** | **13333** | **7** | **19.51** | **2.52E-05** | **33** | **32500** | **5** | **20.30** | **1.76E-06** | **33** | **15000** | **7** | **18.83** | **1.07E-04** |
| **48A** | **15.1** | **3.0** | **2.5** | **60.3** | **31** | **16667** | **6** | **20.16** | **4.42E-05** | **32** | **32500** | **13** | **20.64** | **2.08E-06** | **32** | **15000** | **8** | **19.91** | **6.92E-05** |
| **48B** | **15.1** | **3.0** | **2.5** | **60.3** | **31** | **15000** | **6** | **20.16** | **4.42E-05** | **32** | **32500** | **13** | **20.64** | **2.08E-06** | **32** | **15000** | **8** | **19.91** | **6.92E-05** |
| **48C** | **15.1** | **3.0** | **2.5** | **60.3** | **31** | **13333** | **6** | **20.16** | **4.42E-05** | **32** | **32500** | **13** | **20.64** | **2.08E-06** | **32** | **15000** | **8** | **19.91** | **6.92E-05** |
| **49A** | **11.3** | **3.5** | **2.5** | **44.3** | **30** | **7333** | **8** | **19.25** | **2.79E-05** | **36** | **32500** | **13** | **17.95** | **2.12E-06** | **24** | **15000** | **17** | **15.70** | **9.56E-06** |
| **49B** | **11.3** | **3.5** | **2.5** | **44.3** | **30** | **6000** | **8** | **19.25** | **2.79E-05** | **36** | **32500** | **13** | **17.95** | **2.12E-06** | **24** | **15000** | **17** | **15.70** | **9.56E-06** |
| **49C** | **11.3** | **3.5** | **2.5** | **44.3** | **30** | **4667** | **8** | **19.25** | **2.79E-05** | **36** | **32500** | **13** | **17.95** | **2.12E-06** | **24** | **15000** | **17** | **15.70** | **9.56E-06** |
| **50A** | **9.7** | **3.0** | **2.0** | **55.5** | **33** | **16667** | **7** | **19.28** | **4.04E-05** | **33** | **32500** | **23** | **19.58** | **1.86E-06** | **24** | **15000** | **19** | **15.51** | **5.51E-06** |
| **50B** | **9.7** | **3.0** | **2.0** | **55.5** | **33** | **15000** | **7** | **19.28** | **4.04E-05** | **33** | **32500** | **23** | **19.58** | **1.86E-06** | **24** | **15000** | **19** | **15.51** | **5.51E-06** |
| **50C** | **9.7** | **3.0** | **2.0** | **55.5** | **33** | **13333** | **7** | **19.28** | **4.04E-05** | **33** | **32500** | **23** | **19.58** | **1.86E-06** | **24** | **15000** | **19** | **15.51** | **5.51E-06** |
| **51A** | **12.5** | **2.5** | **3.0** | **35.6** | **31** | **16667** | **8** | **18.08** | **3.76E-05** | **34** | **32500** | **13** | **19.95** | **1.90E-06** | **19** | **15000** | **13** | **16.30** | **3.68E-06** |
| **51B** | **12.5** | **2.5** | **3.0** | **35.6** | **31** | **15000** | **8** | **18.08** | **3.76E-05** | **34** | **32500** | **13** | **19.95** | **1.90E-06** | **19** | **15000** | **13** | **16.30** | **3.68E-06** |
| **51C** | **12.5** | **2.5** | **3.0** | **35.6** | **31** | **13333** | **8** | **18.08** | **3.76E-05** | **34** | **32500** | **13** | **19.95** | **1.90E-06** | **19** | **15000** | **13** | **16.30** | **3.68E-06** |

| | | | | | | | | | | | | | | | | | | |
|---|---|---|---|---|---|---|---|---|---|---|---|---|---|---|---|---|---|---|
| **52A** | **9.0** | **3.0** | **3.0** | **65.7** | **30** | **16667** | **7** | **18.94** | **3.02E-05** | **35** | **32500** | **11** | **20.20** | **2.02E-06** | **32** | **32500** | **21** | **18.48** | **3.63E-06** |
| **52B** | **9.0** | **3.0** | **3.0** | **65.7** | **30** | **15000** | **7** | **18.94** | **3.02E-05** | **35** | **32500** | **11** | **20.20** | **2.02E-06** | **32** | **32500** | **21** | **18.48** | **3.63E-06** |
| **52C** | **9.0** | **3.0** | **3.0** | **65.7** | **30** | **13333** | **7** | **18.94** | **3.02E-05** | **35** | **32500** | **11** | **20.20** | **2.02E-06** | **32** | **32500** | **21** | **18.48** | **3.63E-06** |
| **53A** | **10.6** | **2.5** | **3.0** | **57.7** | **31** | **16667** | **9** | **18.56** | **1.55E-05** | **34** | **32500** | **14** | **18.79** | **2.31E-06** | **35** | **32500** | **14** | **19.84** | **2.20E-06** |
| **53B** | **10.6** | **2.5** | **3.0** | **57.7** | **31** | **15000** | **9** | **18.56** | **1.55E-05** | **34** | **32500** | **14** | **18.79** | **2.31E-06** | **35** | **32500** | **14** | **19.84** | **2.20E-06** |
| **53C** | **10.6** | **2.5** | **3.0** | **57.7** | **31** | **13333** | **9** | **18.56** | **1.55E-05** | **34** | **32500** | **14** | **18.79** | **2.31E-06** | **35** | **32500** | **14** | **19.84** | **2.20E-06** |
| **54A** | **9.4** | **3.0** | **3.0** | **81.7** | **30** | **16667** | **8** | **19.17** | **5.94E-05** | **33** | **32500** | **14** | **19.00** | **2.85E-06** | **37** | **32500** | **8** | **20.54** | **2.04E-06** |
| **54B** | **9.4** | **3.0** | **3.0** | **81.7** | **30** | **15000** | **8** | **19.17** | **5.94E-05** | **33** | **32500** | **14** | **19.00** | **2.85E-06** | **37** | **32500** | **8** | **20.54** | **2.04E-06** |
| **54C** | **9.4** | **3.0** | **3.0** | **81.7** | **30** | **13333** | **8** | **19.17** | **5.94E-05** | **33** | **32500** | **14** | **19.00** | **2.85E-06** | **37** | **32500** | **8** | **20.54** | **2.04E-06** |
| **55A** | **2.1** | **3.0** | **3.0** | **4.8** | **24** | **16667** | **11** | **15.40** | **6.59E-06** | **33** | **17500** | **0** | **20.21** | **1.37E-01** | **32** | **17500** | **0** | **20.37** | **8.68E-02** |
| **55B** | **2.1** | **3.0** | **3.0** | **4.8** | **24** | **15000** | **11** | **15.40** | **6.59E-06** | **33** | **17500** | **0** | **20.21** | **1.37E-01** | **32** | **17500** | **0** | **20.37** | **8.68E-02** |
| **55C** | **2.1** | **3.0** | **3.0** | **4.8** | **24** | **13333** | **11** | **15.40** | **6.59E-06** | **33** | **17500** | **0** | **20.21** | **1.37E-01** | **32** | **17500** | **0** | **20.37** | **8.68E-02** |
| **56A** | **1.7** | **2.5** | **3.0** | **6.3** | **24** | **16667** | **17** | **16.51** | **6.20E-06** | **31** | **17500** | **0** | **20.44** | **1.12E-01** | **34** | **17500** | **0** | **20.05** | **1.04E-01** |
| **56B** | **1.7** | **2.5** | **3.0** | **6.3** | **24** | **15000** | **17** | **16.51** | **6.20E-06** | **31** | **17500** | **0** | **20.44** | **1.12E-01** | **34** | **17500** | **0** | **20.05** | **1.04E-01** |
| **56C** | **1.7** | **2.5** | **3.0** | **6.3** | **24** | **13333** | **17** | **16.51** | **6.20E-06** | **31** | **17500** | **0** | **20.44** | **1.12E-01** | **34** | **17500** | **0** | **20.05** | **1.04E-01** |
| **57A** | **2.0** | **3.0** | **3.0** | **3.3** | **21** | **16667** | **7** | **16.27** | **8.82E-06** | **30** | **17500** | **0** | **20.22** | **1.02E-01** | **41** | **37500** | **0** | **21.67** | **1.60E-01** |
| **57B** | **2.0** | **3.0** | **3.0** | **3.3** | **21** | **15000** | **7** | **16.27** | **8.82E-06** | **30** | **17500** | **0** | **20.22** | **1.02E-01** | **41** | **37500** | **0** | **21.67** | **1.60E-01** |
| **57C** | **2.0** | **3.0** | **3.0** | **3.3** | **21** | **13333** | **7** | **16.27** | **8.82E-06** | **30** | **17500** | **0** | **20.22** | **1.02E-01** | **41** | **37500** | **0** | **21.67** | **1.60E-01** |
| **58A** | **2.0** | **2.5** | **2.5** | **3.8** | **24** | **16667** | **5** | **15.97** | **5.28E-06** | **33** | **17500** | **0** | **20.43** | **6.23E-02** | **40** | **37500** | **0** | **22.01** | **1.27E-01** |
| **58B** | **2.0** | **2.5** | **2.5** | **3.8** | **24** | **15000** | **5** | **15.97** | **5.28E-06** | **33** | **17500** | **0** | **20.43** | **6.23E-02** | **40** | **37500** | **0** | **22.01** | **1.27E-01** |
| **58C** | **2.0** | **2.5** | **2.5** | **3.8** | **24** | **13333** | **5** | **15.97** | **5.28E-06** | **33** | **17500** | **0** | **20.43** | **6.23E-02** | **40** | **37500** | **0** | **22.01** | **1.27E-01** |
| **59A** | **2.4** | **3.0** | **3.5** | **3.1** | **27** | **16667** | **15** | **15.80** | **1.40E-06** | **34** | **17500** | **0** | **20.26** | **1.17E-01** | **44** | **65500** | **0** | **23.68** | **8.63E-02** |
| **59B** | **2.4** | **3.0** | **3.5** | **3.1** | **27** | **15000** | **15** | **15.80** | **1.40E-06** | **34** | **17500** | **0** | **20.26** | **1.17E-01** | **44** | **65500** | **0** | **23.68** | **8.63E-02** |
| **59C** | **2.4** | **3.0** | **3.5** | **3.1** | **27** | **13333** | **15** | **15.80** | **1.40E-06** | **34** | **17500** | **0** | **20.26** | **1.17E-01** | **44** | **65500** | **0** | **23.68** | **8.63E-02** |
| **60A** | **2.3** | **3.5** | **3.0** | **3.9** | **24** | **16667** | **15** | **16.02** | **7.82E-06** | **32** | **17500** | **0** | **20.29** | **6.06E-02** | **43** | **65500** | **0** | **23.72** | **8.01E-02** |
| **60B** | **2.3** | **3.5** | **3.0** | **3.9** | **24** | **15000** | **15** | **16.02** | **7.82E-06** | **32** | **17500** | **0** | **20.29** | **6.06E-02** | **43** | **65500** | **0** | **23.72** | **8.01E-02** |
| **60C** | **2.3** | **3.5** | **3.0** | **3.9** | **24** | **13333** | **15** | **16.02** | **7.82E-06** | **32** | **17500** | **0** | **20.29** | **6.06E-02** | **43** | **65500** | **0** | **23.72** | **8.01E-02** |
| **61A** | **1.9** | **2.5** | **3.5** | **3.2** | **24** | **16667** | **13** | **17.92** | **7.14E-06** | **41** | **37500** | **0** | **21.69** | **1.54E-01** | **27** | **6000** | **3** | **15.31** | **3.50E-07** |
| **61B** | **1.9** | **2.5** | **3.5** | **3.2** | **24** | **15000** | **13** | **17.92** | **7.14E-06** | **41** | **37500** | **0** | **21.69** | **1.54E-01** | **27** | **6000** | **3** | **15.31** | **3.50E-07** |
| **61C** | **1.9** | **2.5** | **3.5** | **3.2** | **24** | **13333** | **13** | **17.92** | **7.14E-06** | **41** | **37500** | **0** | **21.69** | **1.54E-01** | **27** | **6000** | **3** | **15.31** | **3.50E-07** |
| **62A** | **2.7** | **2.5** | **2.5** | **3.4** | **23** | **16667** | **15** | **15.73** | **4.03E-06** | **40** | **37500** | **0** | **22.17** | **1.18E-01** | **29** | **6000** | **2** | **14.96** | **2.18E-07** |
| **62B** | **2.7** | **2.5** | **2.5** | **3.4** | **23** | **15000** | **15** | **15.73** | **4.03E-06** | **40** | **37500** | **0** | **22.17** | **1.18E-01** | **29** | **6000** | **2** | **14.96** | **2.18E-07** |
| **62C** | **2.7** | **2.5** | **2.5** | **3.4** | **23** | **13333** | **15** | **15.73** | **4.03E-06** | **40** | **37500** | **0** | **22.17** | **1.18E-01** | **29** | **6000** | **2** | **14.96** | **2.18E-07** |
| **63A** | **2.0** | **2.5** | **3.0** | **5.1** | **24** | **16667** | **18** | **14.87** | **5.37E-06** | **40** | **37500** | **0** | **21.71** | **1.10E-01** | **28** | **6000** | **1** | **15.54** | **5.08E-07** |
| **63B** | **2.0** | **2.5** | **3.0** | **5.1** | **24** | **15000** | **18** | **14.87** | **5.37E-06** | **40** | **37500** | **0** | **21.71** | **1.10E-01** | **28** | **6000** | **1** | **15.54** | **5.08E-07** |
| **63C** | **2.0** | **2.5** | **3.0** | **5.1** | **24** | **13333** | **18** | **14.87** | **5.37E-06** | **40** | **37500** | **0** | **21.71** | **1.10E-01** | **28** | **6000** | **1** | **15.54** | **5.08E-07** |
| **64A** | **1.7** | **2.0** | **3.0** | **2.7** | **24** | **16667** | **17** | **16.95** | **6.30E-06** | **40** | **37500** | **0** | **21.94** | **8.79E-02** | **30** | **15000** | **7** | **19.63** | **6.31E-05** |
| **64B** | **1.7** | **2.0** | **3.0** | **2.7** | **24** | **15000** | **17** | **16.95** | **6.30E-06** | **40** | **37500** | **0** | **21.94** | **8.79E-02** | **30** | **15000** | **7** | **19.63** | **6.31E-05** |
| **64C** | **1.7** | **2.0** | **3.0** | **2.7** | **24** | **13333** | **17** | **16.95** | **6.30E-06** | **40** | **37500** | **0** | **21.94** | **8.79E-02** | **30** | **15000** | **7** | **19.63** | **6.31E-05** |

| | | | | | | | | | | | | | | | | | | |
|---|---|---|---|---|---|---|---|---|---|---|---|---|---|---|---|---|---|---|
| **65A** | **1.8** | **3.0** | **3.0** | **3.0** | **25** | **16667** | **11** | **16.17** | **5.64E-06** | **39** | **37500** | **0** | **21.78** | **2.87E-02** | **30** | **15000** | **7** | **18.71** | **2.87E-05** |
| **65B** | **1.8** | **3.0** | **3.0** | **3.0** | **25** | **15000** | **11** | **16.17** | **5.64E-06** | **39** | **37500** | **0** | **21.78** | **2.87E-02** | **30** | **15000** | **7** | **18.71** | **2.87E-05** |
| **65C** | **1.8** | **3.0** | **3.0** | **3.0** | **25** | **13333** | **11** | **16.17** | **5.64E-06** | **39** | **37500** | **0** | **21.78** | **2.87E-02** | **30** | **15000** | **7** | **18.71** | **2.87E-05** |
| **66A** | **2.3** | **3.0** | **3.0** | **3.5** | **23** | **16667** | **17** | **15.41** | **6.16E-06** | **39** | **37500** | **0** | **22.00** | **6.13E-02** | **29** | **6000** | **6** | **19.42** | **4.02E-05** |
| **66B** | **2.3** | **3.0** | **3.0** | **3.5** | **23** | **15000** | **17** | **15.41** | **6.16E-06** | **39** | **37500** | **0** | **22.00** | **6.13E-02** | **29** | **6000** | **6** | **19.42** | **4.02E-05** |
| **66C** | **2.3** | **3.0** | **3.0** | **3.5** | **23** | **13333** | **17** | **15.41** | **6.16E-06** | **39** | **37500** | **0** | **22.00** | **6.13E-02** | **29** | **6000** | **6** | **19.42** | **4.02E-05** |
| **67A** | **2.1** | **3.5** | **2.0** | **3.4** | **24** | **16667** | **14** | **17.37** | **4.81E-06** | **44** | **65500** | **0** | **23.13** | **1.13E-01** | **23** | **15000** | **14** | **17.32** | **6.34E-06** |
| **67B** | **2.1** | **3.5** | **2.0** | **3.4** | **24** | **15000** | **14** | **17.37** | **4.81E-06** | **44** | **65500** | **0** | **23.13** | **1.13E-01** | **23** | **15000** | **14** | **17.32** | **6.34E-06** |
| **67C** | **2.1** | **3.5** | **2.0** | **3.4** | **24** | **13333** | **14** | **17.37** | **4.81E-06** | **44** | **65500** | **0** | **23.13** | **1.13E-01** | **23** | **15000** | **14** | **17.32** | **6.34E-06** |
| **68A** | **2.4** | **2.5** | **2.0** | **5.0** | **28** | **16667** | **11** | **16.13** | **4.94E-06** | **44** | **65500** | **0** | **23.28** | **1.81E-01** | **21** | **15000** | **6** | **15.01** | **2.80E-06** |
| **68B** | **2.4** | **2.5** | **2.0** | **5.0** | **28** | **15000** | **11** | **16.13** | **4.94E-06** | **44** | **65500** | **0** | **23.28** | **1.81E-01** | **21** | **15000** | **6** | **15.01** | **2.80E-06** |
| **68C** | **2.4** | **2.5** | **2.0** | **5.0** | **28** | **13333** | **11** | **16.13** | **4.94E-06** | **44** | **65500** | **0** | **23.28** | **1.81E-01** | **21** | **15000** | **6** | **15.01** | **2.80E-06** |
| **69A** | **2.0** | **2.0** | **2.5** | **5.6** | **19** | **16667** | **8** | **15.98** | **5.15E-06** | **43** | **65500** | **0** | **23.18** | **1.26E-01** | **23** | **15000** | **10** | **15.88** | **4.54E-06** |
| **69B** | **2.0** | **2.0** | **2.5** | **5.6** | **19** | **15000** | **8** | **15.98** | **5.15E-06** | **43** | **65500** | **0** | **23.18** | **1.26E-01** | **23** | **15000** | **10** | **15.88** | **4.54E-06** |
| **69C** | **2.0** | **2.0** | **2.5** | **5.6** | **19** | **13333** | **8** | **15.98** | **5.15E-06** | **43** | **65500** | **0** | **23.18** | **1.26E-01** | **23** | **15000** | **10** | **15.88** | **4.54E-06** |
| **70A** | **3.0** | **3.5** | **3.0** | **2.6** | **28** | **16667** | **16** | **15.33** | **3.68E-06** | **44** | **65500** | **0** | **23.14** | **1.11E-01** | **33** | **32500** | **9** | **19.14** | **1.62E-06** |
| **70B** | **3.0** | **3.5** | **3.0** | **2.6** | **28** | **15000** | **16** | **15.33** | **3.68E-06** | **44** | **65500** | **0** | **23.14** | **1.11E-01** | **33** | **32500** | **9** | **19.14** | **1.62E-06** |
| **70C** | **3.0** | **3.5** | **3.0** | **2.6** | **28** | **13333** | **16** | **15.33** | **3.68E-06** | **44** | **65500** | **0** | **23.14** | **1.11E-01** | **33** | **32500** | **9** | **19.14** | **1.62E-06** |
| **71A** | **1.3** | **3.5** | **3.5** | **2.9** | **25** | **16667** | **11** | **15.16** | **7.38E-06** | **43** | **65500** | **0** | **23.27** | **8.30E-02** | **34** | **32500** | **15** | **18.81** | **1.87E-06** |
| **71B** | **1.3** | **3.5** | **3.5** | **2.9** | **25** | **15000** | **11** | **15.16** | **7.38E-06** | **43** | **65500** | **0** | **23.27** | **8.30E-02** | **34** | **32500** | **15** | **18.81** | **1.87E-06** |
| **71C** | **1.3** | **3.5** | **3.5** | **2.9** | **25** | **13333** | **11** | **15.16** | **7.38E-06** | **43** | **65500** | **0** | **23.27** | **8.30E-02** | **34** | **32500** | **15** | **18.81** | **1.87E-06** |
| **72A** | **1.8** | **2.5** | **2.5** | **4.1** | **26** | **16667** | **13** | **14.74** | **5.01E-06** | **44** | **65500** | **0** | **23.12** | **1.05E-01** | **34** | **32500** | **13** | **19.60** | **1.97E-06** |
| **72B** | **1.8** | **2.5** | **2.5** | **4.1** | **26** | **15000** | **13** | **14.74** | **5.01E-06** | **44** | **65500** | **0** | **23.12** | **1.05E-01** | **34** | **32500** | **13** | **19.60** | **1.97E-06** |
| **72C** | **1.8** | **2.5** | **2.5** | **4.1** | **26** | **13333** | **13** | **14.74** | **5.01E-06** | **44** | **65500** | **0** | **23.12** | **1.05E-01** | **34** | **32500** | **13** | **19.60** | **1.97E-06** |
| **73A** | **2.0** | **3.0** | **2.5** | **3.2** | **21** | **16667** | **10** | **15.55** | **6.15E-06** | **27** | **6000** | **3** | **16.08** | **1.05E-07** | **33** | **17500** | **0** | **19.92** | **1.52E-01** |
| **73B** | **2.0** | **3.0** | **2.5** | **3.2** | **21** | **15000** | **10** | **15.55** | **6.15E-06** | **27** | **6000** | **3** | **16.08** | **1.05E-07** | **33** | **17500** | **0** | **19.92** | **1.52E-01** |
| **73C** | **2.0** | **3.0** | **2.5** | **3.2** | **21** | **13333** | **10** | **15.55** | **6.15E-06** | **27** | **6000** | **3** | **16.08** | **1.05E-07** | **33** | **17500** | **0** | **19.92** | **1.52E-01** |
| **74A** | **2.0** | **2.5** | **3.0** | **5.5** | **23** | **16667** | **6** | **15.17** | **3.57E-06** | **28** | **6000** | **3** | **15.53** | **4.58E-07** | **36** | **17500** | **0** | **20.49** | **1.92E-01** |
| **74B** | **2.0** | **2.5** | **3.0** | **5.5** | **23** | **15000** | **6** | **15.17** | **3.57E-06** | **28** | **6000** | **3** | **15.53** | **4.58E-07** | **36** | **17500** | **0** | **20.49** | **1.92E-01** |
| **74C** | **2.0** | **2.5** | **3.0** | **5.5** | **23** | **13333** | **6** | **15.17** | **3.57E-06** | **28** | **6000** | **3** | **15.53** | **4.58E-07** | **36** | **17500** | **0** | **20.49** | **1.92E-01** |
| **75A** | **2.6** | **3.0** | **2.5** | **5.2** | **23** | **16667** | **14** | **16.19** | **3.20E-06** | **28** | **6000** | **1** | **15.58** | **6.94E-07** | **41** | **37500** | **0** | **21.68** | **1.07E-01** |
| **75B** | **2.6** | **3.0** | **2.5** | **5.2** | **23** | **15000** | **14** | **16.19** | **3.20E-06** | **28** | **6000** | **1** | **15.58** | **6.94E-07** | **41** | **37500** | **0** | **21.68** | **1.07E-01** |
| **75C** | **2.6** | **3.0** | **2.5** | **5.2** | **23** | **13333** | **14** | **16.19** | **3.20E-06** | **28** | **6000** | **1** | **15.58** | **6.94E-07** | **41** | **37500** | **0** | **21.68** | **1.07E-01** |
| **76A** | **2.1** | **3.0** | **3.0** | **4.1** | **25** | **16667** | **13** | **15.61** | **4.85E-06** | **30** | **15000** | **3** | **15.94** | **5.35E-07** | **39** | **37500** | **0** | **22.11** | **8.51E-02** |
| **76B** | **2.1** | **3.0** | **3.0** | **4.1** | **25** | **15000** | **13** | **15.61** | **4.85E-06** | **30** | **15000** | **3** | **15.94** | **5.35E-07** | **39** | **37500** | **0** | **22.11** | **8.51E-02** |
| **76C** | **2.1** | **3.0** | **3.0** | **4.1** | **25** | **13333** | **13** | **15.61** | **4.85E-06** | **30** | **15000** | **3** | **15.94** | **5.35E-07** | **39** | **37500** | **0** | **22.11** | **8.51E-02** |
| **77A** | **2.0** | **3.0** | **2.5** | **4.1** | **21** | **16667** | **18** | **16.86** | **4.58E-06** | **28** | **6000** | **2** | **14.85** | **5.14E-07** | **43** | **65500** | **0** | **23.45** | **5.41E-02** |
| **77B** | **2.0** | **3.0** | **2.5** | **4.1** | **21** | **15000** | **18** | **16.86** | **4.58E-06** | **28** | **6000** | **2** | **14.85** | **5.14E-07** | **43** | **65500** | **0** | **23.45** | **5.41E-02** |
| **77C** | **2.0** | **3.0** | **2.5** | **4.1** | **21** | **13333** | **18** | **16.86** | **4.58E-06** | **28** | **6000** | **2** | **14.85** | **5.14E-07** | **43** | **65500** | **0** | **23.45** | **5.41E-02** |

| | | | | | | | | | | | | | | | | | | |
|---|---|---|---|---|---|---|---|---|---|---|---|---|---|---|---|---|---|---|
| **78A** | **2.0** | **2.5** | **3.0** | **3.2** | **25** | **16667** | **16** | **16.71** | **7.00E-06** | **28** | **6000** | **2** | **15.26** | **6.18E-07** | **43** | **65500** | **0** | **23.49** | **1.33E-01** |
| **78B** | **2.0** | **2.5** | **3.0** | **3.2** | **25** | **15000** | **16** | **16.71** | **7.00E-06** | **28** | **6000** | **2** | **15.26** | **6.18E-07** | **43** | **65500** | **0** | **23.49** | **1.33E-01** |
| **78C** | **2.0** | **2.5** | **3.0** | **3.2** | **25** | **13333** | **16** | **16.71** | **7.00E-06** | **28** | **6000** | **2** | **15.26** | **6.18E-07** | **43** | **65500** | **0** | **23.49** | **1.33E-01** |
| **79A** | **2.3** | **2.5** | **2.0** | **4.3** | **22** | **16667** | **18** | **15.90** | **6.01E-06** | **28** | **6000** | **2** | **16.39** | **2.75E-07** | **26** | **6000** | **2** | **15.16** | **5.41E-07** |
| **79B** | **2.3** | **2.5** | **2.0** | **4.3** | **22** | **15000** | **18** | **15.90** | **6.01E-06** | **28** | **6000** | **2** | **16.39** | **2.75E-07** | **26** | **6000** | **2** | **15.16** | **5.41E-07** |
| **79C** | **2.3** | **2.5** | **2.0** | **4.3** | **22** | **13333** | **18** | **15.90** | **6.01E-06** | **28** | **6000** | **2** | **16.39** | **2.75E-07** | **26** | **6000** | **2** | **15.16** | **5.41E-07** |
| **80A** | **1.7** | **4.0** | **3.0** | **4.7** | **24** | **16667** | **10** | **15.63** | **5.90E-06** | **27** | **6000** | **1** | **16.06** | **7.40E-07** | **28** | **6000** | **3** | **15.53** | **6.78E-07** |
| **80B** | **1.7** | **4.0** | **3.0** | **4.7** | **24** | **15000** | **10** | **15.63** | **5.90E-06** | **27** | **6000** | **1** | **16.06** | **7.40E-07** | **28** | **6000** | **3** | **15.53** | **6.78E-07** |
| **80C** | **1.7** | **4.0** | **3.0** | **4.7** | **24** | **13333** | **10** | **15.63** | **5.90E-06** | **27** | **6000** | **1** | **16.06** | **7.40E-07** | **28** | **6000** | **3** | **15.53** | **6.78E-07** |
| **81A** | **1.9** | **2.5** | **2.5** | **3.7** | **25** | **16667** | **9** | **16.49** | **2.59E-06** | **28** | **6000** | **1** | **14.93** | **3.58E-07** | **29** | **6000** | **4** | **15.42** | **3.48E-07** |
| **81B** | **1.9** | **2.5** | **2.5** | **3.7** | **25** | **15000** | **9** | **16.49** | **2.59E-06** | **28** | **6000** | **1** | **14.93** | **3.58E-07** | **29** | **6000** | **4** | **15.42** | **3.48E-07** |
| **81C** | **1.9** | **2.5** | **2.5** | **3.7** | **25** | **13333** | **9** | **16.49** | **2.59E-06** | **28** | **6000** | **1** | **14.93** | **3.58E-07** | **29** | **6000** | **4** | **15.42** | **3.48E-07** |
| **82A** | **11.3** | **3.5** | **3.0** | **41.9** | **34** | **38334** | **8** | **20.42** | **2.29E-06** | **27** | **6000** | **8** | **18.51** | **2.65E-05** | **30** | **15000** | **7** | **19.13** | **3.97E-05** |
| **82B** | **11.3** | **3.5** | **3.0** | **41.9** | **34** | **32500** | **8** | **20.42** | **2.29E-06** | **27** | **6000** | **8** | **18.51** | **2.65E-05** | **30** | **15000** | **7** | **19.13** | **3.97E-05** |
| **82C** | **11.3** | **3.5** | **3.0** | **41.9** | **34** | **26667** | **8** | **20.42** | **2.29E-06** | **27** | **6000** | **8** | **18.51** | **2.65E-05** | **30** | **15000** | **7** | **19.13** | **3.97E-05** |
| **83A** | **14.4** | **3.0** | **3.0** | **72.9** | **35** | **38334** | **15** | **20.31** | **2.35E-06** | **29** | **6000** | **7** | **19.72** | **5.24E-05** | **34** | **15000** | **5** | **19.47** | **5.89E-05** |
| **83B** | **14.4** | **3.0** | **3.0** | **72.9** | **35** | **32500** | **15** | **20.31** | **2.35E-06** | **29** | **6000** | **7** | **19.72** | **5.24E-05** | **34** | **15000** | **5** | **19.47** | **5.89E-05** |
| **83C** | **14.4** | **3.0** | **3.0** | **72.9** | **35** | **26667** | **15** | **20.31** | **2.35E-06** | **29** | **6000** | **7** | **19.72** | **5.24E-05** | **34** | **15000** | **5** | **19.47** | **5.89E-05** |
| **84A** | **13.2** | **2.5** | **3.0** | **61.9** | **33** | **38334** | **25** | **19.43** | **1.27E-06** | **32** | **15000** | **7** | **19.35** | **7.15E-05** | **30** | **15000** | **7** | **19.25** | **5.81E-05** |
| **84B** | **13.2** | **2.5** | **3.0** | **61.9** | **33** | **32500** | **25** | **19.43** | **1.27E-06** | **32** | **15000** | **7** | **19.35** | **7.15E-05** | **30** | **15000** | **7** | **19.25** | **5.81E-05** |
| **84C** | **13.2** | **2.5** | **3.0** | **61.9** | **33** | **26667** | **25** | **19.43** | **1.27E-06** | **32** | **15000** | **7** | **19.35** | **7.15E-05** | **30** | **15000** | **7** | **19.25** | **5.81E-05** |
| **85A** | **14.4** | **3.5** | **3.0** | **61.1** | **34** | **38334** | **16** | **20.00** | **1.85E-06** | **32** | **15000** | **6** | **18.94** | **4.17E-05** | **23** | **15000** | **4** | **14.93** | **5.45E-06** |
| **85B** | **14.4** | **3.5** | **3.0** | **61.1** | **34** | **32500** | **16** | **20.00** | **1.85E-06** | **32** | **15000** | **6** | **18.94** | **4.17E-05** | **23** | **15000** | **4** | **14.93** | **5.45E-06** |
| **85C** | **14.4** | **3.5** | **3.0** | **61.1** | **34** | **26667** | **16** | **20.00** | **1.85E-06** | **32** | **15000** | **6** | **18.94** | **4.17E-05** | **23** | **15000** | **4** | **14.93** | **5.45E-06** |
| **86A** | **8.3** | **3.0** | **3.0** | **69.6** | **31** | **38334** | **10** | **19.49** | **1.73E-06** | **32** | **15000** | **8** | **18.98** | **3.96E-05** | **24** | **15000** | **12** | **16.58** | **7.49E-06** |
| **86B** | **8.3** | **3.0** | **3.0** | **69.6** | **31** | **32500** | **10** | **19.49** | **1.73E-06** | **32** | **15000** | **8** | **18.98** | **3.96E-05** | **24** | **15000** | **12** | **16.58** | **7.49E-06** |
| **86C** | **8.3** | **3.0** | **3.0** | **69.6** | **31** | **26667** | **10** | **19.49** | **1.73E-06** | **32** | **15000** | **8** | **18.98** | **3.96E-05** | **24** | **15000** | **12** | **16.58** | **7.49E-06** |
| **87A** | **11.5** | **2.0** | **2.5** | **75.9** | **36** | **38334** | **17** | **19.07** | **2.35E-06** | **31** | **15000** | **8** | **20.17** | **3.44E-05** | **23** | **15000** | **16** | **16.65** | **7.40E-06** |
| **87B** | **11.5** | **2.0** | **2.5** | **75.9** | **36** | **32500** | **17** | **19.07** | **2.35E-06** | **31** | **15000** | **8** | **20.17** | **3.44E-05** | **23** | **15000** | **16** | **16.65** | **7.40E-06** |
| **87C** | **11.5** | **2.0** | **2.5** | **75.9** | **36** | **26667** | **17** | **19.07** | **2.35E-06** | **31** | **15000** | **8** | **20.17** | **3.44E-05** | **23** | **15000** | **16** | **16.65** | **7.40E-06** |
| **88A** | **8.0** | **2.5** | **3.5** | **45.7** | **33** | **38334** | **8** | **20.14** | **1.33E-06** | **31** | **15000** | **7** | **18.91** | **4.53E-05** | **33** | **32500** | **14** | **18.55** | **8.29E-07** |
| **88B** | **8.0** | **2.5** | **3.5** | **45.7** | **33** | **32500** | **8** | **20.14** | **1.33E-06** | **31** | **15000** | **7** | **18.91** | **4.53E-05** | **33** | **32500** | **14** | **18.55** | **8.29E-07** |
| **88C** | **8.0** | **2.5** | **3.5** | **45.7** | **33** | **26667** | **8** | **20.14** | **1.33E-06** | **31** | **15000** | **7** | **18.91** | **4.53E-05** | **33** | **32500** | **14** | **18.55** | **8.29E-07** |
| **89A** | **12.2** | **3.0** | **3.0** | **77.6** | **32** | **38334** | **7** | **19.75** | **2.73E-06** | **30** | **15000** | **8** | **18.66** | **4.67E-05** | **34** | **32500** | **15** | **19.71** | **1.83E-06** |
| **89B** | **12.2** | **3.0** | **3.0** | **77.6** | **32** | **32500** | **7** | **19.75** | **2.73E-06** | **30** | **15000** | **8** | **18.66** | **4.67E-05** | **34** | **32500** | **15** | **19.71** | **1.83E-06** |
| **89C** | **12.2** | **3.0** | **3.0** | **77.6** | **32** | **26667** | **7** | **19.75** | **2.73E-06** | **30** | **15000** | **8** | **18.66** | **4.67E-05** | **34** | **32500** | **15** | **19.71** | **1.83E-06** |
| **90A** | **12.0** | **3.0** | **3.5** | **43.9** | **34** | **38334** | **16** | **19.57** | **3.19E-06** | **32** | **15000** | **7** | **19.53** | **5.23E-05** | **34** | **32500** | **11** | **20.28** | **2.50E-06** |
| **90B** | **12.0** | **3.0** | **3.5** | **43.9** | **34** | **32500** | **16** | **19.57** | **3.19E-06** | **32** | **15000** | **7** | **19.53** | **5.23E-05** | **34** | **32500** | **11** | **20.28** | **2.50E-06** |
| **90C** | **12.0** | **3.0** | **3.5** | **43.9** | **34** | **26667** | **16** | **19.57** | **3.19E-06** | **32** | **15000** | **7** | **19.53** | **5.23E-05** | **34** | **32500** | **11** | **20.28** | **2.50E-06** |

| | | | | | | | | | | | | | | | | | | |
|---|---|---|---|---|---|---|---|---|---|---|---|---|---|---|---|---|---|---|
| **91A** | **14.9** | **2.0** | **3.0** | **45.7** | **32** | **38334** | **10** | **19.90** | **1.80E-06** | **24** | **15000** | **17** | **15.55** | **7.71E-06** | **33** | **17500** | **0** | **20.48** | **1.11E-01** |
| **91B** | **14.9** | **2.0** | **3.0** | **45.7** | **32** | **32500** | **10** | **19.90** | **1.80E-06** | **24** | **15000** | **17** | **15.55** | **7.71E-06** | **33** | **17500** | **0** | **20.48** | **1.11E-01** |
| **91C** | **14.9** | **2.0** | **3.0** | **45.7** | **32** | **26667** | **10** | **19.90** | **1.80E-06** | **24** | **15000** | **17** | **15.55** | **7.71E-06** | **33** | **17500** | **0** | **20.48** | **1.11E-01** |
| **92A** | **14.3** | **2.0** | **3.0** | **51.0** | **34** | **38334** | **14** | **20.39** | **1.99E-06** | **26** | **15000** | **12** | **16.02** | **6.77E-06** | **36** | **17500** | **0** | **20.39** | **1.40E-01** |
| **92B** | **14.3** | **2.0** | **3.0** | **51.0** | **34** | **32500** | **14** | **20.39** | **1.99E-06** | **26** | **15000** | **12** | **16.02** | **6.77E-06** | **36** | **17500** | **0** | **20.39** | **1.40E-01** |
| **92C** | **14.3** | **2.0** | **3.0** | **51.0** | **34** | **26667** | **14** | **20.39** | **1.99E-06** | **26** | **15000** | **12** | **16.02** | **6.77E-06** | **36** | **17500** | **0** | **20.39** | **1.40E-01** |
| **93A** | **13.0** | **3.0** | **2.5** | **69.8** | **33** | **38334** | **19** | **19.98** | **2.34E-06** | **25** | **15000** | **17** | **15.59** | **5.36E-06** | **40** | **37500** | **0** | **21.97** | **7.08E-02** |
| **93B** | **13.0** | **3.0** | **2.5** | **69.8** | **33** | **32500** | **19** | **19.98** | **2.34E-06** | **25** | **15000** | **17** | **15.59** | **5.36E-06** | **40** | **37500** | **0** | **21.97** | **7.08E-02** |
| **93C** | **13.0** | **3.0** | **2.5** | **69.8** | **33** | **26667** | **19** | **19.98** | **2.34E-06** | **25** | **15000** | **17** | **15.59** | **5.36E-06** | **40** | **37500** | **0** | **21.97** | **7.08E-02** |
| **94A** | **9.5** | **3.0** | **3.0** | **45.7** | **37** | **38334** | **15** | **19.84** | **2.80E-06** | **25** | **15000** | **12** | **15.96** | **6.46E-06** | **39** | **37500** | **0** | **22.03** | **1.09E-01** |
| **94B** | **9.5** | **3.0** | **3.0** | **45.7** | **37** | **32500** | **15** | **19.84** | **2.80E-06** | **25** | **15000** | **12** | **15.96** | **6.46E-06** | **39** | **37500** | **0** | **22.03** | **1.09E-01** |
| **94C** | **9.5** | **3.0** | **3.0** | **45.7** | **37** | **26667** | **15** | **19.84** | **2.80E-06** | **25** | **15000** | **12** | **15.96** | **6.46E-06** | **39** | **37500** | **0** | **22.03** | **1.09E-01** |
| **95A** | **9.6** | **2.5** | **2.5** | **64.5** | **36** | **38334** | **17** | **19.90** | **2.35E-06** | **27** | **15000** | **17** | **14.26** | **5.32E-06** | **43** | **65500** | **0** | **23.59** | **7.93E-02** |
| **95B** | **9.6** | **2.5** | **2.5** | **64.5** | **36** | **32500** | **17** | **19.90** | **2.35E-06** | **27** | **15000** | **17** | **14.26** | **5.32E-06** | **43** | **65500** | **0** | **23.59** | **7.93E-02** |
| **95C** | **9.6** | **2.5** | **2.5** | **64.5** | **36** | **26667** | **17** | **19.90** | **2.35E-06** | **27** | **15000** | **17** | **14.26** | **5.32E-06** | **43** | **65500** | **0** | **23.59** | **7.93E-02** |
| **96A** | **4.8** | **3.0** | **2.5** | **65.5** | **31** | **38334** | **6** | **19.74** | **2.26E-06** | **26** | **15000** | **16** | **16.08** | **4.31E-06** | **44** | **65500** | **0** | **22.96** | **1.43E-01** |
| **96B** | **4.8** | **3.0** | **2.5** | **65.5** | **31** | **32500** | **6** | **19.74** | **2.26E-06** | **26** | **15000** | **16** | **16.08** | **4.31E-06** | **44** | **65500** | **0** | **22.96** | **1.43E-01** |
| **96C** | **4.8** | **3.0** | **2.5** | **65.5** | **31** | **26667** | **6** | **19.74** | **2.26E-06** | **26** | **15000** | **16** | **16.08** | **4.31E-06** | **44** | **65500** | **0** | **22.96** | **1.43E-01** |
| **97A** | **9.7** | **2.0** | **2.0** | **62.1** | **35** | **38334** | **16** | **19.16** | **1.68E-06** | **24** | **15000** | **12** | **16.91** | **5.60E-06** | **28** | **6000** | **2** | **15.45** | **6.36E-07** |
| **97B** | **9.7** | **2.0** | **2.0** | **62.1** | **35** | **32500** | **16** | **19.16** | **1.68E-06** | **24** | **15000** | **12** | **16.91** | **5.60E-06** | **28** | **6000** | **2** | **15.45** | **6.36E-07** |
| **97C** | **9.7** | **2.0** | **2.0** | **62.1** | **35** | **26667** | **16** | **19.16** | **1.68E-06** | **24** | **15000** | **12** | **16.91** | **5.60E-06** | **28** | **6000** | **2** | **15.45** | **6.36E-07** |
| **98A** | **6.3** | **3.0** | **3.0** | **67.4** | **32** | **38334** | **22** | **20.25** | **1.85E-06** | **23** | **15000** | **9** | **16.42** | **5.06E-06** | **28** | **6000** | **1** | **15.40** | **5.17E-07** |
| **98B** | **6.3** | **3.0** | **3.0** | **67.4** | **32** | **32500** | **22** | **20.25** | **1.85E-06** | **23** | **15000** | **9** | **16.42** | **5.06E-06** | **28** | **6000** | **1** | **15.40** | **5.17E-07** |
| **98C** | **6.3** | **3.0** | **3.0** | **67.4** | **32** | **26667** | **22** | **20.25** | **1.85E-06** | **23** | **15000** | **9** | **16.42** | **5.06E-06** | **28** | **6000** | **1** | **15.40** | **5.17E-07** |
| **99A** | **13.8** | **3.0** | **3.5** | **44.4** | **34** | **38334** | **15** | **20.69** | **2.41E-06** | **23** | **15000** | **8** | **16.35** | **4.39E-06** | **28** | **6000** | **3** | **16.44** | **3.77E-07** |
| **99B** | **13.8** | **3.0** | **3.5** | **44.4** | **34** | **32500** | **15** | **20.69** | **2.41E-06** | **23** | **15000** | **8** | **16.35** | **4.39E-06** | **28** | **6000** | **3** | **16.44** | **3.77E-07** |
| **99C** | **13.8** | **3.0** | **3.5** | **44.4** | **34** | **26667** | **15** | **20.69** | **2.41E-06** | **23** | **15000** | **8** | **16.35** | **4.39E-06** | **28** | **6000** | **3** | **16.44** | **3.77E-07** |
| **100A** | **13.7** | **2.5** | **2.5** | **73.4** | **34** | **38334** | **6** | **19.33** | **3.12E-06** | **33** | **32500** | **12** | **20.25** | **2.41E-06** | **29** | **6000** | **6** | **19.29** | **5.18E-05** |
| **100B** | **13.7** | **2.5** | **2.5** | **73.4** | **34** | **32500** | **6** | **19.33** | **3.12E-06** | **33** | **32500** | **12** | **20.25** | **2.41E-06** | **29** | **6000** | **6** | **19.29** | **5.18E-05** |
| **100C** | **13.7** | **2.5** | **2.5** | **73.4** | **34** | **26667** | **6** | **19.33** | **3.12E-06** | **33** | **32500** | **12** | **20.25** | **2.41E-06** | **29** | **6000** | **6** | **19.29** | **5.18E-05** |
| **101A** | **11.4** | **3.0** | **2.5** | **61.5** | **35** | **38334** | **12** | **21.05** | **2.38E-06** | **34** | **32500** | **11** | **19.62** | **1.81E-06** | **31** | **15000** | **7** | **18.78** | **4.43E-05** |
| **101B** | **11.4** | **3.0** | **2.5** | **61.5** | **35** | **32500** | **12** | **21.05** | **2.38E-06** | **34** | **32500** | **11** | **19.62** | **1.81E-06** | **31** | **15000** | **7** | **18.78** | **4.43E-05** |
| **101C** | **11.4** | **3.0** | **2.5** | **61.5** | **35** | **26667** | **12** | **21.05** | **2.38E-06** | **34** | **32500** | **11** | **19.62** | **1.81E-06** | **31** | **15000** | **7** | **18.78** | **4.43E-05** |
| **102A** | **9.9** | **2.5** | **3.0** | **69.7** | **34** | **38334** | **11** | **19.58** | **1.20E-06** | **36** | **32500** | **11** | **20.09** | **2.40E-06** | **31** | **15000** | **7** | **19.21** | **3.45E-05** |
| **102B** | **9.9** | **2.5** | **3.0** | **69.7** | **34** | **32500** | **11** | **19.58** | **1.20E-06** | **36** | **32500** | **11** | **20.09** | **2.40E-06** | **31** | **15000** | **7** | **19.21** | **3.45E-05** |
| **102C** | **9.9** | **2.5** | **3.0** | **69.7** | **34** | **26667** | **11** | **19.58** | **1.20E-06** | **36** | **32500** | **11** | **20.09** | **2.40E-06** | **31** | **15000** | **7** | **19.21** | **3.45E-05** |
| **103A** | **11.4** | **3.0** | **2.5** | **46.9** | **36** | **38334** | **15** | **19.53** | **2.29E-06** | **33** | **32500** | **17** | **19.03** | **1.84E-06** | **25** | **15000** | **8** | **14.80** | **4.95E-06** |
| **103B** | **11.4** | **3.0** | **2.5** | **46.9** | **36** | **32500** | **15** | **19.53** | **2.29E-06** | **33** | **32500** | **17** | **19.03** | **1.84E-06** | **25** | **15000** | **8** | **14.80** | **4.95E-06** |
| **103C** | **11.4** | **3.0** | **2.5** | **46.9** | **36** | **26667** | **15** | **19.53** | **2.29E-06** | **33** | **32500** | **17** | **19.03** | **1.84E-06** | **25** | **15000** | **8** | **14.80** | **4.95E-06** |

| | | | | | | | | | | | | | | | | | | |
|---|---|---|---|---|---|---|---|---|---|---|---|---|---|---|---|---|---|---|
| **104A** | **15.8** | **3.5** | **3.0** | **60.7** | **33** | **38334** | **15** | **19.07** | **1.94E-06** | **35** | **32500** | **12** | **18.56** | **8.12E-07** | **26** | **15000** | **13** | **16.97** | **6.54E-06** |
| **104B** | **15.8** | **3.5** | **3.0** | **60.7** | **33** | **32500** | **15** | **19.07** | **1.94E-06** | **35** | **32500** | **12** | **18.56** | **8.12E-07** | **26** | **15000** | **13** | **16.97** | **6.54E-06** |
| **104C** | **15.8** | **3.5** | **3.0** | **60.7** | **33** | **26667** | **15** | **19.07** | **1.94E-06** | **35** | **32500** | **12** | **18.56** | **8.12E-07** | **26** | **15000** | **13** | **16.97** | **6.54E-06** |
| **105A** | **15.0** | **2.5** | **2.5** | **71.7** | **34** | **38334** | **15** | **19.15** | **1.84E-06** | **34** | **32500** | **18** | **20.23** | **4.34E-07** | **22** | **15000** | **10** | **15.15** | **4.46E-06** |
| **105B** | **15.0** | **2.5** | **2.5** | **71.7** | **34** | **32500** | **15** | **19.15** | **1.84E-06** | **34** | **32500** | **18** | **20.23** | **4.34E-07** | **22** | **15000** | **10** | **15.15** | **4.46E-06** |
| **105C** | **15.0** | **2.5** | **2.5** | **71.7** | **34** | **26667** | **15** | **19.15** | **1.84E-06** | **34** | **32500** | **18** | **20.23** | **4.34E-07** | **22** | **15000** | **10** | **15.15** | **4.46E-06** |
| **106A** | **9.7** | **2.5** | **3.0** | **73.5** | **35** | **38334** | **11** | **19.03** | **1.85E-06** | **34** | **32500** | **11** | **20.54** | **8.57E-07** | **34** | **32500** | **10** | **19.85** | **1.62E-06** |
| **106B** | **9.7** | **2.5** | **3.0** | **73.5** | **35** | **32500** | **11** | **19.03** | **1.85E-06** | **34** | **32500** | **11** | **20.54** | **8.57E-07** | **34** | **32500** | **10** | **19.85** | **1.62E-06** |
| **106C** | **9.7** | **2.5** | **3.0** | **73.5** | **35** | **26667** | **11** | **19.03** | **1.85E-06** | **34** | **32500** | **11** | **20.54** | **8.57E-07** | **34** | **32500** | **10** | **19.85** | **1.62E-06** |
| **107A** | **11.5** | **2.5** | **2.0** | **58.9** | **34** | **38334** | **10** | **19.95** | **1.41E-06** | **33** | **32500** | **17** | **20.84** | **1.84E-06** | **32** | **32500** | **17** | **18.36** | **2.33E-06** |
| **107B** | **11.5** | **2.5** | **2.0** | **58.9** | **34** | **32500** | **10** | **19.95** | **1.41E-06** | **33** | **32500** | **17** | **20.84** | **1.84E-06** | **32** | **32500** | **17** | **18.36** | **2.33E-06** |
| **107C** | **11.5** | **2.5** | **2.0** | **58.9** | **34** | **26667** | **10** | **19.95** | **1.41E-06** | **33** | **32500** | **17** | **20.84** | **1.84E-06** | **32** | **32500** | **17** | **18.36** | **2.33E-06** |
| **108A** | **7.6** | **2.0** | **3.0** | **35.3** | **35** | **38334** | **10** | **20.82** | **1.79E-06** | **34** | **32500** | **11** | **18.63** | **1.59E-06** | **34** | **32500** | **13** | **19.32** | **2.66E-06** |
| **108B** | **7.6** | **2.0** | **3.0** | **35.3** | **35** | **32500** | **10** | **20.82** | **1.79E-06** | **34** | **32500** | **11** | **18.63** | **1.59E-06** | **34** | **32500** | **13** | **19.32** | **2.66E-06** |
| **108C** | **7.6** | **2.0** | **3.0** | **35.3** | **35** | **26667** | **10** | **20.82** | **1.79E-06** | **34** | **32500** | **11** | **18.63** | **1.59E-06** | **34** | **32500** | **13** | **19.32** | **2.66E-06** |
| **109A** | **4.8** | **2.0** | **3.5** | **65.2** | **32** | **16667** | **1** | **15.86** | **3.58E-07** | **28** | **6000** | **2** | **15.16** | **2.65E-05** | **33** | **17500** | **0** | **22.96** | **7.08E-02** |
| **109B** | **4.8** | **2.0** | **3.5** | **65.2** | **32** | **15000** | **1** | **15.86** | **3.58E-07** | **28** | **6000** | **2** | **15.16** | **2.65E-05** | **33** | **17500** | **0** | **22.96** | **7.08E-02** |
| **109C** | **4.8** | **2.0** | **3.5** | **65.2** | **32** | **13333** | **1** | **15.86** | **3.58E-07** | **28** | **6000** | **2** | **15.16** | **2.65E-05** | **33** | **17500** | **0** | **22.96** | **7.08E-02** |
| **110A** | **8.5** | **2.0** | **3.0** | **58.3** | **33** | **16667** | **7** | **15.99** | **5.24E-05** | **32** | **15000** | **7** | **15.42** | **7.15E-05** | **33** | **32500** | **17** | **20.54** | **1.99E-06** |
| **110B** | **8.5** | **2.0** | **3.0** | **58.3** | **33** | **15000** | **7** | **15.99** | **5.24E-05** | **32** | **15000** | **7** | **15.42** | **7.15E-05** | **33** | **32500** | **17** | **20.54** | **1.99E-06** |
| **110C** | **8.5** | **2.0** | **3.0** | **58.3** | **33** | **13333** | **7** | **15.99** | **5.24E-05** | **32** | **15000** | **7** | **15.42** | **7.15E-05** | **33** | **32500** | **17** | **20.54** | **1.99E-06** |
| **111A** | **6.3** | **3.0** | **2.5** | **62.4** | **34** | **16667** | **7** | **15.66** | **7.15E-05** | **22** | **15000** | **12** | **17.32** | **1.84E-06** | **31** | **17500** | **0** | **21.97** | **1.09E-01** |
| **111B** | **6.3** | **3.0** | **2.5** | **62.4** | **34** | **15000** | **7** | **15.66** | **7.15E-05** | **22** | **15000** | **12** | **17.32** | **1.84E-06** | **31** | **17500** | **0** | **21.97** | **1.09E-01** |
| **111C** | **6.3** | **3.0** | **2.5** | **62.4** | **34** | **13333** | **7** | **15.70** | **7.15E-05** | **22** | **15000** | **12** | **17.32** | **1.84E-06** | **31** | **17500** | **0** | **21.97** | **1.09E-01** |
| **112A** | **12.5** | **2.5** | **4.0** | **53.7** | **32** | **16667** | **6** | **16.39** | **4.17E-05** | **33** | **32500** | **11** | **15.01** | **8.12E-07** | **32** | **15000** | **7** | **19.29** | **2.65E-05** |
| **112B** | **12.5** | **2.5** | **4.0** | **53.7** | **32** | **15000** | **6** | **16.39** | **4.17E-05** | **33** | **32500** | **11** | **15.01** | **8.12E-07** | **32** | **15000** | **7** | **19.29** | **2.65E-05** |
| **112C** | **12.5** | **2.5** | **4.0** | **53.7** | **32** | **13333** | **6** | **16.40** | **4.17E-05** | **33** | **32500** | **11** | **15.01** | **8.12E-07** | **32** | **15000** | **7** | **19.29** | **2.65E-05** |
| **113A** | **2.0** | **1.5** | **1.5** | **2.9** | **24** | **16667** | **7** | **15.55** | **6.30E-06** | **44** | **65500** | **0** | **19.92** | **1.52E-01** | **44** | **65500** | **0** | **21.69** | **8.30E-02** |
| **113B** | **2.0** | **1.5** | **1.5** | **2.9** | **24** | **15000** | **7** | **15.55** | **6.30E-06** | **44** | **65500** | **0** | **19.92** | **1.52E-01** | **44** | **65500** | **0** | **21.69** | **8.30E-02** |
| **113C** | **2.0** | **1.5** | **1.5** | **2.9** | **24** | **13333** | **7** | **15.55** | **6.30E-06** | **44** | **65500** | **0** | **19.92** | **1.52E-01** | **44** | **65500** | **0** | **21.69** | **8.30E-02** |
| **114A** | **1.8** | **3.0** | **2.0** | **3.8** | **33** | **38334** | **3** | **16.02** | **5.64E-06** | **32** | **17500** | **0** | **20.49** | **1.92E-01** | **28** | **6000** | **8** | **16.39** | **6.36E-07** |
| **114B** | **1.8** | **3.0** | **2.0** | **3.8** | **33** | **32500** | **3** | **16.02** | **5.64E-06** | **32** | **17500** | **0** | **20.49** | **1.92E-01** | **28** | **6000** | **8** | **16.39** | **6.36E-07** |
| **114C** | **1.8** | **3.0** | **2.0** | **3.8** | **33** | **26667** | **3** | **16.02** | **5.64E-06** | **32** | **17500** | **0** | **20.49** | **1.92E-01** | **28** | **6000** | **8** | **16.39** | **6.36E-07** |
| **115A** | **2.1** | **2.5** | **3.0** | **3.1** | **35** | **38334** | **17** | **15.59** | **6.16E-06** | **33** | **17500** | **0** | **21.68** | **1.07E-01** | **35** | **32500** | **13** | **16.97** | **1.85E-06** |
| **115B** | **2.1** | **2.5** | **3.0** | **3.1** | **35** | **32500** | **17** | **15.59** | **6.16E-06** | **33** | **17500** | **0** | **21.68** | **1.07E-01** | **35** | **32500** | **13** | **16.97** | **1.85E-06** |
| **115C** | **2.1** | **2.5** | **3.0** | **3.1** | **35** | **26667** | **17** | **15.59** | **6.16E-06** | **33** | **17500** | **0** | **21.68** | **1.07E-01** | **35** | **32500** | **13** | **16.97** | **1.85E-06** |
| **116A** | **1.6** | **4.0** | **2.5** | **3.4** | **26** | **16667** | **5** | **15.96** | **4.81E-06** | **33** | **15000** | **7** | **18.94** | **6.36E-07** | **30** | **17500** | **0** | **19.92** | **1.52E-01** |
| **116B** | **1.6** | **4.0** | **2.5** | **3.4** | **26** | **15000** | **5** | **15.96** | **4.81E-06** | **33** | **15000** | **7** | **18.94** | **6.36E-07** | **30** | **17500** | **0** | **19.92** | **1.52E-01** |
| **116C** | **1.6** | **4.0** | **2.5** | **3.4** | **26** | **13333** | **5** | **15.96** | **4.81E-06** | **33** | **15000** | **7** | **18.94** | **6.36E-07** | **30** | **17500** | **0** | **19.92** | **1.52E-01** |

| | | | | | | | | | | | | | | | | | | |
|---|---|---|---|---|---|---|---|---|---|---|---|---|---|---|---|---|---|---|
| **117A** | **1.7** | **2.0** | **3.5** | **3.9** | **22** | **16667** | **13** | **14.26** | **4.94E-06** | **28** | **6000** | **1** | **18.98** | **5.17E-07** | **33** | **15000** | **6** | **19.21** | **5.18E-05** |
| **117B** | **1.7** | **2.0** | **3.5** | **3.9** | **22** | **15000** | **13** | **14.26** | **4.94E-06** | **28** | **6000** | **1** | **18.98** | **5.17E-07** | **33** | **15000** | **6** | **19.21** | **5.18E-05** |
| **117C** | **1.7** | **2.0** | **3.5** | **3.9** | **22** | **13333** | **13** | **14.26** | **4.94E-06** | **28** | **6000** | **1** | **18.98** | **5.17E-07** | **33** | **15000** | **6** | **19.21** | **5.18E-05** |
| **118A** | **2.1** | **1.5** | **1.5** | **4.2** | **35** | **38334** | **13** | **16.08** | **5.15E-06** | **32** | **15000** | **3** | **20.17** | **3.77E-07** | **33** | **32500** | **6** | **14.80** | **4.95E-06** |
| **118B** | **2.1** | **1.5** | **1.5** | **4.2** | **35** | **32500** | **13** | **16.08** | **5.15E-06** | **32** | **15000** | **3** | **20.17** | **3.77E-07** | **33** | **32500** | **6** | **14.80** | **4.95E-06** |
| **118C** | **2.1** | **1.5** | **1.5** | **4.2** | **35** | **26667** | **13** | **16.08** | **5.15E-06** | **32** | **15000** | **3** | **20.17** | **3.77E-07** | **33** | **32500** | **6** | **14.80** | **4.95E-06** |
| **119A** | **2.2** | **2.0** | **3.0** | **3.0** | **34** | **38334** | **23** | **16.91** | **3.68E-06** | **24** | **15000** | **22** | **16.02** | **4.95E-06** | **32** | **17500** | **0** | **21.78** | **1.28E-01** |
| **119B** | **2.2** | **2.0** | **3.0** | **3.0** | **34** | **32500** | **23** | **16.91** | **3.68E-06** | **24** | **15000** | **22** | **16.02** | **4.95E-06** | **32** | **17500** | **0** | **21.78** | **1.28E-01** |
| **119C** | **2.2** | **2.0** | **3.0** | **3.0** | **34** | **26667** | **23** | **16.91** | **3.68E-06** | **24** | **15000** | **22** | **16.02** | **4.95E-06** | **32** | **17500** | **0** | **21.78** | **1.28E-01** |
| **120A** | **1.8** | **3.0** | **2.5** | **4.3** | **36** | **38334** | **13** | **16.42** | **7.38E-06** | **34** | **32500** | **15** | **17.92** | **6.54E-06** | **34** | **15000** | **3** | **20.20** | **2.35E-05** |
| **120B** | **1.8** | **3.0** | **2.5** | **4.3** | **36** | **32500** | **13** | **16.42** | **7.38E-06** | **34** | **32500** | **15** | **17.92** | **6.54E-06** | **34** | **15000** | **3** | **20.18** | **2.35E-05** |
| **120C** | **1.8** | **3.0** | **2.5** | **4.3** | **36** | **26667** | **13** | **16.42** | **7.38E-06** | **34** | **32500** | **15** | **17.92** | **6.54E-06** | **34** | **15000** | **3** | **20.18** | **2.35E-05** |
| **121A** | **2.4** | **2.5** | **4.0** | **4.0** | **24** | **16667** | **12** | **19.53** | **5.01E-06** | **22** | **15000** | **6** | **15.73** | **4.46E-06** | **36** | **32500** | **23** | **16.08** | **1.62E-06** |
| **121B** | **2.4** | **2.5** | **4.0** | **4.0** | **24** | **15000** | **12** | **19.53** | **5.01E-06** | **22** | **15000** | **6** | **15.73** | **4.46E-06** | **36** | **32500** | **23** | **16.08** | **1.62E-06** |
| **121C** | **2.4** | **2.5** | **4.0** | **4.0** | **24** | **13333** | **12** | **19.53** | **5.01E-06** | **22** | **15000** | **6** | **15.73** | **4.46E-06** | **36** | **32500** | **23** | **16.08** | **1.62E-06** |

# APPENDIX B. MATLAB parameters randomization effect and probability sheet calculation

- **Effect of parameters randomization (**One way ANOVA analysis)

The one-way analysis of variance (ANOVA) is used to determine whether there are any statistically significant differences between the means of three or more independent (unrelated) groups. ANOVA tests the hypothesis ($H_o$) that all group means are equal versus the alternative hypothesis ($H_1$) that at least one group is different from the others.

$H_0$: $\mu_1 = \mu_2 = ... = \mu_k$

$H_1$: not all group means are equal

Where $\mu$ is the group mean and k is the group number. One-way ANOVA analysis was performed using MATLAB for 10 sets of groups for friction angle of silt for its mean value to be $28^o$ and standard deviation of 0.67. Figure B.1 shows the different sets used for the analysis. The resulting p value was equal to 0.9496 > 0.05, which shows that there is no statistical significant difference between the means at 5% significance level.

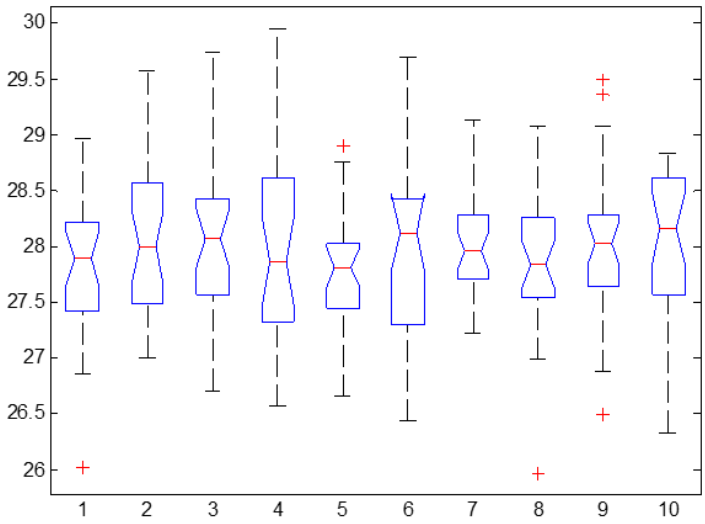


**Figure B.1. Friction angle statistical differences based on ANOVA analysis**

## Table B.1 Probability of exceeding limit state calculation

| Limit state pertinent to Shear Strain at Toe | | | | | L.S.I ($\gamma_{s1}$=1%) | | L.S.II ($\gamma_{s2}$=3%) | | L.S.III ($\gamma_{s3}$=5%) | |
|---|---|---|---|---|---|---|---|---|---|---|
| **Layer** | **μ** | **σ[1]** | **E-/+σ** | **$\gamma_s$ (%)[2]** | **$N_1$= $\gamma_s$ / $\gamma_{s1}$** | **$\Delta N_1$[3]** | **$N_2$= $\gamma_s$ / $\gamma_{s2}$** | **$\Delta N_2$[3]** | **$N_2$= $\gamma_s$ / $\gamma_{s3}$** | **$\Delta N_3$[3]** |
| **Embankment** | 6000 | 1333 | 7333 | 4.8 | 0.208 | 0.077 | 0.625 | 0.232 | 1.042 | 0.387 |
| | | | 4667 | 3.5 | 0.286 | | 0.857 | | 1.429 | |
| | **L.S.I** | **L.S.II** | **L.S.III** | Notations: | | | | | | |
| **Standard deviation[4]** | 0.038 | 0.116 | 0.193 | μ=Expected value of the variable parameter | | | | | | |
| **Mean ($\mu_{\Delta N}$) [5]** | 0.247 | 0.741 | 1.235 | σ=Standard deviation of the variable parameter | | | | | | |
| **C.O.V. ($V_{\Delta N}$) [6]** | 0.156 | 0.156 | 0.156 | LSI=Limit State 1 | | | | | | |
| **Beta (β)[7]** | -9.059 | -2.002 | 1.278 | R=Reliability | | | | | | |
| **R=Φ(β) [8]** | 0 | 0.022 | 0.899 | P(E)=Probability of exceeding the limit state | | | | | | |
| **P(E)=(1-R) [9]** | 1 | 0.977 | 0.100 | | | | | | | |

[1] σ: Standard deviation of the variable parameter based on three-sigma rule $\sigma_v = \frac{HCV - LCV}{6}$ (Duncan, 2000)

[2] $\gamma_s$: Shear strain values measured from PLAXIS finite element analysis for the variable proposed value.

[3] ΔN: Difference in the normalized values of shear strain with respect to the predefined limit states

[4] $\sigma_{\Delta N}$: Standard deviation of ΔN's using the Taylor series technique $\sigma_{\Delta N} = \sqrt{\left(\frac{\Delta N_1}{2}\right)^2_{Embankment}}$ (Wolff, 1994; USACE1997)

[5] $\mu_{\Delta N}$: Mean value for normalized shear strain values.

[6] $V_{\Delta N}$: Coefficient of variation for mean and standard deviation of normalized values. $V_{\Delta N1} = \frac{\sigma_{\Delta N}}{\mu_{\Delta N}}$

[7] $\beta_{ln}$: lognormal distributed reliability index. $\beta_{ln} = \frac{ln\{(\mu_{\Delta N})(\sqrt{1+V_{\Delta N}})\}}{\sqrt{1+V_{\Delta N}}}$ (Duncan, 2000)

[8] R: Reliability value based on normal distribution of the reliability index (Duncan, 2000) $R = \text{NORMSDIST}(\beta_{ln})$

[9] P(E): Probability of exceeding limit state. $P(E) = 1 - R$

# APPENDIX C. MATLAB code and REES tool

The ***REES*** tool consists of the following components (Figure C.1)

1- **Title bar**: shows the tool logo and an about button for some information about the tool, its developer. etc.

2- **Input parameters:** allows the user to input parameters for embankment; geometry (crest width, embankment height, upstream and downstream slope, flood cycles, remedial measures, if any); soil layer properties (friction angle, cohesion, saturated unit weight and permeability). It also allows the conversion between English an SI units and to draw geometry of the embankment.

3- **Consequences of Embankment failure:** allows the user to calculate the consequences of failure in terms of loss of life (LOL) or economic consequences.

4- **Output/ analysis:** runs ANN to predict shear strain values and then probabilities of exceeding limit state values

5- **Risk value:** calculates total risk based on 1000 people PAR, fatality rate from 0 to 3 miles and PE (LSIII).

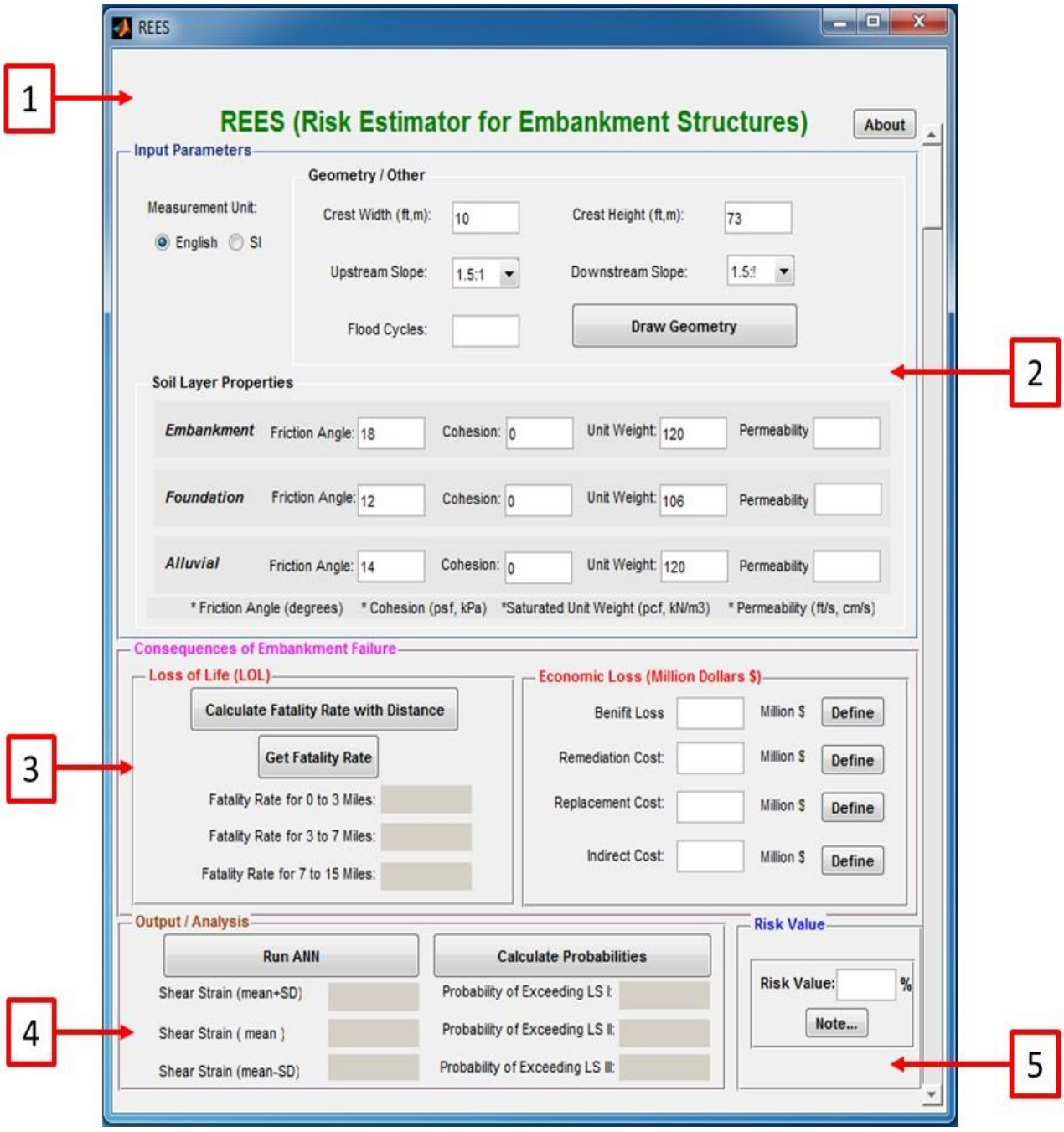


**Figure C.1. REES "Risk Estimator for Embankment Structures" tool interface component**

### Neural Network MATLAB code

```
% Solve an Input-Output Fitting problem with a Neural Network
% Script generated by Neural Fitting app
% Created Sun May 14 21:30:36 EDT 2017
% This script assumes these variables are defined:
%   data - input data.
%   Target_data_2 - target data.
x = data';
t = Target_data_2';
% Choose a Training Function
% For a list of all training functions type: help nntrain
% 'trainlm' is usually fastest.
% 'trainbr' takes longer but may be better for challenging problems.
% 'trainscg' uses less memory. NFTOOL falls back to this in low memory
situations.
trainFcn = 'trainscg'; % Scaled conjugate gradient backpropagation
% Create a Fitting Network
hiddenLayerSize = 7;
net = fitnet(hiddenLayerSize,trainFcn);
net.trainParam.min_grad=1e-10;
net.trainParam.max_fail=100;
% Choose Input and Output Pre/Post-Processing Functions
% For a list of all processing functions type: help nnprocess
net.input.processFcns = {'removeconstantrows','mapminmax'};
net.output.processFcns = {'removeconstantrows','mapminmax'};
% Setup Division of Data for Training, Validation, Testing
% For a list of all data division functions type: help nndivide
net.divideFcn = 'dividerand';  % Divide data randomly
net.divideMode = 'sample';  % Divide up every sample
net.divideParam.trainRatio = 60/100;
net.divideParam.valRatio = 20/100;
net.divideParam.testRatio = 20/100;
% Choose a Performance Function
% For a list of all performance functions type: help nnperformance
net.performFcn = 'mse';  % Mean squared error
```

```
% Choose Plot Functions
% For a list of all plot functions type: help nnplot
net.plotFcns = {'plotperform','plottrainstate','ploterrhist', ...
  'plotregression', 'plotfit'};
% Train the Network
nnNum=10000;
for i=1:nnNum
fprintf('Training %d/%d\n', i, nnNum);
[net,tr] = train(net,x,t);
end
% Test the Network
y = net(x);
e = gsubtract(t,y);
performance = perform(net,t,y)
% Recalculate Training, Validation and Test Performance
trainTargets = t .* tr.trainMask{1};
valTargets = t  .* tr.valMask{1};
testTargets = t  .* tr.testMask{1};
trainPerformance = perform(net,trainTargets,y)
valPerformance = perform(net,valTargets,y)
testPerformance = perform(net,testTargets,y)
% View the Network
view(net)
% Plots
% Uncomment these lines to enable various plots.
figure, plotperform(tr)
%figure, plottrainstate(tr)
%figure, plotfit(net,x,t)
figure, plotregression(t,y)
figure, ploterrhist(e)
% Deployment
% Change the (false) values to (true) to enable the following code blocks.
if (false)
  % Generate MATLAB function for neural network for application deployment
  % in MATLAB scripts or with MATLAB Compiler and Builder tools, or simply
  % to examine the calculations your trained neural network performs.
```

```
  genFunction(net,'myNeuralNetworkFunction');
  y = myNeuralNetworkFunction(x);
end
if (false)
  % Generate a matrix-only MATLAB function for neural network code
  % generation with MATLAB Coder tools.
  genFunction(net,'myNeuralNetworkFunction','MatrixOnly','yes');
  y = myNeuralNetworkFunction(x);
end
if (false)
  % Generate a Simulink diagram for simulation or deployment with.
  % Simulink Coder tools.
  gensim(net);
end
```

**REES MATLAB code**

```
function varargout = RiskEstimator(varargin)
% RISKESTIMATOR MATLAB code for RiskEstimator.fig
% RISKESTIMATOR, by itself, creates a new RISKESTIMATOR or raises the
existing singleton*.
% H = RISKESTIMATOR returns the handle to a new RISKESTIMATOR or the
handle to the existing singleton*.
% RISKESTIMATOR('CALLBACK',hObject,eventData,handles,...) calls the local
% function named CALLBACK in RISKESTIMATOR.M with the given input
arguments.
% RISKESTIMATOR('Property','Value',...) creates a new RISKESTIMATOR or
raises the existing singleton*.  Starting from the left, property value
pairs are applied to the GUI before RiskEstimator_OpeningFcn gets called.
An unrecognized property name or invalid value makes property application
top.  All inputs are passed to RiskEstimator_OpeningFcn via varargin
%      *See GUI Options on GUIDE's Tools menu.  Choose "GUI allows only
one instance to run (singleton)".
% See also: GUIDE, GUIDATA, GUIHANDLES
% Edit the above text to modify the response to help RiskEstimator
% Last Modified by GUIDE v2.5 20-Jul-2017 13:29:33
```

```
% Begin initialization code - DO NOT EDIT
gui_Singleton = 1;
gui_State = struct('gui_Name',       mfilename, ...
                   'gui_Singleton',  gui_Singleton, ...
                   'gui_OpeningFcn', @RiskEstimator_OpeningFcn, ...
                   'gui_OutputFcn',  @RiskEstimator_OutputFcn, ...
                   'gui_LayoutFcn',  [] , ...
                   'gui_Callback',   []);
if nargin && ischar(varargin{1})
    gui_State.gui_Callback = str2func(varargin{1});
end

if nargout
    [varargout{1:nargout}] = gui_mainfcn(gui_State, varargin{:});
else
    gui_mainfcn(gui_State, varargin{:});
end
% End initialization code - DO NOT EDIT
%The following line alerts MATLAB compiler NOT to use overloaded sim
%function that cannot be compiled
%#function network

% --- Executes just before RiskEstimator is made visible.
function RiskEstimator_OpeningFcn(hObject, eventdata, handles, varargin)
% This function has no output args, see OutputFcn.
% hObject    handle to figure
% eventdata  reserved - to be defined in a future version of MATLAB
% handles    structure with handles and user data (see GUIDATA)
% varargin   command line arguments to RiskEstimator (see VARARGIN)

% Choose default command line output for RiskEstimator
handles.output = hObject;

% If there is a splash screen for deployed version, kill it since this
code
% is now running and MCR is no longer loading.
```

```
if isdeployed
    %if ~isempty(varargin)
    %     [pathToFile,nameOfFile,fileExt] = fileparts(varargin{1});
    %     nameOfExe=[nameOfFile,fileExt];
    %     dosCmd = ['taskkill /f /im "' nameOfExe '"'];
         dosCmd = 'taskkill /f /im "REES.exe"';
         dos(dosCmd);
    %end
end

% Update handles structure
guidata(hObject, handles);

% UIWAIT makes RiskEstimator wait for user response (see UIRESUME)
% uiwait(handles.figure1);

% Display parameter1.parameter2 image for parameter3 milliseconds
%splashScreen('splashScreen', 'png', 4000);

% --- Outputs from this function are returned to the command line.
function varargout = RiskEstimator_OutputFcn(hObject, eventdata, handles)
% varargout  cell array for returning output args (see VARARGOUT);
% hObject    handle to figure
% eventdata  reserved - to be defined in a future version of MATLAB
% handles    structure with handles and user data (see GUIDATA)

% Get default command line output from handles structure
varargout{1} = handles.output;

% Declare global variables to be used my multiple functions
global cWidth eHeight eFAngle eCohesion eUWeight eperm fFAngle fCohesion
fUWeight fperm aFAngle aCohesion aUWeight aperm;
global riskValue floodCycle;

initializeVariables(0); % 0 means initializing all variables
```

```
set(handles.crestWidth,'String',cWidth);
set(handles.embankmentHeight,'String',eHeight);
set(handles.EmbankmentFA,'String',eFAngle);
set(handles.EmbankmentC,'String',eCohesion);
set(handles.EmbankmentUW,'String',eUWeight);
set(handles.EmbankmentP,'String',eperm);
set(handles.FoundationFA,'String',fFAngle);
set(handles.FoundationC,'String',fCohesion);
set(handles.FoundationUW,'String',fUWeight);
set(handles.FoundationP,'String',fperm);
set(handles.AlluvialFA,'String',aFAngle);
set(handles.AlluvialC,'String',aCohesion);
set(handles.AlluvialUW,'String',aUWeight);
set(handles.AlluvialP,'String',aperm);
set(handles.riskValue,'String',riskValue);


% --- Initializing variables
function initializeVariables(isPartialInit)

global unitLength cWidth eHeight uSlope dSlope;
global cWidthMin cWidthMax eHeightMin eHeightMax;
global eFAngle eCohesion eUWeight eperm fFAngle fCohesion fUWeight fperm
aFAngle aCohesion aUWeight aperm;
global eFAngleMin fFAngleMin aFAngleMin eFAngleMax fFAngleMax aFAngleMax
cohesionMin cohesionMax epermMin epermMax fpermMin fpermMax apermMin
apermMax;
global eUWeightMin eUWeightMax fUWeightMin fUWeightMax aUWeightMin
aUWeightMax firstANNrun firstLoLCalc;
global riskValue floodCycle floodCycleMin floodCycleMax pLS3 lol1;
%global remedialMeasures;

% Default unit scale is English
unitLength = 'ft';
```

```
cWidthMin = 5.2;
cWidthMax = 65.6;
eHeightMin = 6.56;
eHeightMax = 328.1;
eUWeightMin = 88;
eUWeightMax = 138;
fUWeightMin = 88;
fUWeightMax = 155;
aUWeightMin = 88;
aUWeightMax = 155;

if (isPartialInit) % True when called from function
unitChoice_SelectionChangeFcn()
    return;
end

% These are only initialized when the program runs for the first time
epermMin   = 3.3e-12;
epermMax   = 3.3e-6;
fpermMin   = 6.6e-12;
fpermMax   = 3e-3;
apermMin   = 6.6e-12;
apermMax   = 3e-3;
eFAngleMin = 18;
eFAngleMax = 38;
fFAngleMin = 18;
fFAngleMax = 45;
aFAngleMin = 18;
aFAngleMax = 45;
cohesionMin = 0;
cohesionMax = 543;

cWidth = cWidthMin;
eHeight = eHeightMin;
eFAngle = eFAngleMin;
eCohesion = 209;
```

```
eUWeight = eUWeightMin;
eperm = epermMin;
fFAngle = fFAngleMin;
fCohesion = 209;
fUWeight = fUWeightMin;
fperm = fpermMin;
aFAngle = aFAngleMin;
aCohesion = 209;
aUWeight = aUWeightMin;
aperm = apermMin;
uSlope = 2;
dSlope = 2;
firstANNrun = 1;
firstLoLCalc = 1;
riskValue = 0;
%floodCycleMin = 0;
%floodCycleMax = 10;
floodCycle = 1;
%remedialMeasures = 1;
pLS3 = '';
lol1 = '';

% --- Executes during object creation, after setting all properties.
function axes5_CreateFcn(hObject, eventdata, handles)
% hObject    handle to axes5 (see GCBO)
% eventdata  reserved - to be defined in a future version of MATLAB
% handles    empty - handles not created until after all CreateFcns called

% Hint: place code in OpeningFcn to populate axes5
imshow('Banner.png');

% --- Executes on button press in About.
function About_Callback(hObject, eventdata, handles)
% hObject    handle to About (see GCBO)
% eventdata  reserved - to be defined in a future version of MATLAB
% handles    structure with handles and user data (see GUIDATA)
```

```
textMsg = 'This MATLAB program calculates risks for embankment structures.
It applies Artificial Neural Network (ANN) to estimate risks based on
probabilities of exceeding pre-defined limit states.';
textMsg = strcat(textMsg, '\n\nThe program is developed as part of DHS
Coastal Hazard Center and NC State University collaboration (PI: Dr. M.
Gabr, Dept of Civil, Construction and Environmental Engineering, NCSU,
Raleigh, NC 27695).');
helpdlg(sprintf(textMsg),'About This Software');
%??? Describe more the formula used and flow chart

% --- Executes on button press in loadButton.
function loadButton_Callback(~, eventdata, handles)
% hObject    handle to loadButton (see GCBO)
% eventdata  reserved - to be defined in a future version of MATLAB
% handles    structure with handles and user data (see GUIDATA)

%global fName pName;
[fName, pName] = uigetfile('*.xlsx','Select an Excel Data File');
% Checking errors
if fName == 0
    errordlg('File not loaded!','Error');
    return;
end
file = strcat(pName, fName);
set(handles.loadText,'String',strcat('Data file: ', file));
%{
Excel Practice
filename = 'test.xlsx';
A = {5};
sheet = 1;
xlRange = 'A5';
xlswrite(filename,A,sheet,xlRange);
xlsread(filename, sheet, 'B7:N26');
%}

function crestWidth_Callback(hObject, eventdata, handles)
```

```
% hObject    handle to crestWidth (see GCBO)
% eventdata  reserved - to be defined in a future version of MATLAB
% handles    structure with handles and user data (see GUIDATA)

% Hints: get(hObject,'String') returns contents of crestWidth as text
%        str2double(get(hObject,'String')) returns contents of crestWidth
as a double
global cWidth cWidthMin cWidthMax;
v = str2double(get(hObject,'String'));
if (checkValue(v, cWidthMin, cWidthMax, 'crest width', 1, '') == 1)
    cWidth = v;
else % Give the edit_slice text box focus so user can correct the error
    set(handles.crestWidth,'String',cWidth);
    %uicontrol(hObject);
end

% --- Executes during object creation, after setting all properties.
function crestWidth_CreateFcn(hObject, eventdata, handles)
% hObject    handle to crestWidth (see GCBO)
% eventdata  reserved - to be defined in a future version of MATLAB
% handles    empty - handles not created until after all CreateFcns called

% Hint: edit controls usually have a white background on Windows.
%       See ISPC and COMPUTER.
if ispc && isequal(get(hObject,'BackgroundColor'),
get(0,'defaultUicontrolBackgroundColor'))
    set(hObject,'BackgroundColor','white');
end

function upstreamSlope_Callback(hObject, eventdata, handles)
% hObject    handle to upstreamSlope (see GCBO)
% eventdata  reserved - to be defined in a future version of MATLAB
% handles    structure with handles and user data (see GUIDATA)

% Hints: get(hObject,'String') returns contents of upstreamSlope as text
```

```
%        str2double(get(hObject,'String')) returns contents of
upstreamSlope as a double

% --- Executes during object creation, after setting all properties.
function upstreamSlope_CreateFcn(hObject, eventdata, handles)
% hObject    handle to upstreamSlope (see GCBO)
% eventdata  reserved - to be defined in a future version of MATLAB
% handles    empty - handles not created until after all CreateFcns called

% Hint: edit controls usually have a white background on Windows.
%       See ISPC and COMPUTER.
if ispc && isequal(get(hObject,'BackgroundColor'),
get(0,'defaultUicontrolBackgroundColor'))
    set(hObject,'BackgroundColor','white');
end

function embankmentHeight_Callback(hObject, eventdata, handles)
% hObject    handle to upstreamSlope (see GCBO)
% eventdata  reserved - to be defined in a future version of MATLAB
% handles    structure with handles and user data (see GUIDATA)

% Hints: get(hObject,'String') returns contents of upstreamSlope as text
%        str2double(get(hObject,'String')) returns contents of
upstreamSlope as a double
global eHeight eHeightMin eHeightMax;
v = str2double(get(hObject,'String'));
if (checkValue(v, eHeightMin, eHeightMax, 'embankment height', 1, '') ==
1)
    eHeight = v;
else % Give the edit_slice text box focus so user can correct the error
    set(handles.embankmentHeight,'String',eHeight);
    %uicontrol(hObject);
end

% --- Executes during object creation, after setting all properties.
```

```
function embankmentHeight_CreateFcn(hObject, eventdata, handles)
% hObject    handle to upstreamSlope (see GCBO)
% eventdata  reserved - to be defined in a future version of MATLAB
% handles    empty - handles not created until after all CreateFcns called

% Hint: edit controls usually have a white background on Windows.
%       See ISPC and COMPUTER.
if ispc && isequal(get(hObject,'BackgroundColor'),
get(0,'defaultUicontrolBackgroundColor'))
    set(hObject,'BackgroundColor','white');
end

function downstreamSlope_Callback(hObject, eventdata, handles)
% hObject    handle to downstreamSlope (see GCBO)
% eventdata  reserved - to be defined in a future version of MATLAB
% handles    structure with handles and user data (see GUIDATA)

% Hints: get(hObject,'String') returns contents of downstreamSlope as text
%        str2double(get(hObject,'String')) returns contents of
downstreamSlope as a double



% --- Executes during object creation, after setting all properties.
function downstreamSlope_CreateFcn(hObject, eventdata, handles)
% hObject    handle to downstreamSlope (see GCBO)
% eventdata  reserved - to be defined in a future version of MATLAB
% handles    empty - handles not created until after all CreateFcns called

% Hint: edit controls usually have a white background on Windows.
%       See ISPC and COMPUTER.
if ispc && isequal(get(hObject,'BackgroundColor'),
get(0,'defaultUicontrolBackgroundColor'))
    set(hObject,'BackgroundColor','white');
end
```

```
function EmbankmentFA_Callback(hObject, eventdata, handles)
% hObject    handle to EmbankmentFA (see GCBO)
% eventdata  reserved - to be defined in a future version of MATLAB
% handles    structure with handles and user data (see GUIDATA)

% Hints: get(hObject,'String') returns contents of EmbankmentFA as text
%        str2double(get(hObject,'String')) returns contents of
EmbankmentFA as a double
global eFAngle eFAngleMin eFAngleMax;
v = str2double(get(hObject,'String'));
if (checkValue(v, eFAngleMin, eFAngleMax, 'embankment friction angle', 0,
'degrees') == 1)
    eFAngle = v;
else % Give the edit_slice text box focus so user can correct the error
    set(handles.EmbankmentFA,'String',eFAngle);
    %uicontrol(hObject);
end

% --- Executes during object creation, after setting all properties.
function EmbankmentFA_CreateFcn(hObject, eventdata, handles)
% hObject    handle to EmbankmentFA (see GCBO)
% eventdata  reserved - to be defined in a future version of MATLAB
% handles    empty - handles not created until after all CreateFcns called

% Hint: edit controls usually have a white background on Windows.
%       See ISPC and COMPUTER.
if ispc && isequal(get(hObject,'BackgroundColor'),
get(0,'defaultUicontrolBackgroundColor'))
    set(hObject,'BackgroundColor','white');
end

function EmbankmentC_Callback(hObject, eventdata, handles)
% hObject    handle to EmbankmentC (see GCBO)
% eventdata  reserved - to be defined in a future version of MATLAB
% handles    structure with handles and user data (see GUIDATA)
```

```
% Hints: get(hObject,'String') returns contents of EmbankmentC as text
%        str2double(get(hObject,'String')) returns contents of EmbankmentC
as a double
global eCohesion cohesionMin cohesionMax unitLength;
v = str2double(get(hObject,'String'));
if (strcmp(unitLength,'ft') == 1)
    cUnit = 'psf';
else cUnit = 'kpa';
end
if (checkValue(v, cohesionMin, cohesionMax, 'embankment cohesion', 0,
cUnit) == 1)
    eCohesion = v;
else % Give the edit_slice text box focus so user can correct the error
    set(handles.EmbankmentC,'String',eCohesion);
    %uicontrol(hObject);
end



% --- Executes during object creation, after setting all properties.
function EmbankmentC_CreateFcn(hObject, eventdata, handles)
% hObject    handle to EmbankmentC (see GCBO)
% eventdata  reserved - to be defined in a future version of MATLAB
% handles    empty - handles not created until after all CreateFcns called

% Hint: edit controls usually have a white background on Windows.
%       See ISPC and COMPUTER.
if ispc && isequal(get(hObject,'BackgroundColor'),
get(0,'defaultUicontrolBackgroundColor'))
    set(hObject,'BackgroundColor','white');
end

function edit7_Callback(hObject, eventdata, handles)
% hObject    handle to edit7 (see GCBO)
% eventdata  reserved - to be defined in a future version of MATLAB
```

```
% handles    structure with handles and user data (see GUIDATA)

% Hints: get(hObject,'String') returns contents of edit7 as text
%        str2double(get(hObject,'String')) returns contents of edit7 as a
double

% --- Executes during object creation, after setting all properties.
function edit7_CreateFcn(hObject, eventdata, handles)
% hObject    handle to edit7 (see GCBO)
% eventdata  reserved - to be defined in a future version of MATLAB
% handles    empty - handles not created until after all CreateFcns called

% Hint: edit controls usually have a white background on Windows.
%       See ISPC and COMPUTER.
if ispc && isequal(get(hObject,'BackgroundColor'),
get(0,'defaultUicontrolBackgroundColor'))
    set(hObject,'BackgroundColor','white');
end
function EmbankmentUW_Callback(hObject, eventdata, handles)
% hObject    handle to EmbankmentUW (see GCBO)
% eventdata  reserved - to be defined in a future version of MATLAB
% handles    structure with handles and user data (see GUIDATA)

% Hints: get(hObject,'String') returns contents of EmbankmentUW as text
%        str2double(get(hObject,'String')) returns contents of
EmbankmentUW as a double
global eUWeight eUWeightMin eUWeightMax unitLength;
v = str2double(get(hObject,'String'));
if (strcmp(unitLength,'ft') == 1)
    uwUnit = 'pcf';
else uwUnit = 'kN/m3';
end
if (checkValue(v, eUWeightMin, eUWeightMax, 'embankment unit weight', 0,
uwUnit) == 1)
    eUWeight = v;
else % Give the edit_slice text box focus so user can correct the error
```

```
    set(handles.EmbankmentUW,'String',eUWeight);
    %uicontrol(hObject);
end

% --- Executes during object creation, after setting all properties.
function EmbankmentUW_CreateFcn(hObject, eventdata, handles)
% hObject    handle to EmbankmentUW (see GCBO)
% eventdata  reserved - to be defined in a future version of MATLAB
% handles    empty - handles not created until after all CreateFcns called

% Hint: edit controls usually have a white background on Windows.
%       See ISPC and COMPUTER.
if ispc && isequal(get(hObject,'BackgroundColor'),
get(0,'defaultUicontrolBackgroundColor'))
    set(hObject,'BackgroundColor','white');
end

function EmbankmentP_Callback(hObject, eventdata, handles)
% hObject    handle to EmbankmentP (see GCBO)
% eventdata  reserved - to be defined in a future version of MATLAB
% handles    structure with handles and user data (see GUIDATA)
global eperm epermMin epermMax unitLength;
v = str2double(get(hObject,'String'));
if (strcmp(unitLength,'ft') == 1)
    permUnit = 'cm/s';
else permUnit = 'ft/s';
end
if (checkValue(v, epermMin, epermMax, 'Embankment permeability', 0,
permUnit') == 1)
    eperm = v;
else % Give the edit_slice text box focus so user can correct the error
    set(handles.EmbankmentP,'String',eperm);
end

    %uicontrol(hObject);
% Hints: get(hObject,'String') returns contents of EmbankmentP as text
```

```
%        str2double(get(hObject,'String')) returns contents of EmbankmentP
as a double

% --- Executes during object creation, after setting all properties.
function EmbankmentP_CreateFcn(hObject, eventdata, handles)
% hObject    handle to EmbankmentP (see GCBO)
% eventdata  reserved - to be defined in a future version of MATLAB
% handles    empty - handles not created until after all CreateFcns called

% Hint: edit controls usually have a white background on Windows.
%       See ISPC and COMPUTER.
if ispc && isequal(get(hObject,'BackgroundColor'),
get(0,'defaultUicontrolBackgroundColor'))
    set(hObject,'BackgroundColor','white');
end

% --- Executes during object creation, after setting all properties.
function textEP_CreateFcn(hObject, eventdata, handles)
% hObject    handle to textEP (see GCBO)
% eventdata  reserved - to be defined in a future version of MATLAB
% handles    empty - handles not created until after all CreateFcns called

function FoundationFA_Callback(hObject, eventdata, handles)
% hObject    handle to FoundationFA (see GCBO)
% eventdata  reserved - to be defined in a future version of MATLAB
% handles    structure with handles and user data (see GUIDATA)

% Hints: get(hObject,'String') returns contents of FoundationFA as text
%        str2double(get(hObject,'String')) returns contents of
FoundationFA as a double
global fFAngle fFAngleMin fFAngleMax;
v = str2double(get(hObject,'String'));
if (checkValue(v, fFAngleMin, fFAngleMax, 'Foundation friction angle', 0,
'degrees') == 1)
    fFAngle = v;
```

```
else % Give the edit_slice text box focus so user can correct the error
    set(handles.FoundationFA,'String',fFAngle);
    %uicontrol(hObject);
end

% --- Executes during object creation, after setting all properties.
function FoundationFA_CreateFcn(hObject, eventdata, handles)
% hObject    handle to FoundationFA (see GCBO)
% eventdata  reserved - to be defined in a future version of MATLAB
% handles    empty - handles not created until after all CreateFcns called

% Hint: edit controls usually have a white background on Windows.
%       See ISPC and COMPUTER.
if ispc && isequal(get(hObject,'BackgroundColor'),
get(0,'defaultUicontrolBackgroundColor'))
    set(hObject,'BackgroundColor','white');
end

function FoundationC_Callback(hObject, eventdata, handles)
% hObject    handle to FoundationC (see GCBO)
% eventdata  reserved - to be defined in a future version of MATLAB
% handles    structure with handles and user data (see GUIDATA)

% Hints: get(hObject,'String') returns contents of FoundationC as text
%        str2double(get(hObject,'String')) returns contents of FoundationC
as a double
global fCohesion cohesionMin cohesionMax unitLength;
v = str2double(get(hObject,'String'));
if (strcmp(unitLength,'ft') == 1)
    cUnit = 'psf';
else cUnit = 'kpa';
end
if (checkValue(v, cohesionMin, cohesionMax, 'Foundation cohesion', 0,
cUnit) == 1)
    fCohesion = v;
else % Give the edit_slice text box focus so user can correct the error
```

```
    set(handles.FoundationC,'String',fCohesion);
    %uicontrol(hObject);
end

% --- Executes during object creation, after setting all properties.
function FoundationC_CreateFcn(hObject, eventdata, handles)
% hObject    handle to FoundationC (see GCBO)
% eventdata  reserved - to be defined in a future version of MATLAB
% handles    empty - handles not created until after all CreateFcns called

% Hint: edit controls usually have a white background on Windows.
%       See ISPC and COMPUTER.
if ispc && isequal(get(hObject,'BackgroundColor'),
get(0,'defaultUicontrolBackgroundColor'))
    set(hObject,'BackgroundColor','white');
end

function FoundationUW_Callback(hObject, eventdata, handles)
% hObject    handle to FoundationUW (see GCBO)
% eventdata  reserved - to be defined in a future version of MATLAB
% handles    structure with handles and user data (see GUIDATA)

% Hints: get(hObject,'String') returns contents of FoundationUW as text
%        str2double(get(hObject,'String')) returns contents of
FoundationUW as a double
global fUWeight fUWeightMin fUWeightMax unitLength;
v = str2double(get(hObject,'String'));
if (strcmp(unitLength,'ft') == 1)
    uwUnit = 'pcf';
else uwUnit = 'kN/m3';
end
if (checkValue(v, fUWeightMin, fUWeightMax, 'Foundation unit weight', 0,
uwUnit) == 1)
    fUWeight = v;
else % Give the edit_slice text box focus so user can correct the error
    set(handles.FoundationUW,'String',fUWeight);
```

```
    %uicontrol(hObject);
end
% --- Executes during object creation, after setting all properties.
function FoundationUW_CreateFcn(hObject, eventdata, handles)
% hObject    handle to FoundationUW (see GCBO)
% eventdata  reserved - to be defined in a future version of MATLAB
% handles    empty - handles not created until after all CreateFcns called

% Hint: edit controls usually have a white background on Windows.
%       See ISPC and COMPUTER.
if ispc && isequal(get(hObject,'BackgroundColor'),
get(0,'defaultUicontrolBackgroundColor'))
    set(hObject,'BackgroundColor','white');
end
function FoundationP_Callback(hObject, eventdata, handles)
% hObject    handle to FoundationP (see GCBO)
% eventdata  reserved - to be defined in a future version of MATLAB
% handles    structure with handles and user data (see GUIDATA)

% Hints: get(hObject,'String') returns contents of FoundationP as text
%        str2double(get(hObject,'String')) returns contents of FoundationP
as a double
global fperm fpermMin fpermMax unitLength;
v = str2double(get(hObject,'String'));
if (strcmp(unitLength,'ft') == 1)
    permUnit = 'cm/s';
else permUnit = 'ft/s';
end
if (checkValue(v, fpermMin, fpermMax, 'Foundation permeability', 0,
permUnit) == 1)
    fperm = v;
else % Give the edit_slice text box focus so user can correct the error
    set(handles.FoundationP,'String',fperm);
    %uicontrol(hObject);
end
```

```
% --- Executes during object creation, after setting all properties.
function FoundationP_CreateFcn(hObject, eventdata, handles)
% hObject    handle to FoundationP (see GCBO)
% eventdata  reserved - to be defined in a future version of MATLAB
% handles    empty - handles not created until after all CreateFcns called

% Hint: edit controls usually have a white background on Windows.
%       See ISPC and COMPUTER.
if ispc && isequal(get(hObject,'BackgroundColor'),
get(0,'defaultUicontrolBackgroundColor'))
    set(hObject,'BackgroundColor','white');
end

function AlluvialFA_Callback(hObject, eventdata, handles)
% hObject    handle to AlluvialFA (see GCBO)
% eventdata  reserved - to be defined in a future version of MATLAB
% handles    structure with handles and user data (see GUIDATA)
% Hints: get(hObject,'String') returns contents of AlluvialFA as text
%        str2double(get(hObject,'String')) returns contents of AlluvialFA
as a double
global aFAngle aFAngleMin aFAngleMax;
v = str2double(get(hObject,'String'));
if (checkValue(v, aFAngleMin, aFAngleMax, 'Alluvial friction angle', 0,
'degrees') == 1)
    aFAngle = v;
else % Give the edit_slice text box focus so user can correct the error
    set(handles.AlluvialFA,'String',aFAngle);
    %uicontrol(hObject);
end

% --- Executes during object creation, after setting all properties.
function AlluvialFA_CreateFcn(hObject, eventdata, handles)
% hObject    handle to FoundationFA (see GCBO)
% eventdata  reserved - to be defined in a future version of MATLAB
% handles    empty - handles not created until after all CreateFcns called
```

```
% Hint: edit controls usually have a white background on Windows.
%       See ISPC and COMPUTER.
if ispc && isequal(get(hObject,'BackgroundColor'),
get(0,'defaultUicontrolBackgroundColor'))
    set(hObject,'BackgroundColor','white');
end

function AlluvialC_Callback(hObject, eventdata, handles)
% hObject    handle to AlluvialC (see GCBO)
% eventdata  reserved - to be defined in a future version of MATLAB
% handles    structure with handles and user data (see GUIDATA)
% Hints: get(hObject,'String') returns contents of AlluvialC as text
%        str2double(get(hObject,'String')) returns contents of AlluvialC
as a double
global aCohesion cohesionMin cohesionMax unitLength;
v = str2double(get(hObject,'String'));
if (strcmp(unitLength,'ft') == 1)
    cUnit = 'psf';
else cUnit = 'kpa';
end
if (checkValue(v, cohesionMin, cohesionMax, 'Alluvial cohesion', 0, cUnit)
== 1)
    aCohesion = v;
else % Give the edit_slice text box focus so user can correct the error
    set(handles.AlluvialC,'String',aCohesion);
    %uicontrol(hObject);
end

% --- Executes during object creation, after setting all properties.
function AlluvialC_CreateFcn(hObject, eventdata, handles)
% hObject    handle to FoundationC (see GCBO)
% eventdata  reserved - to be defined in a future version of MATLAB
% handles    empty - handles not created until after all CreateFcns called

% Hint: edit controls usually have a white background on Windows.
%       See ISPC and COMPUTER.
```

```
if ispc && isequal(get(hObject,'BackgroundColor'),
get(0,'defaultUicontrolBackgroundColor'))
    set(hObject,'BackgroundColor','white');
end

function AlluvialUW_Callback(hObject, eventdata, handles)
% hObject    handle to AlluvialUW (see GCBO)
% eventdata  reserved - to be defined in a future version of MATLAB
% handles    structure with handles and user data (see GUIDATA)

% Hints: get(hObject,'String') returns contents of AlluvialUW as text
%        str2double(get(hObject,'String')) returns contents of AlluvialUW
as a double
global aUWeight aUWeightMin aUWeightMax unitLength;
v = str2double(get(hObject,'String'));
if (strcmp(unitLength,'ft') == 1)
    uwUnit = 'pcf';
else uwUnit = 'kN/m3';
end
if (checkValue(v, aUWeightMin, aUWeightMax, 'Alluvial unit weight', 0,
uwUnit) == 1)
    aUWeight = v;
else % Give the edit_slice text box focus so user can correct the error
    set(handles.AlluvialUW,'String',aUWeight);
    %uicontrol(hObject);
end

% --- Executes during object creation, after setting all properties.
function AlluvialUW_CreateFcn(hObject, eventdata, handles)
% hObject    handle to FoundationUW (see GCBO)
% eventdata  reserved - to be defined in a future version of MATLAB
% handles    empty - handles not created until after all CreateFcns called

% Hint: edit controls usually have a white background on Windows.
%       See ISPC and COMPUTER.
```

```
if ispc && isequal(get(hObject,'BackgroundColor'),
get(0,'defaultUicontrolBackgroundColor'))
    set(hObject,'BackgroundColor','white');
end

function AlluvialP_Callback(hObject, eventdata, handles)
% hObject    handle to AlluvialP (see GCBO)
% eventdata  reserved - to be defined in a future version of MATLAB
% handles    structure with handles and user data (see GUIDATA)

% Hints: get(hObject,'String') returns contents of AlluvialP as text
%        str2double(get(hObject,'String')) returns contents of AlluvialP
as a double
global aperm apermMin apermMax unitLength;
v = str2double(get(hObject,'String'));
if (strcmp(unitLength,'ft') == 1)
    permUnit = 'cm/s';
else permUnit = 'ft/s';
end
if (checkValue(v, apermMin, apermMax, 'Alluvila permeability', 0,
permUnit) == 1)
    aperm = v;
else % Give the edit_slice text box focus so user can correct the error
    set(handles.AlluvilaP,'String',aperm);
    %uicontrol(hObject);
end

% --- Executes during object creation, after setting all properties.
function AlluvialP_CreateFcn(hObject, eventdata, handles)
% hObject    handle to AlluvialP (see GCBO)
% eventdata  reserved - to be defined in a future version of MATLAB
% handles    empty - handles not created until after all CreateFcns called

% Hint: edit controls usually have a white background on Windows.
%       See ISPC and COMPUTER.
```

```
if ispc && isequal(get(hObject,'BackgroundColor'),
get(0,'defaultUicontrolBackgroundColor'))
    set(hObject,'BackgroundColor','white');
end



% --- Executes on button press in ANNrunButton.
function ANNrunButton_Callback(hObject, eventdata, handles)
% hObject    handle to ANNrunButton (see GCBO)
% eventdata  reserved - to be defined in a future version of MATLAB
% handles    structure with handles and user data (see GUIDATA)

%The following line alerts MATLAB compiler NOT to use overloaded sim
%function that cannot be compiled

%#function network
global cWidth uSlope dSlope eHeight eFAngle eCohesion eUWeight eperm
fFAngle fCohesion fUWeight fperm aFAngle aCohesion aUWeight aperm;
global net firstANNrun firstLoLCalc floodCycle unitLength SS1 SS2 SS3 lol1
riskValue;
%global remedialMeasures;

if (firstANNrun == 1)
    firstANNrun = 0;

    % This code segment trains & saves a new ANN
    %--- begin train & save ---
    %{
    % Read input and target data from the fixed Excel file
    filename = 'Input Data for ANN.xlsx';
    sheet = 1;
    data = xlsread(filename, sheet, 'A6:O33', 'basic');
    filename = 'Target Data for ANN.xlsx';
    data1 = xlsread(filename, sheet, 'A6:C33', 'basic');
    inputs = data';
```

```
    targets = data1';

    % Create a Fitting Network
    hiddenLayerSize = 2;
    net = fitnet(hiddenLayerSize);

    % Setup Division of Data for Training, Validation, Testing
    net.divideParam.trainRatio = 70/100;
    net.divideParam.valRatio = 15/100;
    net.divideParam.testRatio = 15/100;

    % Train the Network
    net.trainParam.showWindow = false; % Default is true
    [net,tr] = train(net,inputs,targets);
    save preTrainedNet net;
    %}
    %--- end train & save ---

    % Assuming that a pre-trained ANN is already saved in file
    %#function network
    load preTrainedNet;
end

% Convert English unit to SI to match 'Input Data for ANN.xlsx' data type
if (strcmp(unitLength,'ft') == 1)
    lengthConv = 0.3048; % 1 foot = 0.3048 meter
    UWeightConv = 0.15709; % 1 pcf = 0.15709 kN/m3
    CConv = 0.0478803; %1 psf = 0.0478803 kPa
    permConv = 30.48; % 30.48 cm/s = 1 ft/s
else lengthConv = 1;
    UWeightConv = 1;
    CConv =1;
    permConv =1;
end
cWidth1 = cWidth*lengthConv;
```

```
eHeight1 = eHeight*lengthConv;
eCohesion1 = eCohesion*CConv;
eUWeight1 = eUWeight*UWeightConv;
eperm1 = eperm*permConv;
fCohesion1=fCohesion*CConv;
fUWeight1 = fUWeight*UWeightConv;
fperm1 = fperm*permConv;
aUWeight1 = aUWeight*UWeightConv;
aCohesion1=aCohesion*CConv;
aperm1 = aperm*permConv;

% Predict using user input
userData = [cWidth1 uSlope dSlope eHeight1 floodCycle eFAngle eCohesion1
eUWeight1 eperm1 fFAngle fCohesion1 fUWeight1 fperm1 aFAngle aCohesion1
aUWeight1 aperm1]';
SS = sim(net,userData);
set(handles.SS1,'String',num2str(abs(SS(1)),'%.02f'));
set(handles.SS2,'String',num2str(abs(SS(2)),'%.02f'));
set(handles.SS3,'String',num2str(abs(SS(3)),'%.02f'));
SS1 = abs(SS(1));
SS2 = abs(SS(2));
SS3 = abs(SS(3));
%if (firstLoLCalc == 0)
%   riskValue = pLS3 * lol1*1000/1000*100;
%   set(handles.riskValue,'String',riskValue);
%end

% Test the Network
%outputs = net(inputs);
%errors = gsubtract(targets,outputs);
%performance = perform(net,targets,outputs);

% View the Network
%view(net)

% Plots
```

```
% Uncomment these lines to enable various plots.
%figure, plotperform(tr)
%figure, plottrainstate(tr)
%figure, plotfit(net,inputs,targets)
%figure, plotregression(targets,outputs)
%figure, ploterrhist(errors)

% Alternative to above approach
%nnstart;  %Just runs the ANN start GUI

% --- Executes on selection change in popupmenu1.
function popupmenu1_Callback(hObject, eventdata, handles)
% hObject    handle to popupmenu1 (see GCBO)
% eventdata  reserved - to be defined in a future version of MATLAB
% handles    structure with handles and user data (see GUIDATA)

% Hints: contents = cellstr(get(hObject,'String')) returns popupmenu1
contents as cell array
%        contents{get(hObject,'Value')} returns selected item from
popupmenu1
global uSlope;
uSlope = get(hObject,'Value') + 1;

% --- Executes during object creation, after setting all properties.
function popupmenu1_CreateFcn(hObject, eventdata, handles)
% hObject    handle to popupmenu1 (see GCBO)
% eventdata  reserved - to be defined in a future version of MATLAB
% handles    empty - handles not created until after all CreateFcns called

% Hint: popupmenu controls usually have a white background on Windows.
%       See ISPC and COMPUTER.
if ispc && isequal(get(hObject,'BackgroundColor'),
get(0,'defaultUicontrolBackgroundColor'))
    set(hObject,'BackgroundColor','white');
end
```

```
% --- Executes on selection change in popupmenu2.
function popupmenu2_Callback(hObject, eventdata, handles)
% hObject    handle to popupmenu2 (see GCBO)
% eventdata  reserved - to be defined in a future version of MATLAB
% handles    structure with handles and user data (see GUIDATA)

% Hints: contents = cellstr(get(hObject,'String')) returns popupmenu2
contents as cell array
%        contents{get(hObject,'Value')} returns selected item from
popupmenu2
global dSlope;
dSlope = get(hObject,'Value') + 1;



% --- Executes during object creation, after setting all properties.
function popupmenu2_CreateFcn(hObject, eventdata, handles)
% hObject    handle to popupmenu2 (see GCBO)
% eventdata  reserved - to be defined in a future version of MATLAB
% handles    empty - handles not created until after all CreateFcns called

% Hint: popupmenu controls usually have a white background on Windows.
%       See ISPC and COMPUTER.
if ispc && isequal(get(hObject,'BackgroundColor'),
get(0,'defaultUicontrolBackgroundColor'))
    set(hObject,'BackgroundColor','white');
end

% --- Executes on key press with focus on drawButton and none of its
controls.
function drawButton_KeyPressFcn(hObject, eventdata, handles)
% hObject    handle to drawButton (see GCBO)
% eventdata  structure with the following fields (see UICONTROL)
%   Key: name of the key that was pressed, in lower case
%   Character: character interpretation of the key(s) that was pressed
```

```
%   Modifier: name(s) of the modifier key(s) (i.e., control, shift)
pressed
% handles    structure with handles and user data (see GUIDATA)
drawDamGeometry;



% --- Executes on button press in drawButton.
function drawButton_Callback(hObject, eventdata, handles)
% hObject    handle to drawButton (see GCBO)
% eventdata  reserved - to be defined in a future version of MATLAB
% handles    structure with handles and user data (see GUIDATA)
drawDamGeometry;

% --- Draw the dam geometry ---
function drawDamGeometry

global cWidth eHeight uSlope dSlope eHeightMin unitLength;
if (strcmp(unitLength,'ft') == 0)
    lengthConv = 0.3048; % 1 foot = 0.3048 meter
else lengthConv = 1;
end

% Draw the base geometry
figure('Name', 'Dam Geometry');%, 'Units', 'normalized', 'Position',
[0,0,1,1]);
pause(0.00001);
set(get(handle(gcf),'JavaFrame'),'Maximized',1);
min_x = 0;
max_x = 1000*lengthConv + eHeight*uSlope + cWidth + eHeight*dSlope +
1000*lengthConv;
min_y = 0;
max_y = (550 + 150 + 300)*lengthConv + eHeight;
image = imread('Dam.png');
image = image(end:-1:1,:,:); % Flipping the image
imagesc([min_x max_x], [min_y (700*lengthConv + eHeightMin)], image);
```

```
set(gca,'ydir','normal'); % Set the y-axis back to normal
axis([min_x max_x min_y max_y]);
if (strcmp(unitLength,'ft') == 1)
    xlabel('feet');
    ylabel('feet');
else xlabel('meter');
    ylabel('meter');
end
hold on;
%grid on;

% Draw the embankment
cw_x1 = 1000*lengthConv + eHeight*uSlope;
cw_x2 = cw_x1 + cWidth;
cw_y1 = 700*lengthConv + eHeightMin;
cw_y2 = cw_y1 + eHeight;
patch([cw_x1, cw_x2, cw_x2, cw_x1], [cw_y1, cw_y1, cw_y2, cw_y2],
'black'); %Crest
patch([1000*lengthConv, cw_x1, cw_x1], [cw_y1, cw_y1, cw_y2], 'black');
%Upstream embankment
patch([cw_x2, (cw_x2+eHeight*dSlope), cw_x2], [cw_y1, cw_y1, cw_y2],
'black'); %Downstream embankment

% Draw the line and annotation for crest width
h = line([cw_x1 cw_x1], [cw_y2-10*lengthConv, cw_y2+10*lengthConv]);
set(h, 'LineStyle', '--');
h = line([cw_x2 cw_x2], [cw_y2-10*lengthConv, cw_y2+10*lengthConv]);
set(h, 'LineStyle', '--');
x1 = (cw_x1+cw_x2)/2;
y1 = cw_y2+100*lengthConv;
[xaf, yaf] = ds2nfu([x1, x1], [y1, cw_y2]); % Convert data space into
normalized space
cWidthRound = round(cWidth*100)/100;
h = annotation('textarrow', xaf, yaf,'String' , [num2str(cWidthRound) ' '
unitLength ' ']);
set(h, 'LineStyle', ':', 'Color', 'b', 'HeadStyle', 'vback3');
```

```
% Draw the line and annotation for upstream
h = line([1000*lengthConv 1000*lengthConv], [cw_y1-10*lengthConv,
cw_y1+10*lengthConv]);
set(h, 'LineStyle', '--');
x1 = (1000*lengthConv + cw_x1)/2;
y1 = (cw_y1+cw_y2)/2 + 10*lengthConv;
[xaf, yaf] = ds2nfu([x1-15*lengthConv, x1], [y1, y1]); % Convert data
space into normalized space
h = annotation('textarrow', xaf, yaf,'String' , [num2str(uSlope) ':1 ']);
set(h, 'LineStyle', 'none', 'Color', 'b', 'HeadStyle', 'none');

% Draw the line and annotation for downstream
h = line([(max_x-1000*lengthConv) (max_x-1000*lengthConv)], [cw_y1-
10*lengthConv, cw_y1+10*lengthConv]);
set(h, 'LineStyle', '--');
x1 = (max_x - 1000*lengthConv + cw_x2)/2;
y1 = (cw_y1+cw_y2)/2 + 10*lengthConv;
[xaf, yaf] = ds2nfu([x1+40*lengthConv, x1], [y1, y1]); % Convert data
space into normalized space
h = annotation('textarrow', xaf, yaf,'String' , [num2str(dSlope) ':1 ']);
set(h, 'LineStyle', 'none', 'Color', 'b', 'HeadStyle', 'none');

% Draw the line and annotation for embankment height
h = line([1000*lengthConv cw_x1], [cw_y2, cw_y2]);
set(h, 'LineStyle', ':');
%h = drawbrace([1000 cw_y1], [1000 cw_y2]);
%set(h, 'LineStyle', ':', 'Color', 'b');
[xaf, yaf] = ds2nfu([1000*lengthConv, 1000*lengthConv], [cw_y1, cw_y2]); %
Convert data space into normalized space
h = annotation('doublearrow', xaf, yaf);
set(h, 'LineStyle', ':', 'Color', 'b', 'HeadStyle', 'vback3');
y1 = (cw_y1+cw_y2)/2;
[xaf, yaf] = ds2nfu([985*lengthConv, 995*lengthConv], [y1, y1]); % Convert
data space into normalized space
eHeightRound = round(eHeight*100)/100;
```

```
h = annotation('textarrow', xaf, yaf,'String' , [num2str(eHeightRound) ' '
unitLength ' ']);
set(h, 'LineStyle', 'none', 'Color', 'b', 'HeadStyle', 'none');

% Draw the line and annotation for embankment width
h = line([cw_x1 cw_x1], [10*lengthConv, 30*lengthConv]);
set(h, 'LineStyle', '--');
h = line([cw_x2 cw_x2], [10*lengthConv, 30*lengthConv]);
set(h, 'LineStyle', '--');
h = line([1000*lengthConv 1000*lengthConv], [10*lengthConv,
30*lengthConv]);
set(h, 'LineStyle', '--');
h = line([(max_x-1000*lengthConv) (max_x-1000*lengthConv)],
[10*lengthConv, 30*lengthConv]);
set(h, 'LineStyle', '--');
[xaf, yaf] = ds2nfu([1000*lengthConv, cw_x1], [20*lengthConv,
20*lengthConv]); % Convert data space into normalized space
h = annotation('doublearrow', xaf, yaf);
set(h, 'LineStyle', ':', 'Color', 'b', 'HeadStyle', 'vback3');
[xaf, yaf] = ds2nfu([max_x-1000*lengthConv, cw_x2], [20*lengthConv,
20*lengthConv]); % Convert data space into normalized space
h = annotation('doublearrow', xaf, yaf);
set(h, 'LineStyle', ':', 'Color', 'b', 'HeadStyle', 'vback3');
x1 = (1000*lengthConv + cw_x1)/2 + 20*lengthConv;
[xaf, yaf] = ds2nfu([x1, x1], [40*lengthConv, 40*lengthConv]); % Convert
data space into normalized space
h = annotation('textarrow', xaf, yaf,'String' ,
[num2str(round(eHeight*uSlope*100)/100) ' ' unitLength ' ']);
set(h, 'LineStyle', 'none', 'Color', 'b', 'HeadStyle', 'none');
x1 = (max_x - 1000*lengthConv + cw_x2)/2 + 20*lengthConv;
[xaf, yaf] = ds2nfu([x1, x1], [40*lengthConv, 40*lengthConv]); % Convert
data space into normalized space
h = annotation('textarrow', xaf, yaf,'String' ,
[num2str(round(eHeight*dSlope*100)/100) ' ' unitLength ' ']);
set(h, 'LineStyle', 'none', 'Color', 'b', 'HeadStyle', 'none');
```

```
% --- Executes when selected object is changed in unitChoice.
function unitChoice_SelectionChangeFcn(hObject, eventdata, handles)
% hObject    handle to the selected object in unitChoice
% eventdata  structure with the following fields (see UIBUTTONGROUP)
%   EventName: string 'SelectionChanged' (read only)
%   OldValue: handle of the previously selected object or empty if none
was selected
%   NewValue: handle of the currently selected object
% handles    structure with handles and user data (see GUIDATA)
global unitLength cWidth eHeight;
global cWidthMin cWidthMax eHeightMin eHeightMax fHeightMin fHeightMax
aHeightMin aHeightMax;
global eFAngle eCohesion eUWeight eperm fFAngle fCohesion fUWeight fperm
aFAngle aCohesion aUWeight aperm;
global eUWeightMin eUWeightMax fUWeightMin fUWeightMax aUWeightMin
aUWeightMax;

if (strcmp(unitLength,'ft') == 1)
    unitLength = 'm';
    lengthConv = 0.3048; % 1 foot = 0.3048 meter
    UWeightConv = 0.15709; % 1 pcf = 0.15709 kN/m3
    CConv = 0.0478803; %1 psf = 0.0478803 kPa
    permConv = 30.48; % 30.48 cm/s = 1 ft/s
    cWidthMin = round(cWidthMin*lengthConv);
    cWidthMax = round(cWidthMax*lengthConv);
    eHeightMin = round(eHeightMin*lengthConv);
    eHeightMax = round(eHeightMax*lengthConv);
    fHeightMin = round(fHeightMin*lengthConv);
    fHeightMax = round(fHeightMax*lengthConv);
    aHeightMin = round(aHeightMin*lengthConv);
    aHeightMax = round(aHeightMax*lengthConv);
    eUWeightMin = round(eUWeightMin*UWeightConv);
    eUWeightMax = round(eUWeightMax*UWeightConv);
    fUWeightMin = round(fUWeightMin*UWeightConv);
    fUWeightMax = round(fUWeightMax*UWeightConv);
    aUWeightMin = round(aUWeightMin*UWeightConv);
```

```
    aUWeightMax = round(aUWeightMax*UWeightConv);
else initializeVariables(1); % 1 means initializing some variables, not
all
    lengthConv = 3.28084; % 1 meter = 3.28084 foot
    UWeightConv = 1.0/0.15709; % 0.15709 kN/m3 = 1 pcf
    CConv = 1/0.0478803; % 1 psf = 0.0478803 kPa
    permConv = 1/30.48; % 30.48 cm/s = 1 ft/s
end

% Convert other units too
cWidth = cWidth*lengthConv;
eHeight = eHeight*lengthConv;
eUWeight = eUWeight*UWeightConv;
eCohesion = eCohesion*CConv;
aCohesion = aCohesion*CConv;
fCohesion = fCohesion*CConv;
eperm = eperm*permConv;
aperm = aperm*permConv;
fperm = fperm*permConv;
fUWeight = fUWeight*UWeightConv;
aUWeight = aUWeight*UWeightConv;

% Update the form data
set(handles.crestWidth,'String',num2str(cWidth,'%.02f'));
set(handles.embankmentHeight,'String',num2str(eHeight,'%.02f'));
set(handles.EmbankmentFA,'String',eFAngle);
set(handles.EmbankmentC,'String',num2str(eCohesion,'%.02f'));
set(handles.EmbankmentUW,'String',num2str(eUWeight,'%.02f'));
set(handles.EmbankmentP,'String',num2str(eperm,'%10.2e'));
set(handles.FoundationFA,'String',fFAngle);
set(handles.FoundationC,'String',num2str(fCohesion,'%.02f'));
set(handles.FoundationUW,'String',num2str(fUWeight,'%.02f'));
set(handles.FoundationP,'String',num2str(fperm,'%10.2e'));
set(handles.AlluvialFA,'String',aFAngle);
set(handles.AlluvialC,'String',num2str(aCohesion,'%.02f'));
set(handles.AlluvialUW,'String',num2str(aUWeight,'%.02f'));
```

```
set(handles.AlluvialP,'String',num2str(aperm,'%10.2e'));

% --- Executes on button press in FatalityRateCalc.
function FatalityRateCalc_Callback(hObject, eventdata, handles)
% hObject    handle to FatalityRateCalc (see GCBO)
% eventdata  reserved - to be defined in a future version of MATLAB
% handles    structure with handles and user data (see GUIDATA)
global firstLoLCalc; %firstANNrun
%if (firstANNrun == 1)
%    errordlg('Please run ANN first to get probaility of exceeding the
limit states!','Error');
%    return;
%end
filename = 'Loss of Life Potential.xlsx';
winopen(filename);
firstLoLCalc = 0;

% --- Executes on button press in FatalityRateCalc.
function GetFatalityRate_Callback(hObject, eventdata, handles)
% hObject    handle to FatalityRateCalc (see GCBO)
% eventdata  reserved - to be defined in a future version of MATLAB
% handles    structure with handles and user data (see GUIDATA)
global firstLoLCalc firstANNrun pLS3 lol1 riskValue;
%if (firstANNrun == 1)
%    errordlg('Please run ANN first to get probaility of exceeding the
limit states!','Error');
%    return;
%end
if (firstLoLCalc == 1)
    errordlg('Please first calculate the fatality rate with
distance!','Error');
    return;
end
filename = 'Loss of Life Potential.xlsx';
sheet = 'LLP_Calc_sheet';
lol = xlsread(filename, sheet, 'E22:E24', 'basic');
```

```
set(handles.fRate1,'String',lol(1));
set(handles.fRate2,'String',lol(2));
set(handles.fRate3,'String',lol(3));
lol1 = lol(1);
%if (firstANNrun == 0)
%    riskValue = pLS3 * lol1*1000/1000*100;
%    set(handles.riskValue,'String',riskValue);
%end

function riskValue_Callback(hObject, eventdata, handles)
% hObject    handle to riskValue (see GCBO)
% eventdata  reserved - to be defined in a future version of MATLAB
% handles    structure with handles and user data (see GUIDATA)

% Hints: get(hObject,'String') returns contents of riskValue as text
%        str2double(get(hObject,'String')) returns contents of riskValue
as a double

global riskValue;
v = str2double(get(hObject,'String'));
if isnumeric(v)          % It is a number
    if ((v >= 0) && (v <= 99999))
        riskValue = v;
        return;
    end
end
% Give the edit_slice text box focus so user can correct the error
errordlg('Invalid risk value!','Error');
set(handles.riskValue,'String',riskValue);
%uicontrol(hObject);


% --- Executes during object creation, after setting all properties.
function riskValue_CreateFcn(hObject, eventdata, handles)
% hObject    handle to riskValue (see GCBO)
```

```
% eventdata  reserved - to be defined in a future version of MATLAB
% handles    empty - handles not created until after all CreateFcns called

% Hint: edit controls usually have a white background on Windows.
%       See ISPC and COMPUTER.
if ispc && isequal(get(hObject,'BackgroundColor'),
get(0,'defaultUicontrolBackgroundColor'))
    set(hObject,'BackgroundColor','white');
end

function fCycle_Callback(hObject, eventdata, handles)
% hObject    handle to fCycle (see GCBO)
% eventdata  reserved - to be defined in a future version of MATLAB
% handles    structure with handles and user data (see GUIDATA)

% Hints: get(hObject,'String') returns contents of fCycle as text
%        str2double(get(hObject,'String')) returns contents of fCycle as a
double
global floodCycle;
floodCycle = get(hObject,'Value')
% --- Executes during object creation, after setting all properties.
function fCycle_CreateFcn(hObject, eventdata, handles)
% hObject    handle to fCycle (see GCBO)
% eventdata  reserved - to be defined in a future version of MATLAB
% handles    empty - handles not created until after all CreateFcns called

% Hint: edit controls usually have a white background on Windows.
%       See ISPC and COMPUTER.
if ispc && isequal(get(hObject,'BackgroundColor'),
get(0,'defaultUicontrolBackgroundColor'))
    set(hObject,'BackgroundColor','white');
end

% --- Check boundary errors for numeric input ---
function ret = checkValue(val, min, max, name, isLength, unit)
```

```
global unitLength;
if isnumeric(val)           % It is a number
    if ((val >= min) && (val <= max))
        ret = 1;
        return;
    end
end
% Cannot evaluate expression user typed
if (isLength == 1)
    unit = unitLength;
end
msg = strcat({'Invalid '},name,{' value! It should be within '},...
    num2str(min),{' ~ '},num2str(max),{' '},unit);
errordlg(msg,'Error');
ret = 0;
return;

% --- Executes on selection change in remMeasures.
%function remMeasures_Callback(hObject, eventdata, handles)
% hObject    handle to remMeasures (see GCBO)
% eventdata  reserved - to be defined in a future version of MATLAB
% handles    structure with handles and user data (see GUIDATA)
% Hints: contents = cellstr(get(hObject,'String')) returns remMeasures
contents as cell array
%        contents{get(hObject,'Value')} returns selected item from
remMeasures
%global remedialMeasures;
%remedialMeasures = get(hObject,'Value');
%if (remedialMeasures > 1)
%    msg = 'The current version of this tool has no ANN training data
records for remedial measures. Please use default crest width, embankment
height, side slopes of 4:1, and  cycles between 4 and 20.';
%    warndlg(msg, 'Warning');
%end
```

```
% --- Executes during object creation, after setting all properties.
%function remMeasures_CreateFcn(hObject, eventdata, handles)
% hObject    handle to remMeasures (see GCBO)
% eventdata  reserved - to be defined in a future version of MATLAB
% handles    empty - handles not created until after all CreateFcns called

% Hint: popupmenu controls usually have a white background on Windows.
%       See ISPC and COMPUTER.
%if ispc && isequal(get(hObject,'BackgroundColor'),
get(0,'defaultUicontrolBackgroundColor'))
    set(hObject,'BackgroundColor','white');
%end

% --- Executes on button press in note.
function note_Callback(hObject, eventdata, handles)
% hObject    handle to note (see GCBO)
% eventdata  reserved - to be defined in a future version of MATLAB
% handles    structure with handles and user data (see GUIDATA)
textMsg = 'The risk value is calculated for population at risk (PAR) of
1000 people assuming they fill in a fatality area from 0 to 3 miles away
from the structure and for a probability of exceeding Limit State III
(LSIII). User should use caution when PAR changes, and change risk value
accordingly.';
helpdlg(sprintf(textMsg),'How to Calculate Risk Value');

% --- Executes when figure1 is resized.
function figure1_ResizeFcn(hObject, eventdata, handles)
% hObject    handle to figure1 (see GCBO)
% eventdata  reserved - to be defined in a future version of MATLAB
% handles    structure with handles and user data (see GUIDATA)
figPos = get(handles.figure1, 'Position');
panelPos = get(handles.mainPanel, 'Position');
rSlPos = get(handles.rightSlider, 'Position');
bSlPos = get(handles.bottomSlider, 'Position');

% Set panel position
```

```
set(handles.mainPanel, 'Position', [(figPos(3)-panelPos(3)+rSlPos(3)/2)/2,
(figPos(4)-panelPos(4)-bSlPos(4)/2)/2, panelPos(3), panelPos(4)]);

% Adjust right slider
if (figPos(4) > panelPos(4))
    set(handles.rightSlider, 'Visible', 'off');
else rSlPos = [figPos(3)-rSlPos(3), 0, rSlPos(3), figPos(4)];
    set(handles.rightSlider, 'Position', rSlPos);
    set(handles.rightSlider, 'Visible', 'on');
    rightSlider_Callback(hObject, eventdata, handles);
end

% Adjust bottom slider
if (figPos(3) > panelPos(3))
    set(handles.bottomSlider, 'Visible', 'off');
else bSlPos = [0, 0, figPos(3)-rSlPos(3), bSlPos(4)];
    set(handles.bottomSlider, 'Position', bSlPos);
    set(handles.bottomSlider, 'Visible', 'on');
    bottomSlider_Callback(hObject, eventdata, handles);
end

% --- Executes on slider movement.
function rightSlider_Callback(hObject, eventdata, handles)
% hObject    handle to rightSlider (see GCBO)
% eventdata  reserved - to be defined in a future version of MATLAB
% handles    structure with handles and user data (see GUIDATA)

% Hints: get(hObject,'Value') returns position of slider
%        get(hObject,'Min') and get(hObject,'Max') to determine range of
slider

rSlVal = get(handles.rightSlider, 'Value');
panelPos = get(handles.mainPanel, 'Position');
figPos = get(handles.output, 'Position');
```

```
set(handles.mainPanel, 'Position', [panelPos(1), -rSlVal*(panelPos(4)-
figPos(4)), panelPos(3), panelPos(4)]);

% --- Executes during object creation, after setting all properties.
function rightSlider_CreateFcn(hObject, eventdata, handles)
% hObject    handle to rightSlider (see GCBO)
% eventdata  reserved - to be defined in a future version of MATLAB
% handles    empty - handles not created until after all CreateFcns called

% Hint: slider controls usually have a light gray background.
if isequal(get(hObject,'BackgroundColor'),
get(0,'defaultUicontrolBackgroundColor'))
    set(hObject,'BackgroundColor',[.9 .9 .9]);
end

% --- Executes on slider movement.
function bottomSlider_Callback(hObject, eventdata, handles)
% hObject    handle to bottomSlider (see GCBO)
% eventdata  reserved - to be defined in a future version of MATLAB
% handles    structure with handles and user data (see GUIDATA)

% Hints: get(hObject,'Value') returns position of slider
%        get(hObject,'Min') and get(hObject,'Max') to determine range of
slider

bSlVal = get(handles.bottomSlider, 'Value');
panelPos = get(handles.mainPanel, 'Position');
figPos = get(handles.output, 'Position');
set(handles.mainPanel, 'Position', [-bSlVal*(panelPos(3)-figPos(3)),
panelPos(2), panelPos(3), panelPos(4)]);



% --- Executes during object creation, after setting all properties.
function bottomSlider_CreateFcn(hObject, eventdata, handles)
% hObject    handle to bottomSlider (see GCBO)
```

```
% eventdata  reserved - to be defined in a future version of MATLAB
% handles    empty - handles not created until after all CreateFcns called

% Hint: slider controls usually have a light gray background.
if isequal(get(hObject,'BackgroundColor'),
get(0,'defaultUicontrolBackgroundColor'))
    set(hObject,'BackgroundColor',[.9 .9 .9]);
end

% --- Round x upto y decimal precision
function ret = myRound(x, y)
ret = round(x*10^y)/10^y;
return;

function benifitloss_Callback(hObject, eventdata, handles)
% hObject    handle to benifitloss (see GCBO)
% eventdata  reserved - to be defined in a future version of MATLAB
% handles    structure with handles and user data (see GUIDATA)

% Hints: get(hObject,'String') returns contents of benifitloss as text
%        str2double(get(hObject,'String')) returns contents of benifitloss
as a double

% --- Executes during object creation, after setting all properties.
function benifitloss_CreateFcn(hObject, eventdata, handles)
% hObject    handle to benifitloss (see GCBO)
% eventdata  reserved - to be defined in a future version of MATLAB
% handles    empty - handles not created until after all CreateFcns called

% Hint: edit controls usually have a white background on Windows.
%       See ISPC and COMPUTER.
if ispc && isequal(get(hObject,'BackgroundColor'),
get(0,'defaultUicontrolBackgroundColor'))
    set(hObject,'BackgroundColor','white');
end
```

```
function remediationcost_Callback(hObject, eventdata, handles)
% hObject    handle to remediationcost (see GCBO)
% eventdata  reserved - to be defined in a future version of MATLAB
% handles    structure with handles and user data (see GUIDATA)

% Hints: get(hObject,'String') returns contents of remediationcost as text
%        str2double(get(hObject,'String')) returns contents of
remediationcost as a double

% --- Executes during object creation, after setting all properties.
function remediationcost_CreateFcn(hObject, eventdata, handles)
% hObject    handle to remediationcost (see GCBO)
% eventdata  reserved - to be defined in a future version of MATLAB
% handles    empty - handles not created until after all CreateFcns called

% Hint: edit controls usually have a white background on Windows.
%       See ISPC and COMPUTER.
if ispc && isequal(get(hObject,'BackgroundColor'),
get(0,'defaultUicontrolBackgroundColor'))
    set(hObject,'BackgroundColor','white');
end

function replacementcost_Callback(hObject, eventdata, handles)
% hObject    handle to replacementcost (see GCBO)
% eventdata  reserved - to be defined in a future version of MATLAB
% handles    structure with handles and user data (see GUIDATA)

% Hints: get(hObject,'String') returns contents of replacementcost as text
%        str2double(get(hObject,'String')) returns contents of
replacementcost as a double

% --- Executes during object creation, after setting all properties.
function replacementcost_CreateFcn(hObject, eventdata, handles)
% hObject    handle to replacementcost (see GCBO)
```

```
% eventdata  reserved - to be defined in a future version of MATLAB
% handles    empty - handles not created until after all CreateFcns called

% Hint: edit controls usually have a white background on Windows.
%       See ISPC and COMPUTER.
if ispc && isequal(get(hObject,'BackgroundColor'),
get(0,'defaultUicontrolBackgroundColor'))
    set(hObject,'BackgroundColor','white');
end

function indirectcost_Callback(hObject, eventdata, handles)
% hObject    handle to indirectcost (see GCBO)
% eventdata  reserved - to be defined in a future version of MATLAB
% handles    structure with handles and user data (see GUIDATA)

% Hints: get(hObject,'String') returns contents of indirectcost as text
%        str2double(get(hObject,'String')) returns contents of
indirectcost as a double

% --- Executes during object creation, after setting all properties.
function indirectcost_CreateFcn(hObject, eventdata, handles)
% hObject    handle to indirectcost (see GCBO)
% eventdata  reserved - to be defined in a future version of MATLAB
% handles    empty - handles not created until after all CreateFcns called

% Hint: edit controls usually have a white background on Windows.
%       See ISPC and COMPUTER.
if ispc && isequal(get(hObject,'BackgroundColor'),
get(0,'defaultUicontrolBackgroundColor'))
    set(hObject,'BackgroundColor','white');
end

% --- Executes on button press in pushbutton15.
function pushbutton15_Callback(hObject, eventdata, handles)
% hObject    handle to pushbutton15 (see GCBO)
```

```
% eventdata  reserved - to be defined in a future version of MATLAB
% handles    structure with handles and user data (see GUIDATA)


% --- Executes on button press in pushbutton16.
function pushbutton16_Callback(hObject, eventdata, handles)
% hObject    handle to pushbutton16 (see GCBO)
% eventdata  reserved - to be defined in a future version of MATLAB
% handles    structure with handles and user data (see GUIDATA)

% --- Executes on button press in pushbutton17.
function pushbutton17_Callback(hObject, eventdata, handles)
% hObject    handle to pushbutton17 (see GCBO)
% eventdata  reserved - to be defined in a future version of MATLAB
% handles    structure with handles and user data (see GUIDATA)

% --- Executes on button press in pushbutton18.
function pushbutton18_Callback(hObject, eventdata, handles)
% hObject    handle to pushbutton18 (see GCBO)
% eventdata  reserved - to be defined in a future version of MATLAB
% handles    structure with handles and user data (see GUIDATA)

% --- Executes during object creation, after setting all properties.
function axe5_CreateFcn(hObject, eventdata, handles)
% hObject    handle to axes5 (see GCBO)
% eventdata  reserved - to be defined in a future version of MATLAB
% handles    empty - handles not created until after all CreateFcns called

% Hint: place code in OpeningFcn to populate axes5

% --- Executes on button press in CalcProbailities.
function CalcProbailities_Callback(hObject, eventdata, handles)
% hObject    handle to CalcProbailities (see GCBO)
% eventdata  reserved - to be defined in a future version of MATLAB
% handles    structure with handles and user data (see GUIDATA)
```

```
global SS1 SS3 pLS3 pLS lol1 riskValue;
filename = 'Probabilities of Exceeding LS.xlsx';
%winopen(filename);
sheet = 'Probability of exceeding LS';
xlswrite(filename,{SS1},sheet,'F5');
xlswrite(filename,{SS3},sheet,'F6');
filename = 'Probabilities of Exceeding LS.xlsx';
sheet = 'Probability of exceeding LS';
pLS = xlsread(filename, sheet, 'C14:E14', 'basic');
pLS(pLS<0)=0;
set(handles.pLS1,'String',num2str(pLS(1),'%.05f'));
set(handles.pLS2,'String',num2str(pLS(2),'%.05f'));
set(handles.pLS3,'String',num2str(pLS(3),'%.05f'));
pLS3 = pLS(3);
%if (firstANNrun == 0)
   riskValue = pLS3 * lol1*1000/1000*100;
   set(handles.riskValue,'String',num2str(riskValue,'%.03f'));
%end

% --- Executes on button press in note.
function pushbutton21_Callback(hObject, eventdata, handles)
% hObject    handle to note (see GCBO)
% eventdata  reserved - to be defined in a future version of MATLAB
% handles    structure with handles and user data (see GUIDATA)
```